ZooKeys 1031: 1–17 (2021)
doi: 10.3897/zookeys.1031.59361
https://zookeys.pensoft.net

RESEARCH ARTICLE

A peer-reviewed open-access journal
ZooKeys
Launched to accelerate biodiversity research

Redescription of *Emplectonema viride* – a ubiquitous intertidal hoplonemertean found along the West Coast of North America

Cecili B. Mendes[1,2], Paul Delaney[3], James M. Turbeville[3],
Terra Hiebert[4], Svetlana Maslakova[2]

1 *Laboratório de Diversidade Genômica, Departamento de Genética e Biologia Evolutiva, Instituto de Biociências, Universidade de São Paulo, SP, Brazil* **2** *Oregon Institute of Marine Biology, University of Oregon, Charleston, OR, USA* **3** *Department of Biology, Virginia Commonwealth University, Richmond, VA, USA* **4** *Department of Biology, University of Oregon, Eugene, OR, USA*

Corresponding author: Cecili B. Mendes (cecilimendes@gmail.com)

Academic editor: Jon Norenburg | Received 6 October 2020 | Accepted 6 January 2021 | Published 14 April 2021

http://zoobank.org/0889C28B-1CF9-45EF-A7BD-F4AAAA0924CD

Citation: Mendes CB, Delaney P, Turbeville JM, Hiebert T, Maslakova S (2021) Redescription of *Emplectonema viride* – a ubiquitous intertidal hoplonemertean found along the West Coast of North America. ZooKeys 1031: 1–17. https://doi.org/10.3897/zookeys.1031.59361

Abstract

Emplectonema viride Stimpson, 1857, a barnacle predator, is one of the most common and conspicuous intertidal nemerteans found along the West Coast of North America from Alaska to California, but it is currently referred to by the wrong name. Briefly described without designation of type material or illustrations, the species was synonymized with the Atlantic look-alike, *Emplectonema gracile* (Johnston, 1837) by Coe. Here we present morphological and molecular evidence that *E. viride* is distinct from *E. gracile*. The two species exhibit differences in color of live specimens and egg size and are clearly differentiated with species delimitation analyses based on sequences of the partial regions of the 16S rRNA and cytochrome *c* oxidase subunit I genes. In order to improve nomenclatural stability, we re-describe *E. viride* based on specimens from the southern coast of Oregon and discuss which species should be the type species of the genus. *Emplectonema viride* was one of the two species originally included in the genus *Emplectonema* Stimpson, 1857, but subsequent synonymization of *E. viride* with *E. gracile* resulted in acceptance of the Atlantic species, *E. gracile*, as the type species of the genus. We resurrect *E. viride* Stimpson, 1857 and following Corrêa's designation, this should be the type species of the genus *Emplectonema*.

Keywords

Cryptic species, marine diversity, Nemertea, species delimitation

Introduction

The genus *Emplectonema* was established by Stimpson (1857) for two species: a European species *Borlasia camillea* Quatrefages, 1846 and the newly described *Emplectonema viride* Stimpson, 1857 from the Pacific coast of North America (San Francisco Bay, CA). Stimpson did not specify the type species.

The original description of *E. viride* is but a few lines in Latin: "Corpus depressum, lineare v. proteum, supra viride, subtis album. Caput subdiscretum, marginibus albis; foveis elongatis bipartitis; fronte emarginata. Ocellorum acervi quattuor; posteriores distincti, rotundati, ocellis confertis; anteriores marginales juxta foveas, ocellis sparsis. Long. 11; lat. 0.05 poll. *Hab*. In portu 'San Francisco;' littoralis inter lapillos" (Stimpson 1857: 163). It lacks illustrations, apparently owing to loss of Stimpson's plates and material during the great Chicago Fire (Griffin 1898). Griffin (1898), in a posthumously published paper, re-described *E. viride* based on the material collected during his expeditions to the coast of Alaska and Puget Sound. He characterized the species both internally and externally, provided a drawing of the stylet apparatus, and noted that the specimens from Alaska showed a darker color dorsally. He also noted that *E. viride* differs from its Atlantic counterpart *Emplectonema gracile* (Johnston, 1837), by darker body color and "narrower head with sharply defined color patterns" (Griffin 1898). Coe, in his 1901 monograph describing nemerteans from the Harriman Alaska Expedition, synonymized *E. viride* with *E. gracile*. He did not cite Griffin's work (1989) and was apparently unaware of it. Griffin succumbed to pneumonia at the age of 26, shortly before receiving his Doctoral degree from Columbia University.

Emplectonema gracile was first described as *Nemertes gracile* by Johnston (1837) from the Berwick Bay in the North Sea, and it was later included in the genus *Emplectonema* by Coe (1901), as a senior synonym of *E. viride*. Corrêa (1955), in her revision of the genus *Emplectonema*, specified *E. gracile* as the type species of the genus, citing priority. Since then, *Emplectonema gracile* (Johnston, 1837) has been treated as the type species of the genus (Gibson 1995), and all green *Emplectonema* specimens with a curved central stylet and a slender elongated basis are called by that name, regardless of geographic location.

The species currently recognized as *E. gracile* is listed as having a wide geographic distribution in the Northern Hemisphere, including Japan (Hokkaido), Russia (Kamchatka Peninsula), the Aleutian Islands, the Atlantic and Pacific coast of North America, northern coasts of Europe, Mediterranean, the Romanian coast of the Black Sea, and Madeira (Gibson 1995; Turbeville 2011; Maslakova, Delaney and Turbeville unpublished observations). This species is commonly found in great numbers, often with individuals intertwined, among barnacles and mussels in natural and anthropogenic environments, where it feeds upon acorn barnacles.

Here we present molecular and morphological evidence that *E. viride* is a separate species from *E. gracile*. We compare the two cryptic species and re-describe *E. viride*, the type species of the genus *Emplectonema*, as designated by Corrêa (1955).

Materials and methods

Sampling

Clusters of acorn barnacles, typically *Balanus glandula* Darwin, 1854, were collected from intertidal zones at two locations in southern Oregon (Oregon Scientific Take Permits #22780 and 23609) in 2019 and 2020 by C. Mendes and S. Maslakova (Table 1, Suppl. material 1). Some of the worms were removed from the barnacles in the field, but others were entangled, so barnacles were taken to the laboratory, placed in trays, and covered with seawater until the worms crawled out. Worms were removed and kept in 150 ml glass dishes in a sea table with running seawater at ambient sea temperature (12–15 °C). Seven specimens were obtained from pilings near the Charleston Marina in November 2019, and one specimen from the Oregon Institute of Marine Biology (OIMB) Boathouse dock site was collected in October 2019 (Table 1, Suppl. material 1). Additional 10 specimens were collected from the same location in April 2019 (Table 1, Suppl. material 1). Specimens collected by J. Turbeville, in November 2019, from South Carolina were obtained by removing them from mats of the scorched mussel, *Brachidontes exustus* (Linnaeus, 1758), in the field or allowing them to crawl from detached mussel clumps in plastic bags, pyrex dishes, or buckets containing seawater. An additional six specimens from the same site at Pawleys Island, SC, were collected in 2013 and 2014. Specimens collected in November 2019 were shipped alive to the OIMB and kept in isolation to prevent accidental introduction. As some worms had mature gametes, the non-flow-through water from these individuals was changed regularly and treated with 10% hypochlorite before discarding.

Live worms were photographed with external flash using a Canon Eos 5D Mark III. For close ups, worms were anesthetized with a mixture of 1:1 $MgCl_2$ and seawater. Anterior end and proboscis were removed, gently compressed between a glass slide and a cover slip, and photographed using a Spot 5.2 camera mounted on an Olympus BX51 equipped with DIC optics. Eggs, sperm, and larval stages were photographed similarly. The anterior region of each morphological voucher was fixed in 10% formalin, post-fixed in Bouin's solution, and stored in 70% ethanol. The posterior region was preserved in 95% ethanol and kept at -20 °C until DNA extraction.

DNA extraction, PCR amplification, and sequence analysis

Genomic DNA was extracted with DNEasy Blood and Tissue kit (Qiagen) following the manufacturer's protocol. Partial regions of cytochrome *c* oxidase subunit I (COI) and 16S ribosomal DNA (16S rRNA) were amplified using the primer pairs in Table 2. Polymerase chain reactions (PCR) were carried out using GoTaq Green Master Mix (Promega) as follows: initial denaturation at 95 °C for 2 min; 35 cycles of denaturation at 95 °C for 15 or 40 sec; annealing at 45 °C (COI) or 50 °C (16S) for 40 sec, extension at 72 °C for 1 min; and final extension at 72 °C for 2 min. PCR products were purified either with Wizard SV Gel and PCR Clean-Up System (Promega) or enzymatically with

Table 1. Sampling locations, specimen ID, and accession numbers. Morphological vouchers listed in bold. † Sequences previously available in GenBank.

Species	Abbreviation	Sampling location	NMNH #	GenBank accession COI	GenBank accession 16S rRNA
Emplectonema viride	CH_OR_1_E_viride	OIMB Boathouse dock, OR	–	MT649099	MT647808
	CH_OR_2_E_viride		–	MT649110	MT647809
	CH_OR_3_E_viride		–	MT649101	MT647812
	CH_OR_4_E_viride		–	MT649102	MT647811
	CH_OR_5_E_viride		–	MT649109	MT647814
	CH_OR_6_E_viride		–	MT649100	MT647815
	CH_OR_7_E_viride		–	MT649103	MT647816
	CH_OR_8_E_viride		–	MT649104	MT647807
	CH_OR_9_E_viride		–	MT649105	MT647818
	CH_OR_10_E_viride		–	MT649106	MT647817
	CH_OR_11_E_viride	**OIMB Boathouse dock, OR**	**USNM 1638666**	**MT649107**	**MT647813**
	CH_OR_12_E_viride	**Charleston Marina, OR**	**USNM 1638667**	**MT649114**	**MT647820**
	CH_OR_13_E_viride		**USNM 1638668**	**MT649115**	**MT647810**
	CH_OR_14_E_viride		**USNM 1638669**	**MT649108**	**MT647821**
	CH_OR_15_E_viride		**USNM 1638670**	**MT649111**	**MT647824**
	CH_OR_16_E_viride		**USNM 1638671**	**MT649116**	**MT647823**
	CH_OR_17_E_viride		**USNM 1638672**	**MT649112**	**MT647819**
	CH_OR_18_E_viride		**USNM 1638673**	**MT649113**	**MT647822**
	E4H2	Charleston, OR	–	KU197596†	KU197260†
	E5B5		–	KU197597†	KU197261†
	E5B6		–	KU197598†	KU197262†
	E5B7		–	KU197599†	KU197263†
Emplectonema gracile	PI_SC_1_E_gracile	Pawleys Island, SC	–	MT649119	MT647832
	PI_SC_2_E_gracile		–	MT649121	MT647827
	PI_SC_3_E_gracile		–	MT649127	MT647825
	PI_SC_4_E_gracile		–	MT649117	MT647830
	PI_SC_5_E_gracile		–	MT649124	MT647829
	PI_SC_6_E_gracile		–	MT649125	MT647834
	PI_SC_7_E_gracile	**Pawleys Island, SC**	**USNM 1638674**	**MT649126**	**MT647828**
	PI_SC_8_E_gracile		**USNM 1638675**	**MT649122**	**MT647835**
	PI_SC_9_E_gracile		**USNM 1638676**	**MT649123**	**MT647826**
	PI_SC_10_E_gracile		**USNM 1638677**	**MT649118**	**MT647831**
	PI_SC_11_E_gracile		**USNM 1638678**	**MT649120**	**MT647833**
	PI_SC_12_E_gracile		**USNM 1638679**	**–**	**–**
	PI_SC_13_E_gracile		**USNM 1638680**	**–**	**–**
	PI_SC_14_E_gracile		**USNM 1638681**	**–**	**–**
	–	Salcombe, UK	–	AJ436903†	AJ436793†
	DNA10615	Crosby, UK	–	HQ848620†	JF277621†
	NemBar0378	Sweden	–	KU839979†	–
	NemBar0400		–	KU839991†	–
	NemBar0401		–	KU839992†	–
	NemBar0402		–	KU839993†	–
	NemBar0403		–	KU839994†	–
	NemBar0404		–	KU839995†	–
	K21	Spain	–	KU697656†	

Table 2. Primer pairs utilized in this study.

Gene	Forward primer	Reverse primer	Reference
COI	HCO1490 – GGTCAACAAATCATAAAGATATTGG	LCO2198 – AAACTTCAGGGTGACCAAAAAATCA	Folmer et al. 1994
16S rRNA	16SARL – CGCCTGTTTATCAAAAACAT	16SBRH – CCGGTCTGAACTCAGATCACGT	Palumbi et al. 1991
16S rRNA		16SKr – AATAGATAGAAACCAACCTGGC	Jon Norenburg unpublished

the USB ExoSAP (Thermo Fisher). Purified products were sequenced in both directions using PCR primers at Sequetech DNA Inc. (Mountain View, CA) or Genewiz (South Plainfield, NJ). Sequences were trimmed to remove primer regions and low-quality ends, complementary strands proofread against each other using GeneStudioPro (GeneStudio, Inc.), and COI sequences were checked for stop codons. Resulting sequences are deposited in GenBank (Table 1, Suppl. material 1).

Consensus sequences were aligned in the online version of Mafft software v. 7 (Katoh et al. 2019). Additional GenBank sequences of *Emplectonema gracile* from European locations and *Emplectonema viride* (listed as *Emplectonema* sp. 1) from Oregon were included in the final alignments (Table 1, Suppl. material 1). Alignments were used as input for phylogenetic inference in RAxML v. 8.2.12 (Stamatakis 2014), as available in Cipres (Miller et al. 2012), under GTRGAMMA model with 1,000 bootstraps, and *Emplectonema buergeri* as the outgroup (GenBank accession HQ848600 and JF277616). Resulting trees (phylograms) from each dataset were used as input for PTP (Poisson tree process; Zhang et al. 2013) with default parameters. The alignments were also used as input in Automatic Barcoding Gap Discovery (ABGD) online software (Puillandre et al. 2012) with default values for all parameters. FASTA files were converted to Nexus format with PGDSpider v. 2.1.1 (Lischer and Excoffier 2012) and used as input for haplotype network constructions in PopArt v. 1.7 (Leigh and Bryant 2015) using the TCS (Templeton et al. 1992) algorithm. Datasets used in Popart were trimmed to the length of the shortest sequence to avoid biases.

Results

Species delimitation analysis

Independent phylogenetic analyses from each gene region apportioned the specimens into two main clades with high support, corresponding to sampling location. Specimens from the Pacific Ocean (*Emplectonema viride*) form one clade, and specimens from the Atlantic Ocean and North Sea (*Emplectonema gracile*) form another (Fig. 1). Results from the PTP analysis using the maximum likelihood search indicate that these two clades represent a single species each (Fig. 1, Suppl. material 2). The result from the Bayesian solution presents each specimen of *E. viride* as a different species (results not shown). These trees, however, do not show any signs of geographic influence, with specimens from the North Sea distributed among the specimens from the Atlantic coast of North America. ABGD analysis of the COI sequences found a barcoding gap at K2P distance of 0.01–0.16, while analysis of the 16S rRNA sequences found a gap at K2P distance of 0.015–0.10. Both datasets delimit the same two groups found by the phylogenetic analysis.

The haplotype networks show a low diversity with many mutational steps (85 for COI and 33 for 16S rRNA) between specimens from the Pacific and Atlantic Oceans (Fig. 2). Specimens of *E. viride* comprise only two haplotypes, in both networks, with

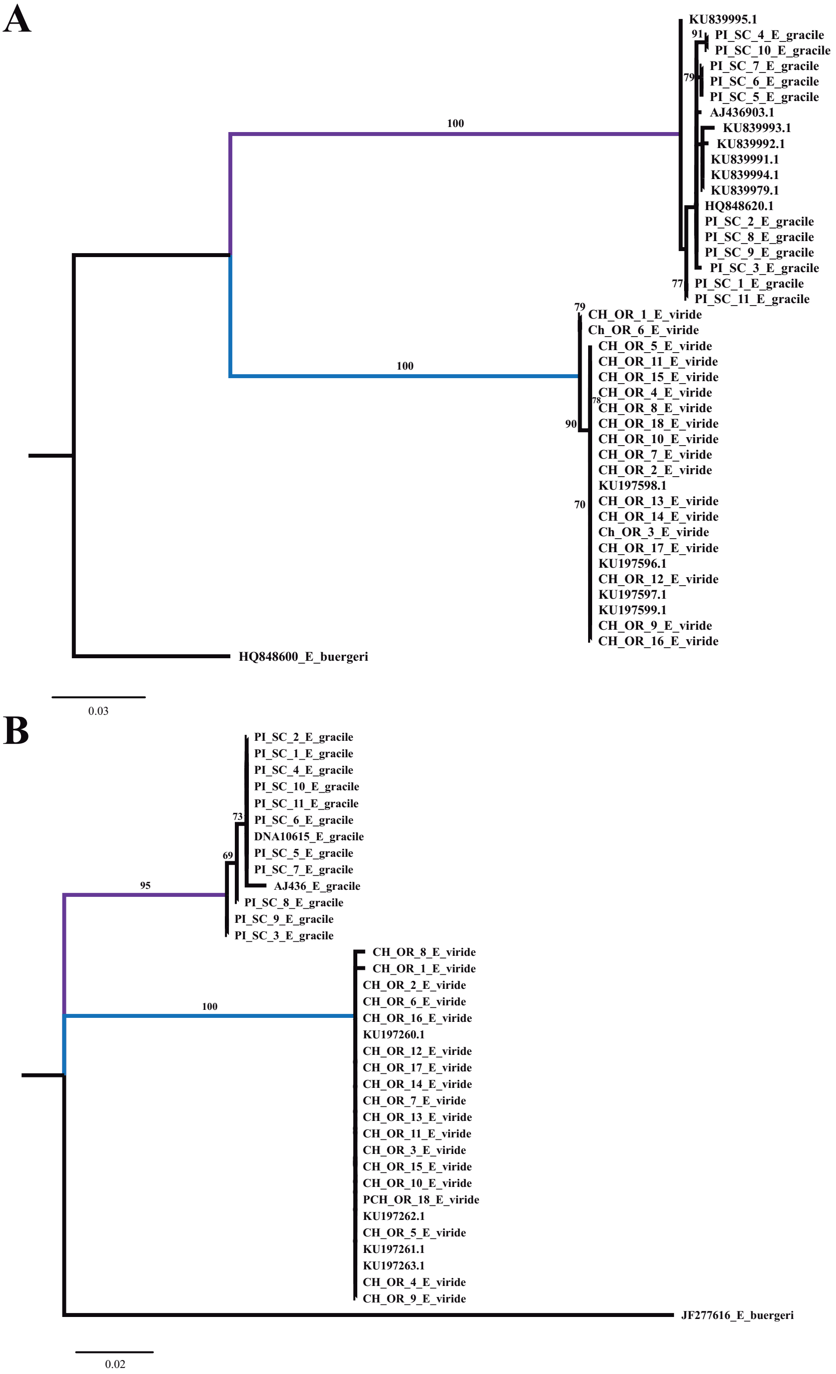

Figure 1. Resulting trees from the Maximum Likelihood analysis with RAxML. A: COI phylogeny (lnL = -1520.573862). B: 16S rRNA phylogeny (lnL = -909.477668). Support values above 50 presented in each branch. Branch in purple comprises specimens of *Emplectonema gracile*. Branch in blue comprises specimens of *Emplectonema viride*.

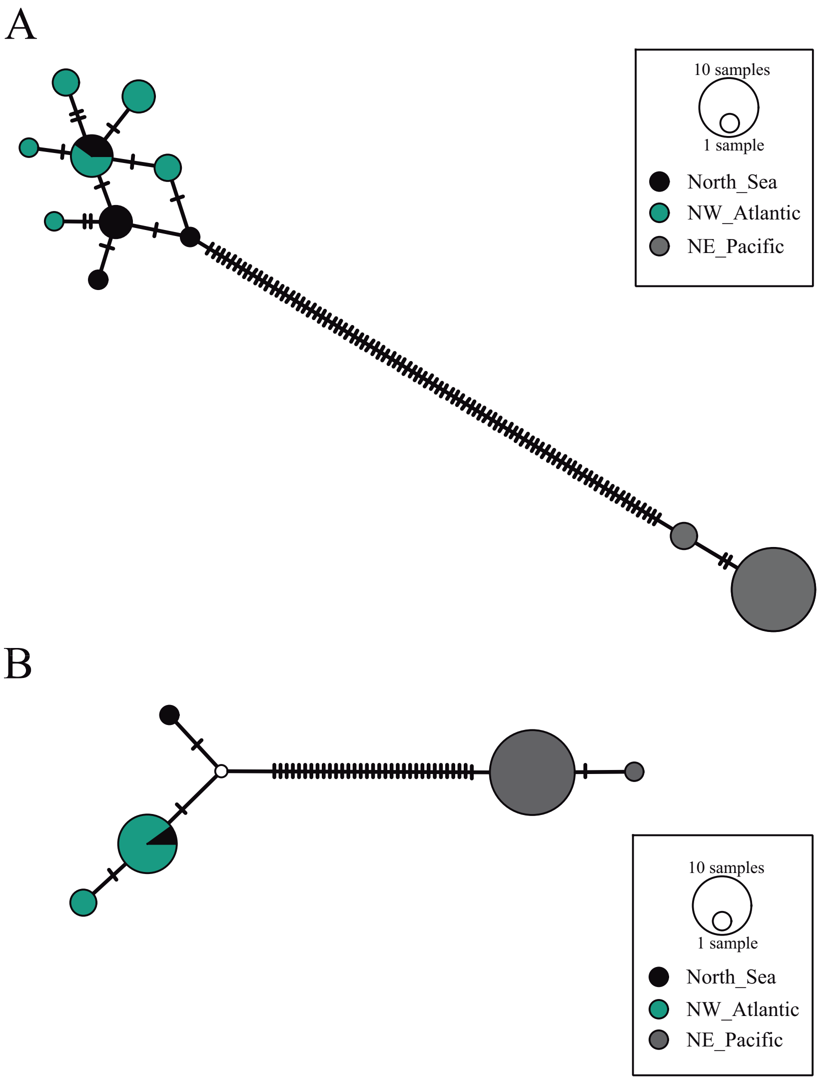

Figure 2. Haplotype networks of *Emplectonema gracile* (North Sea and NW Atlantic) and *Emplectonema viride* (NE Pacific) **A** generated from sequences of COI gene region **B** generated from sequences of 16S rRNA gene region.

one dominant haplotype. The specimens of *E. gracile* comprise nine haplotypes, with only one shared between the Atlantic and the North Sea, and no dominant haplotype for COI sequences. 16S rRNA sequences of *E. gracile* comprise three haplotypes, with one dominant haplotype shared between locations.

Taxonomy

Class HOPLONEMERTEA Hubrecht, 1879
Order Monostilifera Brinkmann, 1917
Suborder Eumonostilifera Chernyshev, 2003
Family Emplectonematidae Bürger, 1904

Genus *Emplectonema* Stimpson, 1857

Type species. *Emplectonema viride* Stimpson, 1857: 163; Griffin 1898: 207.

Emplectonema gracile Coe 1901: 23, fig. 3; Coe 1904: 23, fig. 3; Coe 1905: 207–208, pl. 1, figs 14, 14a, 15, 15a, tex fig. 32; Coe 1940: 252, 278–280, pl. 30, fig. 40; Corrêa 1964: 517–518, 534–536; Kozloff 1999: 98, 100; Roe et al. 2007: 229, 232 pl. 89I.

Material examined. Seven adults from Charleston Marina, OR (43°20.63'N, 124°19.38'W); 27 Nov. 2019; collected from wooden pilings among acorn barnacles, *Balanus glandula* (Table 1, Suppl. material 1). One specimen from OIMB Boathouse dock, OR (43°20.96'N, 124°19.80'W); 10 Oct. 2019; collected from concrete pilings among acorn barnacles, *Balanus glandula* (Table 1, Suppl. material 1). Eggs measured from two specimens collected from the jetty at the north end of Bastendorff Beach, OR (43°21.13'N, 124°20.66'W) on 29 Jan. 2020; and sperm from one male collected at Charleston Marina on 31 Jan. 2020. Voucher material is deposited at the Smithsonian Institution's National Museum of Natural History, Washington, DC: USNM 1638666–USNM 1638673. Each specimen consists of a morphological voucher (anterior end fixed in formaldehyde, post-fixed in Bouin's solution and stored in 70% ethanol) and a tissue sample for DNA extraction (pieces of posterior or midbody in 95% ethanol).

Comparative material. Three females and four non-sexed adults of *E. gracile* from Pawleys Island, SC (33°24.63'N, 79°7.88'W); 29 Nov. 2019; among scorched mussels, *Brachidontes exustus* on granite rocks; GenBank and NMNH accession numbers in Table 1.

Description. Based on specimens from Oregon, body long and thread-like, 35–103 mm long, 0.6–1.0 mm wide. However, Griffin (1898) found specimens nearly 1 m long. Dark green dorsally, cream-colored or pale yellow ventrally (Fig. 3A). Head round, slightly wider than adjacent body when moving freely, with whitish-yellow or cream-colored margins matching the color of the ventral side (Fig. 3B). A pair of small cerebral organ furrows (anterior cephalic furrows), each shaped as a small arch, is located ventrally, anterior to cerebral ganglia (Fig. 3C). Head furrow (posterior cephalic furrow) is shaped as a dorsal posteriorly directed "V" located behind the cerebral ganglia, and only just barely noticeable in some individuals, and not detectable in many individuals. Rhynchostomopore is a small antero-ventral opening. Numerous small ocelli arranged in two groups on each side of head. Each anterior group has 8–10 eyes arranged in a narrow row along the anterior margin of the head. Each posterior group has 10–12 eyes in a dispersed cluster in front of the brain (Fig. 3B). Cerebral ganglia are pinkish and show through the body wall, especially in lighter-colored individuals. Cerebral organs are not easily distinguishable in life, but with slight compression. Posterior tip of body tapered.

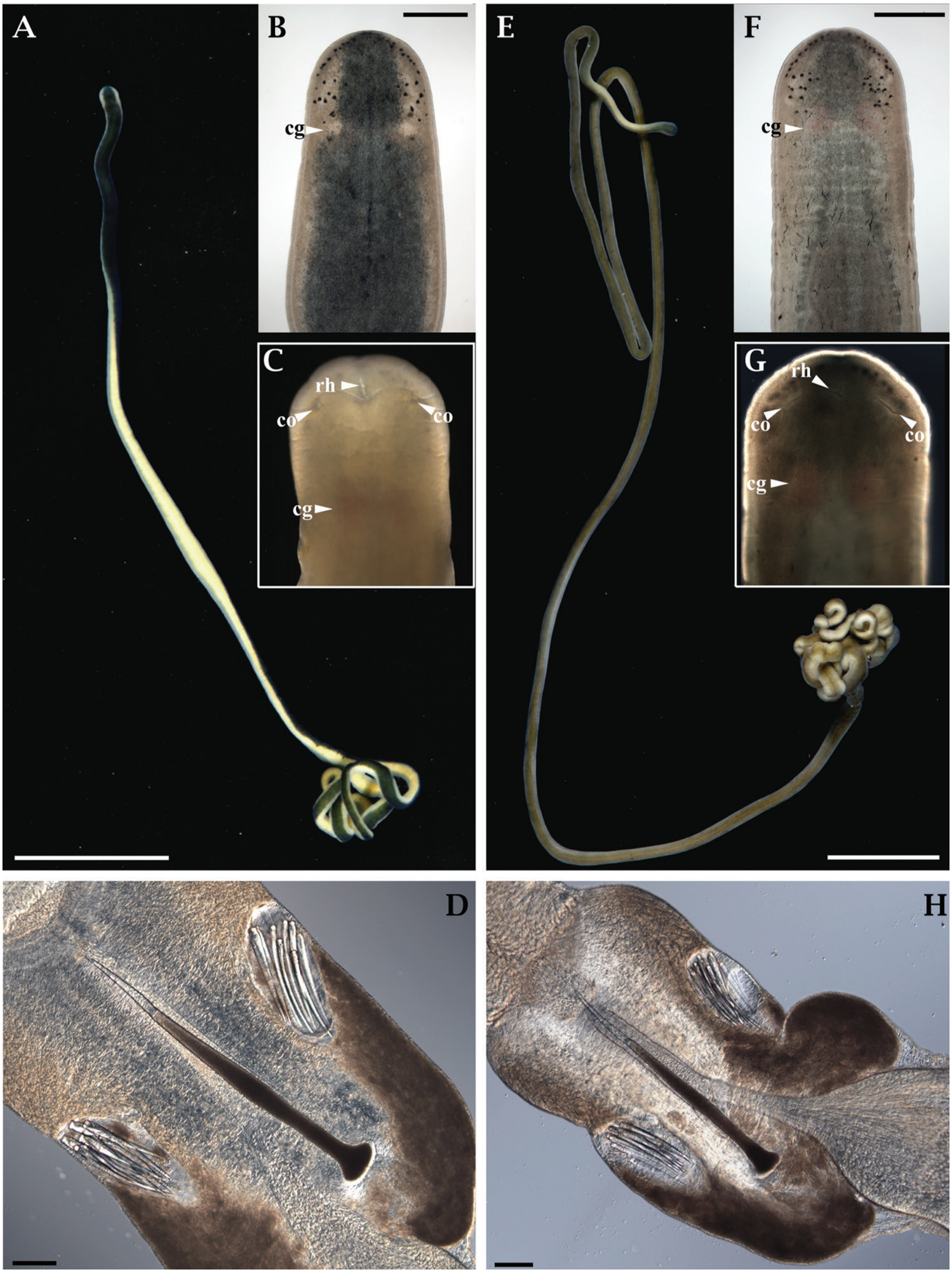

Figure 3. Photomicrographs of *Emplectonema viride* (**A–D**) and *Emplectonema gracile* (**E–H**). Abbreviations: cerebral ganglia, **cg**; rhynchostomopore, **rh**; cerebral organ opening, **co**. Scale bars: 10 mm (**A, E**); 0.5 mm (**B, F**); 100 μm (**D, H**).

Rhynchocoel is short, approximately 1/3 of body length. Central stylet slightly curved, 170–326 μm long (*n* = 7), smooth. Basis is slender, 480–815 μm long (*n* = 7), its distal end abruptly widening into a truncated bulb (Fig. 3C). Basis length/width

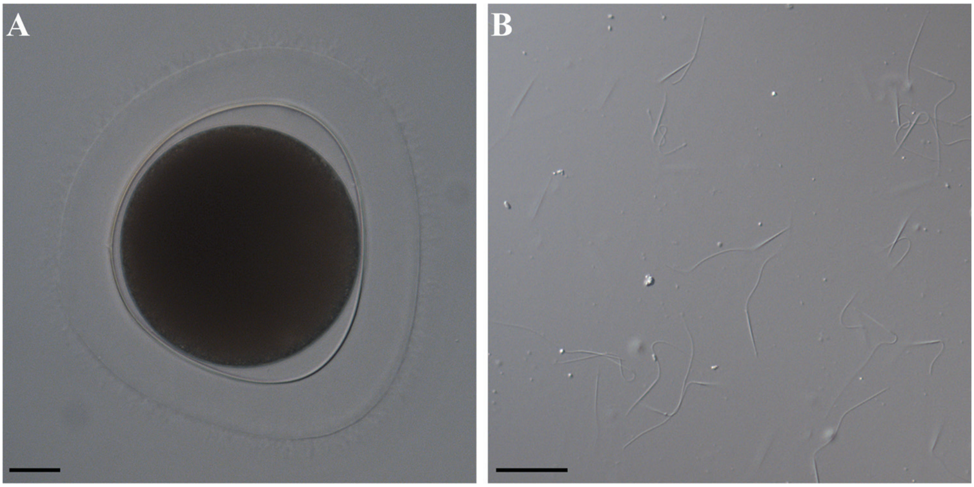

Figure 4. Photomicrography of egg (**A**) and sperm (**B**) of *Emplectonema viride*. Scale bars: 25 µm.

ratio 11.5–16.0. Basis/stylet length ratio 2.0–2.8. Two accessory stylet pouches, each with 9–13 accessory stylets (Fig. 3C). Proboscis bulb elongated. Lateral intestinal diverticula beginning at posterior of rhynchocoel, present until posterior tip of the body. Separate sexes. Gonads serially arranged between intestinal diverticula. Testes of mature males are visible through the body wall as whitish sacs. Ovaries of mature females are visible through the body wall, and the oocytes are orange to light pink, with distinct germinal vesicles. Spermatozoa with elongated head 16–20 µm. Oocytes are 110–140 µm in diameter and surrounded by a tight chorion and a jelly coat (Fig. 4).

Reproduction and larval development. Reproductive individuals of *E. viride* were collected in Charleston, OR, in September 2009, October 2019, January 2020, and June 2020. When ripe, males and females free-spawn gametes into the water, with no known reliable spawning cue. Swimming larvae hatch from the egg chorion after ~30 h and begin feeding on small planktonic crustaceans after developing a functional proboscis and stylet (~4 d). Planktonic period lasts several months (Mendes unpublished observations). Wild-caught larvae of *E. viride* were found in the plankton samples taken with 50–153 µm net at the Charleston Marina, OR, in October 2013, March 2019, February 2020, and June 2020. *Emplectonema viride* larvae are easily recognized by their distinctive green color (Fig. 5).

Distribution. Northeastern Pacific Ocean from Alaska to California. Type locality is San Francisco Bay, California, USA.

Morphological comparison with *Emplectonema gracile*. As has been pointed out by Griffin (1898), specimens of *E. viride* have a darker dorsal surface, with a distinctly lighter colored ventral side and head margins, compared to those of *E. gracile* (Fig. 3). We confirm this finding and can also add that *E. viride* has smaller eggs: 110–140 µm (n = 9), compared to 181–198 µm eggs of *E. gracile* (n = 8). The characteristics of stylet apparatus do not overtly differ in the two species (Fig. 3C, F).

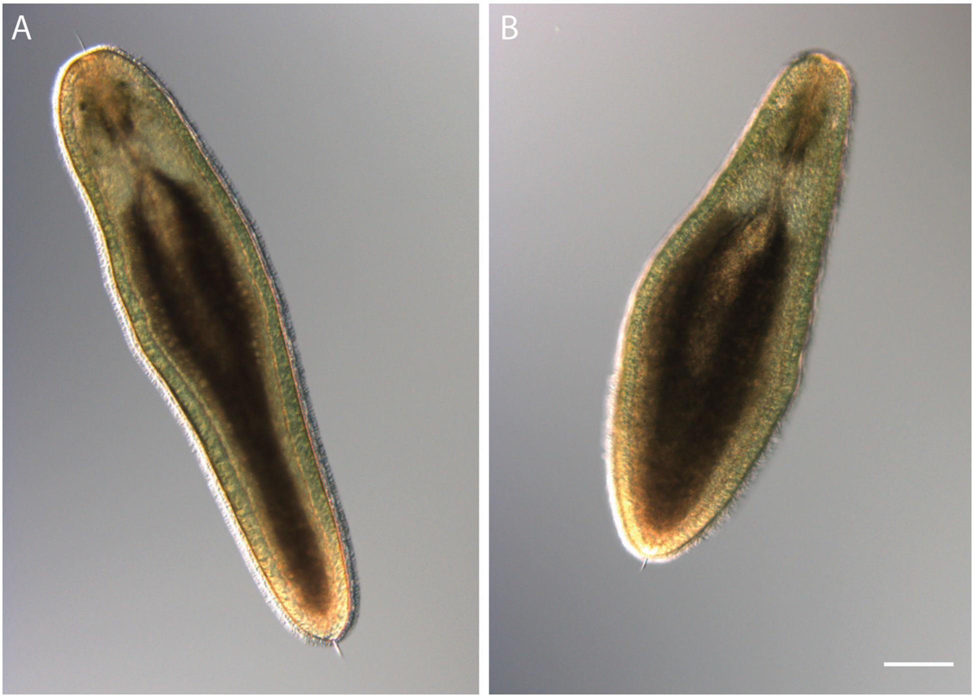

Figure 5. Larva of *Emplectonema viride* collected from plankton in Charleston, OR, on 17 Oct 2013. Same individual is shown in two focal planes to highlight apical tuft (upper left, **A**) and posterior cirrus (lower right, **A**) and green epidermal pigment (**B**). Note paired subepidermal eyes, which are anterior to cerebral organs. Scale bar: 100 µm.

Discussion

Differentiating cryptic species

The simple morphology of nemertean worms makes it notoriously difficult to identify species, and the use of DNA sequence data as well as gamete morphology can help differentiate between morphologically cryptic nemertean species (e.g., Strand and Sundberg 2005; Sundberg et al. 2009a, b, 2016; Chen et al. 2010; Hao et al. 2015; Hiebert and Maslakova 2015; Kajihara et al. 2018; Cherneva et al. 2019). Using mitochondrial sequence data alone can present difficulties in separating phylogenetic and biogeographical signals (Toews and Brelsford 2012 and references therein). However, analyses herein show that both mitochondrial markers exhibit signs of prolonged genetic isolation between the two species. Furthermore, all explicit, non-phylogenetic delimitation analyses in this study (ABGD and the haplotype network) show similar and well-supported results. Importantly, these tests have different strategies of species delimitation. ABGD is based on the pairwise differences between sequences. It uses an algorithm that calculates the divergence between sequences and automatically infers the barcoding gap between groups of sequences (Puillandre et al. 2012). PTP is a tree-based method that uses the number of substitution events as given by branch lengths of an input phylogram to infer intra- and interspecific relationships between sequences (Zhang et al. 2013). The TCS method used to construct haplotype networks has an integrated view of phylogeny and population structure, taking recombination into account. The algorithm collapses sequences into haplotypes, then uses the haplotype frequencies and pairwise comparison to calculate probabilities of relationship between sequences. The haplotypes are only linked when there is over 95% probability of parsimony for their connection (Templeton et al. 1992; Clement et al. 2001). These methods have been used in many delimitation studies with great success (e.g., Jörger et al. 2012; Scarpa et al. 2016; Mills et al. 2017; Pozzi et al. 2020). Therefore, congruent results using these different methods provide strong evidence for separation between *E. viride* and *E. gracile.* The morphological similarities between the two species are likely due to shared recent ancestry, but also possibly due to their similar ecology. Both species live among and prey upon barnacles. This similarity in their ecology is likely a strong factor maintaining the morphological traits even after prolonged isolation between populations (Fišer et al. 2018).

The combination of molecular and morphological data presented here confirms the existence of two cryptic species of North American *Emplectonema*, one from the Pacific and another from the Atlantic coast. Our results support the validity of *E. viride* described from the Pacific coast (Stimpson 1857; Griffin 1898) and suggest that Coe's (1901) synonymization of *E. viride* with *E. gracile* is unjustified.

Genus type fixation

The genus *Emplectonema* was established by Stimpson (1857) for *Emplectonema viride* and *Borlasia camillea* Quatrefages, 1846 (subsequently treated as a synonym of *Amphiporus neesii* Örsted, 1844 by McIntosh (1873–1874), Bürger (1895), and others. However, Stimpson (1857) did not designate a type species. According to the Article 67.2 of the ICZN, only the species originally included are eligible to be fixed as the type species of the genus (ICZN 1999). This makes *E. gracile* ineligible for designation as the type species of the genus. So, which species should become the type of *Emplectonema*?

DNA-based phylogenies (18S rRNA, COI) suggest that *Emplectonema neesii* (Örsted, 1844) is not closely related to *E. gracile* (Strand and Sundberg 2005; Sundberg et al. 2009b). Results of Sundberg et al. (2009b) also show a close relationship between *E. neesii* and *E. buergeri* based on COI data, a relationship also supported by morphological similarities. A more recent multi-locus phylogeny of the phylum (Andrade et al. 2011) shows that *E. gracile* is not closely related to *E. buergeri*, rendering the genus *Emplectonema* polyphyletic. Clearly, the two species originally included and eligible to be fixed as the type species of the genus *Emplectonema* should not belong to the same genus. We follow Correa's designation of *E. gracile* as the type species of the genus. Article 69.2.2 of the Code says "If an author designates as type species a nominal species that was not originally included (or accepts another's such designation) and if, but only if, at the same time he or she places that nominal species in synonymy with one and only one of the originally included species (as defined in Article 67.2), that act constitutes fixation of the latter species as type species of the nominal genus or subgenus" (ICZN 1999). As Corrêa (1955) followed Coe's (1901) taxonomic view that the taxonomic species, *E. gracile* includes the nominal species *Nemertes gracilis* and *E. viride*, but not *Borlasia camillea*, the type species has been validly fixed subsequently by Corrêa (1955) as *Emplectonema viride* (Kajihara personal communication). Therefore, *E. viride* and not *A. neesii* should be the type species of *Emplectonema*. *Amphiporus neesii* is not an *Emplectonema* and is treated here as a species *incertae sedis*.

Acknowledgements

This study was partially funded by São Paulo Research Foundation (FAPESP) grant 2019/10375-8 to CM. TCH was partly supported by the NSF grant OCE-1030453 to Dr Craig Young and SM while carrying out work related to this manuscript. The authors are also thankful to Dr Hiroshi Kajihara, Dr Irina Cherneva, and Dr Jon Norenburg for the helpful comments during the revision of this manuscript.

References

Andrade SC, Strand M, Schwartz M, Chen H, Kajihara H, von Döhren J, Sung S, Junoy J, Thiel M, Norenburg JL, Turbeville JM, Giribet G, Sundberg P (2011) Disentangling ribbon worm relationships: multi-locus analysis supports traditional classification of the phylum Nemertea. Cladistics 28(2): 141–159. https://doi.org/10.1111/j.1096-0031.2011.00376.x

Brinkmann A (1917) Die pelagischen Nemertinen (monographisch dargestellt). A.W. Brøoggers, Kristiania, 194 pp. https://doi.org/10.5962/bhl.title.16138

Bürger O (1895) Die Nemertinen des Golfes von Neapel und der angrenzenden Meeres-Abschnitte. Verlag von R. Friedländer & Sohn, Berlin, 743 pp. https://doi.org/10.5962/bhl.title.14030

Bürger O (1904) Nemertini. Das Tierreich 20: 1–151. https://doi.org/10.1039/pl9042000151

Chen H, Strand M, Norenburg JL, Sun S, Kajihara H, Chernyshev AV, Maslakova SA, Sundberg P (2010) Statistical parsimony networks and species assemblages in cephalotrichid nemerteans (Nemertea). PLoS ONE 5(9): e12885. https://doi.org/10.1371/journal.pone.0012885

Cherneva IA, Chernyshev AV, Ekimova IA, Polyakova NE, Schepetov DM, Turanov SV, Malakhov VV, Neretina T, Chaban EM, Malakhov VV (2019) Species identity and genetic structure of nemerteans of the "*Lineus ruber–viridis*" complex (Muller, 1774) from Arctic waters. Polar Biology 42(3): 497–506. https://doi.org/10.1007/s00300-018-2438-7

Chernyshev AV (2003) Classification system of the higher taxa of enoplan nemerteans (Nemertea, Enopla). Russian Journal of Marine Biology 29(1): S57–S65. https://doi.org/10.1023/B:RUMB.0000011717.06390.30

Clement M, Posada D, Crandall KA (2001) TCS: a computer program to estimate gene genealogies. Molecular Ecology 9(10): 1657–1659. https://doi.org/10.1046/j.1365-294x.2000.01020.x

Coe WR (1901) Papers from the Harriman Alaska Expedition. XX. The nemerteans. Proceedings of the Washington Academy of Sciences 3: 1–110. https://www.jstor.org/stable/24525818

Coe WR (1904) The nemerteans. Harriman Alaska Expedition XI. Doubleday, Page & Company, New York, 220 pp.

Coe WR (1905) Nemerteans of the West and Northwest Coasts of America. Vol. 47. Bulletin of the Museum of Comparative Zoology at Harvard College, Boston, 319 pp.

Coe WR (1940) Revision of the nemertean fauna of the Pacific coasts of North, Central and northern South America. Allan Hancock Pacific Expeditions 2: 247–323.

Corrêa DD (1955) Os géneros *Emplectonema* Stimpson e *Nemertopsis* Bürger (Hoplonemertini Monostilifera). Boletim da Faculdade de Filosofia, Ciências e Letras, Universidade de São Paulo 20: 67–78. https://doi.org/10.11606/issn.2526-3382.bffclzoologia.1955.120212

Corrêa DD (1964) Nemerteans from California and Oregon. Proceedings of the California Academy of Sciences 31: 515–558.

Darwin C (1854) A monography on the sub-class Cirripedia, with figures of all the species. The Ray Society, London, 684 pp.

Fišer C, Robinson CT, Malard F (2018) Cryptic species as a window into the paradigm shift of the species concept. Molecular Ecology 27(3): 613–635. https://doi.org/10.1111/mec.14486

Folmer O, Hoeh WR, Black MB, Vrijenhoek RC (1994) Conserved primers for PCR amplification of mitochondrial DNA from different invertebrate phyla. Molecular Marine Biology and Biotechnology 3(5): 294–299.

Gibson R (1995) Nemertean genera and species of the world: an annotated checklist of original names and description citations, synonyms, current taxonomic status, habitats and recorded zoogeographic distribution. Journal of Natural History 29(2): 271–561. https://doi.org/10.1080/00222939500770161

Griffin BB (1898) Description of some marine nemerteans of Puget Sound and Alaska. Annals of the New York Academy of Sciences 11(1): 193–218. https://doi.org/10.1111/j.1749-6632.1898.tb54969.x

Hao Y, Kajihara H, Chernyshev AV, Okazaki RK, Sun SC (2015) DNA taxonomy of *Paranemertes* (Nemertea: Hoplonemertea) with spirally fluted stylets. Zoological Science 32(6): 571–578. https://doi.org/10.2108/zs140275

Hiebert TC, Maslakova S (2015) Integrative taxonomy of the *Micrura alaskensis* Coe, 1901 species complex (Nemertea: Heteronemertea), with descriptions of a new genus *Maculaura* gen. nov. and four new species from the NE Pacific. Zoological Science 32(6): 615–637. https://doi.org/10.2108/zs150011

Hubrecht AAW (1879) The genera of European nemerteans critically revised, with description of several new species. Notes from the Leyden Museum 1(4): 193–232. https://repository.naturalis.nl/pub/508444

ICZN (1999) International Code of Zoological Nomenclature. Fourth Edition. The International Trust for Zoological Nomenclature, The Natural History Museum, London, 306 pp.

Johnston G (1837) Miscellanea zoologica. II. A description of some planarian worms. Magazine of Zoology and Botany 1: 529–538.

Jörger KM, Norenburg JL, Wilson NG, Schrödl M (2012) Barcoding against a paradox? Combined molecular species delineations reveal multiple cryptic lineages in elusive meiofaunal sea slugs. BMC Evolutionary Biology 12(1): e245. https://doi.org/10.1186/1471-2148-12-245

Kajihara H, Tamura K, Tomioka S (2018) Histology-free descriptions for seven species of interstitial ribbon worms in the genus *Ototyphlonemertes* (Nemertea: Monostilifera) from Vietnam. Species Diversity 23(1): 13–37. https://doi.org/10.12782/specdiv.23.13

Katoh K, Rozewicki J, Yamada KD (2019) MAFFT online service: multiple sequence alignment, interactive sequence choice and visualization. Briefings in Bioinformatics 20(4): 1160–1166. https://doi.org/10.1093/bib/bbx108

Kozloff EN (1999) Marine invertebrates of the Pacific Northwest. University of Washington Press, Seattle and London, 539 pp.

Leigh JW, Bryant D (2015) POPART: full-feature software for haplotype network construction. Methods in Ecology and Evolution 6(9): 1110–1116. https://doi.org/10.1111/2041-210X.12410

Linnaeus C (1758) Systema Naturae per regna tria naturae, secundum classes, ordines, genera, species, cum characteribus, differentiis, synonymis, locis. Editio decima, reformata [10th revised edition], tomus 1. Laurentius Salvius, Holmiae, 824 pp. https://doi.org/10.5962/bhl.title.542

Lischer HE, Excoffier L (2012) PGDSpider: an automated data conversion tool for connecting population genetics and genomics programs. Bioinformatics 28(2): 298–299. https://doi.org/10.1093/bioinformatics/btr642

McIntosh WC (1873) A Monograph of the British Annelids. Part, 1. The Ray Society, London, 668 pp. https://doi.org/10.5962/bhl.title.54725

Miller MA, Pfeiffer W, Schwartz T (2012) The CIPRES science gateway: enabling high-impact science for phylogenetics researchers with limited resources. In: Proceedings of the 1st Conference of the Extreme Science and Engineering Discovery Environment: Bridging from the Extreme to the Campus and Beyond, New York (USA), July 2012, 39: 1–8. https://doi.org/10.1145/2335755.2335836

Mills S, Alcántara-Rodríguez JA, Ciros-Pérez J, Gómez A, Hagiwara A, Galindo KH, Welch DBM, Papakostas S, Riss S, Segers H, Serra M, Shiel R, Smolak R, Snell TW, Stelzer C, Tang CQ, Wallace RL, Fontaneto D, Walsh EJ (2017) Fifteen species in one: deciphering the *Brachionus plicatilis* species complex (Rotifera, Monogononta) through DNA taxonomy. Hydrobiologia 796 (1): 39–58. https://doi.org/10.1007/s10750-016-2725-7

Ørsted AS (1844) Entwurf einer systematischen Eintheilung u. speciellen Beschreibung der Plattwürmer auf mikroscopische Mutersuchungen gegründet. Reitzel, Copenhagen, 118 pp.

Palumbi, SR, Martin A, Romano S, McMillan WO, Stice L, Grabowski G (1991) The Simple Fool's Guide to PCR, Version 2.0. University of Hawaii, Honolulu, 45 pp.

Pozzi L, Penna A, Bearder SK, Karlsson J, Perkin A, Disotell TR (2020) Cryptic diversity and species boundaries within the *Paragalago zanzibaricus* species complex. Molecular Phylogenetics and Evolution 150: 106887. https://doi.org/10.1016/j.ympev.2020.106887

Puillandre N, Lambert A, Brouillet S, Achaz G (2012) ABGD, automatic barcode gap discovery for primary species delimitation. Molecular ecology 21(8): 1864–1877. https://doi.org/10.1111/j.1365-294X.2011.05239.x

Quatrefages AD (1846) Étude sur les types inférieurs de l'embranchement des Annelés. Annales des Sciences Naturelles (Série 3, Zoologie) 6: 173–303.

Roe P, Norenburg JL, Maslakova SA (2007) Nemertea. In: The Light and Smith manual: Intertidal invertebrates from Central California to Oregon. Edited by J.T. Carlton. University of California Press. Berkley, Los Angeles, London, 221–233.

Scarpa F, Cossu P, Lai T, Sanna D, Curini-Galletti M, Casu M (2016) Meiofaunal cryptic species challenge species delimitation: the case of the *Monocelis lineata* (Platyhelminthes: Proseriata) species complex. Contributions to Zoology 85(2): 123–145. https://doi.org/10.1163/18759866-08502001

Stamatakis A (2014) RAxML version 8: a tool for phylogenetic analysis and post-analysis of large phylogenies. Bioinformatics 30(9): 1312–1313. https://doi.org/10.1093/bioinformatics/btu033

Stimpson W (1857) Prodromus descriptionis animalium evertebratorum quae in expeditione ad oceanum pacificum septemtrionalem a republica federata missa. Pars II. Turbellarieorum nemertineorum. Proceedings of the Academy of Natural Sciences of Philadelphia 1857: 159–165. https://doi.org/10.5962/bhl.title.51447

Strand M, Sundberg P (2005) Delimiting species in the hoplonemertean genus *Tetrastemma* (phylum Nemertea): morphology is not concordant with phylogeny as evidenced from mtDNA sequences. Biological Journal of the Linnean Society 86(2): 201–212. https://doi.org/10.1111/j.1095-8312.2005.00535.x

Stricker SA, Cloney RA (1982) Stylet formation in nemerteans. The Biological Bulletin 162(3): 387–403. https://doi.org/10.2307/1540991

Sundberg P, Vodoti ET, Zhou H, Strand M (2009a) Polymorphism hides cryptic species in *Oerstedia dorsalis* (Nemertea, Hoplonemertea). Biological Journal of the Linnean Society 98(3): 556–567. https://doi.org/10.1111/j.1095-8312.2009.01310.x

Sundberg P, Chernyshev AV, Kajihara H, Kånneby T, Strand M (2009b) Character-matrix based descriptions of two new nemertean (Nemertea) species. Zoological Journal of the Linnean Society 157(2): 264–294. https://doi.org/10.1111/j.1096-3642.2008.00514.x

Sundberg P, Andrade SCS, Bartolomaeus T, Beckers P, von Döhren, J, Krämer D, Gibson R, Giribet G, Herrera-Bachiller A, Junoy J, Kajihara H, Kvist S, Kanneby T, Sun S, Thiel M, Turbeville JM, Strand M (2016) The future of nemertean taxonomy (phylum Nemertea) – a proposal. Zoologica Scripta 45(6): 579–582. https://doi.org/10.1111/zsc.12182

Templeton AR, Crandall KA, Sing CF (1992) A cladistic analysis of phenotypic associations with haplotypes inferred from restriction endonuclease mapping and DNA sequence data. III. Cladogram estimation. Genetics 132(2): 619–633. https://doi.org/10.1093/genetics/132.2.619

Toews DP, Brelsford A (2012) The biogeography of mitochondrial and nuclear discordance in animals. Molecular Ecology 21(16): 3907–3930. https://doi.org/10.1111/j.1365-294X.2012.05664.x

Turbeville, JM (2011) The first record of *Emplectonema gracile* (Nemertea: Hoplonemertea) on the Atlantic coast of North America. Marine Biodiversity Records 4: E89. https://doi.org/10.1017/S1755267211000947

Zhang J, Kapli P, Pavlidis P, Stamatakis A (2013) A general species delimitation method with applications to phylogenetic placements. Bioinformatics 29(22): 2869–2876. https://doi.org/10.1093/bioinformatics/btt499

Supplementary material 1

Table S1

Authors: Cecili B. Mendes, Paul Delaney, James M. Turbeville, Terra Hiebert, Svetlana Maslakova

Data type: occurrence

Explanation note: Linked data table of specimens and sequences analyzed in this study. Abbreviations. COI: Cytochrome oxidase I gene fragment; 16S rRNA: 16S ribosomal RNA; †: Sequences previously available in GenBank. Specimens morphologically analyzed marked in bold.

Link: https://doi.org/10.3897/zookeys.1031.59361.suppl1

Supplementary material 2

Figure S2

Authors: Cecili B. Mendes, Paul Delaney, James M. Turbeville, Terra Hiebert, Svetlana Maslakova

Data type: phylogenetic

Explanation note: Species delimitation results from PTP for COI (**A**) and 16S rRNA (**B**) gene regions. Values on branches are posterior probabilities of those taxa form one species under the PTP model and a flat prior. Red branches indicate taxa that should be considered as part of the same lineage.

Link: https://doi.org/10.3897/zookeys.1031.59361.suppl2

ZooKeys 1031: 19–39 (2021)
doi: 10.3897/zookeys.1031.62391
https://zookeys.pensoft.net

RESEARCH ARTICLE

A peer-reviewed open-access journal
ZooKeys
Launched to accelerate biodiversity research

Investigation of the Amathillopsidae (Amphipoda, Crustacea), including the description of a new species, reveals a clinging lifestyle in the deep sea worldwide

Anne-Nina Lörz[1], Tammy Horton[2]

1 *Center of Naturkunde, Universität Hamburg, Martin-Luther King Platz 3, 20146 Hamburg, Germany*
2 *National Oceanography Centre, Southampton, European Way, Southampton SO14 3ZH, UK*

Corresponding author: Anne-Nina Lörz (Anne-Nina.Loerz@uni-hamburg.de)

Academic editor: J. Svavarsson | Received 23 December 2020 | Accepted 2 March 2021 | Published 14 April 2021

http://zoobank.org/D39B776A-5C3D-44A8-9009-D6ECE37B0AA2

Citation: Lörz A-N, Horton T (2021) Investigation of the Amathillopsidae (Amphipoda, Crustacea), including the description of a new species, reveals a clinging lifestyle in the deep sea worldwide. ZooKeys 1031: 19–39. https://doi.org/10.3897/zookeys.1031.62391

Abstract

Amathillopsidae is a widely distributed, but rarely sampled family of deep-sea amphipods. During a recent expedition to the North Atlantic, specimens were filmed clinging to a polychaete tube in situ at abyssal depths by a Remote Operated Vehicle and then sampled for further study. The species was new to science and is described in detail herein. A barcode sequence is provided. Further investigations of photographic and video records revealed the genus *Amathillopsis* to be more widely distributed, both geographically and bathymetrically, than indicated by current literature records, and that these species occur at abyssal depths in all oceans. Specimens of *Amathillopsis* are reported clinging to a variety of different organisms whose erect structures provide the means to raise these charismatic deep-sea predators above the seafloor facilitating feeding opportunities.

Keywords

Benthic, Porcupine Abyssal Plain, Remotely Operated Vehicle (ROV), worldwide distribution

Introduction

During the third expedition of the Icelandic Genetics & Evolution (IceAGE) project on the RV 'Sonne' (Cruise SO267) to the North Atlantic from June to July 2020, large numbers of amphipod crustaceans were collected using a variety of methods. Using the

Remotely Operated Vehicle (ROV) KIEL 6000, an interesting amathillopsid amphipod was observed sitting as a pair clinging to an onuphid worm tube at 4600 m depth at the Porcupine Abyssal Plain. The amathillopsid species was successfully sampled and proved to be new to science. A single specimen of the new species, collected at the Porcupine Abyssal Plain Sustained Observatory site at 4844 m, was also found within the Discovery Collections at the National Oceanography Centre, Southampton, UK. This new species, amongst the deepest confirmed record of the genus, is described herein.

Lowry (2006) included the parepimeriids and the genus *Cleonardopsis* K.H. Barnard, 1916 in the family Amathillopsidae and created three subfamilies: Amathillopsinae, Parepimeriinae and Cleonardopsinae. The new species of *Amathillopsis* described herein is classified within the Amathillopsinae.

Three species of *Amathillopsis* and one species of *Cleonardopsis* have been reported from the North Atlantic to date: *Amathillopsis affinis* Miers, 1881; *Amathillopsis spinigera* Heller, 1875; *Amathillopsis atlantica* Chevreux, 1908; and a probable new species of *Cleonardopsis* which was first reported from off the coast of eastern Greenland by Stephensen (1944) as *Cleonardopsis carinata* K.H. Barnard,1916, and may be the same species as the *Cleonardopsis* sp. sequenced by Jażdżewska et al. (2018).

The Amathillopsidae are rarely collected, and very little is known of their biology and ecology. Most studies of the family relate to the description of new species based on material from a single or very few specimens, from a single locality.

In recent years, the increased use of ROVs to capture high-resolution footage of deep-sea ecosystems has provided an opportunity for the study of poorly known and rarely captured organisms (Macreadie et al. 2018). This is certainly the case with the Amathillopsidae. We provide collated records of ROV footage of a number of as yet unidentified species of *Amathillopsis*, from the deep sea, worldwide; thus confirming that despite the paucity of records and specimens, the genus is cosmopolitan and relatively common.

Materials and methods

Collection methods and locations

During the IceAGE 3 expedition on the RV 'Sonne', the ROV KIEL 6000 sampled the Porcupine Abyssal Plain at station 133-4 (49°47.969'N, 015°12.975'E, 4622 m, 20 July 2020), via photo and video transects, as well as physical sampling. The specimens of the new species of *Amathillopsis* were initially photographed and filmed in situ, after which attempts were made to use the ROV suction to collect them. When this failed the specimens were scooped up by the ROV operator arm using a net and then placed into a sampling box.

Once on board, the single specimen collected was immediately photographed and then placed in RNA*later*. The left first pleopod was then dissected and placed in a separate tube to be used for DNA extraction. The whole specimen and the dissected pleopod sample were then both transferred to the -20 °C freezer for later study.

The type localities and holotype materials of all known species of *Amathillopsis* were collated to aid in future studies of the genus (Table 1). Additional photographic records of other *Amathillopsis* specimens were collated from a variety of sources (Table 3), along with associated metadata, allowing the mapping of specimen localities.

Taxonomic methods

The adult male holotype specimen (ZMH K 60236) was photographed in situ by the ROV KIEL 6000, photographed on board by a Nikon D5 camera with an objective Nikon AF-S Mikro-Nikkor 105 mm 1:2.8, and dissected appendages were photographed using a Keyence 7000 microscope. A video of the *Amathillopsis* in situ can be found in the Suppl. material 1.

Initial observations and photographs were made on board of the RV 'Sonne'.

The pencil drawings were conducted using a LeicaM125 and an Olympus BX53. Pencil drawings were scanned and inked digitally using Adobe Illustrator and a WACOM digitiser tablet (Coleman 2003, 2009). Some setae are omitted from the illustrations for clarity. Type material is deposited in the Zoological Museum Hamburg (**ZMH**) and the Natural History Museum, London (**NHMUK**).

Genetic methods

Isolation of DNA was performed on board using the NucleoSpin tissue extraction kit from MACHEREY-NAGEL GmbH & Co. KG according to the manufacturer's protocol. A fragment of the COI gene (ca. 670 bp fragment) was amplified using primers LCO1490-JJ CHACWAAYCATAAAGATATYGG Forward (Astrin and Stüben 2008) and HCO2198-JJ AWACTTCVGGRTGVCCAAARAATCA Reverse (Astrin and Stüben 2008).

The PCR reaction mixes were prepared to a final volume of 25 μl containing 12.5 μl AccuStart II PCR ToughMix (Quanta Bio), 0.5 μl of each primer (10 pmol/μl), 9.5 μl dH2O and 2 μl template DNA. PCR settings for amplifying CO1 sequences consisted of initial denaturing of 4 min at 95 °C, 5 cycles of 45 s at 95 °C, 90 s at 45 °C, 60 s at 72 °C, following 35 cycles of 45 s at 95 °C, 60 s at 51 °C, 60 s at 72 °C, and final extension 3 min at 72 °C. PCR products were purified using the Exonuclease-I/Shrimp Alkaline Phosphatase (Thermo Fisher) method and were sequenced at Macrogen Inc. Europe. Sequences were edited using Geneious 9.1.8 resulting in a sequence of length of 626 bp excluding primers. Relevant voucher information, taxonomic classifications and sequences are deposited in BOLD.

Setal and mouthpart classifications follow Watling (1989) and Lowry and Stoddart (1992, 1993, 1995).

The following abbreviations have been used:

A	antenna;	**H**	Head;	**Mxp**	maxilliped;	**UL**	upper lip.
E	epimeron;	**LL**	lower lip;	**P**	pereopod;		
Ep	epistome;	**Md**	mandible;	**T**	telson;		
G	gnathopod;	**Mx**	maxilla;	**U**	uropod;		

Systematics

Order Amphipoda Latreille, 1816
Suborder Amphilochidea Boeck, 1871
Infraorder Amphilochida Boeck, 1871
Parvorder Amphilochidira Boeck, 1871
Superfamily Iphimedioidea Boeck, 1871
Family Amathillopsidae Pirlot, 1934
Subfamily Amathillopsinae Pirlot, 1934

Amathillopsis Heller, 1875

Amathillopsis Heller, 1875: 35. – Stebbing 1906: 384. – Gurjanova 1955: 209 (key). – J.L. Barnard 1969: 394. – J.L. Barnard and Karaman 1991: 390.

Acanthopleustes Holmes, 1908: 533 (*Acanthopleustes annectens* Holmes, 1908 by original designation).

Type species. *Amathillopsis spinigera* Heller, 1875 (by original designation).

Diagnosis (after Lowry 2006). ***Head.*** Deeper than long; lateral cephalic lobe subquadrate, truncated apically; anteroventral margin straight, anteroventral margin moderately recessed, anteroventral margin moderately excavate; rostrum short or moderate length; eyes present (round or ovoid) or absent. Body smooth, or dorsally carinate. Antenna 1 subequal in length or longer than antenna 2; peduncle with sparse slender setae; peduncular article 1 shorter than or subequal to article 2; article 2 longer than article 3; article 3 shorter than article 1; accessory flagellum short or minute, 1- or 2-articulate; calceoli present. Antenna 2 medium length; peduncle with sparse slender setae or none; flagellum shorter than or as long as peduncle.

Pereon. Coxae 1–4 longer than broad, overlapping, coxae 1–3 or coxae 1–4 ventrally acute. Coxae 1–3 similar in size or progressively larger. Gnathopod 1 subchelate; carpus shorter than or subequal to propodus; propodus with or without peg-like robust setae along palmar margin. Gnathopod 2 subchelate; coxa smaller than but not hidden by coxa 3 or subequal to but not hidden by coxa 3; carpus short, shorter than propodus. Pereopods: some or none prehensile. Pereopod 4 coxa ventrally acute, with or without small posteroventral lobe. Pereopod 5 coxa equilobate, with posteroventral lobe or with acute posterodistal lobe; basis slightly expanded or linear. Pereopod 6 subequal in length to, or longer than pereopod 7; basis slightly expanded or linear. Pereopod 7 shorter than or subequal in length to pereopod 5; basis slightly expanded or linear.

Pleon. Urosomite 1 carinate, urosomites 1–2 carinate or urosomites not carinate. Uropods 1–2 apices of rami without robust setae. Telson notched, emarginate or entire; dorsal or lateral robust setae absent; apical robust setae absent.

Remarks. *Amathillopsis* is the type genus of the family Amathillopsidae and the genus has a cosmopolitan distribution (Wakabara and Serejo 1999). It currently contains 12 species, five of which are known from the Pacific, *A. annectens* (Holmes, 1908), *A. australis* Stebbing, 1883, *A. grevei* J.L. Barnard, 1961, *A. takahashiae*

Table 1. Type localities of all described species (and subspecies) of *Amathillopsis* and *Cleonardopsis*. The type locality of *Amathillopleustes alticoxa* is included as this likely represents a different species from *Cleonardopsis carinata*, with which it is currently synonymised. All localities are taken from original descriptions. Coordinates of localities for *A. annectens*, *A. pacifica*, and *C. carinata* are inferred from the verbatim type locality.

Species	Verbatim latitude and verbatim longitude	Decimal latitude and longitude	Depth (m)	Geographic locality
Amathillopsis affinis	79°55'N, 51°E	80.5667, 54.7833	unknown	Arctic Ocean
Amathillopsis annectens	SE point Santa Catalina Island, 3.2 miles	33.2735, -118.2705	611–1097	North Pacific, California
Amathillopsis atlantica	39°11'N, 30°24'W	39.1833, -30.4000	1600–1919	North Atlantic, Azores
Amathillopsis australis	12°8'S, 145°10'E	-12.3333, 145.1667	2560	Coral Sea, Celebes Sea, Arafura Sea
Amathillopsis charlottae	66°33.10'S, 68°41.90'W	-66.5528, -68.7083	607	Antarctic Peninsula
Amathillopsis comorensis	12°14.4'S, 46°41.6'E	-11.6520, 43.3726	2500	Indian Ocean, Comoros
Amathillopsis grevei	-44.3, 166.7667	-44.3, 166.7667	3580	Tasman Sea
Amathillopsis pacifica margo	23°59.5'N, 113°11.9'W	23.9847, -113.1858	3479–3515	North Pacific, Baja California
Amathillopsis pacifica	Southern Basin Okhotsk Sea	52.8736, 149.3658	2850	Okhotsk Sea, North Pacific
Amathillopsis roroi	-60.61833, -54.93167	-60.3710, -54.9317	3213	Antarctic Peninsula
Amathillopsis septemdentata	13°46'S, 47°33'E	-13.7667, 47.5500	1490–1600	Indian Ocean, Nosy-Be, Madagascar
Amathillopsis spinigera	79°15'N, 60°E	77.8750, 20.9752	240	Arctic Ocean
Amathillopsis takahashiae	31.43889, 131.67333	31.4389, 131.6733	528	North Pacific, Japan
Amathillopsis inkenae sp. nov.	50.0525, -15.470833	50.0525, -15.4708	4622	North Atlantic, Porcupine Abyssal Plain
Cleonardopsis carinata	36 miles NNE Cape Point	-34.3567, 18.4968	1189	South Africa, South Atlantic
Amathillopleustes alticoxa	2°40'S, 128°37'.5E	-2.9358, 128.6181	835	Ceram Sea, Indonesia

Tomikawa & Mawatari, 2006 and *A. pacifica* Gurjanova, 1955 (and the sub species *A. pacifica margo* J.L. Barnard, 1967),; two from the Antarctic, *A. roroi* Coleman & Coleman, 2008 and *A. charlottae* Coleman, 1998; two from the Indian Ocean, *A. septemdentata* Ledoyer, 1978 and *A. comorensis* Ledoyer, 1986; and three from the North Atlantic and Arctic, *A. affinis* Miers, 1881, *A. spinigera* Heller, 1875 and *A. atlantica* Chevreux, 1908. *Amathillopsis* is a deep-sea specialist, with the shallowest records of the large species, *A. spinigera*, coming from colder Arctic waters at 248 m. All other species are found at depths of 500 to 3580 m. The new species, *A. inkenae*, described here, provides the deepest confirmed records of an *Amathillopsis* to date, at 4622 m and 4844 m. Table 1 summarises the known species in the genus along with the type locality and depth.

Species. *Amathillopsis affinis* Miers, 1881, *A. annectens* (Holmes, 1908), *A. atlantica* Chevreux, 1908, *A. australis* Stebbing, 1883, *A. charlottae* Coleman, 1998, *A. comorensis* Ledoyer, 1986, *A. grevei* J.L. Barnard, 1961, *A. pacifica* Gurjanova, 1955, *A. pacifica margo* J.L. Barnard, 1967, *A. roroi* Coleman & Coleman, 2008, *A. septemdentata* Ledoyer, 1978, *A. spinigera* Heller, 1875, *A. takahashiae* Tomikawa & Mawatari, 2006.

Amathillopsis inkenae sp. nov.

http://zoobank.org/19555683-216D-434B-866C-A5B710BDA2A6

Figures 1–5

Type material. ***Holotype*:** North East Atlantic • Male, 9.4 mm; Porcupine Abyssal Plain; 49°47.969'N, 015°12.975'E, 4622 m; 20 July 2020; RV 'Sonne' cruise 267, station 133–4, gear ROV KIEL 6000; ZMH K-60236. ***Paratype*:** North East

Atlantic • Male, 14 mm; Porcupine Abyssal Plain; 48°58.201'N, 016°53.297'W to 48°55.316'N, 016°49.452'W, 4834–4844 m; 06 June 2018; RRS 'James Cook' Cruise 165, station JC165#064, Otter Trawl Semi-Balloon 14; NHMUK 2021.66.

Type locality. Porcupine Abyssal Plain, 4622 m, 49°47.969'N, 015°12.975'E, RV 'Sonne' cruise 267, station 133–4, gear ROV KIEL 6000.

Diagnosis. Pereonites 3 and 4 with small, rounded mid-dorsal projections. Pereonites 5–7 mid-dorsal projections, small, rounded, increasing in size. Pleonites 1 and 2 mid-dorsal projections small, rounded, reduced to dorsal hump on pleonite 3. Urosomite 1 mid-dorsal projection absent, urosomites 2 and 3 carinate, urosomite 3 with a small mid-dorsal process. Gnathopod 2 posterodistal basis lobe developed. Strong, acute tooth on posterodistal corner of epimeron 3. Telson cleft.

Description. Male holotype 9.4 mm: Head slightly shorter than pereonites 1 and 2 combined, rostrum very short, pointed, lateral cephalic lobe quadrate, eyes present, pigmented, strongly white in fresh specimen. Pereonites 1 and 2 indistinctly keeled dorsally; pereonite 3–5 with short mid-dorsal processes; pereonites 6 and 7 each with short, weakly posteriorly curved mid-dorsal process. Pleonites 1 and 2 each with short weakly posteriorly curved mid-dorsal process; pleonite 3 with low, mid-dorsal rounded process. Epimeral plates 1 and 2 with ventral margin rounded, posteroventral corner rounded; epimeral plate 3 with ventral margin curved and posteroventral corner produced into an acute tooth. Urosomite 1 lacking dorsal armature, urosomites 2–3 dorsally carinate, each with short weakly posteriorly curved mid-dorsal process, urosomite 3 with a small mid-dorsal process. Antenna 1 long, as long as body length, with peduncular articles 1, 2, and 3 in length ratio of 1.0: 1.1: 0.4. Article 1 longer than head length; accessory flagellum uni-articulate, not spine-like; primary flagellum consisting of 64 articles, article 1 long, as long as articles 2–7 combined. Antenna 2 0.8 × as long as antenna 1; peduncular article 3 reaching to mid length of peduncular article 1 of antenna 1; peduncular article 4 long, 1.7 × as long as peduncular article 5, flagellum approximately the same length, as long as peduncle, 54-articulate.

Mouthparts. Upper lip with weakly convex apical margin, bearing two groups of setae. Lower lip with outer lobes broad, setulose; inner lobes indistinct, fused. Mandibles with left incisors bearing eight teeth, left *lacinia mobilis* with four teeth; accessory setal row with nine setae, some bearing a row of minute protuberances. Molar developed, triturative. Palp articles 1, 2, and 3 in length ratio of 1.0: 5.0: 7.1, article 1 lacking setae, article 2 with marginal and submarginal setae, and article 3 with six marginal and three terminal setae. Maxilla 1 with inner plate ovate and bearing four plumose setae; outer plate rectangular, with 11 serrate, robust setae; palp two-articulate, longer than outer plate, terminally with seven long robust setae. Maxilla 2 inner plate slightly broader than outer plate, bearing row of long plumose setae. Maxilliped, inner plate reaching base of palp, with three robust nodular setae on the distomedial margin, distolateral margin with apical robust setae; outer plate exceeding distal margin of palp article 1. Maxillipedal palp long, raptorial, four-articulate; article 2 and 3 heavily setose and widened medially; dactylus as long as article 3.

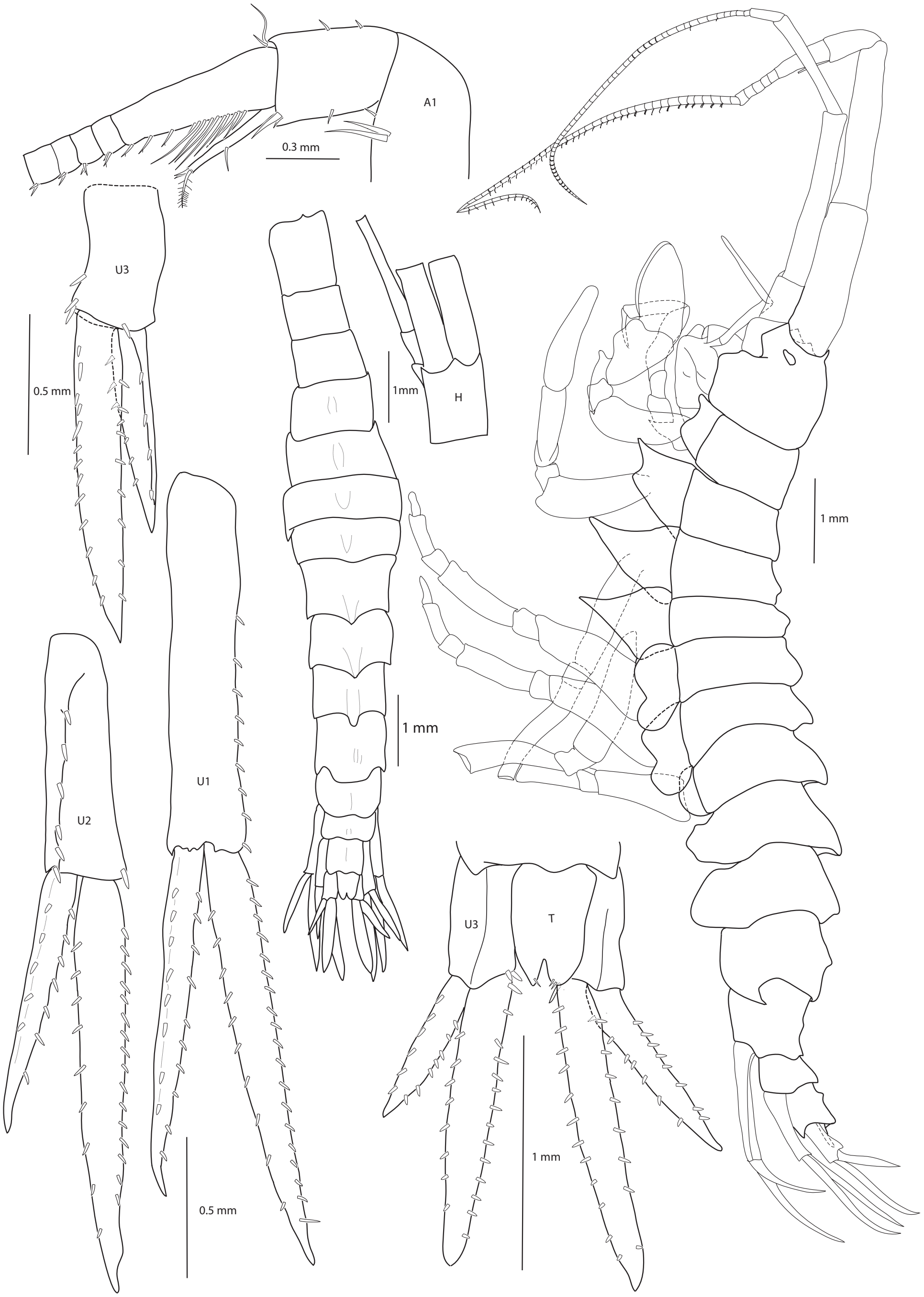

Figure 1. *Amathillopsis inkenae* sp. nov. Holotype: ZMH K-60236, male, 9.4 mm. Habitus lateral and dorsal views, head, antenna 1, uropods 1–3, and telson.

Figure 2. *Amathillopsis inkenae* sp. nov., Holotype: ZMH K-60236, male, 9.4 mm. Upper lip, Lower lip, Maxilliped (left palp external rotation is an artefact of the mounting), maxillae 1, 2, and mandible.

Pereon. Coxae 1 and 2 with acute processes projecting anteroventrally. Coxa 3 subtriangular, Coxa 4 rhomboid, both with acute processes projecting anteroventrally. Coxae 5 and 6 wider than long, bilobate. Coxa 7 small, rounded. Gnathopod 1

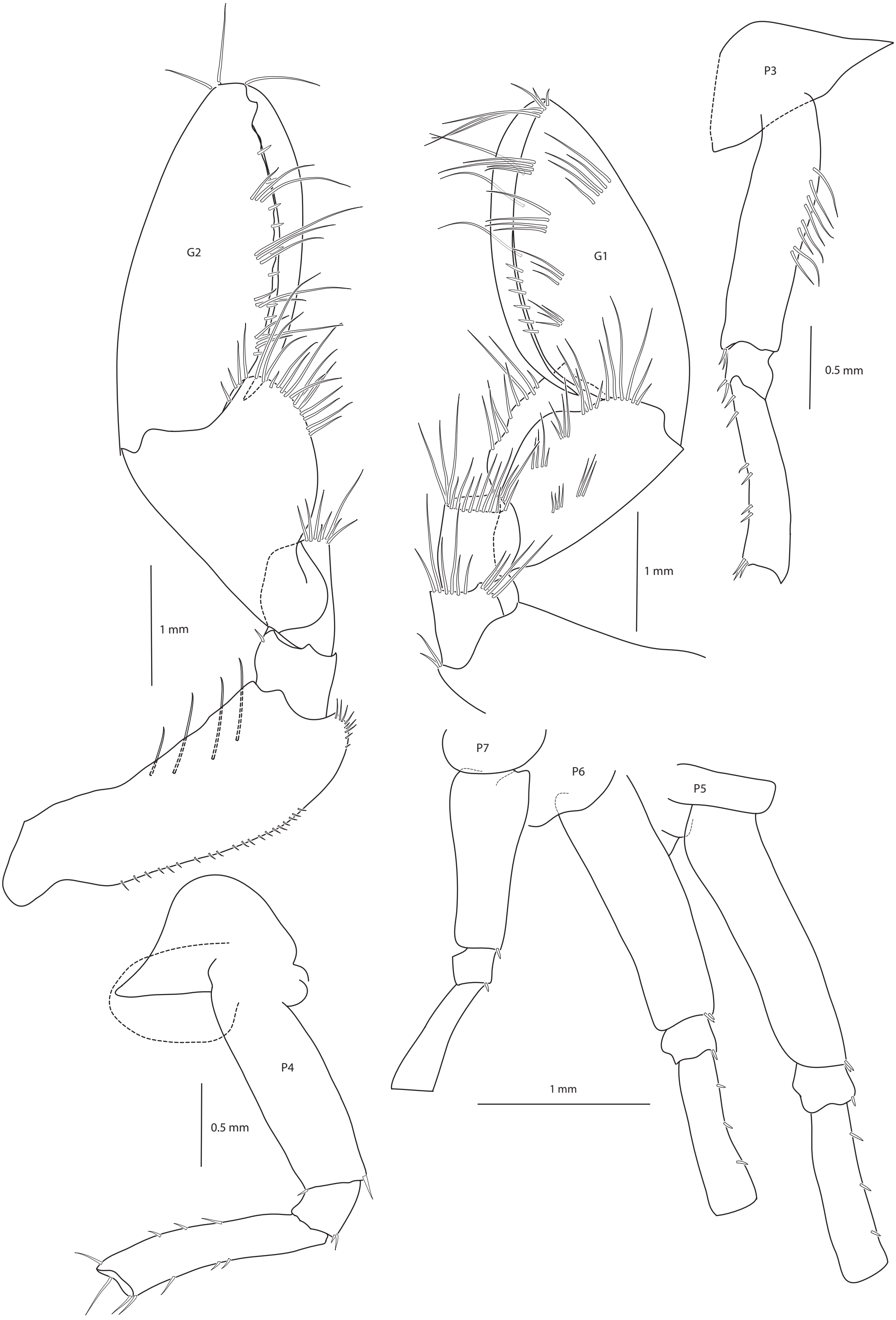

Figure 3. *Amathillopsis inkenae* sp. nov., Holotype: ZMH K-60236, male, 9.4 mm. Gnathopods 1, 2, and pereopods 3–7.

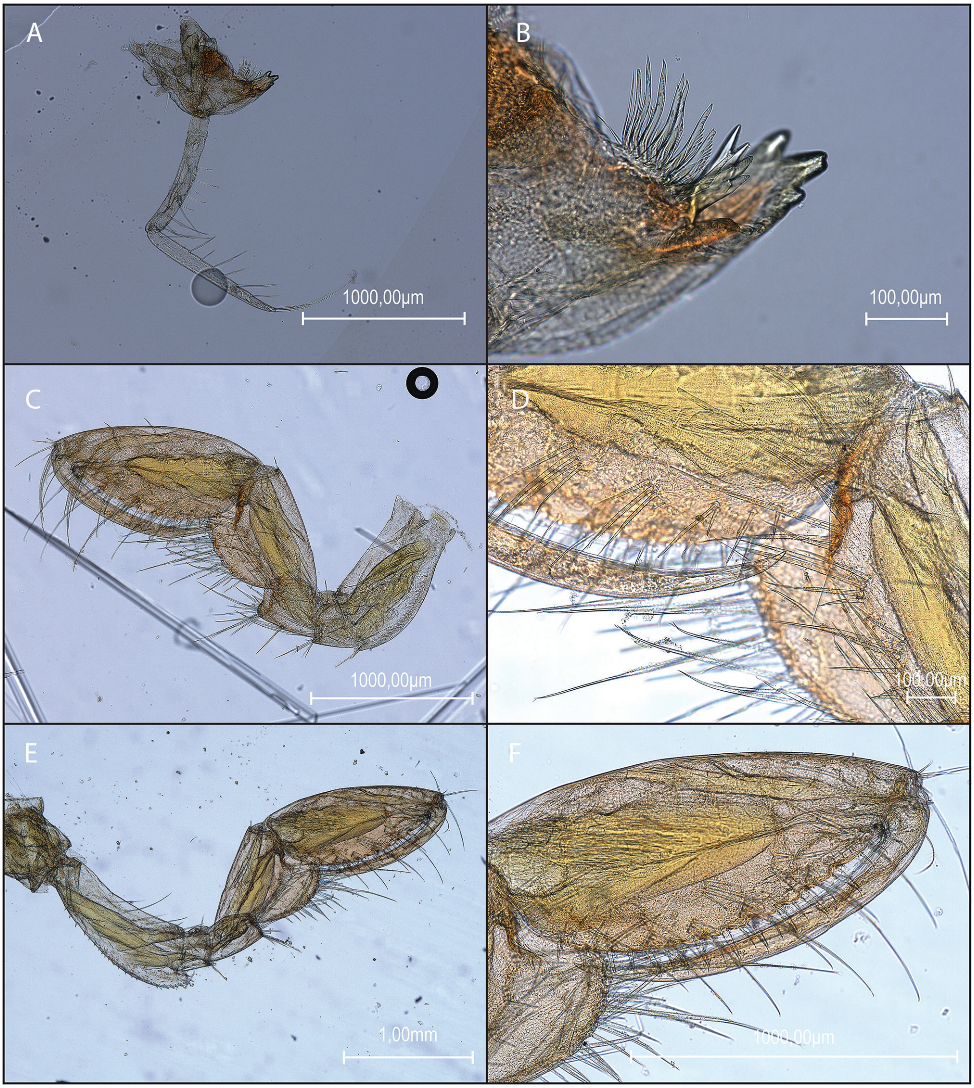

Figure 4. *Amathillopsis inkenae* sp. nov., Holotype: ZMH K-60236, male, 9.4 mm **A** mandible **B** mandible incisor detail **C** gnathopod 1 **D** gnathopod 1 detail **E** gnathopod 2 **F** gnathopod 2 palm detail.

subchelate, basis posterior margin with row of robust setae, posterodistal lobe absent; ischium and merus short; carpus 0.68 × as long as propodus, ventral lobe broad, concave, allowing propodus to retract; propodus stout, tapering distally, with four groups of robust setae, palmar margin with long and short robust setae; dactylus as long as palmar margin, sickle-like. Gnathopod 2 subchelate, basis with posterodistal lobe present, posterior margin with row of robust setae; carpus 0.67 × as long as propodus, ventral lobe broad, concave, allowing propodus to retract; propodus stout, tapering distally, with four groups of robust setae, palmar margin with long and short robust setae; dactylus as long as palmar margin, sickle-like. Pereopod 3 basis with row of robust setae along weakly convex posterior margin, ischium short, as long as wide; merus margins subparallel with slight anterior curvature. Pereopod 4 similar to pereopod 3. Pereopods 5–7 anterior and posterior margins of basis sub-parallel, linear, posterior lobe lacking; ischium short, as long as wide; merus margins subparallel with slight anterior curvature. Carpus, propodus and dactylus missing from pereopods 3–7.

Uropods. Uropod 1 long, peduncle length 0.88 × inner ramus; medial margin of peduncle with robust setae, inner ramus, lateral and medial margins with robust setae, outer ramus 0.88 × as long as inner, lateral and medial margins with robust setae. Uropod 2 with peduncle length 0.57 × inner ramus, lateral margin with robust setae, dorsomedial margin with one robust seta distally; inner ramus, lateral and medial margins with robust setae; outer ramus 0.64 × inner, lateral and medial margins with robust setae. Uropod 3 peduncle length 0.74 × inner ramus; dorsomedial margin of peduncle with three robust setae distally; inner ramus with lateral and medial margins bearing robust setae, outer ramus 0.64 × as long as inner, lateral, and medial margins with robust setae. Telson length 1.44 × width, cleft 22%. Each lobe bearing terminal setae.

Paratype male, 14 mm: As for holotype except the dorsal processes are more pronounced and acute on pereonites 5–7 and pleonites 1 and 2 (Fig. 5c).

Etymology. The name is dedicated to Dr. Inken Suck, the pilot who flew the ROV and sampled the specimen, to honour her dedication to deep-sea biology.

Remarks. In live condition, *Amathillopsis inkenae* sp. nov. has a white coloured body and antennae, the last three segments of both gnathopods as well as the mouthparts are red. Eyes are clearly visible, solid white, in live and fresh condition, but fade after a few days of fixation. Care should be taken in use of the relative sizes of the dorsal processes as these are likely to vary ontogenetically, as for the two specimens available here, where the larger male paratype has more pronounced, acute processes than the smaller male holotype. This is also likely to occur in other species in the genus. The specimens reported by Wakabara and Serejo (1999) as *A. atlantica* are likely to belong to a new species, and the authors point out that the mid-dorsal processes and the telson show some variation. Other characters, such as the reduced lobes on the basis of the gnathopods, also indicate that this is probably a new taxon.

Amathillopsis inkenae sp. nov. differs from known species of *Amathillopsis* by the characters listed in Table 2. *Amathillopsis inkenae* sp. nov. is most similar to *Amathillopsis comorensis* Ledoyer, 1986, which was collected in the Indian Ocean near the Comoros Islands at 2500 m. The new species has a similarly cleft telson, and a similar development of the dorsal processes and of the lobe on the basis of gnathopod 2 only. *Amathillopsis inkenae* differs from *A. comorensis* in having carination on urosomites 2 and 3, with posteriorly directed dorsal processes (lacking in *A. comorensis*), the stronger acute tooth on epimeron 3 posterodistal corner (smaller on *A. comorensis*), the curved article 2 of the mandible palp (straight in *A. comorensis*), and the medially widened articles 2 and 3 of the maxilliped palp (subparallel sided in *A. comorensis*).

Table 2. Morphological tabulation of characters for separating known species of *Amathillopsis*.

Character	*A. inkenae* sp. nov.	*A. affinis*	*A. annectens*	*A. atlantica*	*A. australis*	*A. charlottae*	*A. comorensis*	*A. grevei*	*A. pacifica*	*A.p. margo*	*A. roroi*	*A. septemdentata*	*A. spinigera*	*A. takahashiae*
Pereonites 1–4 mid-dorsal projections	small, rounded on 3 & 4	strong, acute on 1–4	small, rounded on 2–4	absent	keeled on 1–4	keeled on 2–4	small, rounded on 2–4	absent	small, rounded on 2–4	small, rounded on 2–4	absent	absent	strong, acute on 1–4	absent
Pereonites 5–7 mid-dorsal projections	small, rounded, increasing in size on 5–7	strong, acute on 5–7	medium, acute, increasing in size on 5–7	strong, acute, increasing in size on 5–7	strong, acute, increasing in size on 5–7	strong, acute, increasing in size on 5–7	strong, acute, increasing in size on 5–7	medium, acute, increasing in size on 5–7	strong, acute, increasing in size on 5–7	strong, acute, increasing in size on 5–7	absent but trace of keel on 6–7	strong, acute, increasing in size on 5–7	strong, acute on 5–7	rounded hump on 5, acute on 6–7
Pleonites 1–3 mid-dorsal projections	1–2 small, rounded, 3 reduced to dorsal hump	strong, acute on 1–2, 3 small	medium, acute, 1–3, smaller on 3	strong, acute on 1–3	strong, acute on 1–3	strong, acute on 1–2, slightly smaller on 3	medium acute on 1–2 , 3 with tiny upright process	medium, acute, 1–3, decreasing	strong, acute on 1–2, smaller on 3	strong, acute on 1–2, smaller on 3	1–2 short, acute, 3 small upright process	strong, acute on 1–3	strong, acute on 1–3	strong, acute on 1–2, smaller on 3
Urosomite 1 mid-dorsal projection	absent	unknown	absent	absent	absent	absent	absent	absent	absent	absent	absent	present	present	absent
Gnathopod posterodistal basis lobe	developed on G2 only	unknown	absent	well-developed on G1 and G2	developed on G2 only	developed on G1 and G2	developed on G2 only	slightly developed on G2 only	well-developed	well-developed	small	small	small	small
Mandible palp article 3: article 2 length	1.4	unknown	1.2	unknown	1.5	1.1	1.4	unknown	1.4	1.4	1	1.5	0.9	0.9
Telson	cleft	emarginate	entire	emarginate	emarginate	entire	cleft	emarginate	emarginate	emarginate	emarginate	entire	emarginate	emarginate (with dorsal keel)
Antenna 1 Accessory Flagellum	uniarticulate, ordinary	uniarticulate, ordinary	uniarticulate, ordinary	uniarticulate, spine-like, straight	uniarticulate, spine-like, curved	uniarticulate, ordinary	uniarticulate, spine-like	uniarticulate, ordinary	uniarticulate, spine-like, straight	uniarticulate, spine-like, straight	uniarticulate, ordinary	uniarticulate, spine-like, straight	bi-articulate, ordinary	uniarticulate

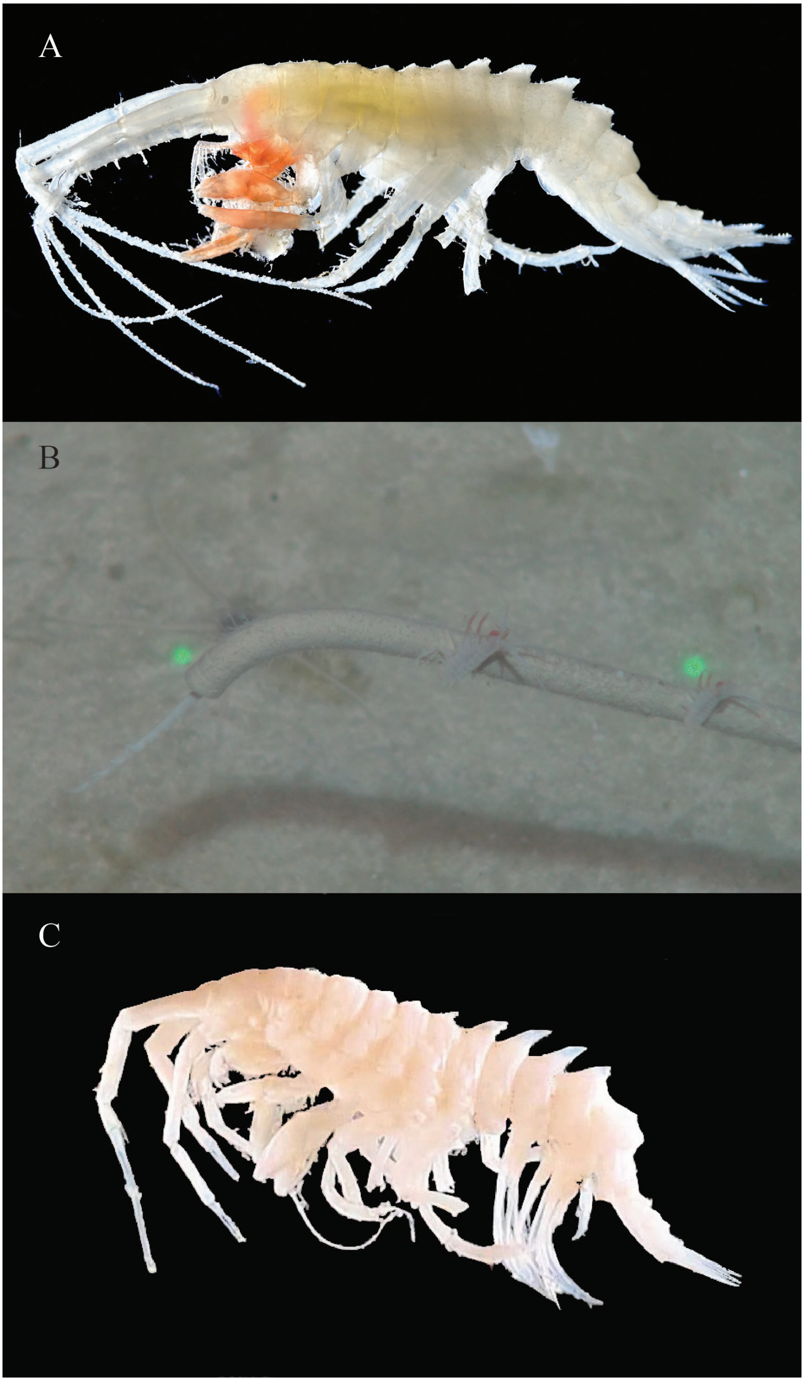

Figure 5. *Amathillopsis inkenae* sp. nov., Holotype: ZMH K-60236, male, 9.4 mm **A** habitus, fresh specimen photograph (S. Zankl) **B** in situ image clinging to a polychaete tube via ROV KIEL 6000. In situ video can be found in Suppl. material 1 **C** *Amathillopsis inkenae* sp. nov., paratype NHMUK 2021.66, male, 14 mm. Habitus, preserved specimen (photograph T. Horton).

The barcode of *Amathillopsis inkenae* sp. nov. is deposited in BOLD:AEF9286 and GenBank MW726208.

Depth range. 4622–4844 m.

Distribution. Only known from the North East Atlantic Ocean, Porcupine Abyssal Plain, between 4622–4844 m.

Discussion

We have described a new species of *Amathillopsis* collected from abyssal depths and differentiated this new species from the known species found globally. Only *A. grevei*, *A. roroi*, and *A. pacifica* have been collected at abyssal depths; all other *Amathillopsis* species were collected shallower than 2000 m. However, photographs and video captured by ROVs are now able to show that the genus is relatively common at bathyal and abyssal depths. *Amathillopsis* species have now been observed by ROVs and other camera systems on a number of occasions, clinging in pairs (and occasionally in larger numbers), to a tubular or stalk-like structure erected from soft substrate, and also on corals attached to hard substrates. We have collated these records and present them alongside the type localities of known *Amathillopsis* species (Table 3, Fig. 7).

All photographic records of *Amathillopsis* collated here are from the Pacific (Fig. 7, purple diamonds), while *Amathillopsis* species are distributed globally (Fig. 7, orange stars). The NOAA Office of Ocean Exploration and Research Benthic Deepwater Animal Identification Guide includes a number of images of amphipods of the genus *Amathillopsis* from the central Pacific at the Northern Mariana Islands (Fig. 6c) and the Pacific Remote Islands Marine National Monument, northeast of Kingman Reef (Fig. 6f). There a number of images of pairs of *Amathillopsis* from abyssal depths in the Eastern Clarion Clipperton Zone (Fig. 6a) from Kiribati waters, and from bathyal depths of the northwest Pacific at the Emperor Seamounts (Fig. 6b) which were collected during AUV and ROV surveys of these areas.

The ROV KIEL 6000 captured images of pairs of *Amathillopsis* clinging to sponges below 4000 m during the DISCOL expedition on RV 'Sonne' to the southeast Pacific in 2015 (Fig. 6d) and to the abyssal plains North of New Zealand (southwest Pacific) in 2017 (Fig. 6e). We have also included in Table 3 and Fig. 7 a recently published record of a specimen of *Amathillopsis*. The specimen shown in Brandt et al. (2018: fig. 6a) is probably a specimen of *A. pacifica*, since it conforms to the illustrations of that species by Gurjanova (1955), and it was collected from a similar geographic locality and depth. We have not made any further attempts to identify the specimens in these images to species, since it is likely that there are new species involved and therefore specimens will be needed for more detailed analyses. It is remarkable that the type localities and the photo localities (see Fig. 7) are so different. While dragged (towed) gear has coincidently sampled occasional specimens of *Amathillopsis*, the advent of technology has resulted in numerous additional records of these animals in situ, work which has been largely focussed in the Pacific Ocean. *Amathillopsis inkenae* sp. nov.

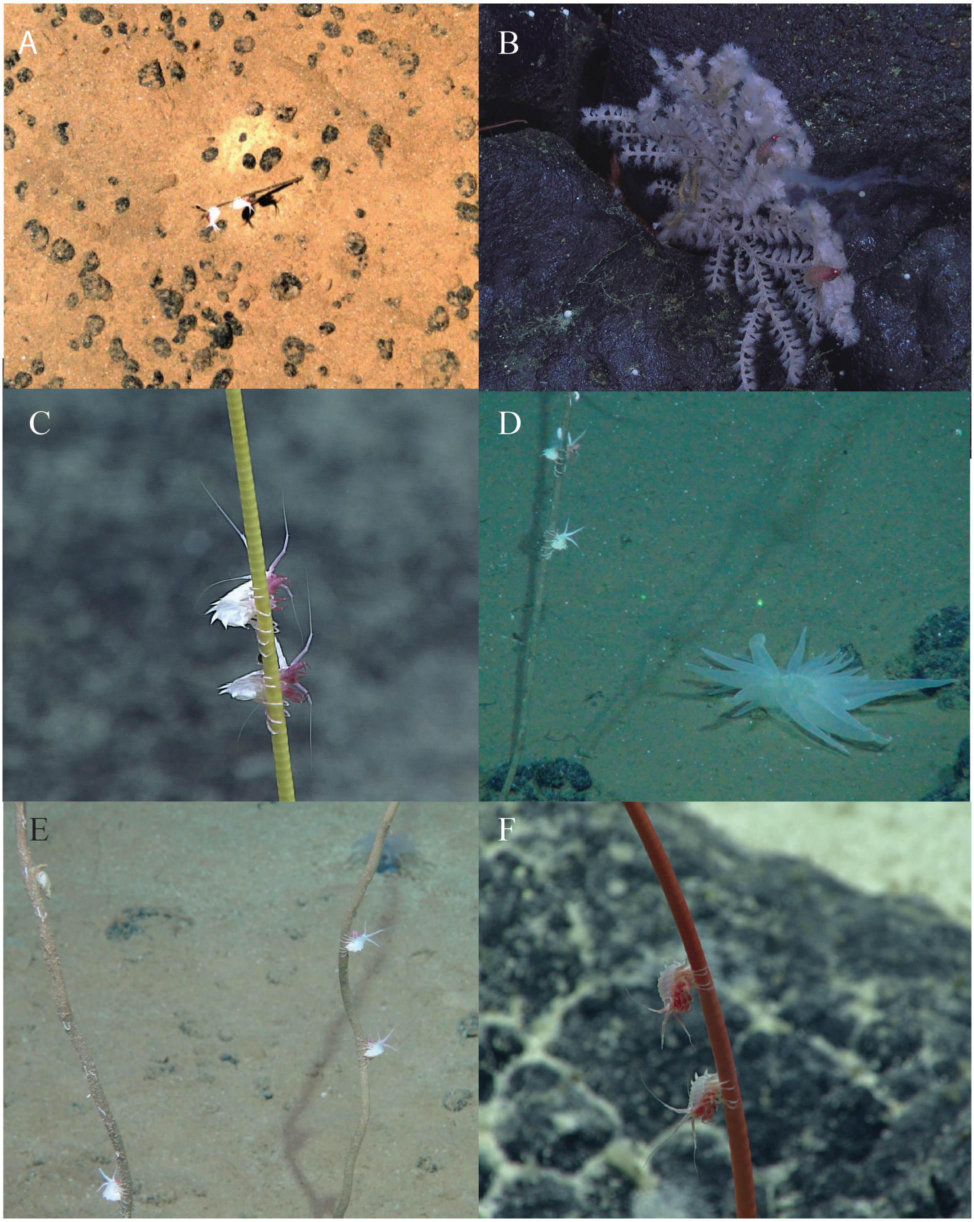

Figure 6. A selection of photographic records of specimens of *Amathillopsis*: **A** Eastern Clarion Clipperton Zone, APEI-6, 4013 m **B** Emperor Seamount Chain, Yomei Seamount, 1470 m **C** Northern Mariana Islands, Fina Nagu Volcanic Chain, 2629 m **D** Peru Basin, DISCOL site, 4149 m **E** New Zealand, Abyssal basin, 4160 m **F** northeast of Kingman Reef, 1930 m. See Table 3 for detailed information.

was observed with two individuals clinging to a polychaete worm tube (video, Suppl. material 1) at 4622 m depth on the Porcupine Abyssal Plain. During the observation time of 20 minutes, the amphipods did not alter their position on the tube. The

Table 3. Locality data for collated photographic records of specimens of *Amathillopsis*. DISCOL = DISturbance and re-COL-onization experiment; APEI = Areas of Particular Environmental Interest; TOML = Tonga Offshore Mining Limited.

Geographic Locality	Latitude and longitude	Depth (m)	Date (dd/mm/yyyy)	Publication/credit
North Atlantic, Porcupine Abyssal Plain	50.0525, -15.4708	4622	20/07/2020	This study
Kiribati (east of the Line Island Group)	5.9903, -156.7402	4660	02/08/2015	https://doi.org/10.3389/fmars.2019.00605
Kiribati (west of the Line Island Group)	2.5704, -162.2069	5111	30/07/2015	https://doi.org/10.3389/fmars.2019.00605
Kiribati (east of the Phoenix Islands Group)	-0.0001, -170.9988	5559	27/07/2015	https://doi.org/10.3389/fmars.2019.00605
Kiribati (east of the Line Island Group)	5.9725, -156.7832	4653	02/08/2015	https://doi.org/10.3389/fmars.2019.00605
Eastern Clarion Clipperton Zone (TOML-C)	15.2734, -129.6792	5002	02/09/2015	https://doi.org/10.1016/j.pocean.2020.102405
Eastern Clarion Clipperton Zone (APEI-6)	17.3400, -122.9007	4005	07/05/2015	https://doi.org/10.1016/j.pocean.2018.11.003
Eastern Clarion Clipperton Zone (APEI-6)	17.3575, -122.9053	4013	07/05/2015	https://doi.org/10.1016/j.pocean.2018.11.003
Eastern Clarion Clipperton Zone (APEI-6)	17.2421, -122.8223	4239	10/05/2015	https://doi.org/10.1016/j.pocean.2018.11.003
Peru Basin – DISCOL site	-7.0736, -88.4653	4130	24/03/2017	https://doi.org/10.1038/s41598-019-44492-w
Peru Basin – DISCOL site	-7.1258, -88.4568	4160	24/03/2017	https://doi.org/10.1038/s41598-019-44492-w
Peru Basin – DISCOL site	-7.0801, -88.4678	4133	24/03/2017	https://doi.org/10.1038/s41598-019-44492-w
Peru Basin – DISCOL site	-7.1252, -88.4506	4149	15/09/2015	courtesy of GEOMAR
Peru Basin – DISCOL site	-7.0898, -88.4463	4140	13/09/2015	courtesy of GEOMAR
New Zealand, Abyssal basin between Three Kings & Colville Ridges	-30.9908, 177.5010	4159	01/02/2017	courtesy of GEOMAR
Northern Mariana Islands, Southern Marianas, Fina Nagu Volcanic Chain	12.7956, 143.7862	2629	27/04/2016	courtesy of NOAA Office of Ocean Exploration and Research
Northern Mariana Islands, Marianas Trench Marine National Monument	21.5679, 145.5185	3300	29/06/2016	courtesy of NOAA Office of Ocean Exploration and Research
Northern Mariana Islands, Marianas Trench Marine National Monument	20.7234, 145.0618	1909	01/07/2016	courtesy of NOAA Office of Ocean Exploration and Research
Pacific Remote Islands Marine National Monument, northeast of Kingman Reef	6.4178, -162.2202	1930	14/05/2017	courtesy of NOAA Office of Ocean Exploration and Research
North West Pacific, Emperor Seamount Chain, Suiko Seamount	44.5561, 170.4798	2252	08/08/2019	Schmidt Ocean Institute, courtesy of NOAA Office of Ocean Exploration and Research
North West Pacific, Emperor Seamount Chain, Yomei Seamount	42.4313, 170.4371	1495	09/08/2019	Schmidt Ocean Institute, courtesy of NOAA Office of Ocean Exploration and Research
North West Pacific, Emperor Seamount Chain, Yomei Seamount	42.4313, 170.4377	1493	09/08/2019	Schmidt Ocean Institute, courtesy of NOAA Office of Ocean Exploration and Research
North West Pacific, Emperor Seamount Chain, Yomei Seamount	42.4318, 170.4357	1479	09/08/2019	Schmidt Ocean Institute, courtesy of NOAA Office of Ocean Exploration and Research
North West Pacific, Emperor Seamount Chain, Yomei Seamount	42.4319, 170.4354	1472	09/08/2019	Schmidt Ocean Institute, courtesy of NOAA Office of Ocean Exploration and Research
North West Pacific, Emperor Seamount Chain, Yomei Seamount	42.4402, 170.4381	1336	09/08/2019	Schmidt Ocean Institute, courtesy of NOAA Office of Ocean Exploration and Research
North West Pacific, Emperor Seamount Chain, Yomei Seamount	42.4320, 170.4350	1470	09/08/2019	Schmidt Ocean Institute, courtesy of NOAA Office of Ocean Exploration and Research
North West Pacific, Emperor Seamount Chain, Nintoku Seamount	40.7519, 170.5925	1490	12/08/2019	Schmidt Ocean Institute, courtesy of NOAA Office of Ocean Exploration and Research
Sea of Okhotsk, Bussol Strait	46.9426, 151.0836	3299	22/07/2015	https://doi.org/10.1016/j.dsr2.2018.05.022
Aleutian Islands	52.4981, -174.9232	2947	27/07/2004	ROV JASON, courtesy of Les Watling

tube belongs to a polychaete worm of the family Onuphidae (Alexandra Kerbl, pers. comm., August 2020). Unfortunately, we only managed to retrieve one of the two specimens. Nevertheless, this is the first confirmed record of an *Amathillopsis* species observed in situ which has been subsequently collected and deposited in a natural history collection. Stills camera and video technology have developed in recent years to a level that enables high resolution images at bathyal and abyssal depths. Until now, the

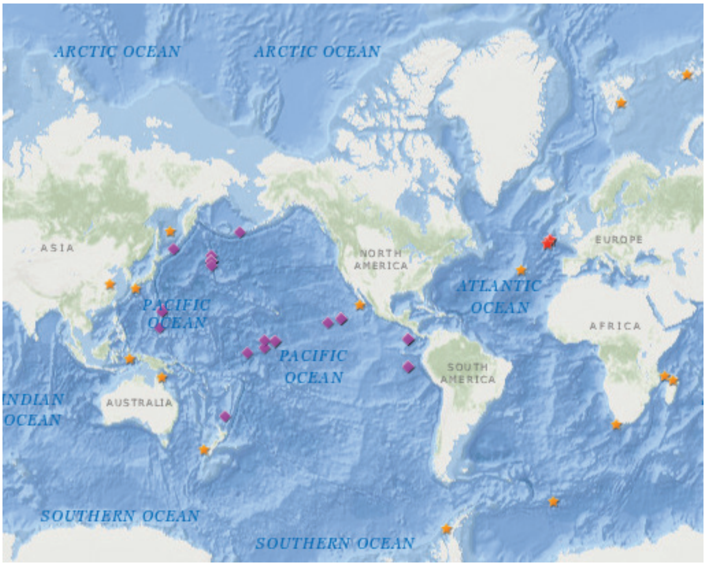

Figure 7. Map showing the type localities of known species of *Amathillopsis* (orange stars), the location of photograph records of *Amathillopsis* species (purple diamonds), and type localities of *Amathillopsis inkenae* sp. nov. (red stars). The types of the two specimens of Cleonardopsinae are included. See Table 3 for detailed locality information.

habits of species of *Amathillopsis* could only be postulated, on the basis of their possession of posterior pereopods adapted to a clinging lifestyle. The functional morphology enabling the gripping of thin structures is expressed by the strongly curved pereopodal dactyli and the pereopods being flexed backwards. These adaptations were described by McCloske (1970) as well-adapted for grasping, in reference to *Dulichia* clinging onto sea urchin spines. While clinging behaviour is known from a number of amphipod families in shallow waters, such as Caprellidae, Podoceridae, and Dulichiidae (e.g., Takeuchi and Hirano 1995; Guerra-García et al. 2002), it is only now that we are able to report that amathillopsids express this behaviour at bathyal and abyssal depths of all oceans. We assume the stem they cling to is simply a means to expose them higher in the water column for feeding. *Amathillopsis inkenae* was found on a worm tube, whereas other *Amathillopsis* species have been photographed clinging to a variety of other organism structures, including sponges and corals.

Based on the raptorial structure of the mouthparts and gnathopods we assume *Amathillopsis* to be predators (or micropredators), capturing their prey, such as zooplankton or small suprabenthic crustaceans from the water column. The red colour of gnathopods and mouthparts may result from the consumption of carotinoids from prey. Amathillopsids have never been caught in baited traps, and therefore we exclude the possibility of them being scavengers. Also remarkable are the well-developed eyes of *Amathillopsis* specimens living below 3000 m. It is probable that they rely on bioluminescence as communication, either for catching prey, avoiding predators or finding mating partners.

Acknowledgements

We are grateful to Saskia Brix, Deutsches Zentrum für Marine Biodiversitätforschung (DZMB) for organizing and leading the IceAGE 3 expedition. We appreciate the extra sampling effort and great in situ images taken by the ROV team led by Fritz Abegg from the GEOMAR Helmholtz Zentrum Kiel. We thank the team of expedition SO197 on board of RV 'Sonne'. Solvin Zankl took the board photographs. Karen Jeskulke (DZMB) is thanked for her technical support with the collection databases. Molecular lab support was provided by Eva Paulus and Nicole Gatzemeier (DZMB). Alexandra Kerbl (CeNak Hamburg), kindly identified the polychaete tube from a photograph. We are grateful to Erik Simon-Lledó (National Oceanography Centre, Southampton), Virginia Moriwake (University of Hawai'i), NOAA Office of Ocean Exploration and Research, Sadie Mills (National Institute of Water & Atmospheric Research, Wellington, New Zealand), Dr. Inken Suck (GEOMAR, Kiel, Germany), and Les Watling (University of Hawai'i at Mānoa & Schmidt Ocean Institute), for allowing us to use photographs of other specimens of *Amathillopsis* from a variety of locations for inclusion in our study. The authors are grateful to the two reviewers whose comments and suggestions greatly improved the manuscript.

Anne-Nina Lörz as well as laboratory consumables and sequencing costs were financed by the Deutsche Forschungsgemeinschaft project IceAGE Amphipoda (LO2543/1-1). Tammy Horton was funded by Climate Linked Atlantic Section Science (CLASS) programme (NE/R015953/1) supported by UK Natural Environment Research Council (NERC) National Capability funding to the National Oceanography Centre.

References

Astrin JJ, Stüben PE (2008) Phylogeny in cryptic weevils: molecules, morphology and new genera of western Palaearctic Cryptorhynchinae (Coleoptera: Curculionidae). Invertebrate Systematics 22: 503–522. https://doi.org/10.1071/IS07057

Barnard JL (1961) Gammaridean Amphipoda from depths of 400–6000 meters. Galathea Report 5: 23–128.

Barnard JL (1967) Bathyal and abyssal Gammaridean Amphipoda of Cedros Trench, Baja California. United States National Museum Bulletin 260: 1–205. https://doi.org/10.5479/si.03629236.260.1

Barnard JL (1969) The families and genera of marine gammaridean Amphipoda. United States National Museum Bulletin 271: 1–535. https://doi.org/10.5479/si.03629236.258.1

Barnard JL, Karaman GS (1991) The families and genera of marine gammaridean Amphipoda (except marine gammaroids). Records of the Australian Museum, Supplement 13: 1–866. https://doi.org/10.3853/j.0812-7387.13.1991.91

Barnard KH (1916) Contributions to the Crustacean Fauna of South Africa n° 5. The Amphipoda. Annals of the South African Museum 15(3): 105–302. https://www.biodiversitylibrary.org/page/11101068

Boeck A (1871) Crustacea amphipoda borealia et arctica. Forhandlinger i Videnskabs-Selskabet i Christiania 1870: 83–280. https://doi.org/10.5962/bhl.title.2056

Brandt A, Alalykina I, Fukumori H, Golovan O, Kniesz K, Lavrenteva A, Lörz AN, Malyutina M, Philipps-Bussau K, Stransky B (2018) First insights into macrofaunal composition from the SokhoBio expedition (Sea of Okhotsk, Bussol Strait and northern slope of the Kuril-Kamchatka Trench). Deep Sea Research Part II: Topical Studies in Oceanography 154: 106–120. https://doi.org/10.1016/j.dsr2.2018.05.022

Chevreux E (1908) Diagnoses d'amphipodes nouveaux provenant des campagnes de la "Princesse-Alice" dans l' Atlantique nord. (suite). Bulletin de l'Institut Océanographique de Monaco 122: 1–8.

Coleman CO (1998) *Amathillopsis charlottae* n. sp., first record of Amathillopsidae (Crustacea, Amphipoda) from the Antarctic Ocean. Bulletin Zoologisch Museum Universiteit van Amsterdam 16(5): 25–32.

Coleman CO (2003) "Digital inking": How to make perfect line drawings on computers. Organism, Diversity and Evolution, Electronic Supplement 14: 1–14. http://senckenberg.de/odes/03-14.htm

Coleman CO (2009) Drawing setae the digital way. Zoosystematics and Evolution 85: 305–310. https://doi.org/10.1002/zoos.200900008

Coleman CD, Coleman CO (2008) *Amathillopsis roroi*, a new species of Amathillopsidae (Crustacea, Amphipoda) from the Antarctic Ocean. Zoosystematics and Evolution 84(2): 143–148. https://doi.org/10.1002/zoos.200800002

Guerra-García JM, Corzo J, García-Gómez JC (2002) Clinging Behaviour of the Caprellidea (Amphipoda) from the Strait of Gibraltar. Crustaceana 75(1): 41–50. https://doi.org/10.1163/156854002317373500

Gurjanova EF (1955) Novye vidy bokoplavov (Amphipoda, Gammaridea) iz severnoi chasti Tikhogo okeana. [New amphipod species (Amphipoda, Gammaridea) from the northern part of the Pacific Ocean]. Akademiya Nauk SSSR, Trudy Zoologicheskogo Instituta 18: 166–218.

Heller C (1875) Neue Crustaceen und Pycnogoniden. Gesammelt während der k.k. österr.-ungar. Nordpol-Expedition. Vorläufige Mittheilung. Sitzungsberichte der mathematisch-naturwissenschaftlichen Classe der Kaiserlichen Akademie der Wissenschaften in Wien 71: 609–612.

Holmes SJ (1908) The Amphipoda collected by the U.S. Bureau of Fisheries Steamer "Albatross" off the West Coast of North America, in 1903 and 1904, with descriptions of a new family and several new genera and species. Proceedings of the United States National Museum 35(1654): 489–543. https://doi.org/10.5479/si.00963801.35-1654.489

Jażdżewska AM, Corbari L, Driskell A, Frutos I, Havermans C, Hendrycks E, Hughes L, Lörz A-N, Stransky B, Tandberg AHS, Vader W, Brix S (2018) A genetic fingerprint of Amphipoda from Icelandic waters – the baseline for further biodiversity and biogeography studies. In: Brix S, Lörz A-N, Stransky B, Svavarsson J (Eds) Amphipoda from the IceAGE-project (Icelandic marine Animals: Genetics and Ecology). ZooKeys 731: 55–73. https://doi.org/10.3897/zookeys.731.19931

Latreille (1816) Nouveau Dictionnaire d'histoire naturelle, appliquée aux arts, à l'Agriculture, à l'Economic rurale et domestique, à la Médecine, etc. Par une Société de Naturalistes et d'Agriculteurs. Nouvelle Édition, Paris 1: 467–469.

Ledoyer M (1978) Contribution à l'étude des Amphipodes gammariens profonds de Madagascar (Crustacea). Téthys 8(4): 365–382.

Ledoyer M (1986) Crustacés Amphipodes Gammariens. Familles des Haustoriidae à Vitjazianidae. Faune de Madagascar 59(2): 599–1112.

Lowry JK, Stoddart HE (1992) A revision of the genus *Ichnopus* (Crustacea: Amphipoda: Lysianassoidea: Uristidae). Records of the Australian Museum 44: 185–245. https://doi.org/10.3853/j.0067-1975.44.1992.32

Lowry JK, Stoddart HE (1993) Crustacea Amphipoda: Lysianassoids from Philippine and Indonesian waters. In: Crosnier A (Ed.) Résultats des campagnes MUSORSTOM. Mémoirs du Muséum Nationale de l'Histoire naturelle 156: 55–109.

Lowry JK, Stoddart HE (1995) The Amphipoda (Crustacea) of Madang Lagoon: Lysianassidae, Opisidae, Uristidae, Wandinidae and Stegocephalidae. Records of the Australian Museum Supplement 22: 97–174. https://doi.org/10.3853/j.0812-7387.22.1995.122

Lowry JK (2006) New families and subfamilies of Amphipod Crustaceans. Zootaxa 1254: 1–28.

Macreadie PI, McLean DL, Thomson P, Partridge JC, Jones DOB, Gates AR, Benfield MC, Collin SP, Booth JB, Smith LL, Techera E, Skropeta D, Horton T, Pattiaratchi C, Bond T, Fowler AM (2018) Eyes in the sea: Unlocking the mysteries of the ocean using industrial, remotely operated vehicles (ROVs). Science of The Total Environment 634: 1077–1091. https://doi.org/10.1016/j.scitotenv.2018.04.049

McCloskey LR (1970) A new species of *Dulichia* (Amphipoda, Podoceridae) commensal with a sea urchin. Pacific Scientist 24(1): 90–98.

Miers EJ (1881) On a small collection of Crustacea and Pycnogonida from Franz-Josef Land, collected by B. Leigh Smith, Esq. Annals and Magazine of Natural History (series 5) 7: 45–51. https://doi.org/10.1080/00222938109459471

NOAA Office of Ocean Exploration and Research (2020) NOAA Office of Ocean Exploration and Research Benthic Deepwater Animal Identification Guide. http://oceanexplorer.noaa.gov/okeanos/animal_guide/animal_guide.html.

Pirlot JM (1934) Les amphipodes de 1'Expedition du Siboga. Deuxieme partie. Les amphipodes gammarides. 11. Les amphipodes de la mer profonde. 2. Hyperiopsidae, Paradaliscidae, Astyridae nov. fam., Tironidae, Calliopiidae, Paramphithoidae, Amathillopsidae nov. fam., Eusiridae, Gammaridae, Aoridae, Photidae, Amphithoidae, Jassidae. Siboga Expeditie 33d: 167–235.

Stebbing TRR (1906) Amphipoda. I. Gammaridea. Das Tiereich. 21: 1–806. [127 figs] http://www.biodiversitylibrary.org/page/998303#page/7/mode/1up

Stebbing TRR (1883) The "Challenger" Amphipoda. Annals and Magazine of Natural History (series 5) 11: 203–207. https://doi.org/10.1080/00222938309459130

Stephensen K (1944) Crustacea Malacostraca. VIII: Amphipoda IV. The Danish Ingolf Expedition 3(13): 1–51.

Takeuchi I, Hirano R (1995) Clinging Behavior of the Epifaunal Caprellids (Amphipoda) Inhabiting the *Sargassum* Zone on the Pacific Coast of Japan, with its Evolutionary Implications. Journal of Crustacean Biology 15(3): 481–492. https://doi.org/10.1163/193724095X00497

Tomikawa K, Mawatari SF (2006) A New Species of the Genus *Amathillopsis* (Crustacea: Amphipoda: Amathillopsidae) from Japan. Species Diversity 11(3): 199–207. https://doi.org/10.12782/specdiv.11.199

Wakabara Y, Serejo CS (1999) Amathillopsidae and Epimeriidae (Crustacea, Amphipoda) from bathyal depths off the Brazilian coast. Zoosystema 21(4): 625–645.

Watling L (1989) A classification system for crustacean setae based on the homology concept. In: Felgenhauer BE, Watling L, Thistle AB (Eds) Functional morphology of feeding and grooming in Crustacea. Crustacean Issues 6: 15–26. https://doi.org/10.1201/9781003079354-2

Supplementary material 1

In situ video

Authors: Anne-Nina Lörz, Tammy Horton

Data type: mp4. video file

Explanation note: *Amathillopsis inkenae* sp. nov., clinging onto a polychaete tube in 4622 m, Porcupine Abyssal Plain, filmed by the ROV KIEL 6000 during the RV 'Sonne' expedition 267, station 133-4.

Link: https://doi.org/10.3897/zookeys.1031.62391.suppl1

ZooKeys 1031: 41–58 (2021)
doi: 10.3897/zookeys.1031.59102
https://zookeys.pensoft.net

RESEARCH ARTICLE

A peer-reviewed open-access journal
ZooKeys
Launched to accelerate biodiversity research

A new species of *Liphistius* from Myanmar and description of the actual male of *L. birmanicus* Thorell, 1897 (Araneae, Mesothelae, Liphistiidae)

Xin Xu[1,2,3], Li Yu[1], Khin Pyae Pyae Aung[4,5], Long Yu[2], Fengxiang Liu[2],
Wai Wai Lwin[4], Men Zing Sang[4], Daiqin Li[6]

1 *College of Life Sciences, Hunan Normal University, 36 Lushan Road, Changsha 410081, Hunan Province, China* **2** *State Key Laboratory of Biocatalysis and Enzyme Engineering, and Centre for Behavioural Ecology and Evolution (CBEE), School of Life Sciences, Hubei University, 368 Youyi Road, Wuhan 430062, Hubei Province, China* **3** *School of Life and Environmental Sciences, University of Sydney, Sydney, NSW, Australia* **4** *Department of Zoology, University of Yangon, Kamayut Township, Pyay Road, Yangon, 11041, Myanmar* **5** *Department of Biology, Taungoo Education College, Taungoo, 08101, Myanmar* **6** *Department of Biological Sciences, National University of Singapore, 14 Science Drive 4, 117543, Singapore*

Corresponding authors: Xin Xu (xuxin@hunnu.edu.cn); Daiqin Li (dbslidq@nus.edu.sg)

Academic editor: G. Blagoev | Received 29 September 2020 | Accepted 17 March 2021 | Published 14 April 2021

http://zoobank.org/78C9CC2B-6D4E-4665-B2BD-E5CB05D09552

Citation: Xu X, Yu L, Aung KPP, Yu L, Liu F, Lwin WW, Sang MZ, Li D (2021) A new species of *Liphistius* from Myanmar and description of the actual male of *L. birmanicus* Thorell, 1897 (Araneae, Mesothelae, Liphistiidae). ZooKeys 1031: 41–58. https://doi.org/10.3897/zookeys.1031.59102

Abstract

Five *Liphistius* Schiödte, 1849 species of the primitively segmented spider family Liphistiidae are currently known from Myanmar. Here, we described a new species, *Liphistius pyinoolwin* **sp. nov.** (♂♀), which was collected from Pyin Oo Lwin, Mandalay Region, Myanmar, diagnosed based on its genital morphology. The specimens (2♂♂, 5♀♀) collected by Walter C. Sedgwick from Pyin Oo Lwin in 1982 were misidentified as *L. birmanicus* Thorell, 1897 and are treated here as the newly described species. Accordingly, we described the males of *L. birmanicus* for the first time, redescribed its female, using newly collected specimens from Yadò, Than Taung and Kalekho Atet townships, Kayin State. We also provided information on the variation in genital morphology of both species, and their relationships within the *birmanicus*-group of species.

Keywords

Morphology, South-east Asia, taxonomy, trapdoor spiders

Introduction

With its unique morphology, lifestyle (living in underground burrows), and often being regarded as 'living fossils' (Bristowe 1975), the primitively segmented spiders of the family Liphistiidae has fascinated many naturalists and arachnologists for over one and a half centuries, since the first species was discovered by Schiödte (1849). Recently, interest in this lineage has resurged because of its pivotal position in fully understanding the arachnid tree of life (Platnick and Gertsch 1976), and application of molecular data (Xu et al. 2015a). As the sister lineage to all other extant spiders, liphistiids bear many plesiomorphic characters, such as the presence of abdominal tergal plates and the position of the spinnerets on the median area of the ventral opisthosoma (Platnick and Gertsch 1976; Coddington and Levi 1991; Haupt 2003). In this study, we focus on the *Liphistius* Schiödte, 1849 from Myanmar, an extremely important yet very poorly studied region, because it is the westernmost distribution of liphistiids according to the current records (Thorell 1897; Platnick and Sedgwick 1984; Schwendinger 1990; Aung et al. 2019; Ono and Aung 2020) and because younger mesothele fossils have also been found in the Middle Cretaceous amber forest in northern Myanmar (Wunderlich 2017, 2019).

The genus *Liphistius* contains 57 nominal species and is limited to Southeast Asia (Indonesia (Sumatra), Laos, Malaysia, Myanmar, and Thailand) (Xu et al. 2015b; World Spider Catalog 2021). Out of 57 species, 32 *Liphistius* species have been reported from Thailand (World Spider Catalog 2021). Given that Myanmar and Thailand share similar landmass, climate and geological topography, a comparable species diversity is expected for Myanmar. However, only five species (*L. birmanicus* Thorell, 1897, *L. hpruso* Aung et al., 2019, *L. lordae* Platnick & Sedgwick, 1984, *L. pinlaung* Aung et al., 2019, and *L. tanakai* Ono & Aung, 2020) have been described from Myanmar so far (Fig. 1). This is probably due to the lack of local arachnologists and the difficulty of accessibility to foreign arachnologists. Working on Myanmar *Liphistius* is thus vital to fully understanding the geographic distribution and species diversity of liphistiids.

In spite of only five described species, the taxonomy of Myanmar *Liphistius*, including *L. birmanicus*, seems to be problematic. The female type of *L. birmanicus*, which was designed as the lectotype by Platnick and Sedgwick (1984), was collected from Yadò Village (Kayin State since 1989, formerly known as Kayah or Karen State), by an Italian explorer, Leonardo Fea, during his expedition to Myanmar between 1885 and 1889, and described by Thorell in 1897. Another specimen, a damaged immature male, recorded by Gravely (1915) from Mawlamyine (formerly Moulmein, Mon State), far south from Yadò, was considered as *L. birmanicus* (Bristowe 1938), but is still unclear (Schwendinger 1990). In 1984, *L. birmanicus* was redescribed based on the specimens collected from Pyin Oo Lwin (formerly Maymyo, Mandalay Region) instead from the type locality Yadò (Platnick and Sedgwick 1984). However, we believe that the specimens from Pyin Oo Lwin might not be *L. birmanicus.* The issue with *L. birmanicus* should thus be addressed before further studying Myanmar *Liphistius* species.

Figure 1. Map showing the localities of six *Liphistius* species in Myanmar including the two species described in this study. The green triangles denote all the recorded sites of adult *L. birmanicus* specimens from the literature, including the misidentified ones.

To resolve the *L. birmanicus* issue, and to document *Liphistius* species diversity, which could allow exploring how geological and climatic events may have shaped its biogeographical history and its diversity in Myanmar, we undertook three expeditions to Myanmar in 2018 and 2019. In this study, we describe *L. birmanicus* males for the first time and redescribe the females based on the female lectotype and newly collected specimens from the type locality. We also diagnose and describe the specimens collected from Pyin Oo Lwin, misidentified as *L. birmanicus* by Platnick and Sedgwick (1984) and Schwendinger (1990), as a new species.

Materials and methods

Specimen collection

All specimens were collected from Pyin Oo Lwin (Mandalay Region), Than Taung and Kalekho Atet townships (Kayin State), Myanmar (Figs 1, 2). They were captured alive and fixed in absolute ethanol. Their right four legs were then removed, preserved in absolute ethanol, and stored at −80 °C for molecular work. The remains of each specimen were preserved in 80% ethanol as vouchers for morphological examination. All type and voucher specimens were deposited at the Centre for Behavioural Ecology and Evolution (**CBEE**), College of Life Sciences, Hubei University, Wuhan, Hubei Province, China.

Morphological examination

Specimens were examined under an Olympic SZX16 stereomicroscope. Female genitalia were cleared using 10 mg/ml trypsase (Bomei Biotech Company, Hefei, Anhui, China) for at least three hours in room temperature to dissolve soft tissues, examine, and photograph with a digital camera CCD mounted on an Olympic BX53 compound microscope. Genital anatomical terminology follows Schwendinger et al. (2019) and Aung et al. (2019). All measurements were carried out under a Leica M205 digital microscope using the software of Leica Application Suite v4 and are given in millimetres. Leg and palp measurements are given in the following order: total leg length (femur + patella + tibia + metatarsus + tarsus), total palp length (femur + patella + tibia + tarsus). Abbreviations used in the text are: **ALE** = anterior lateral eye; **AME** = anterior median eye; **CDO** = central dorsal opening; **CT** = contrategulum; **E** = embolus; **GA** = genital atrium; **PC** = paracymbium; **PeP** = paraembolic plate; **PLE** = posterior lateral eye; **PME** = posterior median eye; **PPl** = poreplate; **PS** = posterior stalk; **RC** = receptacular cluster; **ST** = subtegulum; **T** = tegulum; **TiA** = tibial apophysis. **AMNH** = American Museum of Natural History, New York; **IZC** = Invertebrate Zoology Code at AMNH; **MCSNG** = Museo Civico di Storia Naturale, Genova, Italy; **MCZ** = Museum of Comparative Zoology, Harvard University, Cambridge, MA.

Taxonomy

Family Liphistiidae Thorell, 1869
Subfamily Liphistiinae Thorell, 1869

Genus *Liphistius* Schiödte, 1849

Type species. *Liphistius desultor* Schiödte, 1849.

Diagnosis. *Liphistius* differs from all other liphistiid genera by the presence of a tibial apophysis on male palp (Figs 3A–C, 3H–J, 4A–C 8A–C), and by the presence of a poreplate and a median receptacular cluster in female genitalia (Figs 5D–I, 6D–I, 7B–I, 9D–I, 10C–G).

Distribution. Indonesia (Sumatra), Laos, Malaysia, Myanmar, and Thailand.

Liphistius pyinoolwin sp. nov.

http://zoobank.org/781BD6EE-9EC1-4C53-944A-9F45E2F44AE9
Figs 2, 3–7

Liphistius birmanicus Platnick & Sedgwick, 1984: 8 (only 2♂♂ 5♀♀ from Pyin Oo Lwin, Mandalay Region, Myanmar, alt. 1150 m; collected by W. Sedgwick on 13 July 1982; deposited in AMNH (2♂♂ 4♀♀; examined) and MCZ (1♀; not examined)), misidentification, partim; Schwendinger, 1990: 331–332 (illustration based on 2♂♂ 4♀♀ (AMNH)), misidentification.

Type material. ***Holotype*:** Mynamar · ♂; Mandalay Region, Pyin Oo Lwin District, Pyin Oo Lwin township, Anesakhan Village, near Dat Taw Gyaint Waterfall Resort, the View Resort & Restaurant; 21.98°N, 96.38°E; alt. 908 m; 13 July 2018; D. Li, F.X. Liu, X. Xu and L. Yu leg.; XUX–2018–089. ***Paratypes*:** Myanmar · 7 ♂♂, 15 ♀♀; same data as for the holotype; XUX–2018–090, 093, 094, 096, 098, 099A, 102, 103, 103A, 104, 104A, 105, 106, 107–110, 110A, 110B, 110C, 111, 111A.

***Other material*:** Myanmar · 1 ♂, 4 ♀♀ (AMNH; examined); Mandalay, Pyin Oo Lwin; alt. 1150 m; 13 July 1982; W. Sedgwick leg.; AMNH_IZC 00356855 (♂; matured on 14 October 1982, died on 23 February 1983), AMNH_IZC 00356856 (♀; moulted on 28 February 1983, died on 17 April 1983), AMNH_IZC 00356857 (♀; moulted on 27 January 1983, died on 14 February 1983), AMNH_IZC 00356858 (♀; died on 15 October 1982), AMNH_IZC 00356859 (♀; moulted on 6 November 1982, died on 1 March 1983).

Diagnosis. Males of *L. pyinoolwin* sp. nov. can be distinguished from those of *L. birmanicus*, *L. lahu* Schwendinger, 1998, *L. lordae*, and *L. pinlaung* by the presence of a lateral process on the paracymbium (Figs 3A, H, I, 4B); from those of *L. birmanicus* by the larger tibial apophysis (Fig. 3A, B, H, I), the plane cumulus (Figs 3A, B, H–J, 4A), the

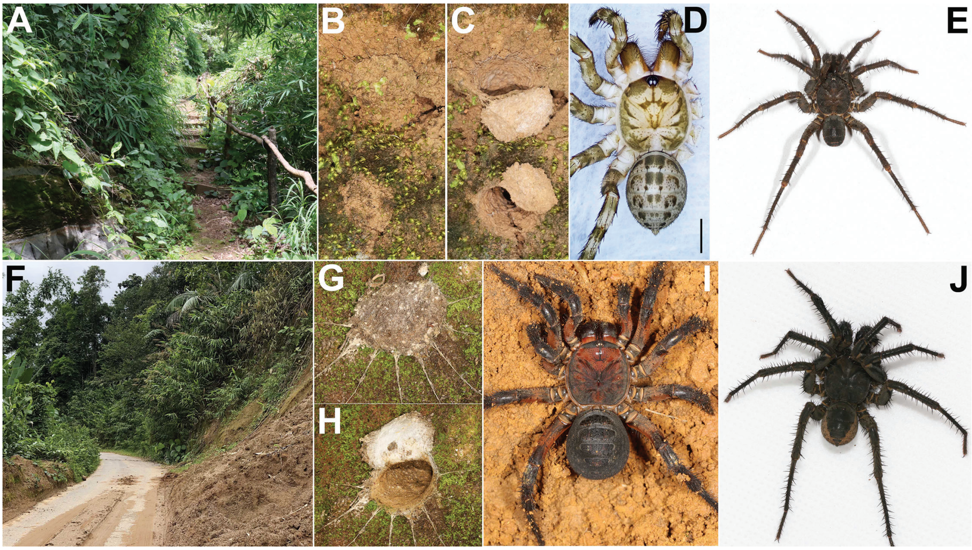

Figure 2. Microhabitats, burrows, and general somatic morphology of *Liphistius pyinoolwin* sp. nov. and *Liphistius birmanicus* Thorell, 1897 **A–E** *L. pyinoolwin* sp. nov. **A** microhabitat **B** a burrow with two trapdoors closed **C** same, trapdoors opened **D** female (XUX–2018–094) **E** male (XUX–2018–110B) **F–J** *L. birmanicus* **F** microhabitat **G** burrow with trapdoor closed **H** same, trapdoor opened **I** female (ARAMYN–090) **J** male (ARAMYN–096); Scale bar: 2 mm (**D**).

smaller paraembolic plate (Figs 3A–J, 4F, G), and the wider shorter contrategular process (Figs 3E, 4F); from those of *L. lahu* by the narrower tegulum (Figs 3C, F, J, 4F, G); from those of *L. lordae* by the wider tibial apophysis at base (Figs 3A, B, H, I, 4B), and the shorter, less regularly arranged setae on the cumulus (Figs 3A, B, H, I, 4A); from those of *L. pinlaung* by the tegulum with a slightly dentated margin (Figs 3C, F, J, 4F). Females of *L. pyinoolwin* sp. nov. resemble those of *L. birmanicus*, *L. hpruso* and *L. pinlaung* by the poreplate with two pairs of lobes, but can be distinguished from those of *L. birmanicus* and *L. pinlaung* by the small, narrower posterior stalk (Figs 5D–I, 6D, E, G, H, 7B–I), as well as the narrower, longer receptacular cluster (Figs 5G–I, 6G–I, 7C, G–I); from those of *L. hpruso* by the poreplate with larger anterior lobes (Figs 5D–I, 6D–I, 7A–I); from those of the other *Liphistius* by the poreplate with four anterior lobes (Figs 5G–I, 6G–H, 7A–I).

Description. ***Male*** (holotype). Total length, excluding chelicerae, 13.95. Carapace 6.03 long and 6.17 wide, black brown, furnished with a few short, scattered bristles. ALE>PLE>PME>AME, eye sizes and interdistances: AME 0.10, ALE 0.60, PME 0.21, PLE 0.42, AME–AME 0.07, AME–ALE 0.09, PME–PME 0.11, PME–PLE 0.08, ALE–PLE 0.09, ALE–ALE 0.06, PLE–PLE 0.36, AME–PME 0.09. Chelicerae robust, promargin of chelicerae groove with 12 strong denticles of variable size. Labium 0.61 long and 1.09 wide, wider than long, fused with sternum. Sternum 2.77 long and 1.03 wide, longer than wide, and a few weakly spined setae on the anterior tip and many long spined setae on the posterior tip, elongated posterior tip. Opisthosoma 6.71 long and 5.00 wide, black, with 12 tergites, the fifth largest, 8 spinnerets. Legs

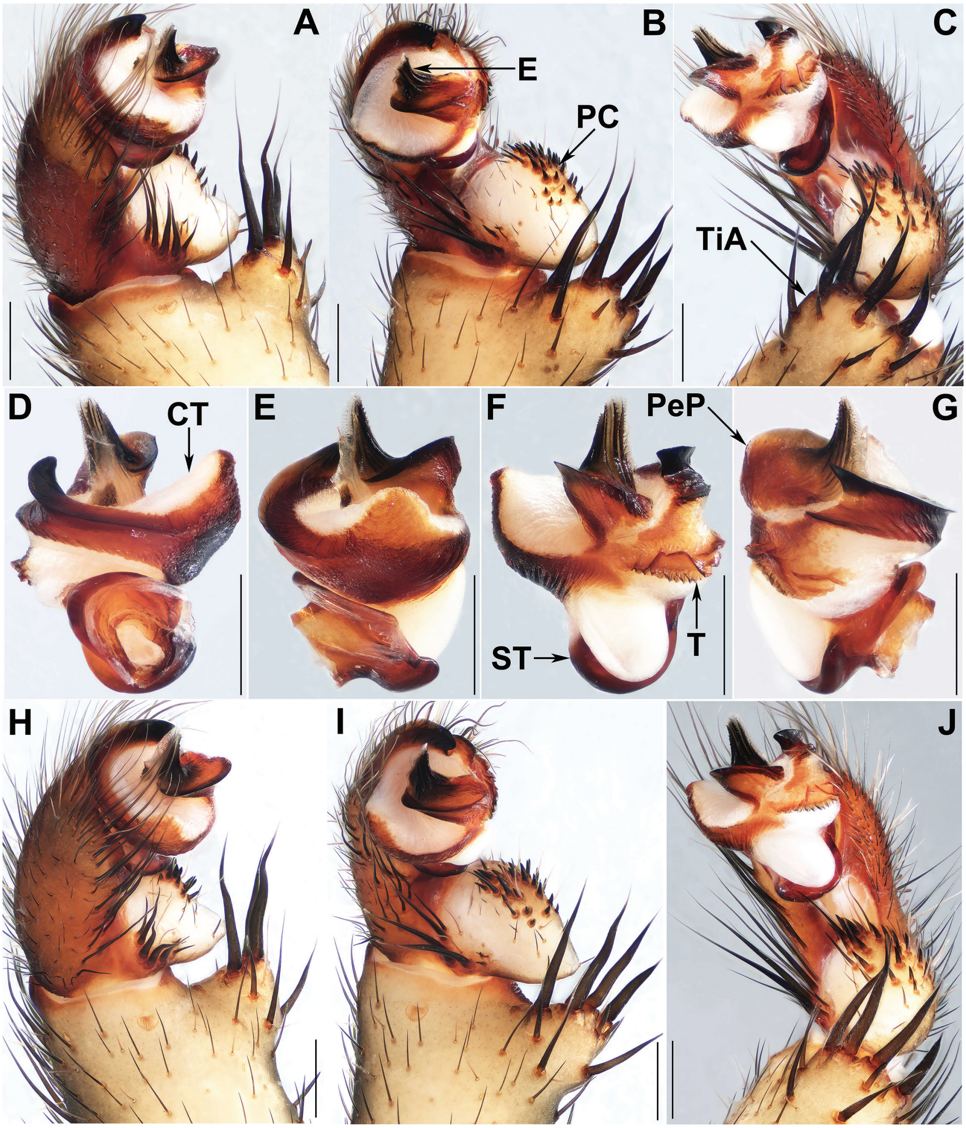

Figure 3. Male genital anatomy of *Liphistius pyinoolwin* sp. nov. **A, H** palp prolateral view **B, I** palp ventral view **C, J** palp retrolateral view **D–G** palp distal view **A–C** XUX–2018–089 **D–G** XUX–2018–110B **H–J** XUX–2018–098; Scale bars: 0.5 mm.

without distinct annulations. Superior tarsal claws of anterior legs with 3 or 4 teeth, of posteriors with 4. Measurements: leg I 15.73 (4.42 + 1.39 + 3.78 + 3.80 + 2.34), leg II 16.16 (4.31 + 1.36 + 3.49 + 4.38 + 2.62), leg III 18.09 (4.15 + 1.34 + 4.16 + 5.68 + 2.76), leg IV 23.69 (5.66 + 1.57 + 5.18 + 7.66 + 3.62).

Palp: Tibial apophysis very broad at base, with four long, stouter setae with similar lengths and a few short spines (Figs 3A–C, H–J, 4A–C); paracymbium wide, with

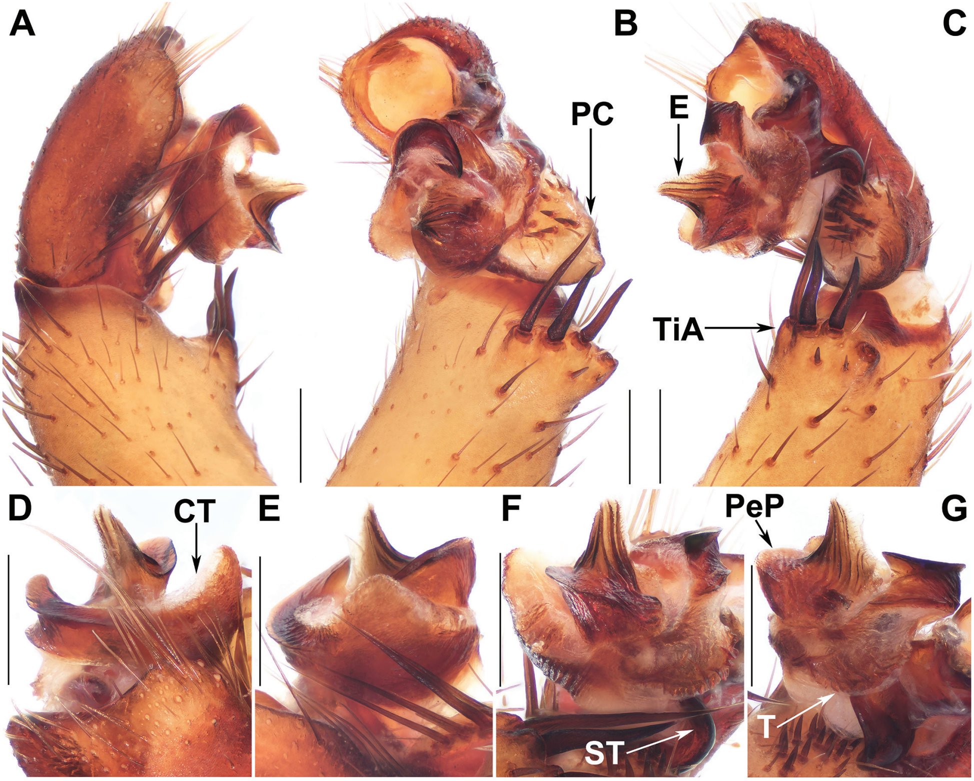

Figure 4. Male genital anatomy of *Liphistius pyinoolwin* sp. nov. (specimens from AMNH, collected by W. Sedgwick) **A** palp prolateral view **B** palp ventral view **C** palp retrolateral view **D–G** palp distal view **A–G** AMNH_IZC 00356855; Scale bars: 0.5 mm.

pointed lateral process and many setae situated at the tip, and several tapering spines on the plane cumulus (Figs 3A, B, H, I, 4A); subtegular apophysis well developed (Figs 3C, F, J, 4F, G); contrategulum with a conical, short, blunt-tipped process (Figs 3D–F, 4E), distal edge widely arched, with a smooth sharp projection (Figs 3B, D, F, G, 4F, G); tegulum small, with a slightly dentated margin (Figs 3C, F, J, 4F, G); paraembolic plate short, widely rounded (Figs 3A–J, 4E–G); embolus short conical, basally sclerotized, with 6 longitudinal ridges that reach the tip, embolic parts adjacent (Figs 3A–J, 4C–G).

Female (XUX–2018–094, Fig. 2D). Total length, excluding chelicerae, 10.40. Carapace 4.79 long, 4.72 wide, light brown, furnished with few short, scattered bristles (Fig. 2D). Eight eyes on darkened ocular tubercle, ALE > PLE > PME > AME. Eye sizes and interdistances: AME 0.06, ALE 0.45, PME 0.19, PLE 0.35; AME–AME 0.08, AME–ALE 0.10, PME–PME 0.05, PME–PLE 0.10, ALE–PLE 0.05, ALE–ALE 0.10, PLE–PLE 0.33, AME–PME 0.06. Chelicerae light and glabrous proximally, robust, dark brown; promargin of chelicerae groove with 11–12 denticles of variable size. Labium 0.59 long, 1.25 wide. Sternum 2.55 long, 1.23 wide, light brown with several

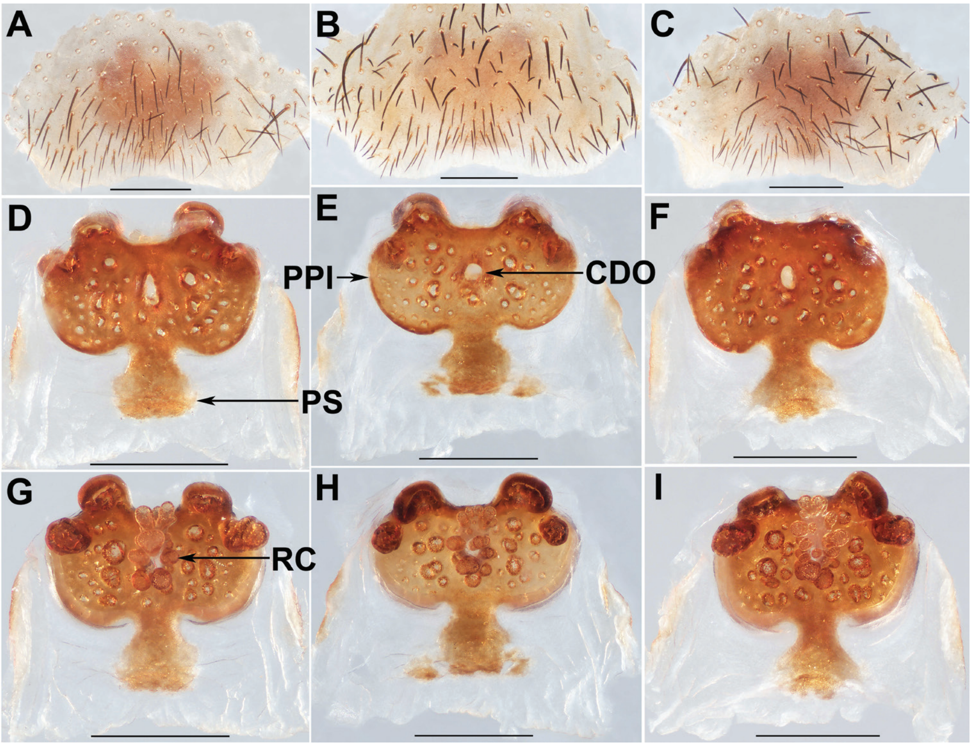

Figure 5. Female genital anatomy of *Liphistius pyinoolwin* sp. nov. **A–C** plate ventral view **D–F** vulva dorsal view **G–I** vulva ventral view **A, D, G** XUX–2018–094 **B, E, H** XUX–2018–096 **C, F, I** XUX–2018–104; Scale bars: 0.5 mm.

setae. Opisthosoma 5.44 long, 3.84 wide, brown, with 12 tergites, and 8 spinnerets. Legs brown with strong hairs and spines, long and short black sparse setae, with three tarsal claws. Measurements: palp 7.89 (2.84 + 1.05 + 1.98 + 2.02), leg I 10.16 (3.33 + 1.32 + 2.22 + 1.90 + 1.39), leg II 9.95 (3.15 + 1.07 + 2.14 + 2.03 + 1.56), leg III 11.10 (3.18 + 1.19 + 2.55 + 2.58 + 1.60), leg IV 15.60 (4.41 + 1.24 + 3.53 + 3.91 + 2.51).

Female genitalia: Posterior margin of genital sternite curved (Figs 5A–C, 6A–C, 7A); approximately rectangular poreplate wider than long, with a pair of large, well separated anterior lobes and a pair of small anterolateral lobes; the anterior lobes very close to the anterolateral lobes (Figs 5D–I, 6D–I, 7B–I); transition between poreplate and posterior stalk distinct (Figs 5D–I, 6D, E, G, H, 7B–I); posterior stalk long, narrow; racemose receptacular cluster long and narrow, central dorsal opening sphere-shaped (Figs 5D–F, 6D–F, 7D–F).

Etymology. The species epithet "pyinoolwin" is a toponym referring to the type locality.

Distribution. Myanmar (Mandalay Region).

Variation. Body size: males (*N*=8): BL 8.63–13.95, CL 4.23–6.03, CW 4.87–6.17, OL 3.76–6.71, OW 2.85–5.17; females (*N*=15): BL 10.40–14.21, CL

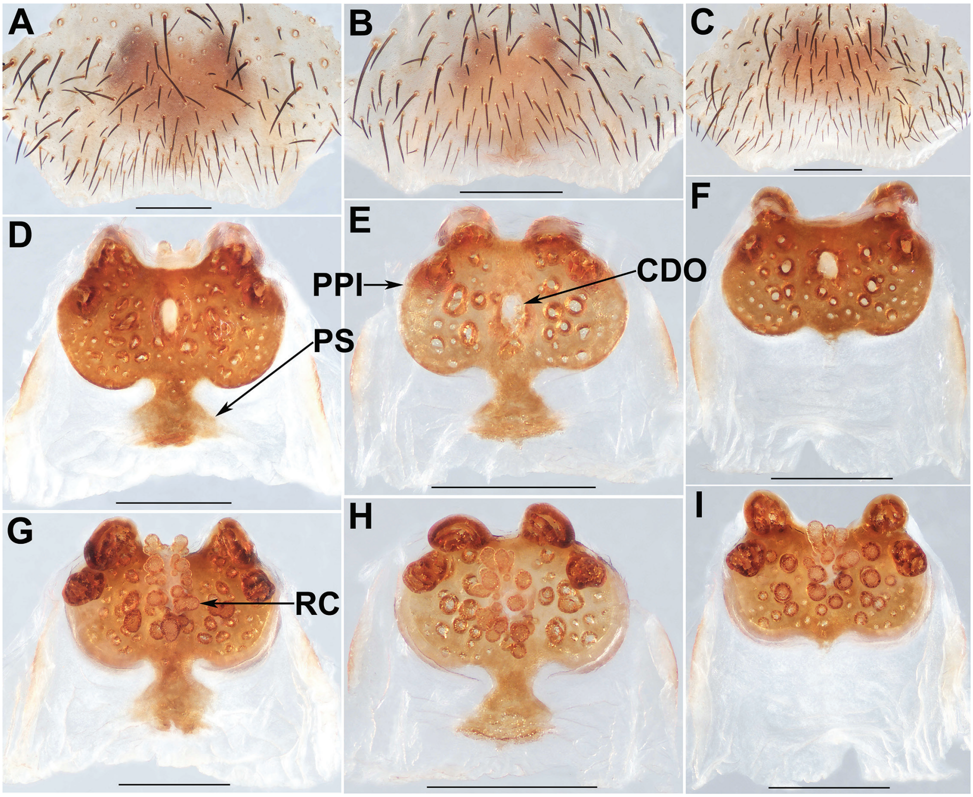

Figure 6. Female genital anatomy of *Liphistius pyinoolwin* sp. nov. **A–C** plate ventral view **D–F** vulva dorsal view **G–I** vulva ventral view **A, D, G** XUX–2018–105 **B, E, H** XUX–2018–109 **C, F, I** XUX–2018–110; Scale bars: 0.5 mm.

4.79–6.37, CW 4.55–5.91, OL 5.44–8.10, OW 3.84–6.27; The examined females have different genitalia, including the specimen XUX–2018–110, which lack the posterior stalk (Fig. 6F, 6I); the shape of the anterior and anterolateral lobes of the poreplate is variable (Figs 5G–I, 6G–I, 7C, 7G–I); In some specimens, the receptacular cluster is beyond the anterior margin of the poreplate dorsally (Figs 5D, 6D, 7A, D, E), whereas in others are not (Figs 5E, F, 6E, F, 7B, F), and the size and shape of the receptacular cluster may be slightly different (Figs 5G–I, 6G–I, C, G–I); the shape and size of the central dorsal opening are also variable (Figs 5D–F, 6D–F, 7B, D–F).

Remarks. We examined 8 males and 15 females collected from Pyin Oo Lwin by us, as well as 1 male and 4 females collected by W. Sedgwick on 13 July 1982, which were used to redescribe *L. birmanicus* by Platnick and Sedgwick (1984) and reviewed by Schwendinger (1990). After examined the male and females collected by W. Sedgwick, even though the male palp was distorted (Fig. 4A–C), we can still identify it as the same as the descriptions and illustrations by Platnick and Sedgwick (1984), and the same as the males and females collected by us at Pyin Oo Lwin.

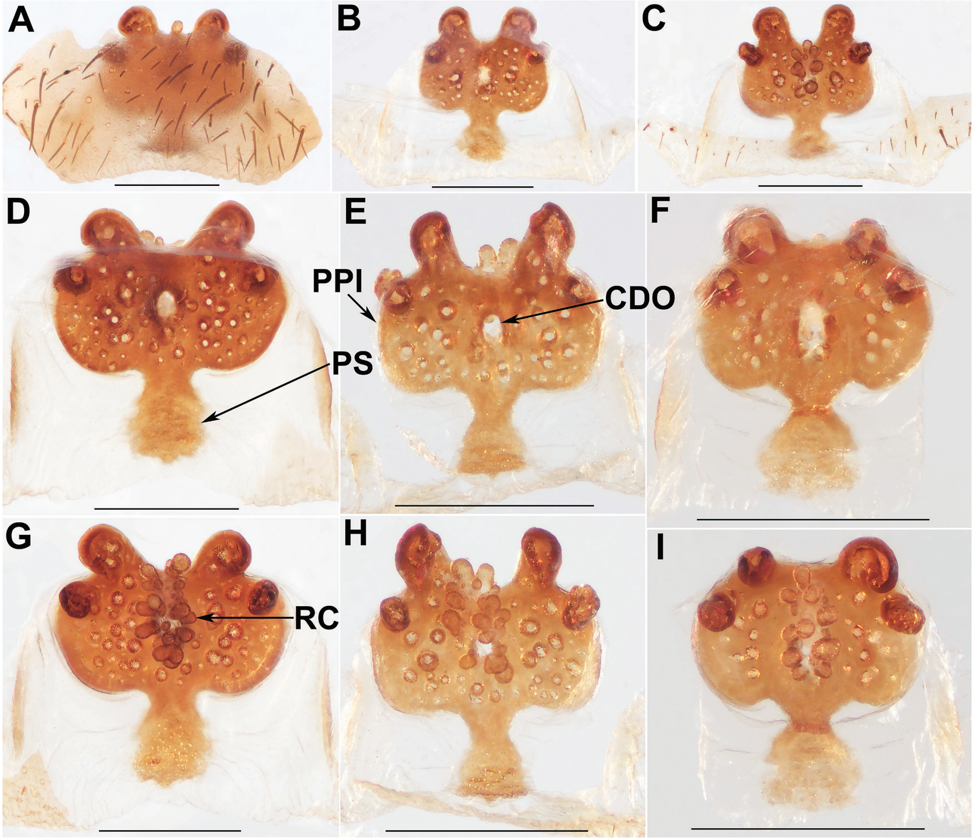

Figure 7. Female genital anatomy of *Liphistius pyinoolwin* sp. nov. (specimens from AMNH, collected by W. Sedgwick) **A** plate ventral view **B, D–F** vulva dorsal view **C, G–I** vulva ventral view **A, D, G** AMNH_IZC 00356859 **B, C** AMNH_IZC 00356856 **E, H** AMNH_IZC 00356857 **F, I** AMNH_IZC 00356858; Scale bars: 0.5 mm.

***Liphistius birmanicus* Thorell, 1897**

Figs 2, 8–10

Liphistius birmanicus Thorell, 1897: 162 (♀, from Yadò, Kayin State, Myanmar; alt. 1200–1300 m; 1885–1889, collected by L. Fea; deposited in MCSNG, examined); Pocock, 1900: 156; Bristowe, 1933: 1029; Haupt, 1983: 280.

Material examined. Mynamar · 7♀♀; Kayin State, Than Taung township, Yadò; 19.33°N, 96.81°E; alt. 1062–1090 m; ARAMYN–496, 497, 498, 501, 504, 505, 506; 2♂♂, 3♀♀; Kayin State, Kalekho Atet township; 19.31°N, 96.75°E; alt. 554–564 m; 15 November 2018; D. Li and L. Yu leg.; ARAMYN–090, 091, 092, 095, 096. ***Other material*:** Mynamar · 1♀ (lectotype); Kayin State (formerly Kayah State: Platnick and Sedgwick 1984; Karen State: Schwendinger 1990), Yadò, Mt. Chebà; alt. 1200–1300 m; 1885–1889; L. Fea leg. (MCSNG; examined).

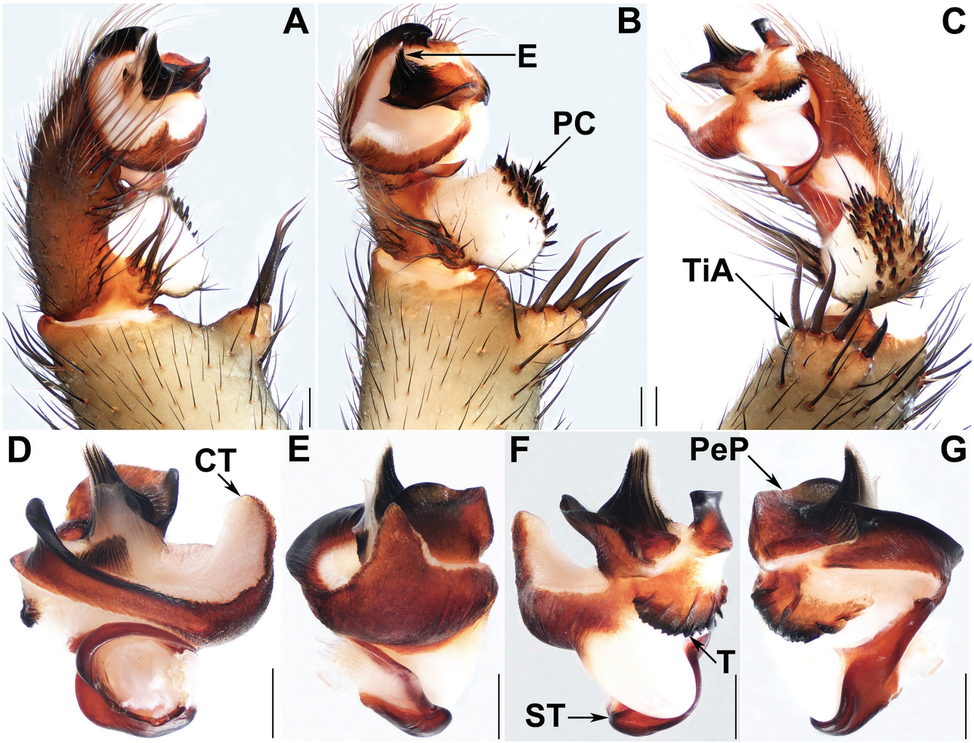

Figure 8. Male genital anatomy of *Liphistius birmanicus* (Thorell, 1897) **A** palp prolateral view **B** palp ventral view **C** palp retrolateral view **D–G** palp distal view **A–C** ARAMYN–096 **D–G** ARAMYN–092; Scale bars: 0.5 mm.

Diagnosis. Males of *L. birmanicus* can be distinguished from those of *L. pyinoolwin* sp. nov. by the lack of the lateral process of the paracymbium (Fig. 8A–C), the cumulus slightly raised (Fig. 8B); the wider paraembolic plate (Fig. 8B, C, F), the narrower, longer contrategular process (Fig. 8D–F), and the slightly smaller tibial apophysis (Fig. 8A–C); differ from those of *L. pinlaung* by the larger tibial apophysis (Fig. 8A–C), and by the raised cumulus with shorter setae (Fig. 8A, B); from those of *L. lahu* by the larger paraembolic plate and the cumulus with shorter setae (Fig. 8B); from those of *L. lordae* by the wider tibial apophysis at base (Fig. 8A, B), and the raised cumulus with shorter, less regularly arranged setae (Fig. 8B); Females of *L. birmanicus* resemble those of *L. hpruso*, *L. pinlaung* and *L. pyinoolwin* sp. nov. by the poreplate with two pair of lobes but can be distinguished from those of *L. hpruso* and *L. pyinoolwin* sp. nov. by the broad posterior stalk and the poreplate slightly longer than wide (Figs 9D–I, 10C–G); from those of *L. pinlaung* by the broader, axe-blade-shaped posterior stalk and the smaller anterolateral lobes of the poreplate (Figs 9C–I, 10E, F); from those of the other *Liphistius* by the poreplate with four anterior lobes (Figs 9G–I, 10E–F).

Description. ***Male*** (ARAMYN–096, Fig. 2J). Total length, excluding chelicerae, 19.90. Carapace 9.50 long and 9.45 wide, black, furnished with few short, scattered

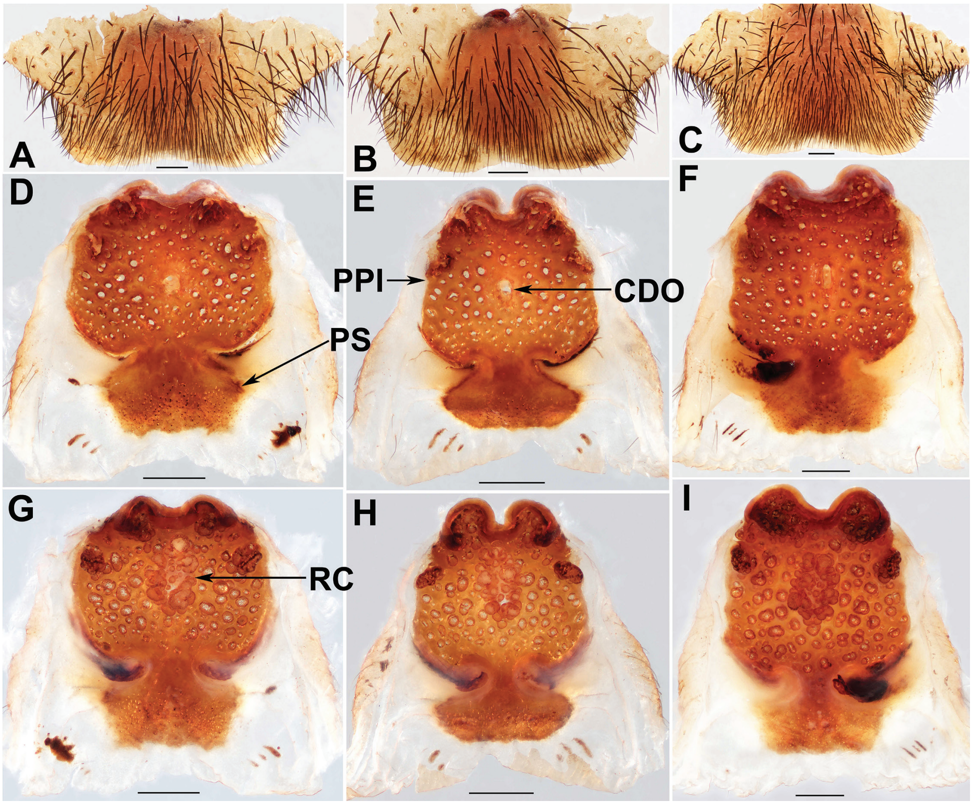

Figure 9. Female genital anatomy of *Liphistius birmanicus* (Thorell, 1897) **A–C** plate ventral view **D–F** vulva dorsal view **G–I** vulva ventral view **A, D, G** ARAMYN–497 **B, E, H** ARAMYN–501 **C, F, I** ARAMYN–506; Scale bars: 0.5 mm.

bristles. ALE>PLE>PME>AME, eye sizes and interdistances: AME 0.14, ALE 0.91, PME 0.33, PLE 0.62, AME–AME 0.11, AME–ALE 0.16, PME–PME 0.09, PME–PLE 0.15, ALE–PLE 0.09, ALE–ALE 0.18, PLE–PLE 0.45, AME–PME 0.06. Chelicerae robust, promargin of chelicerae groove with 11 denticles of variable size. Labium 1.01 long and 1.38 wide, wider than long, fused with sternum. Sternum 4.82 long and 1.12 wide, longer than wide, and strong spined, elongated anterior and posterior tip. Opisthosoma 9.67 long and 7.39 wide, with 12 black tergites, the fifth largest, 8 spinnerets. Legs with strong hairs and spines. Measurements: leg I 16.99 (4.32 + 2.55 + 3.55 + 4.66 + 1.92), leg II 18.06 (4.32 + 2.41 + 3.74 + 5.18 + 2.41), leg III 18.46 (4.44 + 1.85 + 2.83 + 6.68 + 2.66), leg IV 20.40 (3.56 + 1.52 + 4.25 + 8.46 + 2.63).

Palp: Tibial apophysis with four long setae with different lengths (Fig. 8B, C), paracymbium large, wide, with many setae at the tip and several tapering spines on the slightly raised cumulus (Fig. 8A–C); subtegular apophysis well developed (Fig. 8C, F); contrategulum with a triangular process, distal edge widely arched, with a smooth sharp projection (Fig. 8D, E, F); tegulum small, terminal apophysis with finely dentated margin (Fig. 8C, F, G); paraembolic plate base wide with a curved margin (Fig. 8D, G); embolus long and conical, basally sclerotized, with 7 longitudinal ridges that reach the tip, embolic parts adjacent (Fig. 8D–G).

Female (ARAMYN–091). Total length, excluding chelicerae, 22.50. Carapace 11.88 long and 11.06 wide, reddish black, furnished with few short, scattered bristles. Eight eyes on darkened ocular tubercle, ALE > PLE > PME > AME, eye size and interdistances: AME 0.16, ALE 0.92, PME 0.38, PLE 0.71, AME–AME 0.13, AME–ALE 0.18, PME–PME 0.15, PME–PLE 0.12, ALE–PLE 0.09, ALE–ALE 0.20, PLE–PLE 0.68, AME–PME 0.13. Chelicerae proximally glabrous, robust, reddish black; promargin of chelicerae groove with 11 strong denticles of variable size. Labium 1.40 long, 2.01 wide. Sternum 4.42 long, 1.68 wide, strong spined, elongated posterior tip. Opisthosoma 10.46 long, 8.31 wide, black, with 12 tergites, the fifth largest, and 8 spinnerets (Fig. 2I). Legs reddish black with strong hairs and spines, long and short black sparse setae, legs each with three tarsal claws. Measurements: palp 16.92 (6.17 + 2.32 + 4.82 + 3.61), leg I 23.27 (7.81 + 2.78 + 5.38 + 4.65 + 2.65), leg II 24.41 (7.85 + 2.85 + 5.57 + 5.32 + 2.82), leg III 26.88 (7.82 + 3.01 + 5.97 + 6.52 + 3.56), leg IV 35.45 (10.11 + 2.13 + 7.85 + 10.82 + 4.54).

Female genitalia: Posterior margin of genital sternite slightly curved (Figs 9A–C, 10A, H); poreplate almost squared, with a pair of large anterior lobes and a pair of small anterolateral lobes (Figs 9G–I, 10E, F); anterior and anterolateral lobes well separated (Figs 9G–I, 10E, F); indistinct transition between the poreplate and posterior stalk (Figs 9D–I, 10D); posterior stalk broad, large, constricted at base, axe-blade-shaped (Figs 9D–I, 10C–G); racemose receptacular cluster large (Figs 9G–I, 10E, F); central dorsal opening small, spheric (Figs 9D–F, 10C, D, F).

Distribution. Myanmar (Than Taung and Kalekho Atet townships, Kayin State).

Variation. Body size: males (*N*=2): BL 18.58–19.90, CL 9.05–9.50, CW 8.01–9.45, OL 9.08–9.67, OW 6.95–7.39; females (*N*=10): BL 14.45–25.95, CL 6.41–12.26, CW 5.45–12.71, OL 7.65–17.09, OW 6.47–14.76; in ventral view, the shape of the transition between poreplate and posterior stalk is different between the specimens ARAMYN–497, 501, 506 (Fig. 9) and ARAMYN–091, 095 (Fig. 10C–F); anterior lobes larger and close to each other (ARAMYN–501, Fig. 9E, H) compared to other specimens (Figs 9G, I, 10E, F); the size and shape of the receptacular cluster are different (Figs 9G–I, 10E, F); and the shape of central dorsal opening is also variable (Figs 9D–F, 10C, D, G).

Remarks. Only 4 specimens were collected from Myanmar before 1984, all of them identified as *L. birmanicus* in the literature. One female and two juvenile specimens were collected from Yadò and Biapò by Leonardo Fea, most likely in the years of 1887–1888 (Fea 1888) during his expedition to Karen Hills or Kayah-Karen Mountains (Bolotov et al. 2019). These 3 specimens were deposited in MCSNG, Italy. The adult female used to be described as *L. birmanicus* by Thorell in 1897, then redescribed by Pocock (1990), Bristowe (1932), and illustrated by Haupt (1983). Two juvenile specimens were only mentioned in Thorell's description (1897) and have never been mentioned since then. The fourth specimen, an immature male collected from Mawlamyine, was first

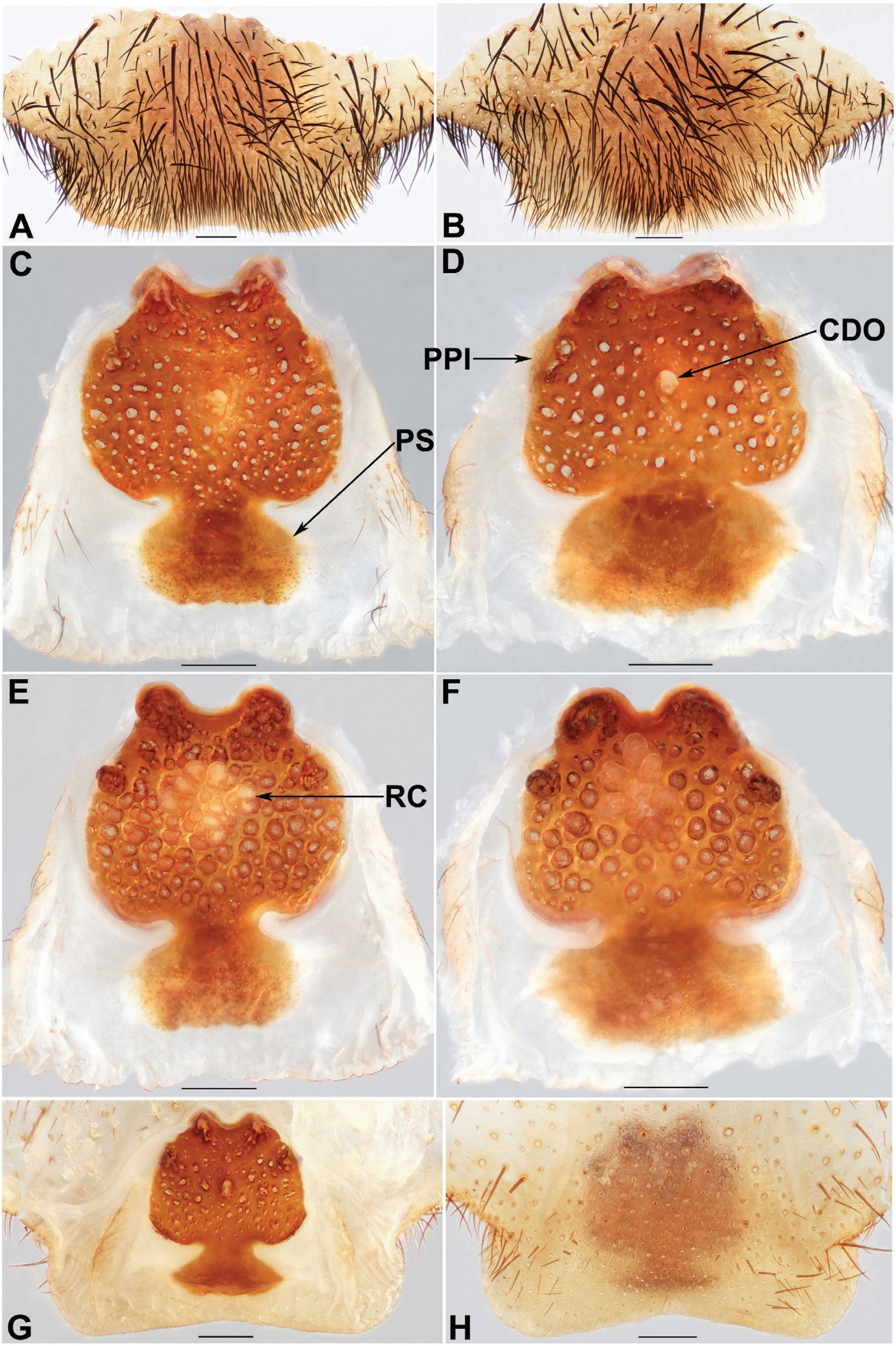

Figure 10. Female genital anatomy of *Liphistius birmanicus* (Thorell, 1897) **A, B** plate ventral view **C, D, G** vulva dorsal view **E, F, H** vulva ventral view **A, C, E** ARAMYN–091 **B, D, F** ARAMYN–095 **G, H** lectotype (specimen from MCSNG, collected by L. Fea); Scale bars: 0.5 mm.

mentioned by Gravely (1915), and considered as *L. birmanicus* by Bristowe (1938). However, Schwendinger (1990) questioned its status, as do we, because the geographic locality is very far from the type locality, Yadò, and it is immature. Nevertheless, new specimens from Mawlamyine are needed to resolve this issue in the future.

One specimen collected outside Myanmar was identified as *L. birmanicus*, but it is actually not a *Liphistius*. Berlard (1932: figure 443) illustrated and assigned a male to *L. birmanicus*, which was collected from the forest of Kha-16, Tonkin, in the district of Song-Luc-Nam, Vietnam. It is obviously not a *Liphistius* since it lacks a palpal tibial apophysis. Simon (1908) first identified it as *L. birmanicus*, but Bristowe (1933) described it as a distinct species, *L. tonkinensis*, presently *Vinathela tonkinensis* (Bristowe, 1933) (Xu et al. 2015a; World Spider Catalog 2021).

Platnick and Sedgwick (1984) provided illustrations and detailed descriptions of *L. birmanicus* after examining the lectotype from Yadò (deposited in MCSNG). Their descriptions of male and female were based on the specimens collected from Pyin Oo Lwin by W. Sedgwick instead of the lectotype. Schwendinger (1990) also provided illustrations and assigned those Pyin Oo Lwin specimens to *L. birmanicus*. As they had noticed, compared to Pyin Oo Lwin females, the female lectotype is much larger (Platnick and Sedgwick 1984; Schwendinger 1990), although the body size is not usually used for identifying a species. Moreover, the poreplate of the lectotype possesses relatively smaller anterior lobes and a much wider posterior stalk as illustrated in Haupt (1983). Thus, we treated the Pyin Oo Lwin specimens as a distinct species, here described as *L. pyinoolwin* sp. nov..

Relationships. *Liphistius pyinoolwin* sp. nov. belongs to the *birmanicus*-group that currently contains *L. birmanicus*, *L. hpruso*, *L. lordae*, *L. lahu*, and *L. pinlaung* based on the male and female genital morphology. Since Schwendinger (1998) provided a detailed discussion about the shared characters among the group members, we give two additional characters within the group here. The *birmanicus*-group can be divided into two types, one including *L. birmanicus*, *L. hpruso*, *L. pinlaung*, and *L. pyinoolwin* sp. nov., the other including *L. lahu* and *L. lordae*, based on the following synapomorphies: female poreplate of the former four species has four anterior lobes, while female poreplate of the latter two species has only two anterior lobes (Figs 5, 6, 7, 9, 10); the male palp of the former four species has shorter, less regularly arranged setae on the cumulus, and a wider tibial apophysis at base compared with the latter two species (Figs 3A, B, 8A, B).

Acknowledgements

We are deeply indebted to Mr. San Yu, the Yadò Village Head for his permit to stay and collect spiders in the village, for the hospitality from him and his family, and for his assistance in the field. Special thanks to Mr. Thwin Maung Maung , Ko Poo and the drivers for their help in the field in Yadò (Kayin State). We greatly appreciate Prof. Thida Lay Thwe for her advice and support, and Prof. U Moe Moe Dwe for his help in the field. We are also grateful to Dr Ko Myint for his help with the applications for research and spider export permits. We thank Fred Jaya, Alexandre Bragio Bonaldo and an anonymous reviewer for helping edit the language and their constructive comments on the manuscript. We would also like to thank Myanmar Department of Forestry for research permit (NGA/CITES/9/6825/2018) and spider export permit (NWCD/CITES/9/8038/2018) as well as Agri-Food & Veterinary Authority (AVA) of Singapore for spider import permits. We also thank Prof. Lorenzo Prendini and Louis Sorkin (AMNH) and Dr. Maria Tavano (MCSNG) for kindly providing specimens for comparison. This study was supported by the grants from the National Natural Sciences Foundation of China (NSFC) (31272324; 32070430), the Singapore Ministry of Education AcRF Tier 1 grant (R-154-000-A52-114), ASEAN University Network funding, and Special PhD Program on Zoology from Hubei University.

References

Aung KPP, Xu X, Lwin WW, Sang MZ, Yu L, Liu H, Liu FX, Li D (2019) Two new species of the primitively segmented spider genus *Liphistius* Schiödte, 1849 (Mesothelae, Liphistiidae) from Myanmar. Zookeys 882: 29–39. https://doi.org/10.3897/zookeys.882.38811

Bolotov IN, Vikhrev IV, Lopes-Lima M, Gofarov MY, Konopleva ES, Lyubas AA, Lunn Z, Chan N, Bogan AE (2019) *Unio sella* and *U. sula*: a review of enigmatic taxonomic names linked to *Gibbosula laosensis* (Lea, 1863) (Bivalvia: Margaritiferidae: Gibbosulinae). Raffles Bulletin of Zoology 67: 440–447.

Bristowe WS (1933) The liphistiid spiders. With an appendix on their internal anatomy by J. Millot. Proceedings of Zoological Society of London 102: 1015–1057. https://doi.org/10.1111/j.1096-3642.1932.tb01575.x

Bristowe WS (1938) A supplementary note on the liphistiid spiders. Proceedings of Zoological Society of London (B) 108: 661–662.

Bristowe WS (1975) A family of living fossil spiders. Endeavour 34: 115–117. https://doi.org/10.1016/0160-9327(75)90130-1

Coddington JA, Levi HW (1991) Systematics and evolution of spiders (Araneae). Annual Review of Ecology and Systematics 22: 565–592. https://doi.org/10.1146/annurev.es.22.110191.003025

Fea L (1888) Net Carin Indipendenti (con una Cartina nel testo e due disegni). Estratto dal Bollettino della Societa Geografica Italyana 1888: 1–15.

Gravely FH (1915) Notes on Indian mygalomorph spiders. Records of the Indian Museum, Calcutta 11: 257–287.

Haupt J (1983) Vergleichende Morphologie der Genitalorgane und Phylogenie der liphistiomorphen Webspinnen (Araneae: Mesothelae). I. Revision der bisher bekannten Arten. Zeitschrift für Zoologische Systematik und Evolutionsforschung 21: 275–293. https://doi.org/10.1111/j.1439-0469.1983.tb00296.x

Haupt J (2003) The Mesothelae – monograph of an exceptional group of spiders (Araneae: Mesothelae) (Morphology, behaviour, ecology, taxonomy, distribution and phylogeny). Zoologica 154: 1–102.

Ono H, Aung MM (2020) A new species of the genus Liphistius (Araneae: Mesothelae) from Lampi Island, Tanintharyi Region, Southern Myanmar. Bulletin of the National Museum of Nature and Science Tokyo (A) 46: 89–95.

Platnick NI, Gertsch WJ (1976) The suborders of spiders: a cladistic analysis (Arachnida, Araneae). American Museum Novitates 2607: 1–15.

Platnick NI, Sedgwick WC (1984) A revision of the spider genus *Liphistius* (Araneae, Mesothelae). American Museum Novitates 2781: 1–31.

Pocock RI (1900) The Fauna of British India, Including Ceylon and Burma. Taylor & Francis, London, 279 pp.

Schiödte JC (1849) Om en afvigende Slægt af Spindlernes Orden. Naturhistorisk Tidsskrift 2: 617–624.

Schwendinger PJ (1990) On the spider genus *Liphistius* (Araneae: Mesothelae) in Thailand and Burma. Zoologica Scripta 19: 331–351. https://doi.org/10.1111/j.1463-6409.1990.tb00262.x

Schwendinger PJ (1998) Five new *Liphistius* species (Araneae, Mesothelae) from Thailand. Zoologica Scripta 27: 17–30. https://doi.org/10.1111/j.1463-6409.1998.tb00426.x

Schwendinger PJ, Syuhadah N, Lehmann-Graber C, Price L, Huber S, Hashim R, Bhassu S, Monod L (2019) A revision of the trapdoor spider genus *Liphistius* (Mesothelae: Liphistiidae) in Peninsular Malaysia; part 2. Revue Suisse de Zoologie 126(2): 321–353. https://doi.org/10.35929/RSZ.0017

Thorell T (1869) On European spiders. Part I. Review of the European genera of spiders, preceded by some observations on zoological nomenclature. Nova Acta Regiae Societatis Scientiarum Upsaliensis 7(3): 1–108.

World Spider Catalog (2021) World Spider Catalog, Version 22.0. Natural History Museum Bern. http://wsc.nmbe.ch [access on 11 March 202]

Wunderlich J (2017) New and rare fossil spiders (Araneae) in mid Cretaceous amber from Myanmar (Burma), including the description of new extinct families of the suborders Mesothelae and Opisthothelae as well as notes on the taxonomy, the evolution and the biogeography of the Mesothelae. In: Wunderlich J (Ed.) Ten Papers on Fossil and Extant Spiders (Araneae). Beiträge zur Araneologie, Hirschberg, 72–279.

Wunderlich J (2019) What is a spider? Cretaceous fossils modify strongly phylogenetics as well as diagnoses of families, superfamilies and even suborders of spiders (Araneida) and other arthropods. Beiträge zur Araneologie 12: 1–32.

Xu X, Liu FX, Chen J, Ono H, Li D, Kuntner M (2015a) A genus level taxonomic review of primitively segmented spiders (Mesothelae, Liphistiidae). ZooKeys 488: 121–151. https://doi.org/10.3897/zookeys.488.8726

Xu X, Liu FX, Cheng R-C, Chen J, Xu X, Zhang ZS, Ono H, Pham DS, Norma-Rashid Y, Arnedo MA, Kuntner M, Li D (2015b) Extant primitively segmented spiders have recently diversified from an ancient lineage. Proceedings of the Royal Society B: Biological Sciences 282: e20142486. https://doi.org/10.1098/rspb.2014.2486

ZooKeys 1031: 59–84 (2021)
doi: 10.3897/zookeys.1031.60129
https://zookeys.pensoft.net

RESEARCH ARTICLE

A peer-reviewed open-access journal
ZooKeys
Launched to accelerate biodiversity research

Natural history of *Platypria* (*Platypria*) *hystrix* (Fabricius, 1798) on Fabaceae host plants, with notes on other *Platypria* species in India (Chrysomelidae, Cassidinae, Hispini)

Sachin Ranade[1], Kaniyarikkal Divakaran Prathapan[2],
Hemant V. Ghate[3], Caroline S. Chaboo[4]

1 *Bombay Natural History Society, Vulture Conservation Breeding Center, Rani – 781131, Kamrup District, Assam, India* **2** *Department of Entomology, Kerala Agricultural University, Vellayani P. O., Trivandrum – 695 522, Kerala, India* **3** *Post-Graduate Research Centre, Department of Zoology, Modern College of Arts, Science and Commerce, Shivajinagar, Pune 411 005, India* **4** *University of Nebraska State Museum, Systematics Research Collections, W436 Nebraska Hall, University of Nebraska, Lincoln, Nebraska 68588-0514, USA.*

Corresponding author: Caroline S. Chaboo (cchaboo2@unl.edu)

Academic editor: M. Schmitt | Received 29 October 2020 | Accepted 7 March 2021 | Published 14 April 2021

http://zoobank.org/52D90B93-3285-48ED-AE49-BE6AA1338693

Citation: Ranade S, Prathapan KD, Ghate HV, Chaboo CS (2021) Natural history of *Platypria* (*Platypria*) *hystrix* (Fabricius, 1798) on Fabaceae host plants, with notes on other *Platypria* species in India (Chrysomelidae, Cassidinae, Hispini). ZooKeys 1031: 59–84. https://doi.org/10.3897/zookeys.1031.60129

Abstract

The leaf-beetle genus *Platypria* Guérin-Méneville, 1840 comprises two subgenera and 34 species (Chrysomelidae: Cassidinae: Hispini). Host plants are documented for eight species and indicate mostly perennial species of Fabaceae and Rhamnaceae. Larvae and pupae have been documented for two *Platypria* species. This paper presents novel natural history data, based on a field study of populations of *Platypria* (*Platypria*) *hystrix* (Fabricius, 1798) on *Erythrina stricta* Roxb. and *Pueraria phaseoloides* (Roxb.) Benth. in Kerala, south India and on *Erythrina variegata* L., *Pueraria montana* var. *lobata* (Willd.) Maes. & S. Almeida and *Mucuna pruriens* (L) DC in Assam, northeast India. Three new Fabaceae hosts are reported for *P.* (*P.*) *hystrix*. Brief notes and new host records, based on field observations, are also provided for the other three species of *Platypria* in India – *P.* (*P.*) *chiroptera* Gestro, 1899, *P.* (*P.*) *echidna* Guérin-Méneville, 1840 and *P.* (*P.*) *erinaceus* (Fabricius, 1801). *Platypria* females slit the leaf to lay a single egg which is covered with secretions that harden as an ootheca, the egg covering in Cassidinae *s. l.* There are five larval stages, each with the typical 'hispine' mining form and behaviour – a flattened cream-coloured body, chitinised head capsule and claws, and feeding on mesophyll and leaving irregular blotch mines on the host leaves. Pupation occurs in an independent pupal mine and lasts about a week. These observations suggest new potential phylogenetic character hypotheses that can stimulate better data collection on leaf-mining Cassidinae and help resolve evolutionary patterns amongst these basal mining genera.

Keywords

Leaf miner, life history, hispine, *Erythrina*, *Gouania*, *Mucuna*, *Pueraria*, *Ziziphus*

Introduction

The Old World cassidine tribe Hispini Gyllenhal, 1813 (Coleoptera: Chrysomelidae: Cassidinae) currently comprises 25 genera and 627 species, including three fossil species (Staines 2015). Tribal monophyly is well-supported by the distinct long stiff spines on the pronotum and elytra (Würmli 1975; Chen et al. 1986), particularly the spinose lateral elytral edges (Chaboo 2007:179).

The genus *Platypria* Guérin-Méneville, 1840 comprises two subgenera (*Platypria*, *Dichirispa*) and 34 species (Staines 2015). The two subgenera are separated by the elytra margins expanded both at the humeri and posteriorly, with long spines and with "windows" in the nominotypical subgenus (fenestrate; Würmli 1975, 1978). This paper focuses on four species found in India (Fig. 1). Adults of Indian *Platypria* are morphologically distinct (Figs 2–5): the body is oblong, but the margins of the pronotum and elytra are expanded into broad rounded lobes and have prominent spinose extensions (Maulik 1919; Uhmann 1954b; Würmli 1975). The antenna has nine antennomeres, as the last three are apparently fused (Maulik 1919). *Platypria* is distributed across the Afrotropical and Oriental Regions. Hosts are known for eight of the 34 species in the genus (Table 1). Kalshoven (1957) noted that *Platypria* is amongst a few Oriental hispine genera atypically associated with eudicotyledonous plants, often belonging to unrelated families; other such genera are *Notosacantha* Chevrolat, 1837 (Rane et al. 2000), *Oncocephala* Agassiz 1846 (Calcetas et al. 2020), *Dactylispa*, *Dicladispa*, *Hispa* and *Monohispa* (Staines 2015).

Juveniles were briefly noted for *P.* (*P.*) *erinaceus* (Fabricius, 1801) (= *P.* (*P.*) *andrewesi* in Beeson 1941, Uhmann 1957, 1958b), *P.* (*Dichirispa*) *coronata* (Guérin-Méneville, 1840) (Uhmann 1958a) and *P.* (*P.*) *melli* Uhmann, 1954a (Chen 1982). Larvae and pupae of *P.* (*P.*) *melli* were further studied on *Hovenia acerba* Lindl. (Rhamnaceae) by Liao et al. (2014). *Platypria* species have been reported as pests of pear and plum (Chen 1982; Qi et al. 1995) and soybean in China (Kezhen 1992) and as minor pests of trees and shrubs of Fabaceae and Rhamnaceae (Kalshoven 1957). The pest status has been confirmed by others (Ayyar 1940; Mathur and Singh 1959; Nair 1986; Balikai 1999; Rani and Sridhar 2004; Liu et al. 2019).

Four species of *Platypria* have been documented in India (Staines 2015): *P.* (*P.*) *chiroptera* Gestro, 1899 (Fig. 2), *P.* (*P.*) *echidna* Guérin-Méneville, 1840 (Fig. 3), *P.* (*P.*) *erinaceus* (Fabricius, 1801) (Fig. 4) and *P.* (*P.*) *hystrix* Maulik, 1919 (Fig. 5). Maulik (1919) indicated seven species, but some have since been synonymised. Würmli (1975) recorded *P.* (*P.*) *fenestrata* Pic, 1924, which occurs in China and Vietnam, from

1

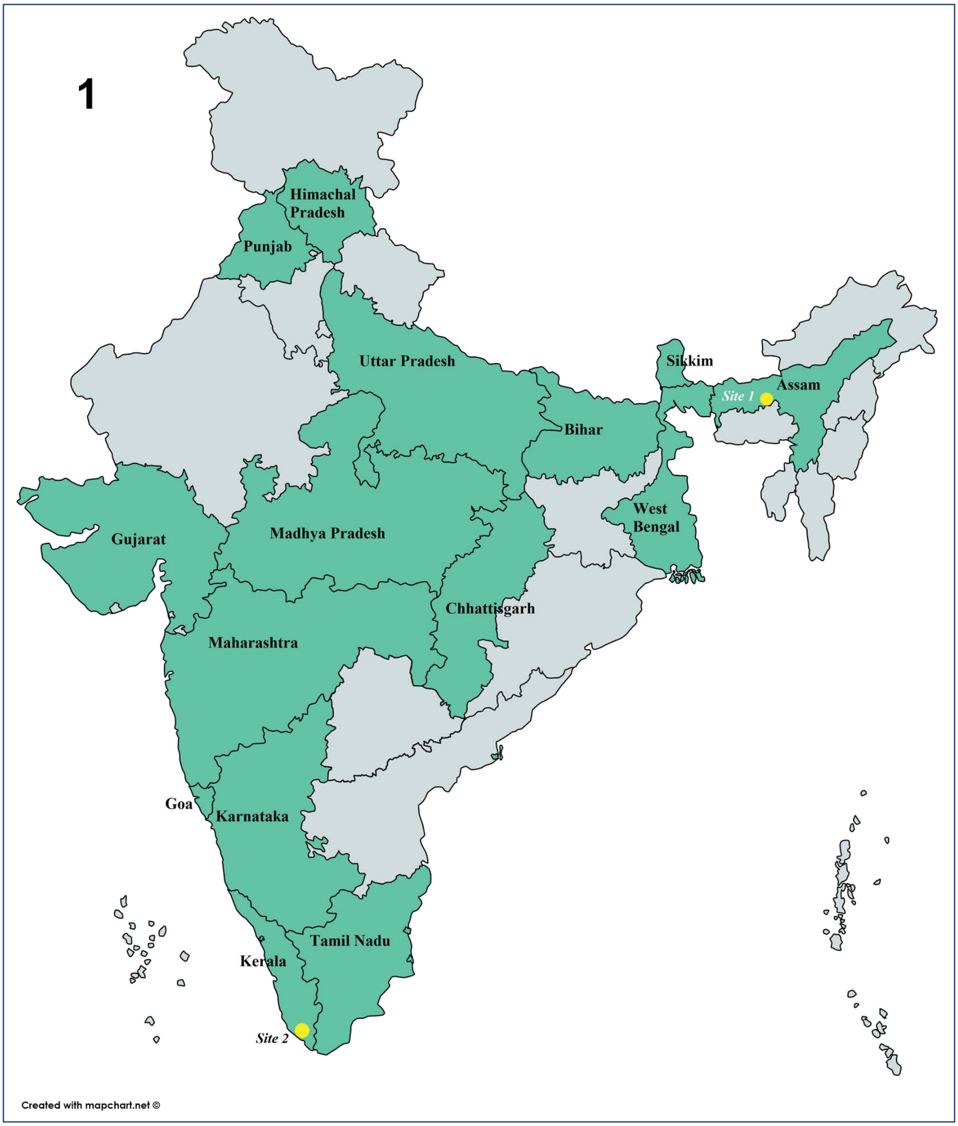

Figure 1. Map showing distribution of *Platypria* in India by state (in green) and our two field sites (yellow circles).

the Nilgiri Hills in south India; however, this was questioned by Kimoto (1999) who suggested that it could be *P. parva* Chen & Sun, 1964, which occurs in China and Vietnam. Staines (2015) cited *P.* (*P.*) *fenestrata* as a fifth species for India. However, we never encountered this species in India, despite extensive fieldwork in the country.

We present the first natural history notes on *P.* (*P.*) *hystrix* from two widely-separated localities in India. This species is widespread in southeast Asia and is documented from 16 States in India – Assam, Bihar, Chhattisgarh, Goa, Gujarat, Himachal Pradesh,

Table 1. Host plants of *Platypria* species (Cassidinae: Hispini). New host records are indicated by bold font and '*'.

Species	Host family	Host species	Reference
***Platypria* (*Platypria*) sp.**	Fagaceae	*Quercus semecarpifolia* Sm.	Stebbing 1914
***Platypria* (*Platypria*) *chiroptera* Gestro 1899** (=*Platypria garthwaitei* Bhasin 1942)	Rhamnaceae	***Gouania microcarpa* DC.**	**This paper***
		Ziziphus incurva Roxb.	Bhasin 1942; Mathur and Singh 1961
***Platypria* (*Dichirispa*) *coronata* (Guérin-Méneville 1840)**	Fabaceae	*Desmodium repandum* (Vahl) Poir.	Uhmann 1958a
		Pueraria phaseoloides (Roxburgh) Bentham	Bernon and Graves 1979
***Platypria* (*Platypria*) *echidna* Guérin-Méneville 1840**	Euphorbiaceae	*Mallotus* Lour. sp.	Hua 2002
	Fabaceae	*Desmodium gangeticum* (L.) DC	Beeson 1941
		Erythrina L. sp.	Beeson 1941; Ayyar 1940
		Erythrina subumbrans (Hassk.) Merr. (= *Erythrina lithosperma* Blume ex. Miq.)	Fletcher 1921; Chatterjee and Bhasin 1936; Kalshoven 1957; Mathur and Singh 1959; Zaka-Ur-Rab 1991
		Erythrina variegata L. (=*Erythrina indica* Lam.)	Zaka-Ur-Rab 1991
		Erythrina variegata orientalis Murr.	Hua 2002
		Pueraria tuberosa (Roxb. ex Willd.) DC.	Beeson 1941
	Rhamnaceae	*Ziziphus* Mill. sp.	Beeson 1941; Mathur and Singh 1961
		***Ziziphus mauritiana* Lam.**	**This paper***
		***Ziziphus nummularia* (Burm.f.) Wight & Arn.**	**This paper***
		Ziziphus oenoplia (L.) Mill.	Chatterjee and Bhasin 1936
		***Ziziphus rugosa* Lam.**	**This paper***
		***Ziziphus xylopyrus* (Retz.) Willd.**	**This paper***
***Platypria* (*Platypria*) *erinaceus* (Fabricius 1801b)** (=*Platypria andrewesi* Weise 1904)	Fabaceae	*Desmodium gangeticum* (L.) DC.	Beeson 1941
		Erythrina L. sp.	Beeson 1941; Kalshoven 1957
		Pueraria tuberosa (Roxb. ex Willd.) DC.	Beeson 1941
	Poaceae	*Oryza sativa* L.	Anand 1989
		Saccharum L. sp. ("sugar-cane")	Maulik 1919, 1937
	Rhamnaceae	*Ziziphus* Mill. spp.	Maulik 1919, 1937; Chatterjee and Bhasin 1936; Beeson 1941; Mathur and Singh 1961
		Ziziphus jujuba Lam. (= *Ziziphus mauritiana* Lam.)	Maxwell-Lefroy 1909; Stebbing 1914; Beeson 1919; Maulik 1919, 1937; Fletcher 1921; Ayyar 1940; Speyer 1954; Kalshoven 1957; Mathur and Singh 1961; Nair 1986; Zaka-Ur-Rab 1991; Balikai 1999; Kalaichelvan and Verma 2005
		***Ziziphus nummularia* (Burm.f.) Wight & Arn.**	**This paper**
***Platypria* (*Platypria*) *hystrix* (Fabricius 1798)**	Fabaceae	*Cajanus cajan* (L.) Millsp.	Uhmann 1954a
		Cajanus indicus Spreng.	Kalshoven 1957
		Desmodium gangeticum (L.) DC	Beeson 1941
		Dolichos lablab L.	Fletcher 1921; Ayyar 1940; Kalshoven 1957; Nair 1986; Zaka-Ur-Rab 1991
		Erythrina L. sp.	Fletcher 1914, 1921; Ayyar 1940; Beeson 1941; Kalshoven 1951, 1957
		Erythrina arborescens Roxb. (swarming only)	Chatterjee and Bhasin 1936; Kalshoven 1957
		***Erythrina stricta* Roxb.**	**This paper***
		Erythrina subumbrans (Hassk.) Merr. (=*Erythrina lithosperma* Blume ex Miq.)	Zaka-Ur-Rab 1991
		Erythrina variegata L. (= *Erythrina indica* Zoll.)	Maulik 1919, 1937; Beeson 1919; Chatterjee and Bhasin 1936; Gressitt and Kimoto 1963; Gressitt 1950; Kalshoven 1951; Speyer 1954; Mathur and Singh 1959; Zaka-Ur-Rab 1991

Species	Host family	Host species	Reference
***Platypria* (*Platypria*) *hystrix* (Fabricius 1798)**	Fabaceae	*Erythrina variegata orientalis* Murr.	Hua 2002
		Glycine max (L.) Merr. ("soybean")	Kezhen 1992
		Mucuna pruriens (L.) DC	Rani and Sridhar 2004
		Phaseolus spp.	Kezhen 1992
		***Pueraria montana* var. *lobata* (Willd.) Maes. & S. Almeida**	**This paper***
		***Pueraria phaseoloides* (Roxb.) Benth.**	**This paper***
		Pueraria tuberosa (Roxb. ex Willd.) DC.	Beeson 1941
		Sesbania Scop. sp. ("agathi")	Fletcher 1921; Kalshoven 1957; Nair 1986
		Sesbania aculeata (Schreb.) Poir.	Zaka-Ur-Rab 1991; Hua 2002
		Sesbania grandiflora (L.) Poir.	Beeson 1919; Chatterjee and Bhasin 1936; Speyer 1954; Kalshoven 1957; Zaka-Ur-Rab 1991
		Sesbania Scop. sp. ("agathi")	Fletcher 1921; Chatterjee and Bhasin 1936; Nair 1986
		Tephrosia candida DC.	Kalshoven 1951; 1957
	Fagaceae	*Castanea* Mill. sp. ("chestnut")	Nair 1986
	Myricaceae	*Myrica* L. sp. (swarming only)	Chatterjee and Bhasin 1936; Kalshoven 1957
		Myrica rubra (Lour.) Siebold & Zucc.	Hua 2002
	Rhamnaceae	*Ziziphus* Mill. spp.	Beeson 1941; Mathur and Singh 1961
	Rosaceae	*Rubus* L. *sp.*	Hua 2002
		Rubus ellipticus Sm. (swarming only)	Chatterjee and Bhasin 1936; Kalshoven 1957
	Rubiaceae	*Uncaria gambir* (W. Hunter) Roxb.	Kalshoven 1957
***Platypria* (*Platypria*) *melli* Uhmann 1954**	Poaceae	*Oryza sativa* L.	Gressitt and Kimoto 1963
	Rhamnaceae	*Hovenia* acerba Lindl.	Chen et al. 1986; Liao et al. 2014; Liu et al. 2019
		Paliurus ramosissimus Poir.	Chen 1982; Hua 2002
		Ziziphus jujuba Lam.	Chen et al. 1986; Hua 2002; Liu et al. 2019
***Platypria* (*Dichirispa*) *paucispinosa* Gestro 1904**	Icacinaceae	*Icacina mannii* Oliv.	Uhmann 1954
***Platypria* sp.**	Rosaceae	*Pyrus* sp. ("pear")	Qi et al. 1995
		Prunus sp. ("plum")	Qi et al. 1995

Karnataka, Kerala, Madhya Pradesh, Maharashtra, Pondicherry, Punjab, Sikkim, Tamil Nadu, Uttar Pradesh and West Bengal (Fig. 1) (Maulik 1919; Basu 1999; Borowiec and Świętojańska 2007; Borowiec and Sekerka 2010; Staines 2015). At present, 20 host plants in six families have been recorded for this species (Table 1). We report observations of the species on four host plants, three being new records for this species. We also present brief biological notes for the other three Indian *Platypria* species based on field observations and provide a key to identify these four species in India. This paper is the first step in an ongoing process; a detailed comparative morphology study is our next goal.

Materials and methods

The study is based on independent observations by SR and KDP of live populations of *P.* (*P.*) *hystrix* at two sites in India, 2,500 km apart (Fig. 1). Authors SR, KDP and HVG started observations independently and now are collaborating; we pool data here in this phase 1 of a long-term study.

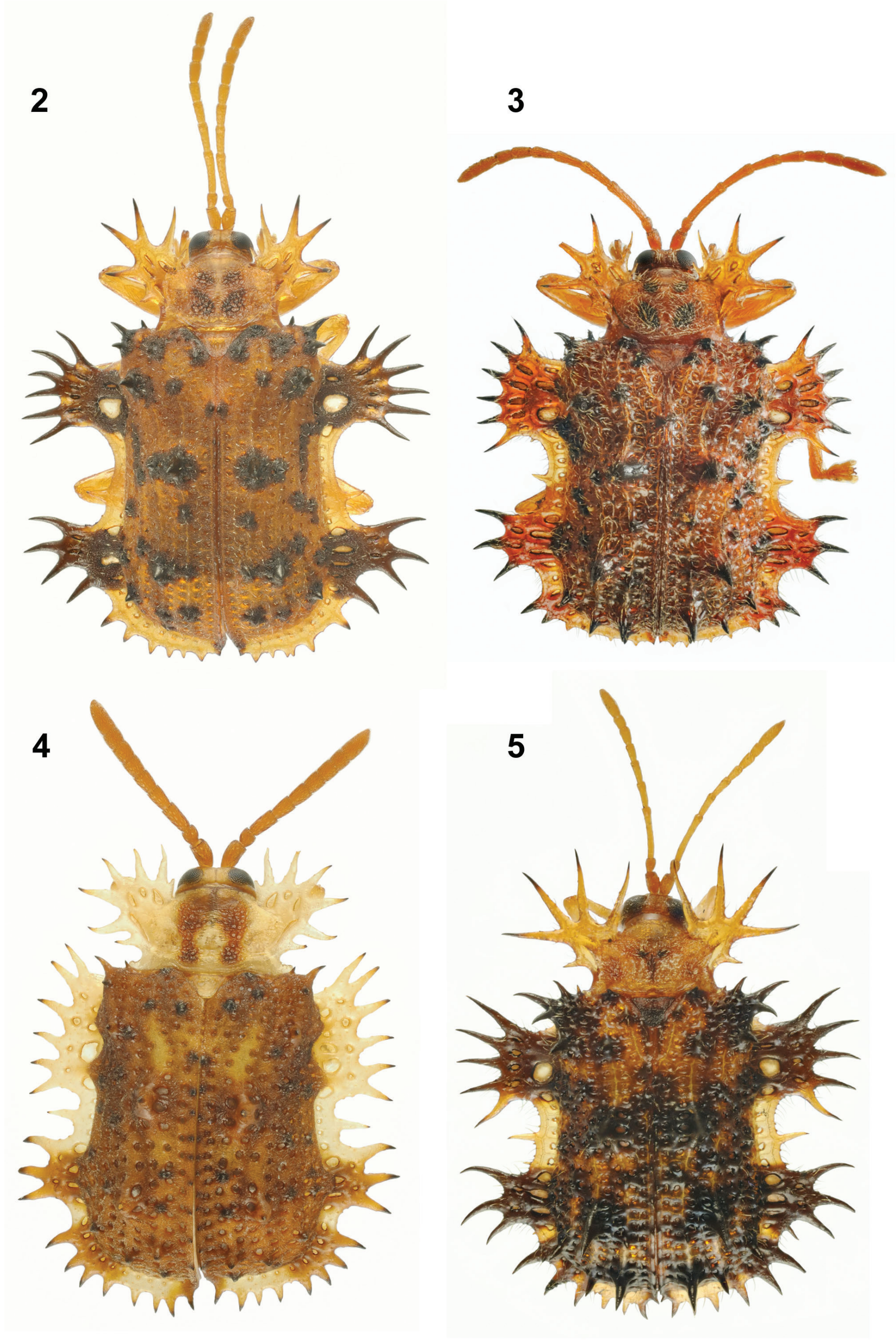

Figures 2–5. *Platypria* species in India (photos: K.D. Prathapan) **2** *Platypria* (*Platypria*) *chiroptera* Gestro, 1899 **3** *Platypria* (*Platypria*) *echidna* Guérin-Méneville, 1840 **4** *Platypria* (*Platypria*) *erinaceus* (Fabricius, 1801) **5** *Platypria* (*Platypria*) *hystrix* Maulik, 1919.

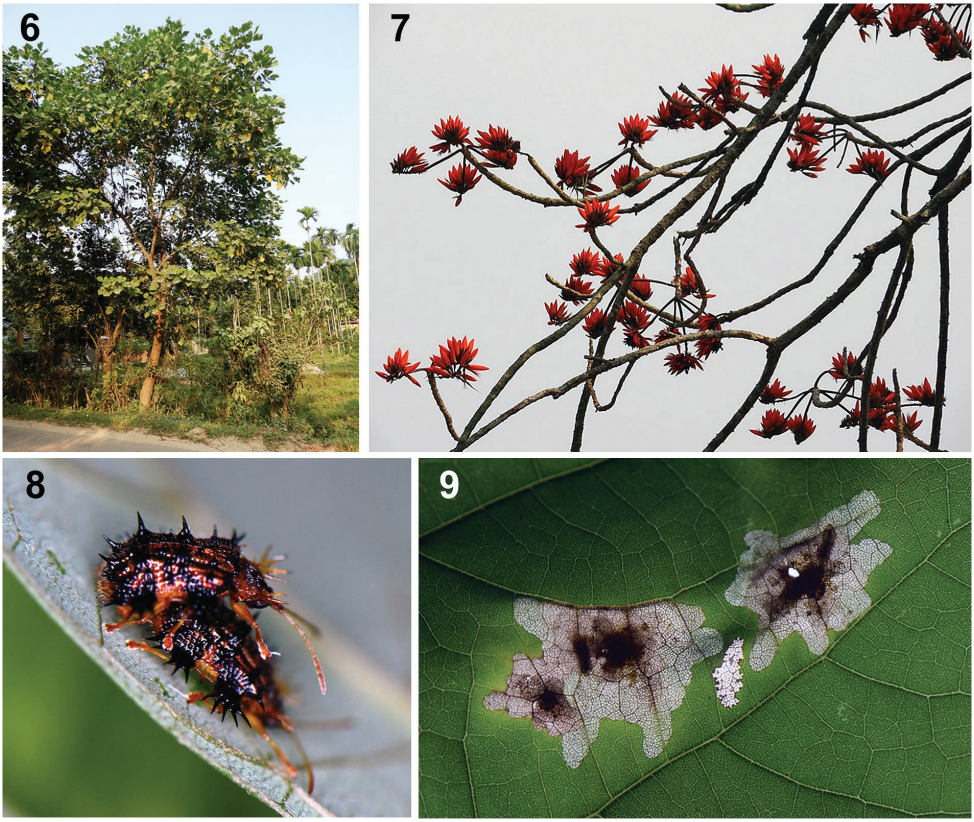

Figures 6–9. Natural history of *Platypria* (*Platypria*) *hystrix* on *Erythrina variegata* L., Assam, India **6** host tree **7** flowers **8** adults in copula **9** larval mines. (Photos: S. Ranade).

Site 1: INDIA: Assam, Kamrup District, 26°0'0.9"N, 91°32'53.7936"E, 190 m elev., September 2019–May 2020 (Figs 6–9). Beetles were observed by SR on a single tree, *Erythrina variegata* L. (Fabaceae) that was visited frequently to record natural history data. Specimens were not collected at that time, but photographs and movies with a SLR camera were recorded. Populations were also observed on two perennial vines *Mucuna pruriens* (L.) DC and *Pueraria montana* var. *lobata* (Willd.) Maes. & S. Almeida (Fabaceae) at the same location, October–November 2020. We are continuing with the natural history study of this population.

Site 2: INDIA: Kerala, Vellayani, Kerala Agricultural University campus, 8°25'46.3"N, 76°59'07.8"E, 39 m elev. Author KDP observed this population for ca. three months in 2007 and again from October 2019 to May 2020. During 2007, populations were observed on *Erythrina stricta* Roxb. (Figs 10–13) and *Pueraria phaseoloides* (Roxb.) Benth. (Figs 14–21) (both Fabaceae). However, the entire population of *Erythrina* was decimated following the invasion of the *Erythrina* gall wasp, *Quadrastichus erythrinae* Kim (Hymenoptera: Eulophidae) (Faizal et al. 2006). In 2019 and 2020, the beetles were found only on *P. phaseoloides* at Vellayani (Figs 14–21).

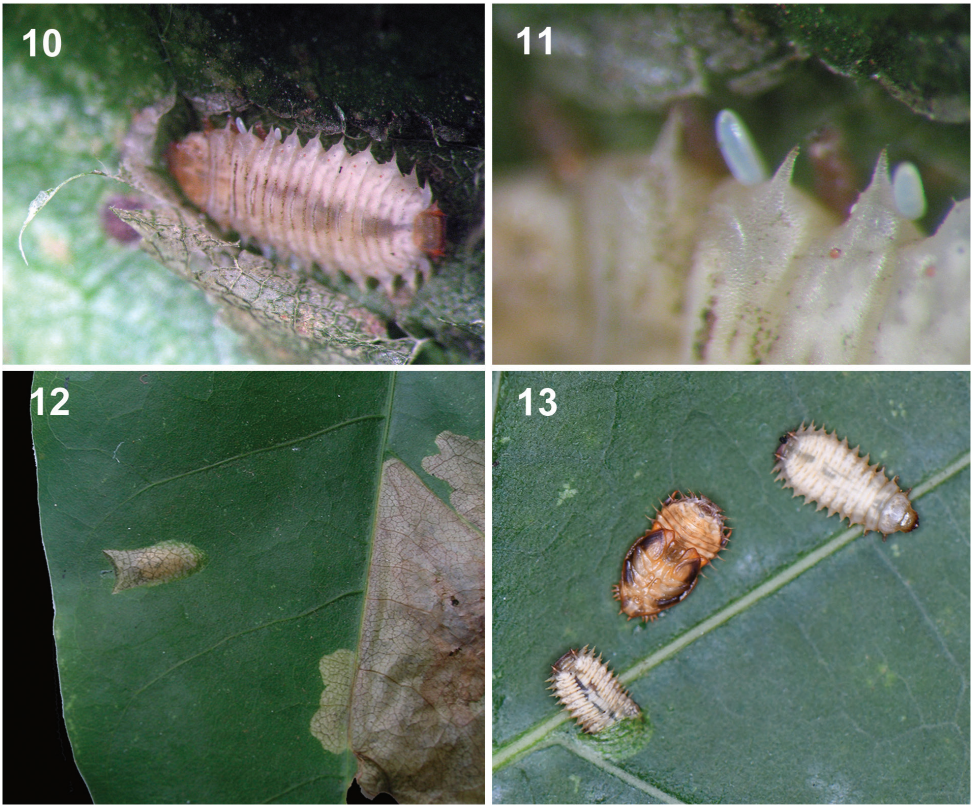

Figures 10–13. Juveniles of *Platypria* (*Platypria*) *hystrix* on *Erythrina* L. spp. in India **10** Larva **11** Eggs of parasitoid wasp on larva. (Photos: K.D. Prathapan in Kerala; on *E. stricta* Roxb.) **12** Pupal chamber **13** Pupae and a last instar larva initiating pupal mine (Photo: S. Ranade in Assam; on *E. variegata* L.).

Rearing

We marked and numbered leaves with larval mines to observe their behaviour and development. In Assam, we followed 15 larvae and four successfully reached adulthood. In Kerala, about 20 larval and pupal mines were studied. Some specimens were taken to the lab to rear and collect certain life stages for vouchers, photography and measurements.

In addition to the detailed study of *P.* (*P.*) *hystrix* above, HVG, PKD and SR observed and collected the other three Indian *Platypria* species on *Ziziphus* and other hosts in India and provide these brief notes below.

Natural history notes on *Platypria* (*Platypria*) *chiroptera* Gestro, 1899

PKD and M. K. Shameem collected this species in six localities in the southern Western Ghats, India: Karnataka, Kalasa, 11.V.2011, Shameem K. (2 specimens); Kottigehara, 22.IX.2004, Prathapan Coll. (1 specimen); Kottigehara, 13°7'7.7"N/ 75°30'7.9"E,

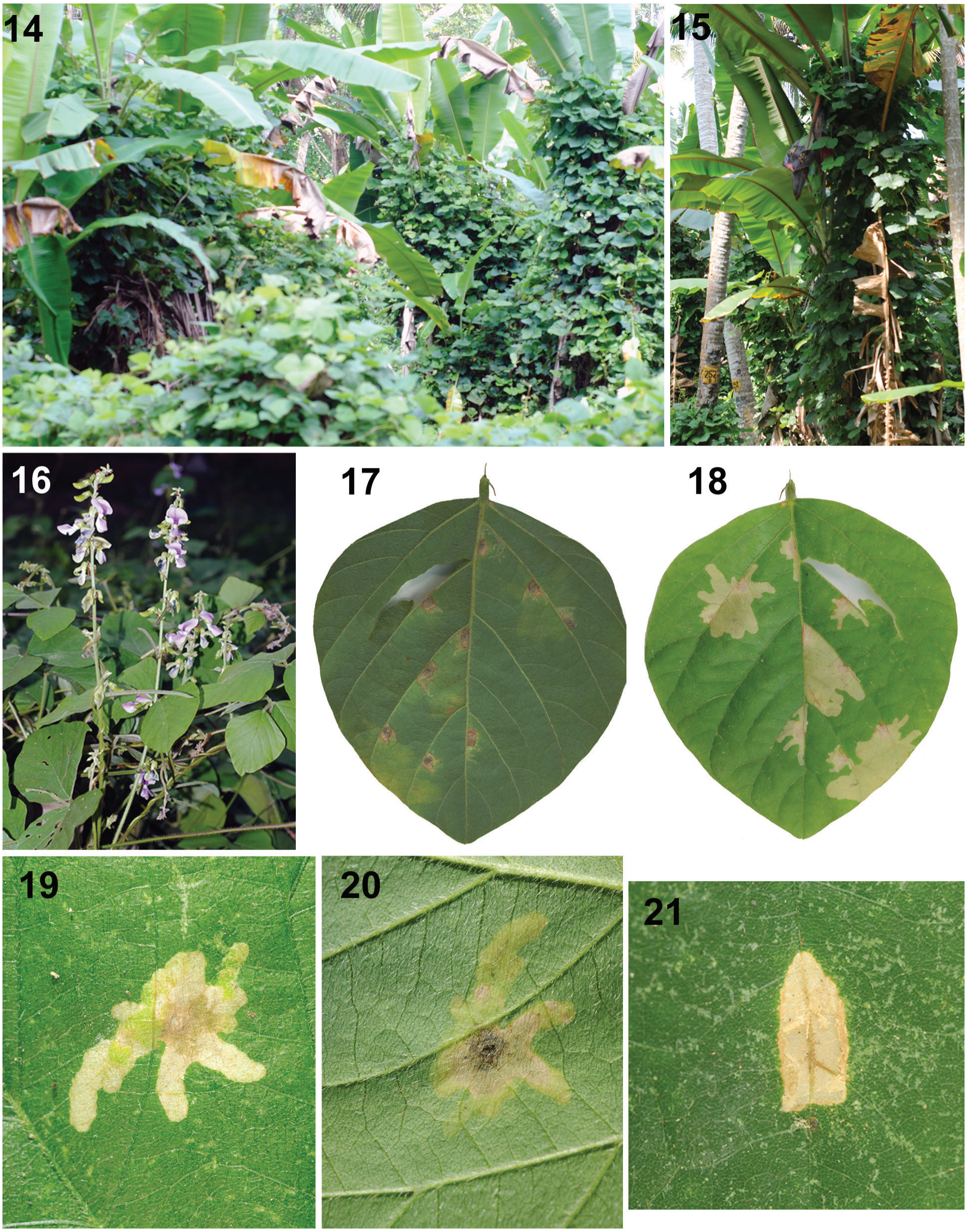

Figures 14–21. Natural history of *Platypria* (*Platypria*) *hystrix* on *Pueraria phaseoloides*, Kerala, India (Photos: K.D. Prathapan) **14** Vine growing over all plants in a banana plantation **15** Plant growing over banana **16** Inflorescence **17** Leaf with six larval mines, abaxial view **18** Leaf with six larval mines, adaxial view **19** Larval mine, view from adaxial side of the leaf **20** Larval mine, view from abaxial side of the leaf with ootheca at the centre **21** Pupal chamber.

938 m a.s.l., 8.v.2011, Prathapan and Shameem (2 specimens); Kerala, Neyyar W. L. San., 8.II.2002, Prathapan Coll. (1 specimen); Elappara, 1.III.2011, Shameem K. (1 specimen); Kuttiyadi, Janakikkadu, 14.iii.2013 (1 specimen); Silent Valley Nat. Park, Sairandhri, 11°5'35.8"N/ 76°26'47.7"E, 1030 m a.s.l., 15.xi.2013, Prathapan and Shameem (4 specimens, KAU). The host plant is *Gouania microcarpa* DC. (Rhamnaceae) (M.K. Shameem, personal communication). Bhasin (1942) and Mathur and Singh (1961) recorded *P.* (*P.*) *chiroptera* (as *Platypria garthwaitei* Bhasin, 1942) on *Ziziphus incurva* (Rhamnaceae).

Natural history notes for *Platypria* (*Platypria*) *echidna* Guérin-Méneville, 1840 (Figs 26–28)

Authors HVG and SR observed live populations on four different hosts, all new records, in India. Locality 1: Pune District, Tamhini-Dongarwadi, Mulshi, 18°26'48.1488"N, 73°25'29.3808"E, June–September (monsoon season) 1997–2001. Locality 2: Pune, Paud Road, 18°30'24.066"N, 73°46'58.2708"E, 10 April 2011. These adults were noted feeding by scraping the upper leaf surface, *Ziziphus rugosa* Lam. Localities 3–4: Adults were observed feeding on *Z. nummularia* and on *Z. mauritiana* Lam. at Pune District, Bhimashankar, 19°4'36.1848"N, 73°32'6.8784"E, August 1999 and on *Ziziphus xylopyrus* (Retz.) Willd., Pashan, Pune, 18°32'12.1884"N, 73°47'22.6284"E, May 1999. Locality 5: Larvae, pupae, and adults together were observed only on *Z. mauritiana*, at Taljai Tekadi Pune, 18°31'13.548"N, 73°51'24.2784"E, September 2007.

Natural history notes for *Platypria* (*Platypria*) *erinaceus* (Fabricius, 1801)

HVG and SR observed this species on the host plant, *Z. mauritiana* Lam. (Formerly *Z. jujuba* Lamk.) in several sites in India. Locality 1: Pune District, Chatushrungi, 18°32'12.4872"N, 73°49'42.69"E, 27 May 1999. Locality 2: Pashan, 18°32'12.1884"N, 73°47'22.6284"E, 27 May 1999. Locality 3: West Bengal, Kolkata, Baruipur 22°22.770"N, 88°26.154"E, 9 m a.s.l., 19.vi.2013, KDP Coll. (3, KAU). Locality 4: Tamil Nadu, Manavur, 13°05'48.44"N, 79°47'37.66"E, 54 m a.s.l., Ex. *Ziziphus*, 24.ix.2016, Shameem KM Coll. (1, KAU). Locality 5: Pune, Paud, NDA Road, on *Z. nummularia* (Burm.f.) Wight & Arn. (HVG); adults were feeding by scraping the upper surface of leaf. Mating pairs, larvae and pupae were also noted.

Taxonomic identifications

Erythrina stricta (Fabaceae) was identified by A. K. Pradeep, Calicut University Herbarium, previously for Faizal et al. (2006). No plant voucher was collected at that time as no flowers were produced under Vellayani conditions; now the plant has become locally extinct. *Pueraria phaseoloides* was identified by A. P. Balan, Malabar Botanical Garden. *Erythrina variegata*, *P. montana* var. *lobata* and *M. pruriens* (all Fabaceae) from

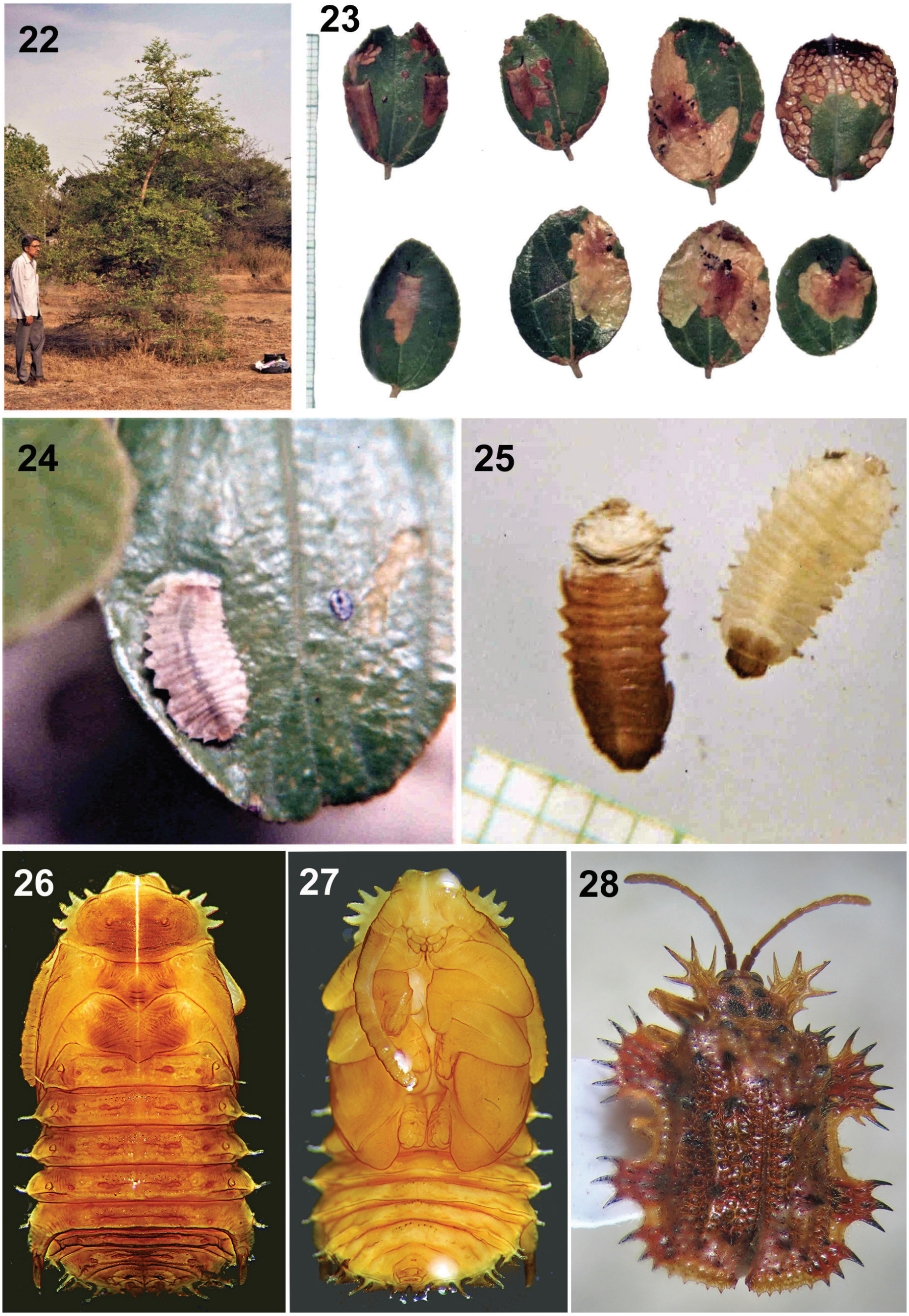

Figures 22–28. 22–25 Natural history of *Platypria* (*Platypria*) *erinaceus* on *Ziziphus nummularia* (Burm.f.) Wight & Arn., Maharashtra, India, (Photos: S. Ranade) **22** *Ziziphus xylopyrus* (with author HVG standing) **23** larval mines in small, rounded leaves of *Ziziphus nummularia* **24** larva **25** mature larva and pupa **26–28** *Platypria* (*Platypria*) *echidna* **26** Pupa, dorsal view **27** pupa, ventral view **28** adult, dorsal view. (Photos: H.V. Ghate).

Assam were identified by G. Krishna, Central National Herbarium (CAL), Botanical Survey of India. The beetles were identified independently by authors KDP and SR as *P.* (*P.*) *hystrix* using the species key by Maulik (1919) and compared with photos of type specimens deposited in Berlin Museum of Natural History and Kiel University, Germany. A key to identify the four *Platypria* species in India is developed.

Specimen collections and repository

Specimens collected by KDP and associates over years from various localities in India are deposited in the Travancore Insect Collection, Kerala Agricultural University, Vellayani (KAU). In addition to KAU, specimens of beetles will be deposited also at the National Bureau of Agricultural Insect Resources, Bengaluru, India (NBAIR). Specimens of *P.* (*P.*) *echidna* and *P.* (*P.*) *erinaceus* are deposited at the Modern College of Arts, Science and Commerce, Pune, India. Additionally, a specimen series of *P.* (*P.*) *hystrix* is on loan from KDP to CSC for further study. Vouchers of *P. phaseoloides* (Accession no. 7019), *P. montana* var. *lobata* (Accession no. 7030, 7031) and *M. pruriens* (Accession no. 7037, 7038) are deposited in the Calicut University Herbarium, Department of Botany, University of Calicut, Kerala.

Host plant ecology

The four Fabaceae hosts are native to southeast Asia. Each is used for multiple purposes in agro-ecosystems. *Erythrina stricta* is a spinose tree on which cultivated black pepper (*Piper nigrum* L.) is trailed. It is also grown as a hedge plant and shade tree. Leaves are used as fodder for sheep and rabbit (Prathapan, personal observations; Sastri 1952). *Erythrina variegata* (Fig. 6) is a tropical soft-wood tree, closely resembling *E. stricta*; however, its stem is usually unarmed. It is cultivated as an avenue tree and a live fence and it is used as a shade tree in plantations of tea and coffee and to trail betel vine and black pepper (Sastri 1952; Prathapan, personal observations). *Pueraria phaseoloides* (Figs 14–18; tropical kudzu) is a perennial climbing vine, trailing over trees, shrubs, bananas and grasses in and around the Instructional Farm of Kerala Agricultural University, Vellayani, India. It is grown as a cover crop in rubber plantations and for fodder (see Keung 2002). *Pueraria montana* var. *lobata*, known for rapid and competitive growth, is used as a pasture, fodder and hay crop in North America (Lindgren et al. 2013). *Mucuna pruriens* is used for its medicinal properties and as fodder (Choudhary et al. 2012; Patiri and Borah 2007). These five hosts have moderately large, trifoliate leaves.

The genus *Ziziphus* Mill. includes about 58 species of spiny shrubs and trees (El Maaiden et al. 2020). It is extensively used in folk and traditional medicine in arid and semi-arid regions for the treatment of diarrhoea, dysentery, cholera, diabetes, hypertension, inflammation, intestinal spasm, liver, malaria and other diseases (El Maaiden et al. 2020). *Ziziphus mauritiana* Lam., called Indian jujube or ber, is a tropical shrub or small tree, of considerable commercial importance and is widely cultivated for its fruits. *Ziziphus rugosa* Lam., called wild jujube, is a thorny tree or straggling shrub, common in foothills and low mountains in India (Chadha 1976). Fruits are collected from the wild for consumption. *Ziziphus xylopyrus* (Retz.) Willd., locally called 'kath ber', is an erect shrub or small tree, common in dry and deciduous forests (Chadha 1976). *Ziziphus nummularia* (Burm.f.) Wight & Arn., occurring in semi-arid areas from Iran to the Indian subcontinent, is a multipurpose branched thorny shrub reaching a height of 1–3 m, with medicinal, nutritional, industrial and economic values (Zandifar et al. 2020).

Photographs

Specimens were colour-photographed using a AF Micro Nikkor 60 mm macrolens, mounted on a Nikon D3000 SLR camera. The camera was mounted on a Wemacro stack rail, positioned vertically. Three Ikea 201.696.58 Jansjo Desk Work LED Lamps, with suitable diffusers, were used to uniformly illuminate the specimen. A Wemacro rail android Bluetooth control app, installed on a smartphone, was used to remotely control the imaging system. Multiple images at different depths of plane were taken and were stacked together using Helicon focus software. The high-resolution images, thus obtained, were edited with Adobe Photoshop 2020. Field photographs were taken using a Canon EFS 55–250 mm lens mounted on a Canon EOS 1300D SLR camera or Micro Nikkor 60 mm macrolens mounted on a Nikon D3000 SLR camera.

Measurements

Life stages of *P.* (*P.*) *hystrix* were measured using a standardised ocular micrometer placed in one eyepiece of a stereoscopic microscope. Measurements of host plant leaves and leaf mines were taken using a Vernier caliper. In our Assam lab, we measured three adults, one instar I, one instar III, one instar V, one pupa and one pupal mine. In our Kerala lab, we measured 10 adults, 20 pupal mines, 10 pupae, and seven oothecae.

Taxonomy

We use the current plant names according to the online catalogue (Tropicos 2020) and current beetle names according to the catalogue of Staines (2015).

Results

Key to species of *Platypria* in India

1 Antenna thick, hardly extending beyond scutellum over pronotum; third antennomere not longer than 2.5 times width ..... ***P.* (*P.*) *erinaceus* (F.) (Fig. 4)**

– Antenna thin, extending well beyond scutellum over pronotum; third antennomere about four times as long as wide **2**

2 Anterior lateral lobe on each side of elytra has five spines; feeds on Fabaceae... .... ***P.* (*P.*) *hystrix* (F.) (Fig. 5)**

– Anterior lateral lobe on each side of elytra has six spines; feeds on Rhamnaceae **3**

3 Elytra covered with white pubescence; punctures large, subquadrate and contiguous; anterior and posterior lateral lobes on elytra reddish .... ***P.* (*P.*) *echidna* Guérin-Méneville (Fig. 3)**

– Elytra glabrous; punctures rounded, separated by broad interstices; anterior and posterior lateral lobes of elytra blackish.......... ***P.* (*P.*) *chiroptera* Gestro (Fig. 2)**

Natural history of *Platypria* (*Platypria*) *hystrix*

We report *Erythrina stricta*, *Pueraria montana* var. *lobata* and *Pueraria phaseoloides* as new hosts for *P.* (*P.*) *hystrix* (Figs 6–21). In India, this beetle has been reported on other species in these genera, as well as on species of *Cajanus*, *Desmodium* and *Dolichos* (Table 1, all citations therein).

Starting on 17 September 2019, SR observed irregular blotch mining on leaves of a young tree of *E. variegata* (Fig. 9). Eggs were observed on *E. variegata* in Assam as well as on *P. phaseoloides* in Kerala. They were laid singly on the adaxial side of leaves. Up to four eggs were observed on a single leaflet. Individual eggs were inserted into a depression made on the mesophyll and were covered with a creamy-brown secretion to form the oblong-oval ootheca, that measured 1.03–1.32 mm (1.10 mm – mean of 7 observations) long and 1.07–1.48 times (1.24 times – mean of 7 observations) longer than wide. A characteristic, long, thread-like process, arising from the middle of the ootheca, enabled easy identification of the ootheca under low power of the microscope. From the abaxial side, the ootheca appeared like a minute, brown speck. The egg appeared soft and was easily ruptured when we attempted to separate it from the oothecal covering. The thread-like process and the outer wall of the ootheca remained intact even after hatching and formation of the leaf mine. In Assam, a female was observed on the host plant for ten days; oviposition and egg hatch were noted. Twenty-one leaflets were observed, each with about 3–4 beetle eggs. These eggs hatched in about 4–7 days. Many eggs remained unhatched or the larvae died prematurely.

The larva hatched out of the egg mines into the adjacent mesophyll without breaking the oothecal covering. It feeds and moves within the leaf creating mines by consuming mesophyll tissue. The first instar larva grew up to 1.8 mm. The larva has chitinous brown head and translucent-greenish body. The alimentary canal appears dark green due to the presence of food. While observing it against sunlight, the mines appeared occupied and small larvae were apparent through the epidermis. The larval mine in *P. phaseoloides* appeared less apparent in the abaxial view (Fig. 17), but clear and rather transparent from the adaxial side of the leaf lamina (Fig. 18). The larval mines are irregular blotch mines. Six leaf mines were observed on a 65 mm wide leaflet of *P. phaseoloides* (Figs 17–18) at Vellayani. The mines contained excreta, exuviae and often remnants of dead larvae. The leaf mines of the late instars were noticeable as some of them were approximately 1 cm wide and 10 cm long and irregularly shaped. The final instar was about 5 mm long.

Pupation

The pupation takes place in a separate pupal mine. Emergence from the larval mine and construction of the pupal mine were observed in Assam. The mature larva (Fig. 13) exits the larval mine, moves towards the other leaf end and initiates the pupal mine. Construction of the pupal mine by a single larva that was observed took 23 minutes to conceal itself. Four pupal mines were observed in Assam on *E. variegata*. The average size of the pupal mine was 9 × 4 mm (n = 4). Excreta was present next to every pupal mine's single opening. The pupal period in Assam lasted for about seven days. On four occasions, the pupa was observed moving out of the mine and adults emerged in early morning.

About 20 pupal mines were observed on *P. phaseoloides* at Vellayani. The length of pupal mines ranged from 7.5–10.1 mm (9.98 mm; mean of 10 observations) and width 3.5–4.5 mm (4.01; mean of 10 observations). All, except two, were formed along a leaf vein. Two were formed between the veins on the leaf lamina. The pupal mines are U-shaped, resembling a pocket, with its distal end closed and the proximal end, from where the larva initiated the mine, remaining open. The resident pupa has the head orientated to the closed end and its rear end towards the mine opening. In Assam, we observed that a pupating larva spent one day in the pupal mine, then cast the last larval skin and pupated. This individual took 9 days from formation of the pupal mine to adult emergence. Generally, 1–2 pupal mines were observed on a single leaflet on both *E. variegata* in Assam and *P. phaseoloides* in south India (Vellayani, Kerala). The fresh pupa is yellow in colour that turns coffee-brown in a few days. Prior to the emergence of the adult, the pupa exited the mine and shed the exuviae. In the case of the single individual observed by PKD in the laboratory, the exuviae of the pupa remained about 3 cm away from the pupal mine. Thus, the pupa can move out of the mine to eclose.

The adults (n = 10; length 4.29–5.24 mm) were observed feeding mainly by scraping on adaxial surface of leaves. Sexual dimorphism was not distinct to the naked eye. Copulation was recorded in the morning as well as in the evening. Pairs were in copula for more than an hour.

Dormancy and aestivation

In Assam, the adults were seen until the first week of December 2019, after which they were not found anymore. They appeared on the same plant in the first week of March 2020. Further south, at Vellayani in Kerala, the population of *P.* (*P.*) *hystrix* on *P. phaseoloides* was active throughout the year, as adults and leaf mines were observed even during the summer months of March and April. Apparently, no dormant stage of the insect occurs in Kerala as extremes of climate are absent in this part of the country.

Longevity

Although our observations are still in progress, we noticed that adults emerging in September 2019 in Assam were active, with mating and egg laying observed during March 2020. We suspect that the adults survive for at least one year.

Mating behaviour

Copulation was observed in the third week of March after several thunder showers in Assam. On 23 March, we noted four pairs on *E. variegata*. In the case of two pairs, a single female was pursued by two males. The male mounted the female, keeping fore- and middle legs on the elytra of the female, the hind legs being on the substratum. The pair remained coupled for more than one hour per observation. On a few occasions, coupled pairs were observed for 4–6 hours. The female moved around, carrying the male and even fed while in copula. During a single sighting, we found a maximum of eight beetles on a single sapling of *Erythrina* at Assam, indicating that it is not a major pest.

Natural enemies

At the Vellayani site, we observed a Braconidae wasp (Hymenoptera) parasitising a mature larva of *P.* (*P.*) *hystrix* (Fig. 11) and ant (Hymenoptera: Formicidae) predation of a pupa. Both the wasp and ant specimens are deposited at KAU. In the Pune locality, we observed a chalcid wasp (Hymenoptera) laying its egg on a late larval instar on 27 May 1999 and subsequently, we detected a chalcid infestation of the larval and pupal stages of *P.* (*P.*) *erinaceus*. Bernon and Graves (1979) is the only other report of Hymenoptera parasites of *Platypria*; they noted that *Platypria* was an alternative host of the Hymenoptera parasites of the *Coelaenomenodera* pest.

Discussion

Santiago-Blay (2004) has discussed many aspects of leaf mining by Chrysomelidae and Chaboo (2007: 46–47) provides an overview of Cassidinae pupation. We discuss here aspects of the biology and behaviour of *Platypria* species and compare with the other members of the tribe and Cassidinae *s. l.* generally. We discuss refinements for the current morphology and behaviour-based phylogenetic characters of Chaboo (2007).

Plant relations

Platypria is associated mainly with two plant families, Fabaceae and Rhamnaceae (Table 1). We found several citations in Indian literature about the genus that should be added to the online catalogue of Staines (2015). Records on other plants – Fagaceae

[Nair (1986), Euphorbiaceae (Hua 2002) and Poaceae (Anand 1989; Maulik 1919, 1937)] – need confirmation as there is little information on immatures from these observations. We can call only those plants as 'hosts' where larval development occurs successfully. In that sense, *P.* (*P.*) *echidna* may sometimes feed on *Z. nummularia*, but we have never observed larvae or pupa of this species on *Z. nummularia*. Similarly, we never observed larvae/pupae of any *Platypria* species on *Z. xylopyrus* (Retz.) Willd. which we [HVG and SR] regularly visited to study bionomics of another cassidine. Further, although *Z. oenoplia* (L.) Mill. is reported as a host of one *Platypria* species (see Table 1), HVG never observed *Z. oenoplia* in Pune harbouring any *Platypria*.

Kalshoven (1957) noted that *Platypria* is one amongst a few unusual Oriental hispine genera associated with dicotyledonous plants, often belonging to different families. He also commented that *Platypria* is unusual as it is one of the few hispine taxa specific to dicots and exhibits trophic selections between unrelated host plant families.

Pest status

Ayyar (1940) recorded *P.* (*P.*) *hystrix* as a leaf-feeding pest on *Dolichos lablab*, *Sesbania* sp. and *Erythrina* sp. in south India. He also noted *P.* (*P.*) *echidna* on *Erythrina* sp. in south India and *P.* (*P.*) *erinaceus* on *Z. jujuba*. Nair (1986) recorded *P.* (*P.*) *erinaceus* as a pest on *Z. jujuba*, as well as *P.* (*P.*) *hystrix* on *D. lablab*, *Sesbania* sp. and *Castanea* sp. (Fagaceae, chestnut) in India. Rani and Sridhar (2004) recorded *P.* (*P.*) *hystrix* as a pest damaging leaves of *Mucuna pruriens* L. (DC) var. *utilis* in south India (this plant is used as a nerve tonic and aphrodisiac in Indian traditional medicine). However, *P.* (*P.*) *melli* is known as a significant pest of Rhamnaceae fruit trees, *Hovenia acerba* and *Ziziphus jujuba*, in China (Liu et al. 2019). In India, there have been no reports of outbreaks or severe crop damage.

Life cycle

All life stages of *P.* (*P.*) *hystrix* (egg to adults) were observed in both south and northeast India. The natural history of the populations observed in Assam, northeast India and in Kerala, south India were rather identical, irrespective of the host species, though the populations are separated by a distance of > 2,500 km and climates are distinct. The south Indian population at Vellayani was active throughout the year as harsh winter or summer is absent here, while the northeast Indian population vanished as the winter peaked and re-appeared only after receipt of rains in summer, thus disappearing for at least three months from December to March.

Information is limited on the eggs and associated maternal behaviour for leaf-mining hispines. In *P.* (*P.*) *hystrix*, we observed females excavating a depression on the abaxial surface of leaves and laying a single egg there. Then she covered the egg with a yellow secretion that turned red brown on drying and formed a crusty oothecal covering. Thrusting single eggs into the leaf lamina is known in some leaf-mining hispines (Chen 1982; Chaboo et al. 2010; Shameem et al. 2016; Liao et al. 2018b), although Taylor (1937) noted that females of *Promecotheca* species may oviposit on the leaf surface or sink the egg into the leaf and the natal larva starts the mine. In *Prionispa champaka* Maulik, 1919 (Oncocephalini), the female oviposits 5–6 eggs into a channel she cuts on the leaf (Liao et al. 2018a). Chaboo (2007: 244) proposed two egg features (egg stalk and faecal cover) for phylogeny reconstruction; our data here suggest at least three new potential character hypotheses about the oviposition site (externally on leaf surface or thrust into the leaf tissue), egg grouping (single or massed) and maternal covering (naked with no covering, oothecal secretion, faecal/plant covering or oothecal secretion + faecal/plant covering). Verma and Kalaichelvan (2004) reported observations on oothecal structures in Indian Cassidinae; however, our observations of such secretions in *Platypria* indicate the behaviour of maternal coverings is more widespread across the cassidine tree of life. It is very important to document such information in fine detail to achieve better resolved phylogenies of Cassidinae *s. l.*

We observed all larvae of the four Indian species of *Platypria* making a blotch mine, as in some other mining Cassidinae (Bernon and Graves 1979; Chen 1982; Lee et al. 2009; Liao et al. 2014, 2018a). Figs 17–18 show six mines in one leaf; however, we are uncertain how many larvae can be sustained by the single leaflet to reach pupation and adulthood. We observed a single larva per mine, agreeing with observations in *Javeta pallida* Baly, 1858 (Shameem et al. 2016) and *Chaeridiona thailandica* Kimoto, 1998 (Świętojańska and Kovac 2007). This contrasts with those mining species whose larvae live gregariously in a common mine (e.g. *Pr. champaka*, Liao et al. 2018a).

In our *Platypria* species, the mature larva exits the larval mine and constructs a separate leaf mine for pupation (Figs 12, 13 and 21; see Suppl. material 1 on Pensoft's Youtube channel: https://www.youtube.com/channel/UC3mfJg-mxTVrXO-jE3XrkAMw). This is different from *P.* (*P.*) *melli* Uhmann, 1954 (Liao et al. 2014) where the larva mines into the mid-rib to pupate; such a mid-rib pupation mine is also known in *C. thailandica* (Oncocephalini; Świętojańska and Kovac 2007). The behaviour of a different pupation mine within the leaf blade is also known in some mining cassidines – *Cassidispa relicta* Medvedev, 1957 (Hispini; Liao et al. 2018b), *Oncocephala promontorii* Péringuey, 1898 (Oncocephalini; Chaboo et al. 2010), *Notosacantha vicaria* (Spaeth, 1913) (Notosacanthini; Rane et al. 2000) and *Pr. champaka* (Liao et al. 2018a). In contrast, other leaf-mining cassidines pupate within the larval mine. Species of *Dactylispa* Weise (Hispini), which feed on either monocots or dicots, pupate within the larval leaf mine (Zaitsev 2012). The rice pest, *Dicladispa armigera* (Olivier, 1808) (Hispini) and the palm-feeder, *Javeta pallida* (Shameem et al. 2016), both have pupation within the larval mine.

The structure of the pupal mine appeared very similar in our observed *Platypria* species. In *C. thailandica* (Oncocephalini), the mature larva exits the larval mine, bores into the mid-rib forming a pupal chamber and then pupates with the head orientated towards the stem of the plant (Świętojańska and Kovac 2007). Members of Hispini, Notosacanthini and Oncocephalini, that live on eudicots, create more or less similar pupal mines.

Chaboo (2007: 244) proposed Character 18 with four states for different pupation sites across Cassidinae *s. l.* Our new observations here suggest that the origin of the pupation mine can provide an additional character hypothesis with two states – within a larval mine or a separate mine.

The pupal mines of *P.* (*P.*) *hystrix* are U-shaped and the resident pupa is positioned such that its rear end is orientated to the single opening at the wider end. This facilitates respiration with the erect, tubular spiracles. Even in rains when the pupal mine may become flooded, the pupa can be seen projecting spiracles out of the opening; the pupa is motile and not glued like other Cassidinae. Similar pupal mines have been reported for *P.* (*P.*) *echidna* and *P.* (*P.*) *erinaceus* and some other basal Cassidinae, such as *Chaeridiona picea* Baly (personal observations SR; Oncocephalini), *Notoscantha* (Rane et al. 2000; Notosacanthini), and *Oncocephala tuberculata* Olivier,1792 (Oncocephalini). Notosacanthini is one of the historic transitional tribes between crown-clade Cassidinae, based on adult morphology and basal "hispines" (Chaboo 2007). The similarity of its pupal chamber to that of *Platypria* and Oncocephalini underscores the need for re-assessment of its taxonomic placement.

Chatterjee and Bhasin (1936) and Kalshoven (1957) reported *Platypria* adults as exhibiting swarming behaviour on *Rubus ellipticus* Sm. (Rosaceae) in India. We did not observe such behaviour. Swarming has been reported for only one other Cassidinae, *Caelaenomenodera elaeidis* Maulik (Bernon and Graves 1979), where this behaviour appears to be cyclical. It could provide another set of phylogenetically informative characters.

Platypria females attract many males in a mating frenzy. Once a male is chosen, copulation lasts several hours. (See our supplementary movie file on the life cycle of *Platypria* in India).

Conclusions

This paper provides a first step in ongoing fieldwork and study of the four Indian species of *Platypria*. We discovered new hosts and note the specialisation of these species on Fabaceae and Rhamnaceae. We characterise aspects of the oviposition behaviour, egg, larvae, pupae, mining behaviour and adult courtship. A detailed morphological study is our next goal.

Acknowledgements

We thank Ayilliath Kuttiyeri Pradeep, Calicut University, for confirming the identity of the plant *Erythrina stricta* and A. P. Balan, Malabar Botanical Garden, for identifying *Pueraria phaseoloides*. Gopal Krishna, Central National Herbarium (CAL), Botanical Survey of India identified the host plants from Assam. We thank Yongying Ruan and Ruie Nie, Chinese Academy of Sciences, Beijing, China for translating Chinese texts, Michael Schmitt, University of Greifswald for translating sections of Uhmann (1957, 1958) and Hugh Rowell for a complete translation of Würmli (1975). We thank Rashmi Kant Shukla and Subodh Kr. Bajpai, the National Forest Library and Information Centre, Dehra Dun for Chatterjee and Bhasin (1936) and Mathur and Singh (1959, 1961). SR acknowledges Vibhu Prakash for his encouragement and the Bombay Natural History Society for support. We also thank Charles Staines for sending several references. KDP thanks Koormath Mohammed Shameem for collaboration and camaraderie during fieldwork; SR and HVG also thank Neelesh Sunil Rane for collaboration during fieldwork. We thank Michael Geiser and Dmitry Telnov, British Museum of Natural History, London, United Kingdom, for a loan of specimens and Bernd Jaeger, Museum für Naturkunde, Berlin, Germany, for photographs of a lectotype and specimen information. Sangamesh Hiremath prepared the map of India. Chaboo thanks the U.S. National Science Foundation for Eager Grant #1663680 that supported her effort. HVG thanks the authorities of Modern College for access to facilities. We thank the three anonymous reviewers and editor Michael Schmitt for comments that improved the final manuscript. Finally, we all thank our respective institutions for support during this work.

References

Anand RK (1989) Taxonomy of hispid pests (Coleoptera: Chrysomelidae) in India. Annals of Entomology (Dehra Dun) 7: 1–10.

Ayyar TVR (1940) Handbook of Economic Entomology for South India. Government Press, Madras, 528 pp.

Balikai RA (1999) Pest scenario of ber (*Zyzyphus mauritiana* Lamarck) in Karnataka. Pest Management in Horticultural Ecosystems 5(1): 67–69.

Baly JS (1858) Catalogue of Hispidae in the collection of the British Museum. London, 172 pp.

Basu CR (1999) On the collection of Hispinae (Coleoptera: Chrysomelidae) preserved in the Zoological Survey of India, Calcutta. Records of the Zoological Survey, India (Part 3): 149–190. https://citeseerx.ist.psu.edu/viewdoc/download?doi=10.1.1.893.6766&rep=rep1&type=pdf

Beeson CFC (1919) The food plants of Indian Forest Insects. Part II. Indian Forester, Allahabad 45: 139–153. http://www.southasiaarchive.com/Content/sarf.120200/220452

Beeson CFC (1941) The Ecology and Control of the Forest Insects of India and the Neighbouring Countries. Dehra Dun: Vasant Press, 1007 pp.

Bernon G, Graves RC (1979) An outbreak of the oil palm leaf miner beetle in Ghana with reference to a new alternate host for its parasite complex. Environmental Entomology 8(1): 108–112. https://doi.org/10.1093/ee/8.1.108

Bhasin GD (1942) A new species of Chrysomelidae from Burma. The Indian Journal of Entomology 4: 9–10.

Borowiec L, Sekerka L (2010) Cassidinae. In: Löbl I, Smetana A (Eds) Catalogue of Palearctic Coleoptera (Vol. 6). Apollo Books, 64–65. [368–390.]

Borowiec L, Świętojańska J (2007) Cassidinae collected during Czech-Polish Expedition to Maharashtra, India (Coleoptera: Chrysomelidae). Genus 18(2): 279–295.

Calcetas OA, Adorada JR, Staines CL, Calilung VJ, Caoili BL, Jamias SB (2020) Two new species of *Oncocephala* Agassiz, 1846 (Coleoptera: Chrysomelidae: Cassidinae: Oncocephalini) in Africa. Proceedings of the Entomological Society of Washington 122(3): 566–576. https://doi.org/10.4289/0013-8797.122.3.566

Chaboo CS (2007) Biology and phylogeny of the Cassidinae Gyllenhal *sensu lato* (tortoise and leaf-mining beetles) (Coleoptera: Chrysomelidae). Bulletin of the American Museum of natural History 305: 1–250. https://doi.org/10.1206/0003-0090(2007)305[1:BAPOTC]2.0.CO;2

Chaboo CS, Grobbelaar E, Heron HDC (2010) An African Leaf Miner, *Oncocephala promontorii* Péringuey, 1898 (Chrysomelidae: Cassidinae: Oncocephalini): Biological Notes and Host Records. The Coleopterists Bulletin 64(1): 21–29. https://doi.org/10.1649/0010-065X-64.1.21

Chadha YR (1976) The Wealth of India. A Dictionary of Indian Raw Materials and Industrial Products. Raw Materials XI: X–Z, Council of Scientific & Industrial Research, New Delhi, 385 pp. https://www.cabdirect.org/cabdirect/abstract/19630308468

Chatterjee NC, Bhasin GD (1936) Entomological investigations on the spike disease of sandal, (27) Chrysomelidae (Col.). Indian Forest Records New Series (Entomology) 1(13): 243–318. http://docs.kfri.res.in/KFRI-RR/KFRI-RR454.pdf

Chen Q-Y (1982) Preliminary study on *Platypria melli* Uhm. Entomological Knowledge 19(3): 32–33.

Chen S, Yu P, Sun C, Zia Y (1986) Coleoptera Hispidae. Fauna Sinica (Insecta). Science Press, Beijing, 653 pp.

Choudhary RK, Srivastava RC, Das AK, Lee J (2012) Floristic diversity assessment and vegetation analysis of Upper Siang district of eastern Himalaya in North East India. Korean Journal of Plant Taxonomy 42: 222–246. https://doi.org/10.11110/kjpt.2012.42.3.222

El Maaiden E, El Kharrassi Y, Qarah NAS, Essamadi AK, Moustaid K, Nasser B (2020) Genus *Ziziphus*: A comprehensive review on ethnopharmacological, phytochemical and pharmacological properties. Journal of Ethnopharmacology 259: e112950. https://doi.org/10.1016/j.jep.2020.112950

Fabricius JC (1798) Supplementum Entomologiae Systematicae. Hafinae, 572 pp. https://doi.org/10.5962/bhl.title.123559

Fabricius JC (1801) Systema Eleutheratorum Seundum Ordines, Genera, Species, Adiectis Synonymis, Locis, Observationibus; Descriptionibus. Tomus II. Kiliae. Bibliopoli Academici Novi, 687 pp.

Faizal MH, Prathapan KD, Anith KN, Mary CA, Lekha M, Rini CR (2006) Erythrina gall wasp *Quadrastichus erythrinae*, yet another invasive pest new to India. Current Science 90(8): 1061–1062. http://www.ias.ac.in/currsci

Fletcher TB (1914) Some South Indian Insects and Other Animals of Economic Importance Considered Especially from an Economic Point of View. Government Press, Madras, 565 pp. https://doi.org/10.5962/bhl.title.9207

Fletcher TB (1921) Annotated List of Indian Crop-Pests. Government Printing, Calcutta, 282 pp.

Gestro R (1899) Nuove forme del gruppo delle *Platypria*. Annali del Museo Civico di Storia Naturale di Genova (2) 20(40): 172–176.

Gressitt JL (1950) The hispine beetles of China (Chrysomelidae: Cassidinae). Lingnan Science Journal 23(1–2): 53–142.

Gressitt JL, Kimoto S (1963) The Chrysomelidae (Coleopt.) of China and Korea. Part 2. Pacific Insects Monograph 1B: 301–1026.

Guérin-Méneville FE (1840) Description de cinq espèces d'Hispes, formant une division distincte dans ce genre. Revue Zoologique 3: 139–142.

Hua L-Z (2002) List of Chinese Insects (Vol. 2). Zhongshan University Press, Guangzhou, 612 pp.

Kalaichelvan T, Verma KK (2005) Checklist of leaf beetles (Coleoptera: Chrysomelidae) of Bhilai-Durg. Zoos' Print Journal 20(4): 1838–1842. https://doi.org/10.11609/JoTT.ZPJ.1114.1838-42

Kalshoven LGE (1951) Pests of Crops of Indonesia. Ichtiar Baru-W. Van Hoeve, Jakarta, 701 pp.

Kalshoven LGE (1957) An analysis of ethological, ecological and taxonomic data on Oriental Hispinae (Coleoptera, Chrysomelidae). Tijdschrift voor Entomologie 100: 12–24.

Kezhen L (1992) Observations on the life habit of *Platypria hystrix* (Fabricius). Journal of Guangxi Agricultural University 3: 57–63.

Keung WM (2002) *Pueraria*. The genus *Pueraria*. Medicinal and Aromatic Plants-Industrial Profiles. In: Keung WM (Ed.) Medicinal and Aromatic Plants–Industrial Profiles (Vol. 23). Taylor & Francis, London, 290 pp.

Kimoto S (1998) Descriptions of three new species of hispid beetles (Coleoptera: Chrysomelidae) from Thailand, Cambodia and Vietnam. Serangga 3(1): 1–6.

Kimoto S (1999) Chrysomelidae (Coleoptera) of Thailand, Cambodia, Laos and Vietnam. VI. Hispinae. Bulletin of the Institute of Comparative Studies of International Cultures and Societies 23: 59–159.

Lee CF, Świętojańska J, Staines CL (2009) *Prionispa houjayi* (Coleoptera: Chrysomelidae: Cassidinae: Oncocephalini), a newly recorded genus and new species from Taiwan, with a description of its immature stages and notes on its bionomy. Zoological Studies 51: 832–861.

Liao CQ, Xu JS, Dai XH, Zhao XL (2014) Study on the biological characteristics of *Platypria melli*. Northern Horticulture 03: 118–120.

Liao CQ, Liu P, Xu JS, Staines CL, Dai XH (2018a) Description of the last-instar larva and pupa of a leafmining hispine – *Prionispa champaka* Maulik, 1919 (Coleoptera, Chrysomelidae, Cassidinae, Oncocephalini). ZooKeys 726: 47–60. https://doi.org/10.3897/zookeys.729.21041

Liao CQ, Zhang Z, Xu JS, Staines CL, Dai XH (2018b) Description of immature stages and biological notes of *Cassidispa relicta* Medvedev, 1957, a newly recorded species from China (Coleoptera, Chrysomelidae, Cassidinae, Hispini). ZooKeys 780: 71–88. https://doi.org/10.3897/zookeys.780.23280

Lindgren CJ, Castro KL, Coiner HA, Nurse RE, Darbyshire SJ (2013) The biology of invasive alien plants in Canada. 12. *Pueraria montana* var. *lobata* (Willd.) Sanjappa & Predeep. Canadian Journal of Plant Science 93: 71–95. https://doi.org/10.4141/cjps2012-128

Liu P, Liao CQ, Xu JS, Staines CL, Dai XH (2019) The Cassidinae beetles of Longnan County (Jiangxi, China): overview and community composition. Biodiversity Data Journal 7: e39053. https://doi.org/10.3897/BDJ.7.e39053

Mathur RN, Singh B (1959) A list of insect pests of forest plants in India and the adjacent countries (Arranged alphabetically according to the plant genera and species, for the use of forest officers). Part 5. List of insect pests of plant genera 'D' to 'F' (*Dactyloclenium* to *Funtumia*). Indian Forest Bulletin 171(4) (New Series) Entomology: 1–165 pp.

Mathur RN, Singh B (1961) A list of insect pests of forest plants in India and the adjacent countries, arranged alphabetically according to the plant genera and species, for the use of forest officers. Part 10. List of insect pests of plant genera 'T' to 'Z' (*Tabernemontana* to *Zizyphus*). Indian Forest Bulletin 171(9): 1–116.

Maulik S (1919) The Fauna of British India, including Ceylon and Burma. Coleoptera Chrysomelidae (Hispinae & Cassidinae) 440 pp. https://www.indianculture.gov.in/rarebooks/fauna-british-india-including-ceyln-and-burma-coleoptera-chrysomelidae

Maulik S (1937) Distributional correlation between Hispine beetles and their host plants. Proceedings of the Zoological Society of London, Ser. A: 129–159.

Maxwell-Lefroy H (1909) Indian Insect Life. Thacker, Spink and Co, Calcutta, 786 pp.

Nair MRGK (1986) Insects and Mites of Crops in India. Indian Council of Agricultural Research, New Delhi, 408 pp.

Olivier GA (1808) Entomologie, ou Histoire Naturelle des Insectes, Avec Leurs Caractères Génériques et Spécifiques, Leur Description, Leur Synonymie, et Leur Figure Enluminée (Vol. 6). Chez Desray, Paris, 612 pp.

Qi S, Huang B, Liu S, Xie Y, Luo K (1995) Two species of *Dactylispa exicisa* and *Platypria* sp. of pear and plum. Entomological Journal of East China 4(1): 110–111.

Patiri B, Borah A (2007) Wild edible plants of Assam. Director Forest Communication, Forest Department, Assam, 169 pp. [+ XXVIII.] http://103.8.249.31/assamforest/publication/wildEdible_plantsAssam.pdf

Péringuey L (1898) Catalogue of the South African Hispinae (Coleoptera), with descriptions of new species. Annals of the South African Museum 1: 113–130.

Rane N, Ranade S, Ghate HV (2000) Some observations on the biology of *Notosacantha vicaria* (Spaeth) (Coleoptera: Chrysomelidae: Cassidinae). Genus 11(2): 197–204. http://www.cassidae.uni.wroc.pl/notosacantha_vicaria.pdf

Rani BJ, Sridhar V (2004) Record of arthropod pests on velvet bean, *Mucuna pruriens* var. *utilis* under Bangalore conditions. Journal of Medicinal and Aromatic Plant Sciences 26: 505–506.

Santiago-Blay JA (2004) Leaf-mining chrysomelids. In: Jolivet PH, Santiago-Blay JA, Schmitt M (Eds) New developments on the biology of Chrysomelidae. SPB Academy Publishing, Hague, 84 pp. https://www.zin.ru/animalia/coleoptera/pdf/santiago-blay_2004.pdf

Sastri BN (1952) The Wealth of India. A dictionary of Indian raw materials and industrial products. Raw Materials (Vol. III.) D – E. Council of Scientific & Industrial Research, New Delhi, 236 pp.

Shameem KM, Prathapan KD, Nasser M, Chaboo CS (2016) Natural history of *Javeta pallida* Baly, 1858 on *Phoenix* palms in India (Chrysomelidae: Cassidinae: Coelaenomenoderini). ZooKeys 597: 39–56. https://doi.org/10.3897/zookeys.597.6876

Spaeth F (1913) Studien über die Gattung *Hoplionota* Hope und Beschreibung einer verwandten neuen Gattung. Verhandlungen der Zoologisch-Botanischen Gesellschaft in Wien 63: 381–534.

Speyer W (1954) Chrysomeliden, Blattkafer. In: Blunck H (Ed.) Handbuch der Pflanzenkrankheiten Fünffer Band. Paul Parey, Berlin, 599 pp.

Stebbing EP (1914) Indian Forest Insects of Economic Importance. Coleoptera. Eyre and Spottiswoode. London, 648 pp. https://doi.org/10.5962/bhl.title.9203

Staines CL (2015) Catalog of the hispines of the World (Coleoptera: Chrysomelidae: Cassidinae). https://naturalhistory.si.edu/research/entomology/collections-overview/coleoptera/catalog-hispines-world [Accessed 17 June 2020]

Świętojańska J, Kovac D (2007) Description of immatures and the bionomy of the Oriental leaf beetle *Chaeridiona thailandica* Kimoto, 1998 (Coleoptera: Chrysomelidae: Cassidinae: Oncocephalini), a leaf-mining hispine beetle. Zootaxa 1637: 21–36. https://doi.org/10.11646/zootaxa.1637.1.2

Taylor THC (1937) The biological control of an insect in Fiji. An account of the coconut leaf-mining beetle and its parasite complex. London: Imperial Institute of Entomology, 283 pp.

Tropicos.org (2020) http://www.tropicos.org, Release 3.1.1. Missouri Botanical Garden [Accessed 26 August 2020].

Uhmann E (1954a) Die Hispinae der Klapperich-Fukien (China)-Expedition April-Juni 1938. II. Teil. 128. Beitrag zur Kenntnis der Hispinae (Coleopt. Chrysom.). Entomologische Blätter 50: 186–215.

Uhmann E (1954b) Die Deckenelemente der *Platypria* (*Dichirispa*)-Arten Afrikas. 143. Beitrag zur Kenntnis der Hispinae (Coleopt. Chrysomelidae). Annales du Musée royal du Congo belge Tervuren, in-4, Zoologie 1: 535–539.

Uhmann E (1957) Hispinae aus dem Britischen Museum. IX. Teil. 184. Beitrag zur Kenntnis der Hispinae (Coleopt. Chrysomelidae). Annals and Magazine of Natural History (12)10: 364–368. https://doi.org/10.1080/00222935708655969

Uhmann E (1958a) Hispinae aus Südafrika. III. Teil. 183. Beitrag zur Kenntnis der Hispinae (Coleopt.: Chrysomelidae). Journal of the Entomological Society of South Africa 21(1): 214–226. https://doi.org/10.1080/00222935808650973

Uhmann E (1958b) Coleopterorum Catalogus Supplementa. Chrysomelidae: Hispinae, Hispinae Africanae, Eurasiaticae, Australicae. W. Junk. s'Gravenhage Pars 35(2): 155–398.

Verma KK, Kalaichelvan T (2004) Observations on the ootheca of some Indian tortoise beetles (Coleoptera: Chrysomelidae: Cassidinae). Entomon 29(2): 129–136.

Würmli M (1975) Gattungsmonographie der altweltlichen Hispinen (Coleoptera: Chrysomelidae: Hispinae). Entomologische Arbeiten aus dem Museum G. Frey 26: 1–83.

Würmli M (1978) Revision der Gattung *Platypria*: die Arten der orientalischen und australischen Region (*Platypria* s. str.) (Coleoptera, Chrysomelidae, Hispinae). Bollettino della Societa entomologica italiana 110: 210–223.

Zaka-ur-Rab M (1991) Leaf mining Coleoptera of the Indian subcontinent. Journal of Entomological Research 15(1): 20–30. http://www.indianjournals.com/ijor.aspx?target=ijor:jer&volume=15&issue=1&article=004

Zaitsev YM (2012) The immature stages of the leaf-beetle genus *Dactylispa* (Coleoptera, Chrysomelidae) from Vietnam. Entomological Review 92: 305–314. https://doi.org/10.1134/S0013873812030074

Zandifar K, Badi HN, Mehrafarin A, Nohooji MG (2020) The phytochemical and morphological diversity analysis of *Ziziphus nummularia* (Burm.f.) Wight & Arn. populations in south of Iran. Notulae Botanicae Horti Agrobotanici Cluj-Napoca 48(2): 588–603. https://doi.org/10.15835/nbha48211845

Supplementary material 1

Movie S1

Authors: Sachin Ranade, Kaniyarikkal Divakaran Prathapan, Hemant V. Ghate, Caroline S. Chaboo

Data type: MP4 movie file

Explanation note: Natural History of *Platypria* (*P.*) *hystrix* (Chrysomelidae: Cassidinae: Hispini) on *Erythrina*, Assam, India. (MP4 format, 3.41 min; film made and narrated by S. Ranade, 2020).

Link: https://doi.org/10.3897/zookeys.1031.60129.suppl1

ZooKeys 1031: 85–124 (2021)
doi: 10.3897/zookeys.1031.62125
https://zookeys.pensoft.net

RESEARCH ARTICLE

A peer-reviewed open-access journal
ZooKeys
Launched to accelerate biodiversity research

Taxonomic complexity in the genus *Merodon* Meigen, 1803 (Diptera, Syrphidae)

Ante Vujić[1], Snežana Radenković[1], Laura Likov[1], Sanja Veselić[1]

[1] *University of Novi Sad, Faculty of Sciences, Department of Biology and Ecology, Trg Dositeja Obradovića 2, 21000 Novi Sad, Serbia*

Corresponding author: Ante Vujić (ante.vujic@dbe.uns.ac.rs)

Academic editor: X. Mengual | Received 16 December 2020 | Accepted 12 March 2021 | Published 14 April 2021

http://zoobank.org/DE30A88C-39E6-48A2-824A-FDC0B67F541E

Citation: Vujić A, Radenković S, Likov L, Veselić S (2021) Taxonomic complexity in the genus *Merodon* Meigen, 1803 (Diptera, Syrphidae). ZooKeys 1031: 85–124. https://doi.org/10.3897/zookeys.1031.62125

Abstract

The genus *Merodon* Meigen, 1803 is distributed across the Palaearctic and Afrotropical Regions. The present work summarizes the knowledge from recent taxonomic and systematic revisions and includes an identification key for the five monophyletic lineages (namely *albifrons*, *aureus*, *avidus-nigritarsis*, *desuturinus* and *natans*), 24 species groups, two species subgroups and 10 unplaced species, along with diagnosis and illustrations. A list of 234 taxa, including 194 described and 40 undescribed species, is appended. Most of the species are distributed in the Palaearctic (209 taxa, 181 described), while 27 species (14 described) are known from the Afrotropical Region. Three lineages (*aureus*, *desuturinus* and *natans*) are present in the Afrotropical Region, as well as in the Palaearctic. The Afrotropical *melanocerus* species group of the *desuturinus* lineage and the *bombiformis* species group of the *aureus* lineage are endemic to the Afrotropical Region, and all other species groups belong to the Palaearctic fauna. The *albifrons* lineage contains six species groups (*albifrons*, *constans*, *equestris*, *geniculatus*, *ruficornis* and *rufus*) and two unplaced taxa. The *aureus* lineage includes five species groups (*aureus*, *bombiformis*, *funestus*, *nanus* and *spinitarsis*). The *avidus-nigritarsis* lineage is divided into 10 species groups (*aberrans*, *aurifer*, *avidus*, *clavipes*, *fulcratus*, *italicus*, *nigritarsis*, *pruni*, *serrulatus* and *tarsatus*) and eight unplaced taxa. The *desuturinus* lineage contains two species groups: the Afrotropical *melanocerus* group, with the *melanocerus* and *planifacies* subgroups plus the species *M. cuthbertsoni* Curran, 1939, and the Palaearctic *murorum* species group. The *natans* lineage consists of the *natans* species group plus the species *M. segetum* Fabricius, 1794.

Keywords

Identification key, integrative taxonomy, lineages, *Merodon*, morphology, species groups, Syrphidae

Introduction

The genus *Merodon* Meigen, 1803 is one of the most species-rich hoverfly genera, distributed across the Palaearctic and Afrotropical Regions (Ståhls et al. 2009; Vujić et al. 2012). It belongs to the tribe Merodontini, formerly named Eumerini. Most recent works used the name Merodontini instead of Eumerini (Skevington and Yeates 2000; Marcos-García et al. 2007; Andrić et al. 2014; Vujić et al. 2015, 2019; Ačanski et al. 2016b; Doczkal et al. 2016; Young et al. 2016; Radenković et al. 2018a; Milić et al. 2019; Šašić Zorić et al. 2019; Likov et al. 2020). However, there is no general consensus on the intratribal structure yet.

The genus *Merodon* was described by Meigen (1803) based on the type species *Syrphus clavipes* Fabricius, 1781. Until now, two synonyms of *Merodon* are recognized: *Lampetia* Meigen, 1800, originally described without included species, was suppressed by ICZN (1963, Opinion 678: 339); and *Exmerodon*, created by Becker (1913) as a subgenus of *Merodon* based on the type species *Exmerodon fulcratus* Becker, 1913, was listed as synonym by Peck (1988). Currently, the genus *Merodon* contains 194 described species and 40 undescribed species listed here. The genus is restricted to the Palaearctic and Afrotropical Regions (Ståhls et al. 2009; Šašić et al. 2016), except for *M. equestris* (Fabricius, 1794) that has been introduced into the Nearctic Region and New Zealand (Speight 2020). The genus is divided in lineages, species groups, species subgroups and species complexes following the system proposed by Šašić et al. (2016) based on different levels of morphological differentiation. Šašić et al. (2016) proposed a system of four levels (ranks) for classification of the genus *Merodon*: (1) the broadest (first) level consists of large monophyletic lineages where each contains multiple morphologically different species groups; (2) the second broadest level involves taxa that constitute morphologically defined species groups within lineages; (3) the third level represents subgroups that include species with very similar morphologies, but exhibiting small, consistent interspecific character variations that facilitate their distinction; (4) the narrowest (fourth) level are species complexes that comprise morphologically inseparable taxa based on classical taxonomical methods, which can only be resolved by employing integrative taxonomy involving molecular markers, morphometry, and ecology.

In Europe, *Merodon* is the most speciose genus with 120 described species (152 including Turkey) (Speight 2020; Vujić, unpublished). The highest species diversity is recorded for the Mediterranean Basin (Vujić et al. 2012), which is associated with a high diversity of bulb plant species that serve as larval host plants (Ricarte et al. 2008, 2017; Andrić et al. 2014; Preradović et al. 2018). Asia Minor and Eastern Europe (especially the Balkan Peninsula) are considered hot spots and regions with high endemism for the genus *Merodon* (Kaloveloni et al. 2015), as documented by several studies in the Eastern Mediterranean Basin (Vujić et al. 2007, 2011, 2013, 2015, 2020a, b, c; Ståhls et al. 2009, 2016; Radenković et al. 2011, 2020; Kaloveloni et al. 2015; Ačanski et al. 2016a, b; Likov et al. 2020). Unlike this area, Afrotropical Region and Eastern Palaearctic are characterized by a low number of species (Vujić, unpublished).

The genus *Merodon* was classified into more than 20 monophyletic species groups, half of which were addressed in Hurkmans' (1993) monograph. Hurkmans (1993) gave the first and most comprehensive revision of the genus, placing 61 species with tapering abdomen into 11 species groups, namely *alagoezicus*, *alexeji*, *avidus*, *clavipes*, *crassifemoris*, *elegans*, *longicornis*, *nigritarsis*, *pruni*, *tarsatus* and *vandergooti*. Mengual et al. (2006) discerned four species groups (*desuturinus*, *albifrons*, *nigritarsis* and *aureus*) based on molecular data among the species occurring in the Iberian Peninsula. Vujić et al. (2019) recognized five monophyletic lineages within the genus *Merodon*, i.e., *albifrons*, *aureus*, *avidus-nigritarsis*, *desuturinus* and *natans*, condensing previous studies from Šašić et al. (2016) and Radenković et al. (2018a). The *albifrons+desuturinus* lineage *sensu* Vujić et al. (2012) is now divided into two lineages, *albifrons* and *desuturinus*.

Nowadays, with the advent of molecular and morphometric techniques, an integrative taxonomic framework has become the standard to study the taxonomy of genus *Merodon.* Combining molecular characters (mtDNA cytochrome *c* oxidase subunit I (COI) and the nuclear 28S rRNA genes) with morphological traits (geometric wing morphometry, surstylus shape and size, and other morphological characters), a number of cryptic and sibling species have been delineated within different species groups. Notable examples are the *ruficornis* species group (Radenković et al. 2002; Milankov et al. 2008c; Francuski et al. 2009; Vujić et al. 2012), *desuturinus* species group (Milankov et al. 2008b; Vujić et al. 2018b), *aureus* and *cinereus* species subgroups (Milankov et al. 2008a; Francuski et al. 2011; Šašić et al. 2016; Veselić et al. 2017; Radenković et al. 2018b), *avidus* species complex (Milankov et al. 2009; Popović et al. 2015; Ačanski et al. 2016b), *albifrons* species group (Milankov et al. 2013), *nigritarsis* species group (Vujić et al. 2013; Likov et al. 2020), *nanus* species group (Vujić et al. 2015; Kočiš Tubić et al. 2018), *serrulatus* species group (Vujić et al. 2020b), *constans* species group (Vujić et al. 2020a), *rufus* species group (Radenković et al. 2020), and all *Merodon* species of Lesvos Island (Ståhls et al. 2009).

The aim of this work is to summarize the knowledge from recent taxonomic and systematic revisions, to help taxonomists to have a central reference for the recent published literature, and to present an identification key for the identification of lineages, species groups, species subgroups and unplaced species of *Merodon*.

Material and methods

A total of 255 species belonging to the tribe Merodontini (genera *Azpeytia* Walker, 1865, *Eumerus* Meigen, 1822, *Megatrigon* Johnson, 1898, *Merodon* and *Platynochaetus* Weidemann, 1830) from the Palaearctic and Afrotropical Regions were studied. All specimens were identified by Ante Vujić and Snežana Radenković. Representative specimens are deposited in the collections of the Department of Biology and Ecology, Faculty of Sciences, University of Novi Sad, Serbia (**FSUNS**).

Morphological terminology follows Thompson (1999), except for the male genitalia that follows Marcos-García et al. (2007). We use the terms "fossette", "hypostomal bridge", "postalar" and "occipital foramen" from Doczkal and Pape (2009), and "oral margin" from Radenković et al. (2018a). For the pollinose markings on abdominal terga we used the term fasciate maculae. These markings are elongate and usually separated medially. Sometimes the fasciate maculae may have joined medially forming an entire fascia or band, but we consistently referred to them as fasciate maculae.

Male genitalia were extracted from dry specimens previously relaxed in a humidity chamber. After genitalia were pulled out with a hook-tipped entomological pin, they were cleared by boiling in warm 10% potassium hydroxide (KOH) for 3–5 min. Acetic acid was then used to neutralize the KOH during 5 s, and genitalia were immersed briefly in ethanol to remove the acid. Prepared genitalia were stored in microvials containing glycerol.

Photographs were taken using a Leica DFC 320 digital camera, attached to a Leica MZ16 stereomicroscope and Nikon Coolpix D7100 digital camera attached to a Nikon SMZ 745T stereomicroscope. Digital photographs were stacked using CombineZ software (Hadley 2006). A Leica MZ16 binocular microscope was used with an FSA 25 PE drawing tube to make the drawings.

Results

Tribe Merodontini

Based on Doczkal and Pape (2009), members of the Merodontini possess six autapomorphic character states: hypostomal bridge close to the occipital foramen with a transverse crest (Suppl. material 1: Fig. S1A: marked with arrow), absent in others (Suppl. material 1: Fig. S1B); presence of a pyramidal tubercle on the postalar wall (Suppl. material 1: Fig. S2A: marked with arrow), flat in others (Suppl. material 1: Fig. S2B: marked with arrow); dorsomedian part of anepimeron setose (Suppl. material 1: Fig. S2C: marked with arrow), bare in others (Suppl. material 1: Fig. S2D: marked with arrow); presence of a well-defined fossette (Suppl. material 1: Fig. S3C: marked with arrow), absent in others (Suppl. material 1: Fig. S3D); wing vein R_1 joining C beyond 0.6 of the distance from Sc to R_{2+3} (Suppl. material 1: Fig. S3A), different in others (Suppl. material 1: Fig. S3B); and distal end of M_1 recurrent, forming an acute outer angle with R_{4+5} (Suppl. material 1: Fig. S3A: marked with arrow), obtuse in others (Suppl. material 1: Fig. S3B: marked with arrow). The first two character states are unique to the Merodontini, whereas the remaining character states are homoplasious with occurrences elsewhere in Syrphidae (Doczkal and Pape 2009). Other autapomorphies of the Merodontini, not present in *Lyneborgimyia* Doczkal & Pape, 2009, are the presence of a lateral sclerite of the aedeagus (Suppl. material 2: Fig. S10F: s) and ventral processes and/or invaginations of the hypandrium (Suppl. material 2: Fig. S10F: marked with arrow) (Doczkal and Pape 2009).

Genus *Merodon*

Merodon Meigen, 1803, Mag. Insektenk, 2, 274. Type-species: *Syrphus clavipes* Fabricius, 1781, by subsequent designation of Guérin-Méneville in Bory de Saint-Vincent 1826: 446.

Lampetia Meigen, 1800, Nouvelle classification des mouches à deux ailes (Diptera L.) d'après un plan tout nouveau J.J. Fuchs, Paris: 34. Type-species: *Syrphus clavipes* Fabricius, 1781, by subsequent designation of Coquillett, 1910: 557. Suppressed by ICZN 1963: Opinion 678: 339.

Differential diagnosis. The genus can be distinguished by the presence of an antero-ventral triangular lamina above the apex of the metafemur (as in Suppl. material 1: Fig. S15D or Suppl. material 1: Fig. S28E, F), wing vein R_{4+5} with a deep loop into cell r_{4+5}, and veins Sc and R_1 connected with a stigmal crossvein (Suppl. material 1: Fig. S3A: marked with asterisk).

As mentioned earlier, there are five monophyletic lineages within the genus *Merodon*: *albifrons*, *aureus*, *avidus-nigritarsis*, *desuturinus*, and *natans* (Vujić et al. 2019). The main morphological features and the list and number of species are presented in Supplementary materials.

Identification key to the *Merodon* lineages

In this section and sections below, we provide several identification keys to the 24 species groups, two species subgroups and 10 unplaced species within the genus *Merodon*. For further species identification inside species groups, species subgroups and species complexes, published revisionary works are cited in brackets.

1 Mesocoxa without long pile posteriorly (Suppl. material 1: Fig. S4B), or if mesocoxa with 1–3 long pile posteriorly then inner side of metafemur with a row of spinae (Suppl. material 1: Fig. S5A) .... ***avidus-nigritarsis* lineage**

– Mesocoxa with at least a few long pile posteriorly (Suppl. material 1: Fig. S4A), inner side of metafemur without a row of spinae..**2**

2 Mesocoxa with more than 10 long pile posteriorly..**4**

– Mesocoxa with a few long pile posteriorly (usually five to seven, or less) (Suppl. material 1: Fig. S5B) **3**

3 Basoflagellomere elongated, twice as long as wide, narrowed in apical third (Suppl. material 1: Fig. S6A); scutum usually with five well defined pollinose longitudinal vittae (Suppl. material 1: Fig. S6C). Anterior surstyle lobe of male genitalia well-developed, oval, without curved distal prolongation (Suppl. material 2: Fig. S13A: al)..***natans* lineage**

– Basoflagellomere less than half as long as wide, narrowed in apical half (Suppl. material 1: Fig. S6B); scutum without pollen or with less distinct pollinose longitudinal vittae (Suppl. material 1: Fig. S6D). Anterior surstyle lobe of male genitalia with curved distal prolongation (Suppl. material 2: Fig. S12E, H: al) .... ***desuturinus* lineage (in part)**

4 Anterior anepisternum with bare area ventral to postpronotum (Suppl. material 1: Fig. S7B) **6**

– Anterior anepisternum with many long pile ventral to postpronotum (Suppl. material 1: Fig. S7A) **5**

5 Postpronotum usually brown or yellow-reddish. Male genitalia: anterior surstyle lobe with curved distal prolongation (Suppl. material 2: Fig. S12E, H: al). Female: pilosity on lateral side of tergum 4 long, medially short and mostly adpressed (Suppl. material 1: Fig. S8A) .... ***desuturinus* lineage (in part)**

– Postpronotum black. Male genitalia: anterior surstyle lobe undeveloped (Suppl. material 2: Fig. S4A: al). Female: all the pilosity on tergum 4 approximately of same length (Suppl. material 1: Fig. S8B) .... ***aureus* lineage**

6 Lateral sclerite of the aedeagus gradually tapered, with the tip curved (Suppl. material 2: Fig. S12C: s); wing microtrichose between veins R_1 and RS (Suppl. material 1: Fig. S9A) .... ***desuturinus* lineage (in part)**

– Lateral sclerite of the aedeagus hammer-like (Suppl. material 2: Fig. S2C: s); wing with bare area in the basal part of wing cell r_1, between veins R_1 and RS (Suppl. material 1: Fig. S9B) .... ***albifrons* lineage**

Key to the species groups and unplaced species of the *albifrons* lineage

1 Postpronotum, lateral sides of scutum and face yellowish (Suppl. material 1: Fig. S31) .... ***Merodon luteihumerus* Marcos-García, Vujić & Mengual, 2007**

– Postpronotum, lateral sides of scutum and face black or dark **2**

2 Pro- and mesolegs strongly modified (Suppl. material 1: Fig. S32A, C) .... ***Merodon mixtum* Vujić, Radenković & Likov, 2019**

– Pro- and mesolegs with usual shape **3**

3 Pilosity on the posterior part of abdomen (at least tergum 4) denser and strikingly golden to reddish-yellow (as in Suppl. material 1: Fig. S33A) contrasting with the colour of the pilosity on the rest of the abdomen .... ***constans* species group (Vujić et al. 2020a)**

– Pilosity on the posterior part of abdomen not denser compared to the anterior part (Suppl. material 3: Fig. S2B) **4**

4 Large (11–17 mm) bumble bee-like species with dense and long body pilosity (Suppl. material 3: Fig. S2A, B); males with strong apical dorsal calcar on metatibia (Suppl. material 1: Fig. S34A) .... ***equestris* species group (Marcos-García et al. 2011)**

– Species with different characters **5**

5 Medium to large sized species (9–13 mm) with black, bronze lustre terga (lack pollinose fasciate maculae), except a pair of small, orange, lateral markings on

tergum 2 (Suppl. material 1: Fig. S33B); scutum and terga covered with erect, mostly yellowish to reddish pilosity, except few black pile medially on terga 3 and 4 (Suppl. material 1: Fig. 33C). Male: metatrochanter can have a calcar, but metatibia always without calcar (Suppl. material 1: Fig. S34B) .... ***rufus* species group (Radenković et al. 2020)**

– Species with different characters; usually with pollinose fasciate maculae on terga **6**

6 Female (genitalia not visible) **9**

– Male (genitalia visible externally) **7**

7 Metaleg with some modifications on metatrochanter, metafemur and/or metatibia; male genitalia often with hook-like posterior surstyle lobe or cercus with prominence(s) **8**

– Metaleg usually without modifications (exception is *Merodon trochantericus* Costa, 1884, see in Suppl. material 1: Fig. S34C); male genitalia with rounded posterior surstyle lobe, biramous anterior surstyle lobe pliers-like (with thorn-like interior accessory lobe process), and cercus without prominences (as in Suppl. material 2: Fig. S2A) .... ***albifrons* species group**

8 Metatrochanter with blunt calcar apically covered with long pile (Suppl. material 1: Fig. S34D); metatibia with apicomedial carina (Suppl. material 1: Fig. S34E); male genitalia with rounded or acute posterior surstyle lobe, biramous anterior surstyle lobe with apical extension more developed, and cercus with prominence(s) (as in Suppl. material 2: Fig. S2G: marked with arrow) .... ***geniculatus* species group (Vujić et al. 2018a)**

– Metatrochanter with sharp apical calcar (Suppl. material 1: Fig. S34F); metafemur usually with ventral tubercle or calcar (as on Suppl. material 1: Fig. S34F: marked with arrow); metatibia usually with apicolateral process (as on Suppl. material 1: Fig. S34F: marked with arrow); male genitalia usually with hook-like posterior surstyle lobe, biramous anterior surstyle lobe with moderately developed interior accessory lobe and apical extension, and cercus without prominences (as in Suppl. material 2: Fig. S3A: c) .... ***ruficornis* species group (Vujić et al. 2012)**

9 Metatibia narrow, not swollen apically (Suppl. material 1: Fig. S34G); terga 3–5 black .... ***ruficornis* species group (Vujić et al. 2012)**

– Metatibia incrassate apically (Suppl. material 1: Fig. S34H); terga 3–5 usually partly reddish **10**

10 Scutum usually with five distinct pollinose vittae (Suppl. material 1: Fig. S35A); terga 2–4 with well-defined pollinose fasciate maculae (Suppl. material 1: Fig. S35B); metatibia with concave ventral margin in apical half (Suppl. material 1: Fig. S34H) .... ***geniculatus* species group (Vujić et al. 2018a)**

– Scutum with indistinct pollinose vittae; terga 2–4 without or with narrower pollinose fasciate maculae (Suppl. material 1: Fig. S35C); metatibia with straight ventral margin in apical half (Suppl. material 1: Fig. S33D) .... ***albifrons* species group**

Key to the groups and unplaced species and species of the *aureus* lineage

1 Female (genitalia not visible) **6**

– Male (genitalia visible externally) **2**

2 Metatrochanter with calcar (Suppl. material 1: Fig. S28B marked with arrow) **5**

– Metatrochanter rounded and smooth, without calcar (Suppl. material 1: Fig. S28A) **3**

3 Hypandrium strongly modified, sinuous in apical half, with subapical ctenidium and stitched theca (cuticle looks like it is sewed) (Suppl. material 2: Fig. S4K) .... ***spinitarsis* species group**

– Hypandrium different, but with apical ctenidium and without stitch on theca (as in Suppl. material 2: Fig. S5C) **4**

4 Pedicel elongated, approximately as long as basoflagellomere (relation pedicel basoflagellomere = 0.9 : 1.1) (Suppl. material 1: Fig. S29A); hypandrium narrowed medially (Suppl. material 2: Fig. S5C: marked with arrow) .... ***bombiformis* species group (Afrotropical Region)**

– Pedicel shorter than basoflagellomere (as in Suppl. material 1: Fig. S29B); hypandrium broad, not narrowed medially (Suppl. material 2: Fig. S4G) .... ***nanus* species group (Vujić et al. 2015; Kočiš Tubić et al. 2018)**

5 Yellow-grey pilosity on terga more dense and striking laterally, as well as on pollinose fasciate maculae of terga 2 and 3, and on tergum 4 (Suppl. material 1: Fig. S30A); pedicel elongated, approximately as long as basoflagellomere (relation pedicel : basoflagellomere = 0.9 : 1.1) (Suppl. material 1: Fig. S29C) .... ***funestus* species group**

– Terga evenly covered with upstanding, dense pilosity (can be differently coloured) (Suppl. material 1: Fig. S30B); pedicel shorter than basoflagellomere (Suppl. material 1: Fig. S29D) .... ***aureus* species group (Šašić et al. 2016, 2018, 2019; Veselić et al. 2017; Radenković et al. 2018b; Vujić et al. 2020c)**

6 Pedicel shorter than basoflagellomere (Suppl. material 1: Fig. S29F) **8**

– Pedicel elongated, approximately as long as basoflagellomere (relation pedicel : basoflagellomere = 0.9 : 1.1) (Suppl. material 1: Fig. S29E) **7**

7 Apical triangular lamina on metafemur weakly serrated, usually with distinct apical dens (Suppl. material 1: Fig. S28E: marked with arrow) .... ***bombiformis* species group (Afrotropical Region)**

– Apical triangular lamina on metafemur markedly serrated (Suppl. material 1: Fig. S28F: marked with arrow) .... ***funestus* species group**

8 Terga without pollinose fasciate maculae, with dense puncta (Suppl. material 1: Fig. S30C) **9**

– Terga 2–4 (at least 2) usually with pollinose medial fasciate maculae, with less dense puncta (Suppl. material 1: Fig. S30D) .... ***aureus* species group (Šašić et al. 2016, 2018, 2019; Veselić et al. 2017; Radenković et al. 2018b; Vujić et al. 2020c)**

9 Tergum 4 covered with short adpressed pile (Suppl. material 1: Fig. S30E); tarsi black (Suppl. material 1: Fig. S28C) .... ***spinitarsis* species group**

– Tergum 4 covered with longer semi-erect pile, longer than basoflegellomere (Suppl. material 1: Fig. S30F); tarsi partly reddish (Suppl. material 1:

Fig. S28D).. .... ***nanus*** **species group (Vujić et al. 2015; Kočiš Tubić et al. 2018)**

Key to the species groups and unplaced species of the *avidus-nigritarsis* lineage

1 Inner side of metafemur with a row of spinae (Suppl. material 1: Fig. S5A). Male with two fossette (small apical one on the inner side, and a large one on the outer side) (Suppl. material 1: Fig. S10A, B); mesocoxa with 1–3 long pile posteriorly .... ***Merodon eumerusi*** **Vujić, Radenković & Likov, 2019**

– Inner side of metafemur without a row of spinae **2**

2 Terga partly brown, reddish or yellow **22**

– Terga black.. **3**

3 Females (genitalia not visible).. **13**

– Males (genitalia visible externally) **4**

4 Male genitalia without ctenidium at hypandrium (Suppl. material 2: Fig. S7K: marked with arrow); small sized species (5–9 mm) with metallic shiny body and distinctly dichoptic eyes, separated by distance almost as long as distance between ocelli (Suppl. material 1: Fig. S11A); metafemur with very small apical triangular lamina apicoventrally (Suppl. material 1: Fig. S12A: marked with arrow) ...... ***fulcratus*** **species group**

– Male genitalia always with ctenidium at hypandrium (as in Suppl. material 2: Fig. S7C: marked with arrow) **5**

5 Large species (15–20 mm) with long body pilosity and broad metafemur covered with long pile (Suppl. material 1: Fig. S12B); basoflagellomere elongated; terga usually covered with pile in different combinations of colours (white, yellow or black) (Suppl. material 3: Fig. S9A, B); surstyle with well-defined and large anterior and posterior lobes (Suppl. material 2: Fig. S7A: al, pl)....... ***clavipes*** **species group**

– Species with shorter pilosity and different combinations of characters **6**

6 Sternum 4 medially clearly divided with membranous structure and with posterolateral tubercles or laminate extensions (Suppl. material 1: Fig. S11C: marked with arrow); sternum 4 from lateral view usually fin-form (Suppl. material 1: Fig. S11D: marked with arrow); basotarsomere of metatarsus usually expanded (Suppl. material 1: Fig. S12C, D) and/or with strong setae ventrally (Suppl. material 1: Fig. S12C, D: marked with arrow) .... ***tarsatus*** **species group**

– Sternum 4 and basotarsomere of metatarsus without such modifications 7

7 Male genitalia: posterior surstyle lobe divided into two branches (Suppl. material 2: Fig. S9J: pl); eyes slightly dichoptic, distance between eyes about two facets long (Suppl. material 1: Fig. S11B) .... ***Merodon hirtus*** **Sack, 1932**

– Male genitalia: posterior surstyle lobe not divided into branches; eyes holoptic ... **8**

8 Abdomen elongated and narrow; terga black; terga 2–4 with a pair of pollinose fasciate maculae (Suppl. material 1: Fig. S11E); metafemur usually long and narrow. Male genitalia: hypandrium with very long lingula (Suppl. material 2: Fig. S6C: l); posterior surstyle lobe with inner lobe covered with long and strong setae (Suppl. material 2: Fig. S6B)... ***aberrans*** **species group**

– Species with different combinations of characters.. **9**

9 Basoflagellomere elongated, at least three times as long as wide (Suppl. material 1: Fig. S13A); posterior surstyle lobe quadratic (Suppl. material 2: Fig. S7D: pl) .... ***italicus* species group (in part)**

– Basoflagellomere less elongated; posterior surstyle lobe different **10**

10 Posterior surstyle lobe with basolateral protrusion (lateral hump) (Suppl. material 2: Fig. S9G: marked with arrow). Metafemur with shorter pilosity ventrally, shorter than width of metafemur (Suppl. material 1: Fig. S14A); basoflagellomere narrow and elongated, two times longer as pedicel (Suppl. material 1: Fig. S13B)............................***serrulatus* species group (in part) (Vujić et al. 2020b)**

– Posterior surstyle lobe of male genitalia without basolateral protrusion (lateral hump)...**11**

11 Basoflagellomere reddish-yellow (Suppl. material 1: Fig. S13C); tarsus of metaleg yellow (at least basotarsomere) (Suppl. material 1: Fig. S14B); metatarsus long, more than three times longer than wide (Suppl. material 1: Fig. S14B); metafemur less incrassate, ca. four times longer than wide (Suppl. material 1: Fig. S14B).. ***Merodon ottomanus* Hurkmans, 1993**

– Basoflagellomere brown to black; tarsi of metaleg dark; metatarsus shorter, two times longer than wide (Suppl. material 1: Fig. S14D); metafemur more incrassate, ca. three times longer than wide (Suppl. material 1: Fig. S14C)...............**12**

12 Basoflagellomere with convex dorsal margin (Suppl. material 1: Fig. S13D); posterior surstyle lobe with the apical hump directed towards cercus (Suppl. material 2: Fig. S10G: marked with arrow).........***Merodon clunipes* Sack, 1913 (in part)**

– Basoflagellomere with concave dorsal margin (Suppl. material 1: Fig. S13E); posterior surstyle lobe without the apical hump directed towards cercus (Suppl. material 2: Fig. S10A: pl)..........................***Merodon auronitens* Hurkmans, 1993**

13 Metafemur more incrassate, ca. three times longer than wide, covered with dense pilosity (Suppl. material 1: Fig. S15A)...**14**

– Metafemur less incrassate, at least three times longer than wide (as in Suppl. material 1: Fig. S15B)..**15**

14 Basoflagellomere shorter, 1.3 times as long as wide, with convex dorsal margin (Suppl. material 1: Fig. S16A); pile on ventral margin of metafemur shorter, ca. one third of width of metafemur (Suppl. material 1: Fig. S15A) ....***Merodon clunipes* Sack, 1913 (in part)**

– Basoflagellomere elongated, two times as long as wide (Suppl. material 1: Fig. S16B); pile on ventral margin of metafemur longer, ca. half of width of metafemur (Suppl. material 1: Fig. S15C) ....***clavipes* species group (in part)**

15 Small sized species (8-11 mm) with metallic shiny body; scutum and terga strongly punctate, without or with very weak pollinose areas (Suppl. material 1: Fig. S17A, B); metafemur with very small apical triangular lamina apicoventrally (Suppl. material 1: Fig. S15D marked with arrow)....................***fulcratus* group**

– Species with different combinations of characters...**16**

16 Metafemur with short pilosity (Suppl. material 1: Fig. S15E)............................ ....***serrulatus* species group (in part) (Vujić et al. 2020b)**

– Metafemur with longer pile (as in Suppl. material 1: Fig. S15B) **17**

17 Abdomen broad, oval (Suppl. material 1: Fig. S17C); terga without pollinosity or with very weak pollinose fasciate maculae; tarsus of metaleg yellow (at least basotarsomere) (Suppl. material 1: Fig. S15B).. ***Merodon ottomanus* Hurkmans, 1993**

– Species with different combinations of characters...**18**

18 Basotarsomere of metatarsus elongated, four times as long as wide (Suppl. material 1: Fig. S15F); basoflagellomere elongated, 2.5 times as long as wide (Suppl. material 1: Fig. S16C); tarsi yellow, tibiae mostly yellowish, except medially brown (Suppl. material 1: Fig. S15F) ....***Merodon murinus* Sack, 1913 (in part)**

– Species with different combinations of characters...**19**

19 Abdomen narrow, elongated (Suppl. material 1: Fig. S17D); metaleg usually narrow (as in Suppl. material 1: Fig. S18A) ....***aberrans* species group**

– Species with broader abdomen and metaleg **20**

20 Tergum 2 without or with indistinct narrow pollinose fasciate maculae (Suppl. material 1: Fig. S19A, B); basotarsomere of metatarsus usually expanded (Suppl. material 1: Fig. S18B) or with strong setae ventrally (Suppl. material 1: Fig. S18B marked with arrow)... ***tarsatus* species group**

– Tergum 2 with broad pollinose fasciate maculae (Suppl. material 1: Fig. S19C); basotarsomere of metatarsus not expanded and without strong setae ventrally (Suppl. material 1: Fig. S18C)..**21**

21 Terga 2–4 strongly punctate; second and third tarsomeres similar in size (Suppl. material 1: Fig. S18D marked with arrow); sterna shiny... ***Merodon auronitens* Hurkmans, 1993**

– Terga 2–4 finely punctate; second tarsomere longer than third (Suppl. material 1: Fig. S18C marked with arrow); sterna dull..............***Merodon hirtus* Sack, 1932**

22 Females (genitalia not visible)...**31**

– Males (genitalia visible externally) **23**

23 Metatibia swollen in apical half (Suppl. material 1: Fig. S20A); basotarsomere of metatarsus strongly modified (Suppl. material 1: Fig. S20A) ....***Merodon caudatus* Sack, 1913**

– Metaleg without such modifications..**24**

24 Posterior surstyle lobe with basolateral protrusion (lateral hump) (Suppl. material 2: Fig. S9G: marked with arrow)..***serrulatus* species group (in part) (Vujić et al. 2020b)**

– Posterior surstyle lobe without basolateral protrusion.......................................**25**

25 Face with a bulge below antennae (Suppl. material 1: Fig. S21A: marked with arrow); posterior surstyle lobe hook-like (Suppl. material 2: Fig. S10J: pl) ....***Merodon crassifemoris* Paramonov, 1925**

– Face without a bulge below antennae **26**

26 Metatrochanter without calcar **28**

– Metatrochanter with distinct calcar (Suppl. material 1: Fig. S20B: marked with arrow) **27**

27 Basoflagellomere 1.2 times as long as wide (Suppl. material 1: Fig. S23A); body pilosity very short; terga 3–4 dark (Suppl. material 1: Fig. S22A)........................ ....***aurifer* species group**

– Basoflagellomere short, as long as wide (Suppl. material 1: Fig. S23B); body pilosity longer; terga 3–4 mostly yellow-red (Suppl. material 1: Fig. S22B) ....***pruni* species group**

28 Basoflagellomere elongated, at least three times as long as wide (Suppl. material 1: Fig. S13A); posterior surstyle lobe quadratic (Suppl. material 2: Fig. S7D: pl) .... ***italicus* species group** (in part)

– Basoflagellomere shorter, less than three times as long as wide (as in Suppl. material 1: Fig. S23C); posterior surstyle lobe different..**29**

29 Eye contiguity very short, approximately four to five facets long (Suppl. material 1: Fig. S21B); male genitalia in Suppl. material 2: Fig. S11D–F......................... ....***Merodon murinus* Sack, 1913 (in part)**

– Eye contiguity more than 10 facets long (as in Suppl. material 1: Fig. S21C); male genitalia different **30**

30 Tarsi yellow dorsally and ventrally (Suppl. material 1: Fig. S20C, D) .... ***avidus* species group (Popović et al. 2015; Ačanski et al. 2016b; Likov et al. 2020)**

– Tarsi dark brown/black dorsally and orange/brown ventrally (Suppl. material 1: Fig. S20E, F)....***nigritarsis* species group (Vujić et al. 2013; Likov et al. 2020)**

31 At least terga 2 and 3 with brown, reddish or yellow markings........................**36**

– Only tergum 2 with brown, reddish or yellow maculae, other terga dark **32**

32 Metatibia swollen in apical half (Suppl. material 1: Fig. S24A); tarsomeres of mesotarsus with strong, black lateral setae (Suppl. material 1: Fig. S24B)........... ....***Merodon caudatus* Sack, 1913**

– Metatibia of normal shape (as in Suppl. material 1: Fig. S24C); tarsomeres of mesotarsus without such lateral setae...**33**

33 Pile on ventral margin of metafemur dense and long, the longest as long as width of metafemur (Suppl. material 1: Fig. S15C).................. ***clavipes* species group**

– Pile on ventral margin of metafemur shorter, maximum as long as half of width of metafemur (as in Suppl. material 1: Fig. S15A)..**34**

34 Basoflagellomere shorter, 1.3 times as long as wide, with convex dorsal margin (Suppl. material 1: Fig. S16A); metafemur incrassate or swollen, ca. three times longer than wide (Suppl. material 1: Fig. S15A).. ....***Merodon clunipes* Sack, 1913 (in part)**

– Basoflagellomere longer, with straight or concave dorsal margin (Suppl. material 1: Fig. S16C); metafemur less incrassate..**35**

35 Tarsi yellow, tibiae mostly yellowish, only medially brown; frons and vertex usually partly reddish to yellow (Suppl. material 1: Fig. S25A) ....***Merodon murinus* Sack, 1913 (in part)**

– Legs mostly black, at least tarsi dark; frons black... ....***serrulatus* species group (in part) (Vujić et al. 2020b)**

36 Basoflagellomere elongated, more than 1.5 times as long as wide (Suppl. material 1: Fig. S26B); metatrochanter with rounded ventral margin (as in Suppl. material 1: Fig. S24D) **38**

– Basoflagellomere shorter, less than 1.3 times as long as wide (Suppl. material 1: Fig. S26A); metatrochanter with angular ventral margin (Suppl. material 1: Fig. S24C: marked with arrow) **37**

37 Basoflagellomere very short, as long as wide (Suppl. material 1: Fig. S26A); metafemur dorsally and ventrally covered with longer outstanding pile (Suppl. material 1: Fig. S24C) .... ***pruni* species group**

– Basoflagellomere longer, 1.2 times as long as wide (Suppl. material 1: Fig. S26C); metafemur covered with short and adpressed pilosity (Suppl. material 1: Fig. S24E) .... ***aurifer* species group**

38 Face with a bulge below antennae (Suppl. material 1: Fig. S25B: marked with arrow) .... ***Merodon crassifemoris* Paramonov, 1925**

– Face without a bulge below antennae **39**

39 Basoflagellomere elongated, at least 2.7 times as long as wide (Suppl. material 1: Fig. S26D); terga 2 and 3 reddish (Suppl. material 1: Fig. S25C) .... ***italicus* species group (in part)**

– Basoflagellomere shorter, less than 2.5 times as long as wide (as in Suppl. material 1: Fig. S26E) **40**

40 Tarsi yellow dorsally and ventrally (as in Suppl. material 1: Fig. S20C, D) ***avidus* species group (Popović et al. 2015; Ačanski et al. 2016b; Likov et al. 2020)**

– Tarsi dark brown/black dorsally and orange/brown ventrally (as in Suppl. material 1: Fig. S20E, F) .... ***nigritarsis* species group (Vujić et al. 2013; Likov et al. 2020)**

Key to the species group, species subgroups and unplaced species of the *desuturinus* lineage

1 Oral margin reduced, covered by microtrichia (Suppl. material 1: Fig. S37A). Distribution: western, central and southern Africa .... ***planifacies* species subgroup (Djan et al. 2020)**

– Oral margin notched, slightly produced forward (as in Suppl. material 1: Fig. S37B) **2**

2 Metatrochanter with sparse pale pile (Suppl. material 1: Fig. S37C) **3**

– Metatrochanter with dense and strong yellow to red brush of pile (Suppl. material 1: Fig. S37D). Distribution: South Africa .... ***melanocerus* species subgroup (Radenković et al. 2018a)**

3 Apical fourth of tibiae and all tarsi bright yellow; Afrotropical species (Zimbabwe) .... ***Merodon cuthbertsoni* Curran, 1939**

– Tarsi partly brown or black; Palaearctic species .... ***murorum* species group (Vujić et al. 2018b)**

Key to the species group and unplaced species of the *natans* lineage

1 Scutum with distinct pollinose ornamentation, vittae and fasciae (Suppl. material 1: Fig. S27D); terga 2–4 with broad pollinose fasciate maculae (Suppl. material 1: Fig. S27A).. ***natans* species group**

– Scutum with indistinct pollinose vittae (Suppl. material 1: Fig. S27E); terga 2–4 without or with narrow pollinose fasciate maculae (Suppl. material 1: Fig. S27B)... ***Merodon segetum* Fabricius, 1794**

Systematic summary

Merodon albifrons lineage

Diagnosis. From small to large sized species (7–19 mm) with non-tapering abdomen and a characteristic structure of male genitalia. It is defined by having the mesocoxa pilose posteriorly (> 10 pile) (Suppl. material 1: Fig. S4A), anterior anepisternum with bare area ventral to postpronotum (Suppl. material 1: Fig. S7B), and male genitalia with a biramous anterior surstyle lobe having an apical extension and interior accessory lobe, and a hammer-like lateral sclerite of the aedeagus (except for the *rufus* species group where the lateral sclerite of the aedeagus is not enlarged apically, but with a slightly curved apex) (Suppl. material 2: Fig. S2C: s).

The *albifrons* lineage comprises 65 species (61 described + 4 undescribed) distributed in six species groups (*albifrons*, *constans*, *equestris*, *geniculatus*, *ruficornis*, and *rufus*) and two unplaced species: *M. luteihumerus* Marcos-García, Vujić & Mengual, 2007 and *M. mixtum* Vujić, Radenković & Likov, 2019 (Suppl. material 5: Table S1).

1) *albifrons* species group (Suppl. material 3: Fig. S1A, B)

Diagnosis. Small to medium-sized species (7–11 mm); abdominal terga at least partly reddish; terga 2–4 usually each with a pair of pollinose fasciate maculae; male metaleg without projections, calcars or spina, except *M. trochantericus* Costa, 1884 on metatrochanter, metafemur and apex of metatibia (Suppl. material 1: Fig. S34C). Male genitalia with characteristic thorn-like interior accessory lobe on the anterior surstyle lobe, and lateral sclerite of the aedeagus hammer-like with pointed end (Suppl. material 2: Fig. S2C: s).

Diversity and distribution. The *albifrons* species group contains eight described species (Suppl. material 5: Table S1) distributed in the Mediterranean Basin, with its highest diversity in the western part.

Identification. An identification key to the species of this group is in preparation (Vujić, unpublished).

2) *constans* species group (Suppl. material 3: Fig. S1C, D)

Diagnosis. Medium to large-sized species (9–18 mm); posterior part of abdomen (at least tergum 4) covered with golden to reddish-yellow pile (as in Suppl. material 1:

Fig. S33A); terga from black (continental species and populations) to reddish (Mediterranean species and populations); terga 2–4 (at least tergum 4) each with a pair of usually elongated pollinose fasciate maculae (Suppl. material 1: Fig. S33A); scutum often with black pile between wing bases; male with tubercle, calcar or lamina on metalegs (on apex of metatibia and ventral margin of metafemur) (Suppl. material 1: Fig. S34I–J). Male genitalia with characteristic rabbit ear-like posterior surstyle lobe, biramous anterior surstyle lobe with moderately developed interior accessory lobe and apical extension, cercus can be with pointed apex (Suppl. material 2: Fig. S1A: c) and lateral sclerite of the aedeagus hammer-like with usually tapering end (Suppl. material 2: Fig. S1F: s).

Diversity and distribution. Predominantly northern and eastern Mediterranean distribution, with no representatives on the Iberian Peninsula (Marcos-García et al. 2007). Its highest diversity is in the Caucasus Region and on the Balkan Peninsula.

Identification. Vujić et al. (2020a) provided an identification key for 15 species of the *constans* species group and distribution maps.

3) *equestris* species group (Suppl. material 3: Fig. S2A, B)

Diagnosis. Medium to large-sized species (11–17 mm) characterised by bumble bee mimicry, with long body pile (Suppl. material 3: Fig. S2A, B); male metatibia with a conspicuous apical calcar (Suppl. material 1: Fig. S34A). Male genitalia with biramous anterior surstyle lobe and with well-developed apical extension curved internally (Suppl. material 2: Fig. S2D: al); lateral sclerite of the aedeagus hammer-like with oval margins (Suppl. material 2: Fig. S2F: s); cercus triangular-shaped (Suppl. material 2: Fig. S2D: c).

Diversity and distribution. Three species belong to the *equestris* species group: *M. confusus* Marcos-García, Vujić, Ricarte & Ståhls, 2011, *M. equestris* and *M. flavus* Sack, 1913, all native to South Europe. *Merodon equestris* has been introduced elsewhere, including Japan, North America and New Zealand (Speight 2020).

Identification. Marcos-García et al. (2011) provided a taxonomic revision of the group with an identification key.

4) *geniculatus* species group (Suppl. material 3: Fig. S2C, D)

Diagnosis. Tergum 2 with reddish lateral maculae; terga 2–4 with distinct pollinose fasciate maculae (Suppl. material 1: Fig. S35B); metatibia in apical third strongly curved, with broad tip (Suppl. material 1: Fig. S34E); metatrochanter in male with a blunt calcar, usually covered with a pile-tuft (Suppl. material 1: Fig. S34D). Male genitalia with biramous anterior surstyle lobe with apical extension more developed, posterior surstyle lobe oval or triangular, cercus with prominence(s) and lateral sclerite of the aedeagus hammer-like with oval margins (Suppl. material 2: Fig. S2I: s).

Diversity and distribution. The *geniculatus* species group comprises 11 described species. Marcos-García et al. (2007) described three new species from the Iberian Peninsula (*M. antonioi* Marcos-García, Vujić & Mengual, 2007, *M. crypticus* Marcos-García, Vujić & Mengual, 2007 and *M. longispinus* Marcos-García, Vujić & Mengual, 2007), in addition to the four previously known Iberian taxa (*M. eques* Fabricius, 1805, *M. escorialensis* Strobl in Czerny and Strobl 1909, *M. geniculatus* Strobl in Czerny and Strobl 1909 and *M. teruelensis* van der Goot, 1966). Vujić et al. (2018a) revealed four species from the Eastern Mediterranean: *M. albifasciatus* Macquart, 1842, *M. chalybeatus* Sack, 1913, *M. luteofasciatus* Vujić, Radenković & Ståhls, 2018 and *M. neofasciatus* Ståhls & Vujić, 2018. In addition, there are four undescribed species in the Western Mediterranean (Suppl. material 5: Table S1).

Identification. A taxonomic revision of the Eastern Mediterranean species is provided by Vujić et al. (2018a), and the revision for the Western Mediterranean species is in preparation (Vujić, unpublished).

5) *ruficornis* species group (Suppl. material 3: Fig. S3A, B)

Diagnosis. Metatrochanter, metafemur and metatibia usually with tubercle, calcar or lamina in the male (Suppl. material 1: Fig. S34F). Male genitalia usually with characteristic hook-like posterior surstyle lobe, biramous anterior surstyle lobe with moderately developed interior accessory lobe and apical extension, cercus without prominences and lateral sclerite of the aedeagus hammer-like with oval margins (Suppl. material 2: Fig. S3C: s). In females, tergum 4 usually with transversal depression (Suppl. material 1: Fig. S36C); terga dark, except tergum 2 with a pair of lateral red-orange maculae; terga 2–4 usually with a pair of white pollinose fasciate maculae; tergum 5 with two small lateral depressions (Suppl. material 1: Fig. S36C); vertex at the level of ocellar triangle shiny black (Suppl. material 1: Fig. S36A).

Diversity and distribution. A total of 18 species are recognized in the *ruficornis* species group (Vujić et al. 2012).The group has a predominantly Eastern Mediterranean distribution with a very high level of endemism. Among the 18 taxa (Suppl. material 5: Table S1), 12 are limited-range endemics and are only found in a few mountain areas or in a small part of the total range of the group. Two regions with a high level of endemism are the Anatolian Peninsula and the Caucasus Region.

Identification. Distributional data and an identification key for 18 species are provided by Vujić et al. (2012).

6) *rufus* species group (Suppl. material 3: Fig. S3C, D)

Diagnosis. In general appearance similar to the members of the *ruficornis* species group. This group comprises black species with bronze reflections that are covered with golden-yellow erect pile, shiny terga and sterna without any trace of pollinosity, and tergum 2 with a pair of small lateral orange maculae (Suppl. material 1: Fig. S33B). Males lack the extensions on the metafemur and metatibia (contrary to the species of the *ruficornis* species group). The male genitalia have biramous anterior surstyle lobe consisting of an interior accessory lobe carrying two spines and protruded apical extension, cercus without prominences (Suppl. material 2: Fig. S3D: c), and with lateral sclerite of the aedeagus curved apically (Suppl. material 2: Fig. S3F: s). In females, the tergum 4 is without a transversal depression (contrary to the female of the *ruficornis* species group), whereas the frons and vertex are shiny, black, and without any pollinosity, with the exception of a narrow line along the eye margin (Suppl. material 1: Fig. S36B).

Diversity and distribution. The European *rufus* species group is composed of four species, three of which belong to recently described species from Mediterranean mountains, namely *M. kozufensis* Radenković & Vujić, 2020, *M. olympius* Vujić & Radenković, 2020, and *M. orjensis* Radenković & Vujić, 2020 (Radenković et al. 2020). The fourth species is *M. rufus* Meigen, 1838.

Identification. Radenković et al. (2020) recognized this group for the first time and provided a revised identification key.

Unplaced species of the *albifrons* lineage

Merodon luteihumerus (Suppl. material 3: Fig. S4A, B) is a very distinctive species with yellowish humeri, postalar calli, antennae, tibiae and tarsi of pro- and mesolegs. This is a large species (14–19 mm) with relatively short body pilosity, small basoflagellomere; whitish pile on frons and face, pollinose vittae on scutum, red-yellow lateral maculae on tergum 2 and a pair of pollinose fasciate maculae on terga 2–4. Male genitalia presented in Suppl. material 2: Fig. S3G–I. *Merodon luteihumerus* is distributed in the Iberian Peninsula and Palaearctic Africa.

Merodon mixtum (Suppl. material 3: Fig. S4C, D) has a unique combination of characters on the legs, including: apomorphic modifications on pro- and mesotibiae and pro- and metafemora in males (Suppl. material 1: Fig. S32A, C, E), less expressed in females (Suppl. material 1: Fig. S32B, D, F); males with small dens on the metatrochanter; ventral margin of metafemur undulating, with basal tubercle and oval central calcar (Suppl. material 1: Fig. S32E). This is a medium sized species (11–13mm), with fascia of black pile between wing bases; tergum 4 with golden pilosity (Suppl. material 1: Fig. S36D). The species was recently described from the Irano–Anatolian Mountains (Vujić et al. 2019).

Merodon aureus lineage

Diagnosis. Posterior part of the mesocoxa pilose (as in Suppl. material 1: Fig. S4A), anterior anepisternum below postpronotum with a pile patch (as in Suppl. material 1: Fig. S7A). Male genitalia with an undeveloped anterior surstyle lobe (as in Suppl. material 2: Fig. S4A: al) and lateral sclerites of the aedeagus very small or absent (as in Suppl. material 2: Fig. S4D: marked with arrow).

The *aureus* lineage contains five species groups: *aureus*, *bombiformis*, *funestus*, *nanus*, and *spinitarsis* with 61 species, 48 of which are described and 13 undescribed (Suppl. material 5: Table S1).

1) *aureus* species group (Suppl. material 3: Figs S5A–D, S6A, B)

Diagnosis. Small to medium sized species (8–12 mm) with a short rounded abdomen, a distinct calcar on the metatrochanter in males. Male genitalia have a characteristic posterior surstyle lobe with parallel margins and rounded apex (as in Suppl. material

2: Fig. S4A: pl) and a narrow, elongated, sickle-shaped hypandrium without lateral sclerite of the aedeagus (as in Suppl. material 2: Fig. S4D: marked with arrow).

Diversity and distribution. The *aureus* species group comprises a large number of previously known and recently discovered taxa distributed mostly in the Mediterranean Region and South Europe with a high number of local endemics. Šašić et al. (2016) defined six species subgroups within the *aureus* species group: *aureus*, *bessarabicus*, *cinereus*, *chalybeus*, *caerulescens* and *dobrogensis*, and one unplaced species (*M. unguicornis* Strobl in Czerny and Strobl 1909). Each of these species subgroups comprises at least one species complex of cryptic species (Šašić et al. 2019), although they may contain multiple complexes of species such as the *bessarabicus* species subgroup (see Veselić et al. 2017). Recent publications (Veselić et al. 2017; Radenković et al. 2018b; Šašić Zorić et al. 2019; Vujić et al. 2020c) increased the number of known species in the *aureus* species group to 45, including eight undescribed cryptic species of the *ambiguus*, *bessarabicus*, and *sapphous* species complexes (Suppl. material 5: Table S1).

Šašić et al. (2016) defined species complexes as morphologically inseparable species, which can only be resolved by employing an integrative taxonomy approach including different data types such as molecular, geometric morphometry, and ecological niche modelling (ENM). Applying this approach for the *aureus* species group has led to the discovery of previously unknown species complexes. In the *cinereus* species subgroup, Šašić et al. (2016) resolved the *atratus* species complex and found that it consisted of three species, two of which were undescribed. Veselić et al. (2017) provided evidence for the presence of four species complexes in the *bessarabicus* species subgroup. Radenković et al. (2018b) resolved *M. luteomaculatus* Vujić, Ačanski & Šašić, 2018 as a complex of six cryptic species. Additionally, the same approach was used to resolve the *caerulescens* species complex (Šašić et al. 2018). *Merodon dobrogensis* Brădescu, 1982, *M. puniceus* Vujić, Radenković & Pérez-Bañón, 2011 and *M. rojoi* Radenković & Vujić, 2019 are distinct species belonging to the *dobrogensis* species complex within the *dobrogensis* species subgroup (Šašić Zorić et al. 2019).

Identification. The identification keys for the various species subgroups have already been published: *aureus* species subgroup (Vujić et al. 2020c), *bessarabicus* species subgroup (Veselić et al. 2017), *cinereus* species subgroup (Šašić et al. 2016), *caerulescens* species subgroup (Šašić et al. 2018) and *dobrogensis* species subgroup (Šašić Zorić et al. 2019). A taxonomic revision of the *chalybeus* species subgroup is in preparation (Vujić, unpublished).

2) *bombiformis* species group (Suppl. material 3: Fig. S6D)

Diagnosis. Elongated pedicel, approximately as long as basoflagellomere (relation pedicel: basoflagellomere = 0.9 : 1.1) (Suppl. material 1: Fig. S29A); broad abdomen (Suppl. material 3: Fig. S6D); metafemur with less serrated apicoventral triangular lamina, usually only the apical dens is distinct (as in Suppl. material 1: Fig. S28H); metatrochanter of males smooth, without calcar. Male genitalia with posterior surstyle lobe usually bent (as in Suppl. material 2: Fig. S5D: pl), and hypandrium narrowed medially (as in Suppl. material 2: Fig. S5F: marked with arrow).

Diversity and distribution. The *bombiformis* species group consists of six related, though clearly morphologically different species distributed in central and southern Africa, of which three have been described (*M. bombiformis* Hull, 1944, *M. multifasciatus* Curran, 1939, and *M. nasicus* Bezzi, 1915) and three remain undescribed (Suppl. material 5: Table S1).

Identification. A taxonomic revision of this species group is in preparation (Vujić, unpublished).

3) *funestus* species group (Suppl. material 3: Fig. S6C)

Diagnosis. The *funestus* and the *bombiformis* species groups differ from other species and species groups of the *aureus* lineage by the elongated pedicel, approximately as long, or even longer, than basoflagellomere (Suppl. material 1: Fig. S29A, C) and the small lateral sclerite of the aedeagus (Suppl. material 2: Fig. S5I: s). The *funestus* species group can be distinguished from the *bombiformis* species group by the presence of a calcar on the metatrochanter in males (Suppl. material 1: Fig. S28G), which is absent in the males of the *bombiformis* species group, and a strongly dentate apicoventral triangular lamina on the metafemur in both sexes (Suppl. material 1: Fig. S28F), which is less dentate in the members of the *bombiformis* species group and usually has a distinct apical dens (Suppl. material 1: Fig. S28E, H).

Diversity and distribution. The *funestus* species group (Suppl. material 3: Fig. S6C) contains two species, *M. funestus* (Fabricius, 1794) and an undescribed species (Suppl. material 5: Table S1). The species group is distributed in South Europe, Turkey, Israel and Libya.

Identification. A taxonomic revision is currently being prepared (Vujić, unpublished).

4) *nanus* species group (Suppl. material 3: Fig. S7B)

Diagnosis. Small to medium-sized species (6–12 mm) with a short rounded abdomen. Differs from the members of the *aureus* species group by the absence of a calcar on the metatrochanter in males and abdominal terga with transverse fasciae of pale pile instead of pollinose fasciate maculae (rarely with indistinct pollinosity). Male genitalia with a broad hypandrium (as in Suppl. material 2: Fig. S4G) with the apical part of the aedeagus large, in a form of biramous pliers (as in Suppl. material 2: Fig. S4H). The studied morphological characters show high morphological similarity in all taxa, with the exception of *M. telmateia* Hurkmans, 1987, which has completely pale and unicoloured tarsi (this character clearly separates this taxon from all other members of the *nanus* species group). The five other species can be distinguished by differences in the partly black to brown tarsi and structure of male genitalia (see Vujić et al. 2015; Kočiš Tubić et al. 2018).

Diversity and distribution. We recognized six taxa within the *nanus* species group (Suppl. material 5: Table 1). All species from the *nanus* species group are widely distributed across the Anatolian Peninsula, which holds the highest diversity for this species group. Besides the Anatolian Peninsula, this species group occurs to the west including Greece, North Macedonia and Serbia, to the north to the Caucasus Region and Crimean Peninsula, and to the east and south to Syria, Lebanon, Israel and Iran.

Identification. Vujić et al. (2015) and Kočiš Tubić et al. (2018) revised the taxonomy of this species group.

5) *spinitarsis* species group (Suppl. material 3: Fig. S7A)

Diagnosis. Members of this species group resemble in their overall appearance species of the *nanus* species group, from which they can be easily distinguished by black tibiae and tarsi (mostly pale in the *nanus* species group), and the structure of the male genitalia: hypandrium of male genitalia strongly modified, anfractuous in apical half, with subapical ctenidium and stitched theca (Suppl. material 2: Fig. S4K), and posterior surstyle lobe narrow and pointed (Suppl. material 2: Fig. S4I: pl). Additionally, males of the *spinitarsis* species group have a basoventral lamina on the metatarsus.

Diversity and distribution. Only two species are known, *M. spinitarsis* Paramonov, 1929, and an undescribed species (Suppl. material 5: Table S1). *Merodon spinitarsis* is distributed in Greece, Romania and Turkey, while the undescribed species is found in Israel and Palestine (Vujić, unpublished).

Identification. A taxonomic revision is currently being prepared (Vujić, unpublished).

Merodon avidus-nigritarsis lineage

Diagnosis. Medium to large-sized species (11–20 mm) usually with white pollinose vittae on scutum (Suppl. material 3: Fig. S8C) and white pollinose fasciate maculae on terga (Suppl. material 3: Fig. S8C); anterior anepisternum bare below the postpronotum (Suppl. material 1: Fig. S7B); abdomen elongate, usually narrow and tapering, longer than scutum and scutellum together (Suppl. material 3: Fig. S10C); posterior part of mesocoxa usually without long pile (except in *M. eumerusi* Vujić, Radenković & Likov, 2019) (Suppl. material 1: Fig. S4B); basoflagellomere usually at most twice as long as wide (Suppl. material 1: Fig. S16B); legs without calcar, spina(e) (except in *M. eumerusi*) or tubercle (Suppl. material 1: Fig. S15C). Male genitalia: anterior surstyle lobe usually of rhomboid shape, covered with dense short pile; posterior surstyle lobe usually longer than anterior one; interior accessory lobe of posterior surstyle lobe narrow and long; cercus rectangular, without prominences; hypandrium usually narrow, elongate and sickle-shaped; posterior end of lateral sclerite of the aedeagus tapering; theca of hypandrium usually with a pair of lateral projections; lingula developed (as in Suppl. material 2: Figs S6I, S8F).

The *avidus-nigritarsis* lineage is divided into 10 species groups (*aberrans*, *aurifer*, *avidus*, *clavipes*, *fulcratus*, *italicus*, *nigritarsis*, *pruni*, *serrulatus*, and *tarsatus*) and eight unplaced taxa: *M. auronitens* Hurkmans, 1993, *M. caudatus* Sack, 1913, *M. clunipes* Sack, 1913, *M. crassifemoris* Paramonov, 1925, *M. eumerusi*, *M. hirtus* Sack, 1932, *M. murinus* Sack, 1913 and *M. ottomanus* Hurkmans, 1993. This lineage comprises 79 species, 66 of which are described and 13 undescribed (Suppl. material 5: Table S1).

1) *aberrans* species group (Suppl. material 3: Fig. S8A)

Diagnosis. Abdomen elongated and narrow with black shiny terga; terga 2–4 with a pair of white pollinose fasciate maculae (Suppl. material 1: Fig. S11E); metafemur usually long and narrow; hypandrium with very long lingula (Suppl. material 2: Fig. S6C: l).

Diversity and distribution. This species group consists of four described species: (*Merodon aberrans* Egger, 1860, *Merodon brevis* Paramonov 1925, *Merodon flavitibius* Paramonov, 1926 and *Merodon hamifer* Sack 1913) and four undescribed species (Suppl. material 5: Table S1) distributed in the Mediterranean and in the east to the Caucasus and Pakistan.

Identification. A taxonomic revision including an identification key and descriptions for the four new species is in preparation (Vujić, unpublished).

2) *aurifer* species group (Suppl. material 3: Fig. S8B)

Diagnosis. Species with short body pilosity, basoflagellomere 1.2 times as long as wide (Suppl. material 1: Fig. S23A), metafemur covered with short and adpressed pile (Suppl. material 1: Fig. S20B).

Diversity and distribution. Besides *M. aurifer* Loew, 1862 distributed in the north Mediterranean and Turkey, the species group consists of at least one additional taxon, an undescribed species from Turkey and Azerbaijan.

Identification. A nomenclatural revision of the species group and the description of the new species is in preparation (Vujić, unpublished).

3) *avidus* species group (Suppl. material 3: Fig. S8C)

Diagnosis. Species with elongated and tapering abdomen (Suppl. material 1: Fig. 22C), at least tergum 2 with reddish-yellow lateral maculae, and reddish-yellow tarsi (Suppl. material 1: Fig. S20C–D).

Diversity and distribution. The *avidus* species group is composed of the *avidus* species complex with four species, and the species *M. femoratus* Sack, 1913 and *M. rutitarsis* Likov, Vujić & Radenković, 2020 (Suppl. material 5: Table S1). This species group is distributed all across Europe, mainly in central and southern zones, and less diverse in the Near and Middle East and in North Africa (Algeria and Libya).

Identification. A taxonomic revision with an identification key are presented in Likov et al. (2020).

4) *clavipes* species group (Suppl. material 3: Fig. S9A, B)

Diagnosis. Large bumble bee-like species (15–20 mm) with long body pilosity and broad metafemur with long pile (Suppl. material 1: Fig. S12B); basoflagellomere elongated; terga usually covered with pile in different combinations of colours (white, yellow or black) (Suppl. material 3: Fig. S9A, B). Male genitalia with well-defined and large anterior and posterior surstyle lobes (Suppl. material 2: Fig. S7A: al, pl).

Diversity and distribution. The *clavipes* species group contains four species (Suppl. material 5: Table 1) distributed in the Mediterranean Region and up to Iran in the east.

Identification. A taxonomic revision of this species group is under preparation (Vujić, unpublished).

5) *fulcratus* species group (Suppl. material 3: Fig. S9C)

Diagnosis. They are small sized species (5–9 mm) with metallic shiny bodies; scutum and terga strongly punctate, without or with very weak pollinose areas (Suppl. material 1: Fig. S17A, B); metafemur with very small apical triangular lamina apicoventrally (Suppl. material 1: Fig. S12A). Males of this species group are clearly separated from other species groups of the *avidus-nigritarsis* lineage by distinctly dichoptic eyes and lack of ctenidium at hypandrium.

Diversity and distribution. Two species are known, *M. dichopticus* Stackelberg, 1968 from Turkey and *M. fulcratus* (Becker, 1913) from Iran.

Identification. A taxonomic revision of this group is under preparation (Vujić, unpublished).

6) *italicus* species group (Suppl. material 3: Fig. S8D)

Diagnosis. Species with elongate basoflagellomere, at least 2.7 times as long as wide (Suppl. material 1: Fig. S13A) and quadratic posterior surstyle lobe (Suppl. material 2: Fig. S7D: pl).

Diversity and distribution. Two species share these morphological features and belong to this species group: *M. italicus* Rondani, 1845 recorded from most of the Mediterranean and *M. erivanicus* Paramonov, 1925 distributed from Croatia to Azerbaijan and Israel.

Identification. A taxonomic revision of this group is in preparation (Vujić, unpublished).

7) *nigritarsis* species group (Suppl. material 3: Fig. S10C)

Diagnosis. Species with elongate, narrow and tapering abdomen, tarsi dark brown/black dorsally and partly orange ventrally. Male genitalia: anterior surstyle lobe more or less rhomboid shape (Suppl. material 2: Fig. S8D: al), except in *alagoezicus* species subgroup where the anterior surstyle lobe is transformed into a narrow, elongate, strongly curved projection (Suppl. material 2: Fig. S8A: al); hypandrium with a pair of apical thorns on the ventral margin directed backwards but often with a pair of lateral projections near the base and well-developed lingula (Suppl. material 2: Fig. S8F: l).

Diversity and distribution. The *nigritarsis* species group includes 17 species revised in Vujić et al. (2013) and Likov et al. (2020) grouped into two species subgroups. Six of them belong to the *alagoezicus* species subgroup (*M. alagoezicus* Paramonov, 1925, *M. hakkariensis* Vujić & Radenković in Vujić et al. 2013, *M. lucasi* Hurkmans, 1993, *Merodon nitidifrons* Hurkmans, 1993, *M. satdagensis* Hurkmans, 1993 and *M. schachti* Hurkmans, 1993) and the other 11 species are members of the *nigritarsis* species subgroup (Suppl. material 5: Table S1). The *nigritarsis* species group comprises taxa with a mainly mountainous distribution, mostly on the Balkan, Anatolian, Apennine and Iberian Peninsulas, in central Europe as well as the Middle and Near East (Likov et al. 2020).

Identification. A taxonomic revision is provided by Vujić et al. (2013) and Likov et al. (2020).

8) *pruni* species group (Suppl. material 3: Fig. S10A, B)

Diagnosis. Medium to large-sized species (10–18 mm) characterised by short body pilosity (scutum and abdomen); short basoflagellomere, as long as broad (Suppl. material 1: Fig. S23B); metafemur dorsally and ventrally covered with medium long outstanding pile (Suppl. material 1: Fig. S20G); and metatrochanter with distinct calcar (Suppl. material 1: Fig. S20H).

Diversity and distribution. Four species belong to this species group: *M. cupreus* Hurkmans, 1993, *M. pallidus* Macquart, 1842 and *M. pruni* Rossi, 1790 and one undescribed taxon from Israel. *Merodon pruni* is distributed in most of the Mediterranean Basin, but the other two described species are more allocated to the east, from Turkey to Israel and Pakistan.

Identification. A taxonomic revision of this group is in preparation (Vujić, unpublished).

9) *serrulatus* species group (Suppl. material 3: Fig. S9D)

Diagnosis. Species with characteristic basolateral protrusion on the posterior surstyle lobe at outer surface (Suppl. material 2: Fig. S9G: marked with arrow); legs mostly black; terga black, tergum 2 usually with a pair of reddish orange lateral maculae; metafemur usually with shorter pilosity ventrally, less than width of metafemur (Suppl. material 1: Fig. S14A); basoflagellomere usually narrow and elongated, dark brown, two times longer as pedicel. They are medium-large (11–15 mm) species with a dark scutum and white pollinose fasciate maculae (at least in females) on the dark olive brown terga 2–4 (Suppl. material 1: Fig. S22D).

Diversity and distribution. This species group includes 13 species (Vujić et al. 2020b). *Merodon serrulatus* Wiedemann in Meigen, 1822 is the species of the genus *Merodon* with the largest distributional range being distributed from the Iberian Peninsula in the south-west, along the Mediterranean and Balkan Peninsula, through Turkey and southern Russia to Siberia and Mongolia in the north-east. Other species of the *serrulatus* species group can be found at the edges of this distributional range, albeit with a much more restricted distribution (see Vujić et al. 2020b).

Identification. This species group is revised by Vujić et al. (2020b), who gave descriptions of seven new species and provided an identification key.

10) *tarsatus* species group (Suppl. material 3: Fig. S11A, B)

Diagnosis. Small to medium sized species (8–14 mm) with usually expanded basotarsomere of metatarsus (Suppl. material 1: Figs S12C, S18B) and/or with strong setae ventrally (Suppl. material 1: Fig. S12D); males with sternum 4 medially clearly divided with membranous structure and lateral tubercles or laminate extensions (Suppl. material 1: Fig. S11C); sternum 4 from lateral view usually fin-form (Suppl. material 1: Fig. S11D).

Diversity and distribution. The *tarsatus* species group consists of seven described and six undescribed species (Suppl. material 5: Table S1). This group of species is geographically restricted to the Near and Middle East, and Central Asia.

Identification. Vujić et al. (2019) and Likov et al. (2020) mentioned this group of species but did not give diagnostic features. A taxonomic revision of the *tarsatus* species group is in preparation (Vujić, unpublished).

Unplaced species of *avidus-nigritarsis* lineage

Merodon auronitens (Suppl. material 3: Fig. S10D) is a species with dark terga, basoflagellomere with concave dorsal margin (Suppl. material 1: Fig. S13E); posterior surstyle lobe with triangular basal extension (Suppl. material 2: Fig. S10A: marked with arrow); in females terga 2–4 strongly punctate; posterior half of tergum 4 with longer whitish, mostly adpressed pile (Suppl. material 1: Fig. S19D). Species has distribution in Turkey and Israel.

Merodon caudatus (Suppl. material 3: Fig. S11C, D) belongs to species with partly reddish terga and unique modification of legs among *avidus-nigritarsis* lineage: metatibia twisted medially in apical half, basotarsomere of metatarsus strongly modified (Suppl. material 1: Fig. S20A); tarsomere of mesotarsus with strong, black lateral setae (Suppl. material 1: Fig. S24B). This species is known from Israel and Palestine.

Merodon clunipes (Suppl. material 3: Fig. S12A, B) is a species with broad metatibiae and dark terga, and has clear apomorphic diagnostic characters, including antennal shape: fossette large, extended from dorsal side to outer, covering half of lateral surface (Suppl. material 1: Fig. S13D), and the characteristic shape of the posterior surstyle lobe with the apical hump directed toward cercus (Suppl. material 2: Fig. S10G: marked with arrow). This species has a North Mediterranean distribution.

Merodon crassifemoris (Suppl. material 3: Fig. S12C, D) is a taxon with tubercle on the face below the antenna (Suppl. material 1: Figs S21A, S25B), and a hook-like posterior surstyle lobe (Suppl. material 2: Fig. S10J: pl) unique among all other taxa of the *avidus-nigritarsis* lineage. It was recently revised and excluded from *M. nigritarsis* group (Likov et al. 2020). The distribution of *M. crassifemoris* extends from the eastern Balkans through the Anatolian Peninsula as far as Ukraine and Azerbaijan.

Merodon eumerusi (Suppl. material 3: Fig. S13A) possesses a line of spinae on the inner side of the apical quarter of metafemur (Suppl. material 1: Fig. S5A), representing a unique character that is absent in all other species of the genus; male genitalia (Suppl. material 2: Fig. S11A–C) similar to *M. ottomanus* (Suppl. material 2: Fig.

S11G–I). Differs from other known species of the *M. avidus-nigritarsis* lineage in having 1–4 fine pile (usually one) on the posterior side of the mesocoxa. In males, the basoflagellomere is elongated with an angular apex, bearing a very large outer fossette and a second inner fossette (Suppl. material 1: Fig. S10A, B), which are absent in almost all other species of the genus except *M. serrulatus* (Vujić et al. 2020b). This species is recently described from high mountain ranges in Tajikistan, Uzbekistan and Kyrgyzstan (Vujić et al. 2019).

Merodon hirtus (Suppl. material 3: Fig. S13B) belongs to species with dark terga, males with posterior surstyle lobe divided in two branches (Suppl. material 2: Fig. S9J: pl); eyes slightly dichoptic, distance between eyes about two facets wide (Suppl. material 1: Fig. S11B); in females terga 2–4 finely punctate; posterior half of tergum 4 with shorter, mostly black and adpressed pile (Suppl. material 1: Fig. S19E). This is an extreme eastern Mediterranean species with a range extending from Turkey to Iran and Israel, as well as Cyprus.

Merodon murinus (Suppl. material 3: Fig. S13C) is a medium to large-sized species (12–15 mm) with yellow tarsi, and tibiae mostly yellowish, except medially where brown (Suppl. material 1: Fig. S15F); basotarsomere of metatarsus elongated, three times as long as wide (Suppl. material 1: Fig. S15F); basoflagellomere elongated, 2.5 times as long as wide (Suppl. material 1: Fig. S16C); males with eye contiguity very short, approximately four to five facets long (Suppl. material 1: Fig. S21B); male genitalia with elongated compact surstyle lobe (Suppl. material 2: Fig. S11D: pl). *Merodon murinus* is a rare species recorded from Turkey and Turkmenistan.

Merodon ottomanus (Suppl. material 3: Fig. S13D) is a species with dark abdomen, reddish-yellow basoflagellomere and yellow tarsi of metaleg (at least basotarsomere); posterior surstyle lobe large, rounded, while anterior surstyle lobe small (Suppl. material 2: Fig. S11G: al, pl). This species has a fragmented distribution including the Iberian Peninsula, Peloponnesus (Greece), Turkey and Iran. It will be taxonomically revised in the future (Vujić, unpublished).

Merodon desuturinus lineage

Diagnosis. The specific shape of the lateral sclerite of the aedeagus (gradually tapered, with the tip curved downwards) is the main synapomorphic character that connects all species from the group (as in Suppl. material 2: Fig. S12I: s). Moreover, the species in this species group have pile on posterior side of mesocoxa; a curved distal prolongation of anterior surstyle lobe (as in Suppl. material 2: Fig. S12E: al); basoflagellomere less than two times as long as wide (Suppl. material 1: Fig. S6B); scutum without pollen or with less distinct pollinose longitudinal vittae (Suppl. material 1: Fig. S6D); wing microtrichose between veins R_1 and RS (Suppl. material 1: Fig. S9A); postpronotum usually brown or yellow-reddish; pilosity on lateral side of tergum 4 in female long, medially short and mostly adpressed (Suppl. material 1: Fig. S8A). The *desuturinus* lineage is closely related to the *albifrons* lineage, which was named *albifrons+desuturinus* clade in Radenković et al. (2018a).

The *desuturinus* lineage contains the Afrotropical *melanocerus* species group with two species subgroups (*melanocerus* and *planifacies*) and the species *M. cuthbertsoni* Curran, 1939 (Radenković et al. 2018a; Djan et al. 2020) (Suppl. material 3: Fig. S14C), and the Palaearctic *murorum* species group with four species (Vujić et al. 2018b). The *desuturinus* lineage comprises 14 described and 10 still undescribed species (Suppl. material 5: Table S1).

1) *melanocerus* species group (Suppl. material 3: Fig. S14A)

Diagnosis. Species with patch of dense yellow pile (dense and strong yellow to red brush of pile) on metatrochanter (Suppl. material 1: Fig. S37D). The *melanocerus* species subgroup has the oral margin notched, slightly produced forward (Suppl. material 1: Fig. S37B) and the *planifacies* species subgroup has the oral margin reduced, covered with microtrichia (Suppl. material 1: Fig. S37A). *Merodon cuthbertsoni*, with an unclear position within the species group, has apical fourth of tibiae and all tarsi bright yellow.

Diversity and distribution. Distribution of the *melanocerus* species subgroup is limited to South Africa, while the *planifacies* species subgroup has broader range: western, central and southern Africa. *Merodon cuthbertsoni* occurs in Zimbabwe.

Identification. Recent revision of the *melanocerus* species subgroup (Radenković et al. 2018a) resulted in the delimitation of five species: *M. capensis* Hurkmans, 2018, *M. commutabilis* Radenković & Vujić, 2018, *M. drakonis* Vujić & Radenković, 2018, *M. flavocerus* Hurkmans, 2018 and *M. melanocerus* Bezzi, 1915. Part of the *planifacies* species subgroup was the subject of a recent molecular analysis, which supported the monophyly of the subgroup (Djan et al. 2020). According to their integrative approach, three species are found within the *planifacies* species subgroup in South Africa: *M. planifacies* Bezzi, 1915, and two species of the *capi* species complex characterized by smooth thecal ridge in male genitalia, namely *M. capi* Vujić & Radenković, 2020 and *M. roni* Radenković & Vujić, 2020. The fourth known species from the species *planifacies* subgroup, *M. stevensoni* Curran, 1939, was described based on one female from Zimbabwe, and its taxonomic status remains unclear until the discovery of additional material, especially male specimens (Djan et al. 2020). Within the *planifacies* species subgroup, populations with folded thecal ridge of hypandrium in male genitalia could represent a group of geographically isolated species, which needs additional taxonomic research based on integrative approach (Djan et al. 2020). Ten undescribed species are already recognized (Suppl. material 5: Table S1) and descriptions are in preparation (Vujić, unpublished).

2) *murorum* species group (Suppl. material 3: Fig. S14B)

Diagnosis. Species without patch of dense yellow pile (dense and strong yellow to red brush of pile) on metatrochanter.

Diversity and distribution. This species group includes four endemo-relicts: *M. cabanerensis* Marcos-García, Vujić & Mengual, 2007, known only from a restricted area in central Spain and Morocco; *M. desuturinus* Vujić, Šimić & Radenković, 1995

(Suppl. material 3: Fig. S14B) localized on high mountains in the Balkans; *M. murorum* Fabricius, 1794 from North-West Africa; and *M. neolydicus* Vujić, 2018, present in several countries in the Eastern Mediterranean (Greece, Turkey, Syria, Lebanon, Israel).

Identification. Vujić et al. (2018b) recently revised this species groups and provided an identification key for the *desuturinus* lineage, including the *murorum* species group.

Merodon natans lineage

Diagnosis. Species with few pile on posterior side of mesocoxa; pile on anterior anepisternum reduced; anterior lobe of surstylus well developed, oval, rounded, pilose, without curved distal prolongation (Suppl. material 2: Fig. S13A: al); basoflagellomere elongated, two times as long as wide, narrowed in apical third (Suppl. material 1: Fig. S27C); scutum usually with five well-defined pollinose longitudinal vittae (Suppl. material 1: Fig. S27D).

The *natans* lineage contains the *natans* species group with three described species (Radenković et al. 2011), one undescribed species (Vujić et al. in prep.), and *M. segetum* Fabricius, 1794 (Suppl. material 5: Table S1). Species belonging to the *natans* lineage have Mediterranean distribution, except for one population of *M. calcaratus* (Fabricus, 1794) recorded in Kenya (Vujić, unpublished).

1) *natans* species group (Suppl. material 3: Fig. S15A)

Diagnosis. Small to medium-sized species (8–13 mm) with distinct pollinose ornamentation, vittae and fasciae, on scutum (Suppl. material 1: Fig. S27D); terga 2–4 with broad pollinose fasciate maculae (Suppl. material 1: Fig. S27A).

Diversity and distribution. The *natans* species group is distributed around the Mediterranean Basin and there is one isolated record in Kenya (Vujić, unpublished).

Identification. A taxonomic revision of this species group is in preparation (Vujić, unpublished).

Unplaced species of the *natans* lineage

Merodon segetum is a large species (14–17 mm) (Suppl. material 3: Fig. S15B), with the scutum with indistinct pollinose vittae (Suppl. material 1: Fig. S27E), and terga 2–4 without or with narrow pollinose fasciate maculae (Suppl. material 1: Fig. S27B). This is a western Mediterranean species occurring in the south of Spain, Algeria, Tunisia and Libya.

Discussion

Out of 194 described species (234 in total including undescribed taxa), 180 (209) species are distributed in the Palaearctic Region and 14 (27) are known from the Afrotropical Region. Three lineages (*aureus*, *desuturinus*, and *natans*) have representatives in both the Afrotropical and the Palaearctic Regions. The Afrotropical *melanocerus* species group of the *desuturinus* lineage and the *bombiformis* species group of the *aureus* lineage are exclusive to the Afrotropical Region, while all other species groups belong to Palaearctic fauna.

The *albifrons* lineage, with 65 species (61 described taxa), contains six species groups (*albifrons*, *constans*, *equestris*, *geniculatus*, *ruficornis*, and *rufus*) and two unplaced taxa.

The *aureus* lineage, with 61 species (48 described), contains five species groups (*aureus*, *bombiformis*, *funestus*, *nanus*, and *spinitarsis*).

The *avidus-nigritarsis* lineage, with 79 species (67 described), is divided into 10 species groups (*aberrans*, *aurifer*, *avidus*, *clavipes*, *fulcratus*, *italicus*, *nigritarsis*, *pruni*, *serrulatus*, and *tarsatus*) and eight unplaced species.

The *desuturinus* lineage, with 24 species (14 described), contains two species groups: the Afrotropical *melanocerus* species group with two species subgroups (*melanocerus* and *planifacies*) and the unplaced species *M. cuthbertsoni*; and the Palaearctic *murorum* species group with four species.

The *natans* lineage contains the *natans* species group, with four species (three described), and the unplaced species *M. segetum*.

At present and based on our results, the regions with the highest species richness are the Mediterranean Peninsulas: Iberian, Balkan and especially Anatolian. Certain areas in the Palaearctic (regions of Pakistan, Central Asia and eastern part of the Middle East) and Afrotropical Regions (Central and Eastern Africa) have been under-sampled and they need additional collecting efforts. Central Asia and Pakistan are characterised by numerous endemics with potential significance to understand the evolutionary scenario of the genus *Merodon*. Finally, the genetic diversity is extremely high in the *aureus* species group and more taxonomic research still needs to be done in this species group and some others, like the *ruficornis*, *avidus* and *equestris* species groups.

Acknowledgements

We thank Branka Božičić Lothrop for valuable comments and editing of the manuscript, and Hugh Lothrop, native English speaker, for linguistic revision. The study was supported by the Ministry of Education, Science and Technological Development, Republic of Serbia, Grant No. 173002, III43002, 451–03–68/2020–14/200358 and 451–03– 68/2020–14/200125, the Provincial Secretariat for Science and Technological Development of the Republic of Serbia (Grant No. 114–451–1125/2014–03 and 114–451–1702/2014–03).

References

Ačanski J, Miličić M, Likov L, Milić D, Radenković S, Vujić A (2016a) Environmental niche divergence of species from *Merodon ruficornis* group (Diptera: Syrphidae). Archives of Biological Sciences 69: 247–259. https://doi.org/10.2298/ABS160303095A

Ačanski J, Vujić A, Djan M, Obreht-Vidaković D, Ståhls G, Radenković S (2016b) Defining species boundaries in the *Merodon avidus* complex (Diptera, Syrphidae) using integrative taxonomy, with the description of a new species. European Journal of Taxonomy 237: 1–25. https://doi.org/10.5852/ejt.2016.237

Andrić A, Šikoparija B, Obreht D, Đan M, Preradović J, Radenković S, Pérez-Bañón C, Vujić A (2014) DNA barcoding applied: identification of the larva of *Merodon avidus* (Diptera: Syrphidae). Acta Entomologica Musei Nationalis Pragae 54: 741–757.

Becker T (1913) Persische Dipteren von den Expeditionen des Herrn N. Zarudny 1898 und 1901. Ezhegodnik Zoologischeskogo Muzeya Imperatorskoi Akadedemii Nauk 17(3–4): 503–654.

Brădescu V (1982) Deux espèces nouvelles du genre *Cheilosia* Meigen et *Merodon* Meigen (Diptera: Syrphidae). Revue Roumaine de Biologie – Serie de Biologie Animale 27: 11–15.

Coquillett DW (1910) The type-species of the North American genera of Diptera (Vol. 37). Smithsonian Institution, United States National Museum. https://doi.org/10.5962/bhl.title.57938

Czerny L, Strobl PG (1909) Spanische Dipteren. III. Verhandlungen der Zoologisch-Botanischen Gesellschaft in Wien 59: 121–301.

Djan M, Ståhls G, Veličković N, Ačanski J, Obreht Vidaković D, Rojo S, Pérez-Bañón C, Radenković S, Vujić A (2020) The *Merodon planifacies* subgroup (Diptera, Syrphidae): congruence of molecular and morphometric evidences reveal new taxa in Drakensberg mountains valleys (Republic of South Africa). Zoologischer Anzeiger 287: 105–120. https://doi.org/10.1016/j.jcz.2020.05.010

Doczkal D, Pape T (2009) *Lyneborgimyia magnifica* gen. et sp. n. (Diptera: Syrphidae) from Tanzania, with a phylogenetic analysis of the Eumerini using new morphological characters. Systematic Entomology 34(3): 559–573. https://doi.org/10.1111/j.1365-3113.2009.00478.x

Doczkal D, Radenković S, Lyneborg L, Pape T (2016) Taxonomic revision of the Afrotropical genus *Megatrigon* Johnson, 1898 (Diptera: Syrphidae). European Journal of Taxonomy 238: 1–36. https://doi.org/10.5852/ejt.2016.238

Edwards FW (1915) Report on the Diptera collected by the British Ornithologists' Union Expedition and the Wollaston Expedition in Dutch New Guinea. With a section on the Asilidae by E. E. Austen. Transactions of the Zoological Society of London 20: 391–424. https://doi.org/10.1111/j.1469-7998.1912.tb07841.x

Fabricius JC (1781) Species insectorum, exhibentes eorum differentias specificas, synonyma auctorum, loca natalia, metamorphosin, adjectis observationibus, descriptionibus (Vol. 1). impensis CE Bohnii, Hamburgi et Kilonii, 494 pp. https://doi.org/10.5962/bhl.title.36509

Fabricius JC (1794) Entomologia Systematica Emendata et Aucta. C.G. Proft, Copenhagen, 472 pp.

Fabricius JC (1805) Systema Antliatorum, secundum ordines, genera, species: adjectis synonymis, locis, observationibus, descriptionibus. C. Reichard, Brunswick, 372 pp. https://doi.org/10.5962/bhl.title.15806

Francuski Lj, Ludoški J, Vujić A, Milankov V (2009) Wing geometric morphometric inferences on species delimitation and intraspecific divergent units in the *Merodon ruficornis* group

(Diptera, Syrphidae) from the Balkan Peninsula. Zoological Science 26(4): 301–308. https://doi.org/10.2108/zsj.26.301

Francuski Lj, Ludoški J, Vujić A, Milankov V (2011) Phenotypic evidence for hidden biodiversity in the *Merodon aureus* group (Diptera, Syrphidae) on the Balkan Peninsula: conservation implication. Journal of Insect Conservation 15(3): 379–388. https://doi.org/10.1007/s10841-010-9311-5

Guérin-Méneville FE (1826) Macrocere (p. 7–8), *Merodon* (p. 446). In: Bory de Saint-Vincent JBBM (Ed.) Dictionnaire classique d'histoire naturelle. Rey & Gravier & Baudouin Freres, Paris. Vol. 10, 642 +[1], 2 folding tables. [1826.06.??]

Hadley A (2006) CombineZ, Ver. 5. Published by the author. http://www.hadleyweb.pwp.blueyonder.co.uk/CZ5/combinez5.htm [accessed 21 May 2020]

Hippa H, Ståhls G (2005) Morphological characters of adult Syrphidae: descriptions and phylogenetic utility. Acta Zoologica Fennica 2005(215): 1–72.

Hull FM (1949) The morphology and inter-relationships of the genera of syrphid flies, recent and fossil. Transactions of the Zoological Society of London 26: 257–408. https://doi.org/10.1111/j.1096-3642.1949.tb00224.x

Hurkmans W (1993) A monograph of *Merodon* (Diptera: Syrphidae). Part 1. Tijdschrift voor Entomologie 136: 147–234.

ICZN [International Commission for Zoological Nomenclature] (1963) Opinion 678. The suppression under plenary powers of the pamphlet published by Meigen, 1800. Bulletin of Zoological Nomenclature 20: 339–342. https://doi.org/10.5962/bhl.part.6607

ICZN [International Commission on Zoological Nomenclature] (1999) International Code of Zoological Nomenclature, Fourth Edition. London: The International Trust for Zoological Nomenclature. https://www.iczn.org/the-code/the-international-code-of-zoological-nomenclature/the-code-online/ [Accessed 22 March 2020]

Johnson CW (1898) Diptera collected by Dr. A. Donaldson Smith in Somaliland, eastern Africa. Proceedings of the Academy of Natural Sciences Philadelphia 50: 157–164.

Kaloveloni A, Tscheulin T, Vujić A, Radenković S, Petanidou T (2015) Winners and losers of climate change for the genus *Merodon* (Diptera: Syrphidae) across the Balkan Peninsula. Ecological Modelling 313: 201–211. https://doi.org/10.1016/j.ecolmodel.2015.06.032

Kočiš Tubić N, Ståhls G, Ačanski J, Djan M, Obreht Vidaković D, Hayat R, Khaghaninia S, Vujić A, Radenković S (2018) An integrative approach in the assessment of species delimitation and structure of the *Merodon nanus* species group (Diptera: Syrphidae). Organisms, Diversity & Evolution 18(4): 479–497. https://doi.org/10.1007/s13127-018-0381-7

Latreille PA (1804) Tableau méthodique des Insectes. Nouveau Dictionnaire d'Histoire Naturelle. Déterville, Paris. Vol. 24: 129–200.

Likov L, Vujić A, Kočiš Tubić N, Đan M, Veličković N, Rojo S, Pérez-Bañón C, Veselić S, Barkalov A, Hayat R, Radenković S (2020) Systematic position and composition of *Merodon nigritarsis* and *M. avidus* groups (Diptera, Syrphidae) with a description of four new hoverflies species. Contributions to Zoology 89(1): 74–125. https://doi.org/10.1163/18759866-20191414

Loew H (1862) Sechs neue europaische Dipteren. Wiener Entomologische Monatsschrift 6: 294–300.

Macquart PJM (1842) Diptéres exotiques nouveaux ou peu connus. Tome deuxieme. 2e partie. Mémoires de la Société des sciences, de l'agriculture et des arts de Lille 1841(1): 65–200.

Marcos-García MÁ, Vujić A, Mengual X (2007) Revision of Iberian species of the genus *Merodon* (Diptera: Syrphidae). European Journal of Entomology 104: 531–572. https://doi.org/10.14411/eje.2007.073

Marcos-García MÁ, Vujić A, Ricarte A, Ståhls G (2011) Towards an integrated taxonomy of the *Merodon equestris* species complex (Diptera: Syrphidae) including description of a new species, with additional data on Iberian *Merodon*. The Canadian Entomologist 143(4): 332–348. https://doi.org/10.4039/n11-013

Meigen JW (1800) Nouvelle classification des mouches a deux ailes, (Diptera L.) d'après un plan tout nouveau. JJ Fuchs, Paris, 44 pp. https://doi.org/10.5962/bhl.title.119764

Meigen JW (1803) Versuch einer neuen Gattungs-Eintheilung der europäischen zweiflügligen Insekten. Magazin für Insektenkunde 2: 259–281.

Meigen JW (1822) Systematische Beschreibung der Bekannten Europaischen Zweiflugeligen Insekten. Dritter Theil, Schulz-Wundermann, Hamm, 416 pp.

Mengual X, Ståhls G, Vujić A, Marcos-García MÁ (2006) Integrative taxonomy of Iberian *Merodon* species (Diptera: Syrphidae). Zootaxa 1377: 1–26.

Milankov V, Ludoški J, Francuski Lj, Ståhls G, Vujić A (2013) Genetic and phenotypic diversity patterns in *Merodon albifrons* Meigen, 1822 (Diptera: Syrphidae): evidence of intraspecific spatial and temporal structuring. Biological Journal of the Linnean Society 110(2): 257–280. https://doi.org/10.1111/bij.12127

Milankov V, Ludoški J, Ståhls G, Stamenković J, Vujić A (2009) High molecular and phenotypic diversity in the *Merodon avidus* complex (Diptera, Syrphidae): cryptic speciation in a diverse insect taxon. Zoological Journal of the Linnean Society 155(4): 819–833. https://doi.org/10.1111/j.1096-3642.2008.00462.x

Milankov V, Ståhls G, Stamenković J, Vujić A (2008a) Genetic diversity of populations of *Merodon aureus* and *M. cinereus* species complexes (Diptera, Syrphidae): integrative taxonomy and implications for conservation priorities on the Balkan Peninsula. Conservation Genetics 9: 1125–1137. https://doi.org/10.1007/s10592-007-9426-8

Milankov V, Ståhls G, Vujić A (2008b) Genetic characterization of the Balkan endemic species, *Merodon desuturinus* (Diptera: Syrphidae). European Journal of Entomology 105: 197–204. https://doi.org/10.14411/eje.2008.028

Milankov V, Ståhls G, Vujić A (2008c) Molecular diversity of populations of the *Merodon ruficornis* group (Diptera, Syrphidae) on the Balkan Peninsula. Journal of Zoological Systematics and Evolutionary Research 46(2): 143–152. https://doi.org/10.1111/j.1439-0469.2007.00448.x

Milić D, Radenković S, Ačanski J, Vujić A (2019) The importance of hidden diversity for insect conservation: a case study in hoverflies (the *Merodon atratus* complex, Syrphidae, Diptera). Journal of Insect Conservation 23(1): 29–44. https://doi.org/10.1007/s10841-018-0111-7

Palma G (1863) Ditteri della fauna napolitana. Annali dell'Accademia degli Aspiranti Naturalisti 3(3): 37–66.

Paramonov SJ (1925) Zur Kenntnis der Gattung *Merodon*. Encyclopédie Entomologique (B II) Diptera 2(1): 143–160.

Peck LV (1988) Syrphidae. In: Soos A, Papp L (Eds) Catalogue of Palaearctic Diptera. Akademia Kiado, Budapest 8: 11–230.

Popović D, Ačanski J, Djan M, Obreht D, Vujić A, Radenković S (2015) Sibling species delimitation and nomenclature of the *Merodon avidus* complex (Diptera: Syrphidae). European Journal of Entomology 112(4): 790–809. https://doi.org/10.14411/eje.2015.100

Preradović J, Andrić A, Radenković S, Šašić Zorić Lj, Pérez-Bañón C, Campoy A, Vujić A (2018) Pupal stages of three species of the phytophagous genus *Merodon* Meigen (Diptera: Syrphidae). Zootaxa 4420(2): 229–242. https://doi.org/10.11646/zootaxa.4420.2.5

Radenković S, Šašić Zorić Lj, Djan M, Obreht Vidaković D, Ačanski J, Ståhls G, Veličković N, Markov Z, Petanidou T, Kočiš Tubić N, Vujić A (2018b) Cryptic speciation in the *Merodon luteomaculatus* complex (Diptera: Syrphidae) from the eastern Mediterranean. Journal of Zoological Systematics and Evolutionary Research 56(2): 170–191. https://doi.org/10.1111/jzs.12193

Radenković S, Veličković N, Ssymank A, Obreht Vidaković D, Djan M, Ståhls G, Veselić S, Vujić A (2018a) Close relatives of Mediterranean endemo-relict hoverflies (Diptera, Syrphidae) in South Africa: morphological and molecular evidence in the *Merodon melanocerus* subgroup. PLoS ONE 13(7): e0200805. https://doi.org/10.1371/journal.pone.0200805

Radenković S, Vujić A, Šimić S (2002) On the identity and synonymy of two species from *Merodon ruficornis* Meigen group (Diptera: Syrphidae). Acta entomologica serbica 7(1–2): 51–57.

Radenković S, Vujić A, Ståhls G, Pérez-Bañón C, Rojo S, Petanidou T, Šimić S (2011) Three new cryptic species of the genus *Merodon* Meigen (Diptera: Syrphidae) from the island of Lesvos (Greece). Zootaxa 2735: 35–56. https://doi.org/10.11646/zootaxa.2735.1.5

Radenković S, Vujić A, Vidaković DO, Djan M, Milić D, Veselić S, Ståhls G, Petanidou T (2020) Sky island diversification in the *Merodon rufus* group (Diptera, Syrphidae) – recent vicariance in south-east Europe. Organisms Diversity & Evolution, 24 PP. https://doi.org/10.1007/s13127-020-00440-5

Ricarte A, Marcos-García MÁ, Rotheray GE (2008) The early stages and life histories of three *Eumerus* and two *Merodon* species (Diptera: Syrphidae) from the Mediterranean region. Entomologica Fennica 19: 129–141. https://doi.org/10.33338/ef.84424

Ricarte A, Souba-Dols GJ, Hauser M, Marcos-García MÁ (2017) A review of the early stages and host plants of the genera *Eumerus* and *Merodon* (Diptera: Syrphidae), with new data on four species. PLoS ONE 12(12): e0189852. https://doi.org/10.1371/journal.pone.0189852

Rondani C (1845) Sulle specie Italiane del genere *Merodon*. Memoria decimaquarta per servire alla ditterologia Italiana. Nuovi annali delle scienze naturali, Bologna 4(2): 254–267.

Rossi P (1790) Fauna Etrusca. Sistens insecta quae in provinciis Florentina et Pisana praesertim collegit (Vol. 2). Liburni [= Livorno], 348 pp. https://doi.org/10.5962/bhl.title.15771

Sack P (1913) Die Gattung *Merodon* Meigen (Lampetia Meig. olim.). Abhandlungen der Senckenbergischen Naturforschenden Gesellschaft 31: 427–462.

Šašić Lj, Ačanski J, Vujić A, Ståhls G, Radenković S, Milić D, Obreht-Vidaković D, Đan M (2016) Molecular and morphological inference of three cryptic species within the *Merodon aureus* species group (Diptera: Syrphidae). PLoS ONE 11: e0160001. https://doi.org/10.1371/journal.pone.0160001

Šašić Zorić Lj, Ačanski J, Đan M, Kočiš-Tubić N, Veličković N, Radenković S, Vujić A (2018) Integrative taxonomy of *Merodon caerulescens* complex (Diptera: Syrphidae)-evidence of cryptic speciation. Zbornik Matice srpske za prirodne nauke 135: 103–118. https://doi.org/10.2298/ZMSPN1835103S

Šašić Zorić Lj, Ačanski J, Vujić A, Ståhls G, Djan M, Radenković S (2019) Resolving the taxonomy of the *Merodon dobrogensis* species subgroup (Diptera: Syrphidae), with the description of a new species. Canadian Entomologist 152(1): 36–59. https://doi.org/10.4039/tce.2019.72

Shannon RC (1927) A review of the South American two-winged flies of the family Syrphidae. Proceedings of the United States National Museum 70(2658): 1–34. https://doi.org/10.5479/si.00963801.70-2658.1

Skevington JH, Yeates DK (2000) Phylogeny of the Syrphoidea (Diptera) inferred from mtDNA sequences and morphology with particular reference to classification of the Pipunculidae (Diptera). Molecular Phylogenetics and Evolution 16(2): 212–224. https://doi.org/10.1006/mpev.2000.0787

Smirnov ES (1924) Zur Kenntnis der Gattung *Cerioides* Rond. Zoologischer Anzeiger 58: 349–352.

Speight MCD (2020) Species accounts of European Syrphidae, 2020. Syrph the Net, the database of European Syrphidae (Diptera). Syrph the Net publications, Dublin, vol. 104, 314 pp.

Stackelberg AA (1968) New hover-flies (Diptera, Syrphidae) from the Caucasus. Entomologicheskoe Obozrenie 47: 227–232.

Ståhls G, Hippa H, Rotheray G, Muona J, Gilbert F (2003) Phylogeny of Syrphidae (Diptera) inferred from combined analysis of molecular and morphological characters. Systematic Entomology 28(4): 433–450. https://doi.org/10.1046/j.1365-3113.2003.00225.x

Ståhls G, Vujić A, Pérez-Bañón C, Radenković S, Rojo S, Petanidou T (2009) COI barcodes for identification of *Merodon* hoverflies (Diptera: Syrphidae) of Lesvos Island, Greece. Molecular Ecology Resources 9: 1431–1438. https://doi.org/10.1111/j.1755-0998.2009.02592.x

Ståhls G, Vujić A, Petanidou T, Cardoso P, Radenković S, Ačanski J, Pérez-Bañón C, Santos R (2016) Phylogeographic patterns of *Merodon* hoverflies in the Eastern Mediterranean region: revealing connections and barriers. Ecology and Evolution 6(7): 2226–2245. https://doi.org/10.1002/ece3.2021

Thompson FC (1972) A contribution to a generic revision of the Neotropical Milesinae (Diptera, Syrphidae). Arquivos de Zoologia 23: 78–215.

Thompson FC (1999) A key to the genera of the flower flies (Diptera: Syrphidae) of the Neotropical Region including descriptions of new genera and species and a glossary of taxonomic terms. Contributions on Entomology International 3: 321–378.

van der Goot VS (1966) Two new species of Syrphidae (Dipt.) from Spain. Entomologische Berichten, Amsterdam 26: 179–183.

Veselić S, Vujić A, Radenković S (2017) Three new Eastern-Mediterranean endemic species of the *Merodon aureus* group (Diptera: Syrphidae). Zootaxa 4254(4): 401–434. https://doi.org/10.11646/zootaxa.4254.4.1

Vujić A, Likov L, Radenković S, Kočiš Tubić N, Djan M, Šebić A, Pérez-Bañón C, Barkalov A, Hayat R, Rojo S, Andrić A, Ståhls G (2020b) Revision of the *Merodon serrulatus* group

(Diptera, Syrphidae). ZooKeys 909: 79–158. https://doi.org/10.3897/zookeys.909.46838.figure10

Vujić A, Marcos-García MÁ, Sarıbıyık S, Ricarte A (2011) New data for the *Merodon* Meigen 1803 fauna (Diptera: Syrphidae) of Turkey including a new species description and status changes in several taxa. Annales de la Societe Entomologique de France 47: 78–88. https://doi.org/10.1080/00379271.2011.10697699

Vujić A, Pérez-Bañón C, Radenković S, Ståhls G, Rojo S, Petanidou T, Šimić S (2007) Two new species of genus *Merodon* Meigen, 1803 (Syrphidae: Diptera) from the island of Lesvos (Greece), in the eastern Mediterranean. Annales de la Societe Entomologique de France 43(3): 319–326. https://doi.org/10.1080/00379271.2007.10697527

Vujić A, Radenković S, Ačanski J, Grković A, Taylor M, Senol GS, Hayat R (2015) Revision of the species of the *Merodon nanus* group (Diptera: Syrphidae) including three new species. Zootaxa 4006(3): 439–462. https://doi.org/10.11646/zootaxa.4006.3.2

Vujić A, Radenković S, Likov L (2018b) Revision of the Palaearctic species of the *Merodon desuturinus* group (Diptera, Syrphidae), ZooKeys 771: 105–138. https://doi.org/10.3897/zookeys.771.20481

Vujić A, Radenković S, Likov L, Andrić A, Gilasian E, Barkalov A (2019) Two new enigmatic species of the genus *Merodon* Meigen (Diptera: Syrphidae) from the north-eastern Middle East. Zootaxa 4555(2): 187–208. https://doi.org/10.11646/zootaxa.4555.2.2

Vujić A, Radenković S, Likov L, Andrić A, Janković M, Ačanski J, Popov G, de Courcy Williams M, Šašić Zorić Lj, Djan M (2020a) Conflict and congruence between morphological and molecular data: revision of the *Merodon constans* group (Diptera : Syrphidae). Invertebrate Systematics 34(4): 406–448. https://doi.org/10.1071/IS19047

Vujić A, Radenković S, Likov L, Trifunov S, Nikolić T (2013) Three new species of the *Merodon nigritarsis* group (Diptera: Syrphidae) from the Middle East. Zootaxa 3640(3): 442–464. https://doi.org/10.11646/zootaxa.3640.3.7

Vujić A, Radenković S, Ståhls G, Ačanski J, Stefanović A, Veselić S, Andrić A, Hayat R (2012) Systematics and taxonomy of the *ruficornis* group of genus *Merodon* (Diptera: Syrphidae). Systematic Entomology 37(3): 578–602. https://doi.org/10.1111/j.1365-3113.2012.00631.x

Vujić A, Šašić Zorić Lj, Ačanski J, Likov L, Radenković S, Djan M, Milić D, Šebić A, Ranković M, Khaghaninia S (2020c) Hide-and-seek with hoverflies: *Merodon aureus* – a species, a complex or a subgroup? Zoological Journal of the Linnean Society 190: 974–1001. https://doi.org/10.1093/zoolinnean/zlaa016

Vujić A, Šimić S, Radenković S (1995) *Merodon desuturinus*, a new hoverfly (Diptera: Syrphidae) from the mountain Kopaonik (Serbia). Ekologija 30: 65–70.

Vujić A, Ståhls G, Ačanski J, Rojo S, Pérez-Bañón C, Radenković S (2018a) Review of the *Merodon albifasciatus* Macquart species complex (Diptera: Syrphidae): the nomenclatural type located and its provenance discussed. Zootaxa 4374(1): 25–48. https://doi.org/10.11646/zootaxa.4374.1.2

Walker F (1865) Descriptions of new species of the dipterous insects of New Guinea. Journal and Proceedings of the Linnaean Society of London, Zoology 8: 109–130. https://doi.org/10.1111/j.1096-3642.1865.tb02426.x

Weidemann CRW (1830) Achias dipterorum genus a Fabricio conditum; illustratum novisque speciebus auctum et conventui physicorum Germanorum oblatum. C.F. Mohr, Kiliae Holsatorium [= Kiel], 16 pp.

Williston SW (1884) On the North American Asilidae (Dasypogoninae, Laphrinae), with a new genus of Syrphidae. Transactions of the American Entomological Society and Proceedings of the Entomological Section of the Academy of Natural Sciences 11(1): 1–35. https://doi.org/10.2307/25076428

Young AD, Lemmon AR, Skevington JH, Mengual X, Ståhls G, Reemer M, Joerdans K, Kelso S, Moriarty Lemmon E, Hauser M, Meyer M, Misof B, Wiegmann BM (2016) Anchored enrichment dataset for true flies (order Diptera) reveals insights into the phylogeny of flower flies (family Syrphidae). BMC Evolutionary Biology 16: 143. https://doi.org/10.1186/s12862-016-0714-0

Supplementary material 1

Figures S1–S37: Figures of morphological characters

Authors: Ante Vujić, Snežana Radenković, Laura Likov, Sanja Veselić

Data type: multimedia

Explanation note: **Figure S1.** Head of male, posterior view. **A** *Platynochaetus setosus* (Fabricius, 1794), hypostomal bridge marked with arrow **B** *Sericomyia silentis* (Harris, 1776). Scale bar: 0.5 mm. **Figure S2.** Parts of thorax of male, lateral view. **A** *Merodon megavidus* Vujić & Radenković, 2016, tubercle **B** *Eristalinus megacephalus* (Rossi, 1794), tubercle **C** *Merodon megavidus*, anepimeron **D** *Sericomyia silentis*, anepimeron. **A, B** tubercle marked with arrow **C, D** dorsomedian part of anepimeron marked with arrow. Scale bar: 0.5 (**A–C**); 1 mm (**D**). **Figure S3. A, B** Wing of male, dorsal view **C–D** Antenna of male, lateral view. **A** *Merodon* aff. *nasicus*, short vein marked with asterisk **B** *Sericomyia silentis* **C** *Merodon ottomanus*, fossette marked with arrow **D** *Microdon analis* (Macquart, 1842). **A, B** outer angle between R_{4+5} and M_1 marked with arrow. Scale bar: 0.5 mm (**A, B, D**); 0.2 mm (C). **Figure S4.** Metacoxa of male. **A** *Merodon albifrons* Meigen, 1822, lateral view **B** *M. nigritarsis* Rondani, 1845, lateral view. **A, B** pile marked with arrow. Scale bar: 0.25 mm. **Figure S5. A** Metafemur of *Merodon eumerusi*, male, lateroventral view, row of spinae marked with arrow **B** Mesocoxa of *M. segetum*, male, lateral view, pile marked with arrow. Scale bar: 1 mm. **Figure S6. A, B** Antenna of male, lateral view **C, D** Thorax of male, dorsal view. **A, C** *Merodon natans* (Fabricius, 1794) **B, D** *M. desuturinus*. Scale bar: 1 mm. **Figure S7.** Thorax (anepisternum) of male, lateral view. **A** *Merodon geniculatus* **B** *M. legionensis* Marcos-García, Vujić & Mengual, 2007. **A, B** pile marked with arrow. **Figure S8.** Abdomen of female, lateral view. **A** *Merodon desuturinus* **B** *M. aureus* Fabricius, 1805. **A,** pile marked with arrow. Scale bar: 1 mm. **Figure S9.** Part of wing of male, dorsal view. **A** *Merodon desuturinus* **B** *M. albifrons*. **A–B** microtrichia marked with arrow. Scale bar: 1 mm. **Figure S10.** Antenna of *Merodon eumerusi*, male, lateral view. **A** outer side **B** inner side. Scale bar: 1 mm. **Figure S11. A, B** Eye contiguity of male, anterior view **C, D** Sternum 4 of male, dorsal (**C**) and lateral (**D**) view **E** Abdomen of male, dorsal view. **A** *Merodon fulcratus* **B** *M. hirtus* **C, D** *M. tarsatus* **E** *M. aberrans*. **C, D** membranous structure and laminate extension marked with arrow. Scale bar: 1 mm (**A, B**); 2 mm (**C–E**). **Figure S12.** Parts of male metaleg, lateral view. **A** *Merodon fulcratus*, metaleg **B** *M. clavipes* (Fabricius, 1781), metafemur and metatibia **C** *M. tarsatus*, metatarsus **D** *M. oidipous* Hurkmans, 1993, metatarsus. **C, D** setae marked with arrrow. Scale bar: 2 mm (**A, B**); 0.5 mm (**C, D**). **Figure S13.** Male antenna, lateral view. **A** *Merodon italicus* **B** *M. serrulatus* **C** *M. ottomanus* **D** *M. clunipes* **E** *M. auronitens*. Scale bar: 2 mm. **Figure S14.** Parts of male metaleg, lateral view. **A** *Merodon serrulatus*, metafemur and metatibia **B** *M. ottomanus*, metaleg **C** *M. clunipes*, metafemur **D** *M. clunipes*, metatarsus. Scale bar: 2 mm. **Figure S15.** Parts of female metaleg, lateral view. **A** *Merodon clunipes*, metafemur and metatibia **B** *M. ottomanus*, metaleg **C** *M. clavipes*, metafemur **D** *M. fulcratus*, metafemur **E** *M. serrulatus*, metafemur **F** *M. murinus*, metatibia and metatarsus. **D**triangular lamina marked with arrow. Scale bar: 2 mm. **Figure S16.** Female antenna, lateral view. **A** *Merodon clunipes* **B** *M. clavipes* **C** *M. murinus*. Scale bar: 2 mm. **Figure S17. A** Female thorax, dorsal view **B–D** Abdomen of female, dorsal view. **A, B** *Merodon fulcratus* **C** *M. ottomanus* **D** *M. aberrans*. Scale bar: 2 mm. **Figure S18.** Parts of female metaleg, lateral view. **A** *Merodon aberrans*, metaleg **B** *M. tarsatus*, metatarsus **C** *M. hirtus*, metatarsus **D** *M. auronitens*, metatarsus. **B** setae marked with arrow **C-D** tarsomerae marked with arrow. Scale bar: 1 mm (**A**); 2 mm (**B–D**). **Figure S19.** Abdomen of female. **A** *Merodon oidipous*, dorsal view **B** *M. tarsatus*, dorsal view **C** *M. auronitens*, dorsal view **D** *M. auronitens*, lateral view **E** *M. hirtus*, lateral view. Scale bar: 2 mm. **Figure S20.** Parts of male metaleg. **A** *Merodon caudatus*, metatibia and metatarsus, lateral view **B** *M. aurifer*, metatrochanter and metafemur, lateral view **C** *M. avidus* (Rossi, 1790), metatarsus, dorsal view **D** *M. avidus*, metatarsus, ventral view **E** *M. nigritarsis*, metatarsus, dorsal view **F** *M. nigritarsis*, metatarsus, ventral view **G** *M. pruni*, part of metafemur, lateral view **H** *M. pruni*, metatrochanter, lateral view. **B** calcar marked with arrow. Scale bar: 0.5 mm (**A–B**); 1mm (**C–G**); 0.25 mm (**H**). **Figure S21. A** *Merodon crassifemoris*, male, head, lateral view **B** *M. murinus*, male, eye contiguity, anterior view **C** *M. nigritarsis*, male, eye contiguity, anterior view. **A** bulge marked with arrow. Scale bar: 1 mm. **Figure S22.** Abdomen, dorsal view. **A** *Merodon aurifer* **B** *M. pruni* **C** *M. avidus* **D** *M. serrulatus*. **A–C** male **D** female. Scale bar: 2 mm. **Figure S23.** Male antenna, lateral view. **A** *Merodon aurifer* **B** *M. pruni* **C** *M. nigritarsis*. Scale bar: 1 mm (**A, C**); 0.5 mm (**B**). **Figure S24.** Parts of metaleg of female. **A** *Merodon caudatus*, metafemur and metatibia, lateral view **B** *M. caudatus*, metatarsus, dorsal view **C** *M. pruni*, metatrochanter, metafemur and metatibia **D** *M. crassifemoris*, metatrochanter, lateral view **E** *M. aurifer*, metafemur and metatibia. **C** metatrochanter marked with arrow. Scale bar: 1 mm (**A, C, E**); 0.5 mm (**B**); 0.75 mm (**D**). **Figure S25. A** *Merodon murinus*, female, head, dorsal view **B** *M. crassifemoris*, female, head, dorsolateral view **C** *M. italicus*, female, abdomen, dorsal view. **B** bulge marked with arrow. Scale bar: 1 mm (**A–B**); 2 mm (**C**). **Figure S26.** Antenna of female, lateral view. **A** *Merodon pruni* **B** *M. crassifemoris* **C** *M. aurifer* **D** *M. italicus* **E** *M. avidus*. Scale bar: 0.5 mm (**A–C, E**); 1 mm (**D**). **Figure S27. A** *Merodon* *natans*, male, abdomen, dorsal view **B** *M. segetum*, male, abdomen, dorsal view **C** *M. natans*, male, antenna, lateral view **D** *M. natans*, male, thorax, dorsal view **E** *M. segetum*, male, thorax, dorsal view. Scale bar: 2 mm (**A–C**); 1 mm (**D**); 0.5 mm (**E**). **Figure S28.** Parts of metaleg. **A** *Merodon bombiformis*, male, metatrochanter, lateral view **B** *M. aureus*, male, metatrochanter, lateral view **C** *M. spinitarsis*, female, metatarsus, dorsal view **D** *M. nanus* (Sack, 1931), female, metatarsus, dorsal view **E** *M. bombiformis*, female, metafemur, lateral view **F** *M. funestus*, female, metafemur, lateral view **G** *M. funestus*, male, metafemur and metatrochanter, lateral view **H** *M. bombiformis*, male, metafemur and metatrochanter, lateral view. **B** calcar on the metatrochanter marked with arrow **E** triangular lamina marked with arrow. Scale bar: 2 mm. **Figure S29.** Antenna, lateral view. **A** *Merodon bombiformis*, male **B** *M. nanus*, male **C** *M. funestus*, male **D** *M. aureus*, male **E** *M. funestus*, female **F** *M. aureus*, female. Scale bar: 2 mm. **Figure S30.** Abdomen. **A** *Merodon funestus*, male, dorsolateral view **B** *M. aureus*, male, lateral view **C** *M. nanus*, female, dorsal view **D** *M. aureus*, female, dorsal view **E** *M. spinitarsis*, female, lateral view **F** *M. nanus*, female, lateral view. Scale bar: 2 mm. **Figure S31.** *Merodon luteihumerus*, male. **A** head, anterior view **B** thorax, dorsolateral view. Scale bar: 2 mm. **Figure S32.** *Merodon mixtum*, legs, lateral view. **A** proleg, male **B** proleg, female **C** mesoleg, male **D** mesoleg, female **E** metaleg, male **F** metaleg, female. Scale bar: 1 mm. **Figure S33. A–C** Abdomen of male **D** Metatibia. **A** *Merodon gudaurensis* Portschinsky, 1877, dorsal view **B** *M. rufus*, dorsal view **C** *M. rufus*, lateral view **D** *M. albifrons*, lateral view. Scale bar: 2 mm. **Figure S34.** Parts of metaleg, lateral view. **A** *Merodon equestris*, male, metatibia **B** *M. rufus*, male, metaleg **C** *M. trochantericus*, male, metaleg **D** *M. albifasciatus*, male, metatrochanter **E** *M. albifasciatus*, male, metatibia **F** *M. trebevicensis* Strobl, 1900, male, metatrochanter, metafemur and metatibia **G** *M. ruficornis* Meigen, 1822, female, metatibia **H** *M. albifasciatus*, female, metatibia **I** *M. gudaurensis*, male, metafemur **J** *M. gudaurensis*, male, metatibia. **E** apicomedial carina marked with arrow **F** ventral tubercle on metafemur and apicolateral process on metatibia marked with arrow. Scale bar: 0.5 mm (**A, B**); 2 mm (**C**); 1 mm (**D–E**); 2 mm (**F**); 2 mm (**G–H**); 2 mm (**I-J**). **Figure S35. A** *Merodon albifasciatus*, female, thorax, dorsal view **B** *M. albifasciatus*, female, abdomen, dorsal view **C** *M. albifrons*, female, abdomen, dorsal view. Scale bar: 2 mm. **Figure S36. A, B** Head of female, dorsal view **C, D** Tip of abdomen, dorsal view. **A** *Merodon ruficornis* **B** *M. rufus* **C** *M. ruficornis*, female **D** *M. mixtum*, male. **B** pollinosity along eye margin marked with arrow **C** transversal depression on tergum 4 and lateral depressions on tergum 5 marked with arrow. Scale bar: 2 mm. **Figure S37. A–B** Head of male, lateral view **C–D** Metatrochanter of male, lateral view. **A** *Merodon planifacies* **B** *M. neolydicus* **C** *M. desuturinus* **D** *M. draconis* Vujić & Radenković, 2018. Scale bar: 1 mm (**A–B**); 2 mm (**C–D**).

Link: https://doi.org/10.3897/zookeys.1031.62125.suppl1

Supplementary material 2

Figures S1–S13: Figures of male genitalia

Authors: Ante Vujić, Snežana Radenković, Laura Likov, Sanja Veselić

Data type: multimedia

Explanation note: **Figure S1.** Male genitalia. **A–C** *Merodon constans* (Rossi, 1794) **D–F** *M. chrysotrichos* Vujić, Radenković & Likov, 2020 **G–I** *M. triangulum* Vujić, Radenković & Hurkmans, 2020. **A, B, D–E, G, H** epandrium **C, F, I** hypandrium. **A, C, D, F, G, I** lateral view **B, E, H** ventral view. Abbreviations: c-cercus, s-lateral sclerite of the aedeagus. Scale bar: 0.5 mm. **Figure S2**. Male genitalia. **A–C** *Merodon albifrons* Meigen, 1822 **D–F** *M. equestris* **G–I** *M. albifasciatus*. **A–B, D–E, G–H** epandrium **C, F, I** hypandrium. **A, C, D, F, G, I** lateral view **B, E, H** ventral view. Abbreviations: al-anterior surstyle lobe, c-cercus, s-lateral sclerite of the aedeagus. Scale bar: 0.4 mm (**A–C**); 0.2 mm (**D–F**); 0.4 mm (**G–I**). **Figure S3.** Male genitalia. **A–C** *Merodon ruficornis* Meigen, 1822 **D–F** *M. rufus* **G–I** *M. luteihumerus* **J–L** *M. mixtum*. **A–B, D–E, G–H, J–K** epandrium **C, F, I, L** hypandrium. **A, C, D, F, G, I, J, L** lateral view **B, E, H, K** ventral view. Abbreviations: c-cercus, s-lateral sclerite of the aedeagus. Scale bar: 0.4 mm (**A–C**); 0.25 mm (**D–F**); 0.2 mm (**G–I**); 0.5 mm (**J–L**). **Figure S4.** Male genitalia. **A–D** *Merodon aureus* Fabricius, 1805 **E–H** *M. nanus* (Sack, 1931) **I–K** *M. spinitarsis*. **A, B, E, F, I, J** epandrium **C, G, K** hypandrium **D, H** part of aedeagus. **A, C, D, E, G, I, K** lateral view **B, F, H, J** ventral view. Abbreviations: al-anterior surstyle lobe, pl-posterior surstyle lobe. **D** place of lateral sclerite of the aedeagus marked with arrow. Scale bar: 0.25 mm (**A–D**); 0.25 mm (**E–H**); 0.5 mm (**I–K**). **Figure S5.** Male genitalia. **A–C** *Merodon bombiformis* **D–F** *M. nasicus* **G–I** *M. funestus*. **A–B, D–E, G–H** epandrium **C, F, I** hypandrium. **A, C, D, F, G, I** lateral view **B, E, H** ventral view. Abbreviations: pl-posterior surstyle lobe, s-lateral sclerite of the aedeagus. **C, F** medially narrowed hypandrium marked with arrow. Scale bar: 0.5 mm. **Figure S6.** Male genitalia. **A–C** *Merodon aberrans* **D–F** *M. aurifer* **G–I** *M. avidus* (Rossi, 1790) **J–L** *M. rutitarsis*. **A–B, D–E, G–H, J–K** epandrium **C, F, I, L** hypandrium. **A, C, D, F, G, I, J, L** lateral view **B, E, H, K** ventral view. Abbreviations: l-lingula. Scale bar: 0.2 mm (**A–C, G–I**); 0.5 mm (**D–F, J–L**). **Figure S7.** Male genitalia. **A–C** *Merodon clavipes* (Fabricius, 1781) **D–F** *M. italicus* **G–I** *M. dichopticus* **J–K** *M. fulcratus*. **A–B, D–E, G–H, J–K** epandrium **C, F, I, L** hypandrium. **A, C, D, F, G, I, J, L** lateral view **B, E, H, K** ventral view. Abbreviations: al-anterior surstyle lobe, pl-posterior surstyle lobe. **C, K** place of ctenidium marked with arrow. Scale bar: 0.2 mm (**A–F, J–L**); 0.5 mm (**G–I**). **Figure S8.** Male genitalia. **A–C** *Merodon alagoesicus* Paramonov, 1925 **D–F** *M. nigritarsis* Rondani, 1845 **G–I** *M. obstipus* Vujić, Radenković & Likov, 2020. **A–B, D–E, G–H** epandrium **C, F, I** hypandrium. **A, C, D, F, G, I** lateral view **B, E, H** ventral view. Abbreviations: al-anterior surstyle lobe. Scale bar: 0.5 mm. **Figure S9.** Male genitalia. **A–C** *Merodon pruni* **D–F** *M. hypochrysos* Hurkmans, 1993 **G–I** *M. serrulatus* **J–L** *M. hirtus*. **A–B, D–E, G–H, J–K** epandrium **C, F, I, L** hypandrium. **A, C, D, F, G, I, J, L** lateral view **B, E, H, K** ventral view. Abbreviations: pl-posterior surstyle lobe. **G** basolateral protrusion marked with arrow. Scale bar: 0.5 mm (**A–C**); 0.2 mm (**D–L**). **Figure**

S10. Male genitalia. **A–C** *Merodon auronitens* **D–F** *M. caudatus* **G–I** *M. clunipes* **J–L** *M. crassifemoris*. **A–B, D–E, G–H, J–K** epandrium **C, F, I, L** hypandrium. **A, C, D, F, G, I, J, L** lateral view **B, E, H, K** ventral view. Abbreviations: pl-posterior surstyle lobe, s-lateral sclerite of the aedeagus. **A** triangular basal extension marked with arrow **F** ventral processes of the hypandrium marked with arrow **G** apical hump marked with arrow. Scale bar: 0.2 mm (**A–C, G–L**); 0.5 mm (**D–F**). **Figure S11.** Male genitalia. **A–C** *Merodon eumerusi* **D–F** *M. murinus* **G–I** *M. ottomanus*. **A–B, D–E, G–H** epandrium **C, F, I** hypandrium. **A, C, D, F, G, I** lateral view **B, E, H** ventral view. Abbreviations: al-anterior surstyle lobe, pl-posterior surstyle lobe. Scale bar: 0.2 mm. **Figure S12.** Male genitalia. **A–C** *Merodon capensis* **D–F** *M. desuturinus* **G–I** *M. neolydicus* **J–L** *M. planifacies*. **A–B, D–E, G–H, J–K** epandrium **C, F, I, L** hypandrium. **A, C, D, F, G, I, J, L** lateral view **B, E, H, K** ventral view. Abbreviations: al-anterior surstyle lobe, s-lateral sclerite of the aedeagus. Scale bar: 0.2 mm. **Figure S13.** Male genitalia. **A–C** *Merodon natans* (Fabricius, 1794) **D–F** *M. segetum*. **A, B, D, E** epandrium **C, F** hypandrium. **A, C, D, F** lateral view **B, E** ventral view. Abbreviations: al-anterior surstyle lobe. Scale bar: 0.2 mm.

Link: https://doi.org/10.3897/zookeys.1031.62125.suppl2

Supplementary material 3

Figures S1–S15: Figures of adults

Authors: Ante Vujić, Snežana Radenković, Laura Likov, Sanja Veselić

Data type: Adobe PDF file

Explanation note: **Figure S1.** Body of male. **A, B** *Merodon albifrons* Meigen, 1822 **C, D** *M. constans* (Rossi, 1794). **A, C** dorsal view **B, D** lateral view. Scale bar: 1 mm. **Figure S2.** Body of male. **A, B** *Merodon equestris* **C, D** *M. geniculatus*. **A, C** dorsal view **B, D** lateral view. Scale bar: 3 mm (**A, B**); 1 mm (**C, D**). **Figure S3.** Body of male. **A, B** *Merodon ruficornis* Meigen, 1822 **C, D** *M. rufus*. **A, C** dorsal view **B, D** lateral view. Scale bar: 1.5 mm. **Figure S4.** Body of male. **A, B** *Merodon luteihumerus* **C, D** *M. mixtum*. **A, C** dorsal view **B, D** lateral view. Scale bar: 2 mm. **Figure S5.** Body of male, dorsal view. **A** *Merodon aureus* Fabricius, 1805 **B** *M. bessarabicus* Paramonov, 1924 **C** *M. cinereus* (Fabricius, 1794) **D** *M. chalybeus* Wiedemann, 1822. Scale bar: 2 mm (**A–C**); 1.5 mm (**D**). **Figure S6.** Body of male, dorsal view. **A** *Merodon caerulescens* Loew, 1869 **B** *M. dobrogensis* **C** *M. funestus* **D** *M. bombiformis*. Scale bar: 1.5 mm (**A, B**), 2 mm (**C, D**). **Figure S7.** Body of male, dorsal view. **A** *Merodon spinitarsis* **B** *M. nanus* (Sack, 1931). Scale bar: 1 mm. **Figure S8.** Body of male, dorsal view. **A** *Merodon aberrans* **B** *M. aurifer* **C** *M. avidus* (Rossi, 1790) **D** *M. italicus*. Scale bar: 2 mm (**A–C**); 1.5 mm (**D**). **Figure S9.** Body of male. **A–B** *Merodon clavipes*

(Fabricius, 1781) **C** *M. fulcratus* **D** *M. serrulatus*. **A, C, D** dorsal view **B** lateral view. Scale bar: 1 mm. **Figure S10.** Body of male. **A, B** *Merodon pruni* **C** *M. nigritarsis* Rondani, 1845 **D** *M. auronitens*. **A, C, D** dorsal view **B** lateral view. Scale bar: 2 mm (**A–C**); 1.5 mm (**D**). **Figure S11.** Body of male. **A, B** *Merodon tarsatus* **C, D** *M. caudatus*. **A, C** dorsal view **B, D** lateral view. Scale bar: 1.5 mm. **Figure S12.** Body of male. **A, B** *Merodon clunipes* **C, D** *M. crassifemoris*. **A, C** dorsal view **B, D** lateral view. Scale bar: 2 mm. **Figure S13.** Body of male, dorsal view. **A** *Merodon eumerusi* **B** M. *hirtus* **C** *M. murinus* **D** *M. ottomanus*. Scale bar: 1.5 mm (**A, C**); 2 mm (**B, D**). **Figure S14.** Body of male, dorsal view. **A** *Merodon melanocerus* **B** *M. desuturinus* **C** *M. cuthbertsoni*. Scale bar: 2 mm (**A–B**). **Figure S15.** Body of male, dorsal view. **A** *Merodon natans* (Fabricius, 1794) **B** *M. segetum*. Scale bar: 1.5 mm (**A**); 2 mm (**B**).

Link: https://doi.org/10.3897/zookeys.1031.62125.suppl3

Supplementary material 4

List of *Merodon* species grouped by *lineage* and species group

Authors: Ante Vujić, Snežana Radenković, Laura Likov, Sanja Veselić

Data type: species data

Link: https://doi.org/10.3897/zookeys.1031.62125.suppl4

Supplementary material 5

Table S1. Classification of the genus *Merodon* in lineages and species groups, including an actual number of species within each

Authors: Ante Vujić, Snežana Radenković, Laura Likov, Sanja Veselić

Data type: species data

Link: https://doi.org/10.3897/zookeys.1031.62125.suppl5

ZooKeys 1031: 125–131 (2021)
doi: 10.3897/zookeys.1031.61846
https://zookeys.pensoft.net

RESEARCH ARTICLE

A peer-reviewed open-access journal
ZooKeys
Launched to accelerate biodiversity research

Belarima violacea (Lucas, 1847) (Coleoptera, Chrysomelidae), a new genus and species for the European fauna

Michele Violi[1], Paola D'Alessandro[2], Maurizio Biondi[2]

1 *Via al Forte 8, 42027 Montecchio Emilia (RE), Reggio Emilia, Italy* **2** *Department of Health, Life and Environmental Sciences, University of L'Aquila, Via Vetoio snc, 67100, Coppito, L'Aquila, Italy*

Corresponding author: Paola D'Alessandro (paola.dalessandro@univaq.it)

Academic editor: Ron Beenen | Received 9 December 2020 | Accepted 8 January 2021 | Published 15 April 2021

http://zoobank.org/9B81134A-B6AA-43DA-B3B6-C9794FE8A6FE

Citation: Violi M, D'Alessandro P, Biondi M (2021) *Belarima violacea* (Lucas, 1847) (Coleoptera, Chrysomelidae), a new genus and species for the European fauna. ZooKeys 1031: 125–131. https://doi.org/10.3897/zookeys.1031.61846

Abstract

Belarima violacea (Lucas) is an uncommon species of the Galerucini tribe (Coleoptera, Chrysomelidae, Galerucinae) distributed in Algeria, Morocco and Tunisia, and recorded here for the first time for the European fauna. One male and one female were found, not far from each other, wandering on the sand among the vegetation of the shifting dunes of the Tuscan coast (Rosignano Solvay, Spiagge Bianche). Some hypotheses are proposed to explain the presence of *B. violacea* on the Italian coast. Morphological descriptions of external habitus, aedeagus and spematheca, the latter here described for the first time, are also provided, accompanied by micro-photographs.

Keywords

Belarima violacea, Chrysomelidae, Europe, Galerucinae, Galerucini, Italy, North Africa

Introduction

Galerucinae are a large subfamily of Chrysomelidae, including about 15,000 species comprised in more than 1100 genera, of which more than 500 genera and about 8000 species in the tribe Alticini, and approximately 540 genera and 7200 species in the tribe Galerucini (Nadein and Bezděk 2014; Nie et al. 2017). Galerucini are widespread in all zoogeographic regions, and occur with 13 genera and 123 species in Europe (Beenen 2013, as Galerucinae).

The genus *Belarima* Reitter, 1913, with the species *violacea* (Lucas, 1847), is here recorded for the first time for the European fauna. *Belarima* currently includes two uncommon species: *B. violacea* from Algeria, Morocco and Tunisia, and *B. obliqua* Beenen, 2019, recently described from Algeria. This genus is separated from *Arima* Chapuis, 1875 by the absence of a basal pronotal margin, which in *Arima* is instead finely margined. In addition, *Belarima* shows some costae on the elytra, absent in *Arima*. Beenen (2019) instead considers *Belarima* as more related to *Galeruca* Geoffroy, 1762, because *Arima* has the sides of the abdominal tergites swollen while they are simple in *Belarima*, as in *Galeruca*. However, *Belarima* lacks the apical spurs on the tibiae, whereas they are present in *Galeruca* (Beenen 2019).

Methods

The specimens were examined, measured and dissected using a Leica M205C stereomicroscope. Photographs were taken using a Leica DFC500 camera and composed using Zerene Stacker version 1.04. Scanning electron micrographs were taken using a Hitachi TM-1000. Terminology follows D'Alessandro et al. (2016) for the median lobe of the aedeagus, and Bezděk (2015) and Rodrigues and Mermudes (2015) for the spermatheca. Geographical coordinates for the localities are reported in degrees, minutes and seconds (WGS84 format).

Abbreviations for biometry

LA	numerical sequence proportional to length of each antennomere;
LAED	length of aedeagus;
LAN	length of antennae;
LB	total length of body (from apical margin of head to apex of abdomen);
LE	length of elytra;
LP	medial length of pronotum;
LSP	maximum length of spermatheca;
WE	maximum combined width of elytra;
WP	maximum width of pronotum.

Results

Belarima violacea (Lucas)

Adimonia violacea Lucas, 1847: plate 44, fig. 7a–c; Lucas 1849: 540–541; Joannis, 1865: 9, 18.

Belarima violacea (Lucas): Warchalowski 2010: 634, pl. LXXV, photo 669; Beenen 2019: 2–4, figs 2, 3b; Beenen 2010: 445.

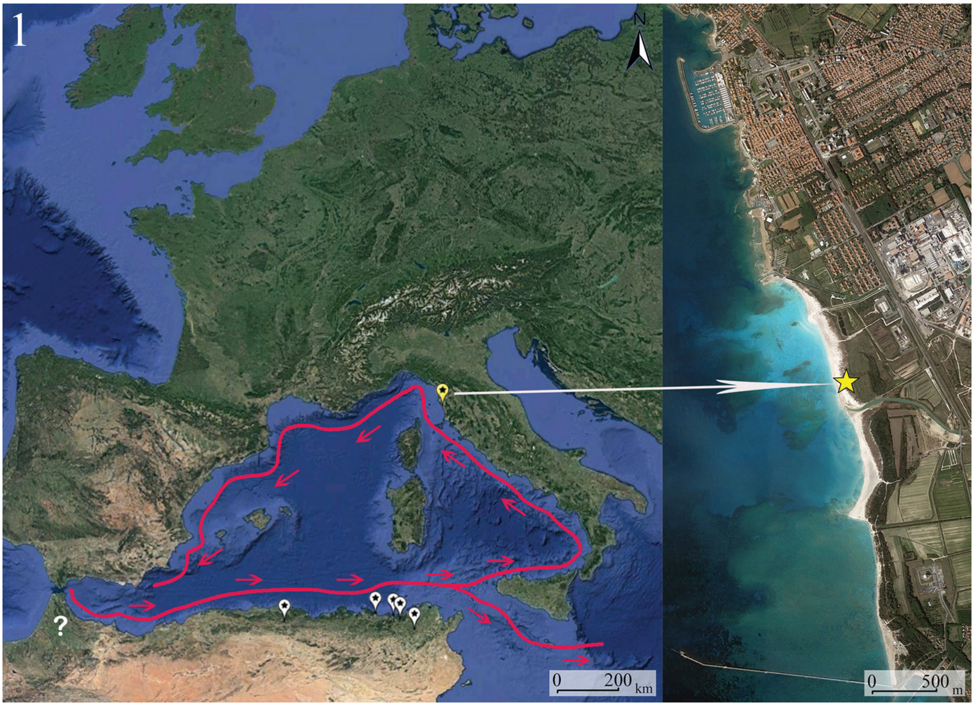

Figure 1. Distribution map of *Belarima violacea* (Lucas). Red line: Algerian current (see text).

Galeruca violacea (Lucas): Jolivet, 1967: 330 (biology).

New material examined. Italy, Tuscany (Livorno), Rosignano Solvay, Spiagge Bianche, 43°22'27.58"N, 10°26'21.27"E, 22.iii.2019, M. Violi leg., 1♂ and 1♀ (University of L'Aquila).

Collecting locality. One male and one female of *B. violacea* were found, not far from each other, wandering on the sand among the vegetation of the shifting dunes of the Spiagge Bianche (Ligurian Sea, Tuscan coast) (Fig. 1). This site is probably the best preserved of the entire beach, away from the aphytoic belt, that is the vegetation-free zone closest to the water, disturbed in summer by bathers and periodic cleaning. The vegetation consists exclusively of herbaceous essences, mainly *Ammophila arenaria arundinacea* H. Lindb. (Poaceae). On the shoreline, and near the place of the finding, there were numerous trunks, branches and other plant debris carried by the storms. The area is part of the Mediterranean macrobioclimate, low meso-Mediterranean belt and low sub-humid umbrotype (Bertacchi et al. 2016). The finding of the specimens occurred around 5.00 pm on a sunny day with sparse clouds. The site was in the portion of the dunes between the mouths of the Fine and Fosso Bianco rivers. The characteristic white color of the sand is due mainly to the waste deposits derived from the production of calcium carbonate and calcium bicarbonate by the Solvay chemical industrial center (opened in 1916 and still in operation), which is located about a

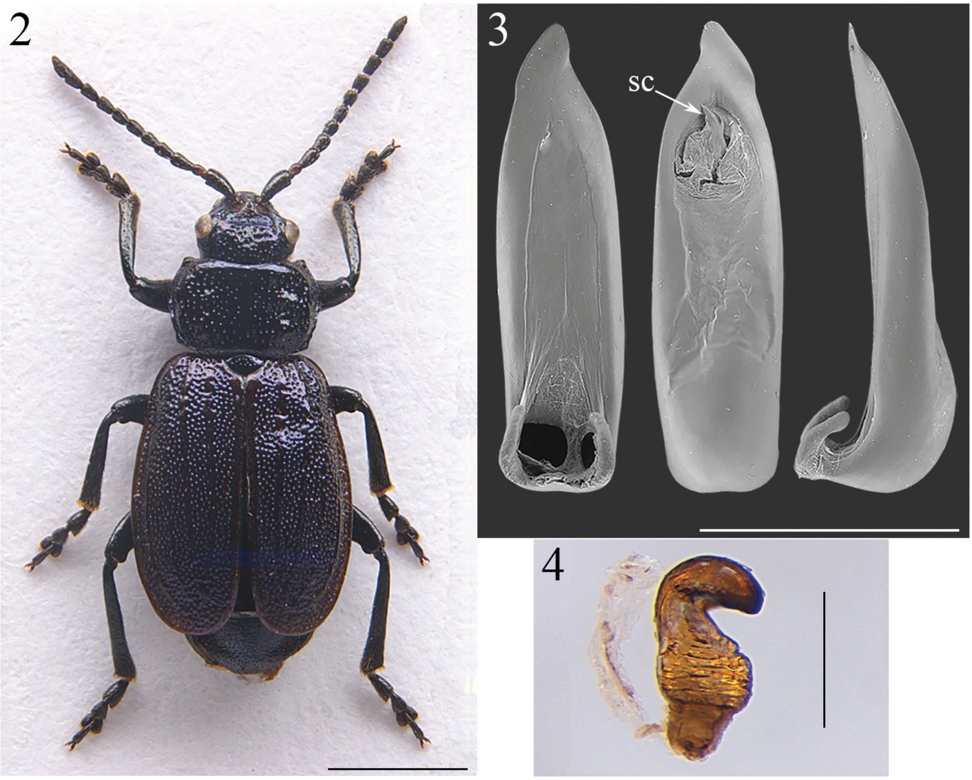

Figures 2–4. *Belarima violacea* (Lucas) **2** habitus (Tuscan coast, Rosignano Solvay, male) **3** median lobe of aedeagus, from left to right in ventral, dorsal and lateral view (Tuscan coast, Rosignano Solvay) **4** spermatheca (Tuscan coast, Rosignano Solvay). sc: sclerite of the internal sac. Scale bars: 2 mm (**2**); 1 mm (**3**); 0.2 mm (**4**).

hundred meters behind the place where *B. violacea* was found. About 1.6 km north lies the village of Rosignano Solvay with the tourist port of Cala de' Medici; about 2.4 km south is the commercial harbor of Vada, a docking point for LNG and ethylene tankers whose contents are destined for Solvay. These two sites would therefore constitute the closest sources for a possible anthropic introduction of the species to this area.

Description of the specimens and differential diagnosis. The collected specimens show shape, sculpture and color typical of the species, as described by Lucas (1847, 1849). The head, pronotum, scutellum and elytra are clearly metallic violaceous in the male (Fig. 2), while they are green-blue in the female. Both the male and the female are apterous. The apices of the elytra are regularly rounded (Fig. 2), differently from *B. obliqua* where the elytra are more strongly curved along the inner margin than along the outer one (Beenen 2019). The median lobe of the aedeagus (Fig. 3) has a little-sclerotized ventral surface, curved sides, and an asymmetrical apex in ventral view; the apex is regularly constricted and ends in a sharp triangle, differently from *B. obliqua* where it is expanded towards the apex and ends in a blunt triangle (Beenen 2019); the median lobe is straight up to the apex in lateral view; the basal part is swollen dorsally and with lateral hook-shaped extensions ventrally; the sclerite of the internal sac ends in three sharp teeth (Fig. 3). The spermatheca (Fig. 4) has hook-like, thickset cornu not inserted into the nodulus; a globose and wrinkled nodulus, as large as the cornu; and ductus with a very robust and conical proximal part.

Biometry. ♂: LB = 7.07 mm; LP = 1.30 mm; WP = 2.21 mm; LE = 4.13 mm; WE = 3.12 mm; LAN = 3.43 mm; LA = 55:20:34:25:25:26:26:30:31:30:41 (right antenna); LAED = 1.9 mm; LE/LP = 3.18; WE/WP = 1.41; WP/LP = 1.70; WE/LE = 0.75; LAN/LB = 0.48; LE/LAED = 2.17. ♀: LB = 6.80 mm; LP = 1.32 mm; WP = 2.24 mm; LE = 4.06 mm; WE = 3.09 mm; LAN = 3.44 mm; LA = 56:23:35:27:24:31:23:25:30:30:40 (right antenna); LSP = 0.32 mm; LE/LP = 3.08; WE/WP = 1.38; WP/LP = 1.70; WE/LE = 0.76; LAN/LB = 0.50; LE/LSP = 12.69.

Distribution. Algeria: Lac Tonga, surroundings of Lacalle [= El Kala]; Djurdjura; Annaba [= Bône] (Lucas 1849; Joannis 1865; Warchalowski 2010); Morocco (Jolivet 1967, indefinite locality), and Tunisia: Aïn Draham and Téboursouk (Beenen 2019); Italy: Tuscany (Livorno), Rosignano Solvay (Fig. 1).

Ecological data. The only data available on the host plants of *B. violacea* are by Jolivet (1967, as *Galeruca violacea*): *Pulicaria odora* L. (Asteraceae), *Rumex acetosella angiocarpus* Murb. and *Rumex scutatus induratus* Boissier (Polygonaceae). However, these data require future confirmation.

Discussion

The occurrence of this North African species on the Tuscan coast is difficult to interpret. The possible hypotheses to explain these findings are essentially three:

a. relict population of a wider past distribution in the north-western Mediterranean. This hypothesis is rather unlikely, considering that other populations, in this case, would have had to survive in suitable areas of the Mediterranean. However, despite the intense research activity that has always involved this area, no other sites of occurrence of the species are known, excluding the North African ones;

b. occurrence due to passive anthropogenic transport between North Africa and this Tuscan locality. This hypothesis cannot be ruled out, although unlikely. The only sites close to the collecting locality that could constitute entry points for a possible passive anthropogenic introduction are the commercial port of Vada (distance 2.4 km S) and the tourist port of Cala de' Medici (distance 1.6 km N);

c. possible colonization of the Tyrrhenian and Ligurian coasts through recent, or relatively recent, passive diffusion of this species from North Africa, vehiculated by assemblages of vegetal debris transported by the sea, possibly along the northern flow branch of the Algerian current. This marine current flows anticlockwise around the Tyrrhenian Sea along the coasts of Sicily and the Italian Peninsula before entering the Channel of Corsica (El-Geziry and Bryden 2010) (Fig. 1). Similar distributions due to possible vehiculation by Mediterranean marine currents have also been hypothesized for other species of Coleoptera (cf. Audisio et al. 2011).

Any hypothesis of active displacement can be excluded considering that the species is unable to fly. Future collecting in this Tuscan locality may provide information on the stability, or otherwise, of populations of *B. violacea* on the Italian coasts. In addition, new material would allow molecular analysis of the specimens and comparison with specimens from the North African populations, to evaluate their genetic distances.

Acknowledgements

We are grateful to our friend Ron Beenen (Nieuwegein, The Netherlands) for confirming the identification of *Belarima violacea* (Lucas) and support in preparing this contribution.

References

Audisio P, Ruzzante G, Leo P (2011) *Dapsa gemina* Audisio & De Biase, 1996, a new species of the European fauna (Coleoptera, Endomychidae). Fragmenta entomologica 23: 153–156. https://doi.org/10.4081/fe.2011.42

Beenen R (2010) Galerucinae. In: Löbl I, Smetana A (Eds) Catalogue of Palaearctic Coleoptera (Vol. 6). Chrysomeloidea. Apollo Books, Stenstrup, 74–75. [443–491.]

Beenen R (2013) Fauna Europaea. Coleoptera, Chrysomelidae, Galerucinae. Fauna Europaea version 2017.06. https://fauna-eu.org

Beenen R (2019) Faunistic, taxonomic and nomenclatural notes on Palaearctic Galerucinae (Coleoptera, Chrysomelidae) with description of six new species and a new genus. Entomologische Blätter und Coleoptera 115: 1–20.

Bertacchi A, Carducci T, Lombardi T (2016) Ecological and phytosociological aspects of foredune vegetation in a neogenic beach of Tuscan coast (Italy). Atti Società Toscana di Scienze Naturali, Memorie, Serie B 123: 83–92.

Bezděk J (2015) *Charaea luzonicum* sp. nov. (Coleoptera: Chrysomelidae: Galerucinae): the first record of Charaea in the Philippines. Revue suisse de Zoologie 122(2): 371–375.

Chapuis F (1875) Tribu XIII. Galérucides. In: Lacordaire T, Chapuis F (Eds) Histoire naturelle des Insectes. Genera des Coléoptères. Tome Onzième. Famille des Phytophages. Librairie Encyclopédique de Roret, Paris, 1–250. https://www.biodiversitylibrary.org/page/9379686

D'Alessandro P, Samuelson A, Biondi M (2016) Taxonomic revision of the genus *Arsipoda* Erichson, 1842 (Coleoptera, Chrysomelidae) in New Caledonia. European Journal of Taxonomy 230: 1–61. https://doi.org/10.5852/ejt.2016.230

El-Geziry TM, Bryden IG (2010) The circulation pattern in the Mediterranean Sea: issues for modeller consideration. Journal of Operational Oceanography 3: 39–46. https://doi.org/10.1080/1755876X.2010.11020116

Geoffroy EL (1762) Histoire abrégée des insectes qui se trouvent aux environs de Paris; dans laquelle ces animaux sont rangés suivant un ordre méthodique. Tome premier. Durand, Paris, [xxvii +] 523 pp. [10 planches] https://www.biodiversitylibrary.org/page/57114112

Joannis L de (1865) Monographie des Galérucides d'Europe, du Nord de l'Afrique et de l'Asie. Gallerucides, tribu de la famille des phytophages, ou chrysomélines. L'Abeille, Mémoires d'Entomologie 3 [1866]: 1–168.

Jolivet P (1967) Notes systematiques et ecologiques sur les Chrysomelides Marocains (Coleoptera) (2e note). Bulletin de la Société des Sciences naturelles et Physiques du Maroc 1966: 305–394.

Lucas PH (1847) Histoire Naturelle des Animaux Articulés. Atlas. Exploration scientifique de L'Algérie pendant les Années 1840, 1841, 1842. Sciences Physiques. Zoologie IV. Imprimerie Nationale, Paris, 121 planches. https://www.biodiversitylibrary.org/page/54761507

Lucas PH (1849) Histoire Naturelle des Animaux Articulés. Deuxiéme Partie. Insectes. Exploration scientifique de L'Algérie pendant les Années 1840, 1841, 1842. Sciences Physiques. Zoologie II. Imprimerie Nationale, Paris, 590 pp. https://www.biodiversitylibrary.org/page/46117987

Nadein KS, Bezděk J (2014) Galerucinae Latreille, 1802. In: Leschen RAB, Beutel RG (Eds) Coleoptera, Beetles. Vol. 3. Morphology and systematics (Phytophaga). De Gruyter, Berlin, 251–259.

Nie R-E, Bezděk J, Yang X-K (2017) How many genera and species of Galerucinae s. str. do we know? Updated statistics (Coleoptera, Chrysomelidae). ZooKeys 720: 91–102. [+ supplementary file] https://doi.org/10.3897/zookeys.720.13517

Reitter E (1913) Fauna Germanica. Die Käfer des Deutschen Reiches. Nach der analytischen Methode bearbeitet. IV. Band [1912]. K.G. Lutz' Verlag, Stuttgart, 236 pp. [plates 129–152]

Rodrigues JMS, Mermudes JRM (2015) Comparative morphology of the type-species of *Isotes* and *Synbrotica* (Coleoptera, Chrysomelidae, Galerucinae), with a new synonymy of species. Iheringia, Série Zoologia, Porto Alegre 105(4): 439–452. https://doi.org/10.1590/1678-476620151054439452

Warchalowski A (2010) The Palaearctic Chrysomelidae. Identification keys (Vol. 2). Warszawska Drukarnia Naukowa, Warszawa, 630–1212. [102 plates]

ZooKeys 1031: 133–141 (2021)
doi: 10.3897/zookeys.1031.63134
https://zookeys.pensoft.net

RESEARCH ARTICLE

A peer-reviewed open-access journal
ZooKeys
Launched to accelerate biodiversity research

Geosesarma sodalis, a new species of vampire crab (Crustacea, Brachyura, Sesarmidae) from a limestone cave in central Sarawak, Malaysia

Peter K. L. Ng[1]

[1] *Lee Kong Chian Natural History Museum, Faculty of Science, National University of Singapore, Kent Ridge, Singapore 119260, Republic of Singapore*

Corresponding author: Peter K.L. Ng (peterng@nus.edu.sg)

Academic editor: L.E. Bezerra | Received 14 January 2021 | Accepted 12 February 2021 | Published 15 April 2021

http://zoobank.org/15B4DD80-14BD-42EA-BB6D-11E8FE9392BA

Citation: Ng PKL (2021) *Geosesarma sodalis*, a new species of vampire crab (Crustacea, Brachyura, Sesarmidae) from a limestone cave in central Sarawak, Malaysia. ZooKeys 1031: 133–141. https://doi.org/10.3897/zookeys.1031.63134

Abstract

A new species of semi-terrestrial crab of the genus *Geosesarma* (Sesarmidae) is described from a limestone cave in central Sarawak, Malaysian Borneo. *Geosesarma sodalis* **sp. nov.** is characterised by its quadrate carapace, absence of a flagellum on the exopod of the third maxilliped, presence of 10 or 11 sharp tubercles on the dactylus of the chela and a diagnostic male first gonopod structure. This is the sixth species of *Geosesarma* reported from Sarawak, and the first member of the genus collected from inside caves.

Keywords

Borneo, cavernicolous, description, *Geosesarma*, karst, new taxon, taxonomy

Introduction

In 2005, Rob Stuebing passed the author several brachyuran crabs he collected while surveying limestone caves in the Bintulu area in central Sarawak. The material included a new species of a cavernicolous gecarcinucid, and in 2006, fresh surveys were made in the caves to obtain more specimens. This new material formed the basis for the description of a new species of *Arachnothelphusa* Ng, 1991, by Grinang and Ng (2021).

Among the original 2005 material collected by Stuebing was a specimen of *Geosesarma* De Man, 1892 (Sesarmidae). Examination of the specimen showed it to be a new species, here named *Geosesarma sodalis* sp. nov. This is also the first record of a *Geosesarma* from inside caves. *Geosesarma* are often called vampire crabs because many species have bright yellow eyes in life (see Ng et al. 2015; Ng 2017). *Geosesarma* is a large genus, with 67 species known from Southeast and East Asia, the Andaman Islands, Papua New Guinea, and the Solomon Islands (Ng et al. 2008; Ng and Wowor 2019; Shy and Ng 2019; Naruse and Ng 2020).

Material and methods

Measurements provided are the carapace width and length. The terminology used in this paper follows Ng et al. (2008) and Davie et al. (2015). The abbreviations G1 and G2 are used for the male first and second gonopods, respectively. The type specimen is deposited in the Zoological Reference Collection (**ZRC**) of the Lee Kong Chian Natural History Museum, National University of Singapore.

Systematic accounts

Family Sesarmidae Dana, 1851

Genus *Geosesarma* De Man, 1892

Type species. *Sesarma* (*Geosesarma*) *nodulifera* De Man, 1892; subsequent designation by Serène and Soh (1970).

Geosesarma sodalis sp. nov.

http://zoobank.org/69A4BE4D-8B0B-4243-9B2D-BA1D559A2C28
Figures 1–3

Material examined. ***Holotype*:** male (10.1 × 9.8 mm) (ZRC 2020.0413), limestone cave, Bukit Sarang, Bintulu, Sarawak, Malaysia, coll. Stuebing RB, early 2005.

Diagnosis. Carapace quadrate, slightly wider than long, width to length ratio 1.03, lateral margins gently concave, subparallel (Fig. 1A, B); dorsal surfaces with well-defined regions, anterior half with low granules, posterior half almost smooth (Fig. 1A, B); frontal margin distinctly deflexed, frontal lobes broad, with truncated margins in dorsal view, separated by wide shallow median concavity; postfrontal and postorbital cristae sharp, distinct (Fig. 1A–C); external orbital angle triangular, directed obliquely anteriorly, extending just beyond lateral carapace margins, outer lateral margin convex; separated from first epibranchial tooth by deep V-shaped cleft; first

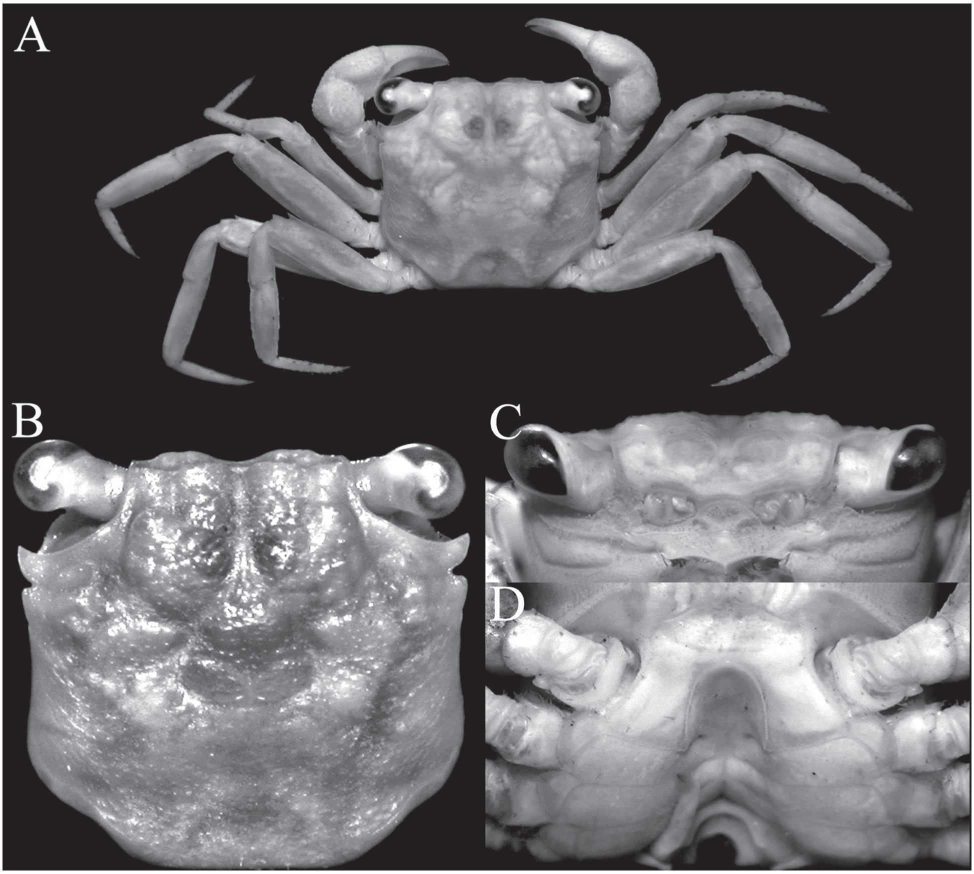

Figure 1. *Geosesarma sodalis* sp. nov., holotype male (10.1 × 9.8 mm) (ZRC 2020.0413), Sarawak **A** overall dorsal view **B** dorsal view of carapace **C** frontal view of cephalothorax **D** anterior thoracic sternites and sternopleonal cavity.

epibranchial tooth distinct, second epibranchial tooth visible only as low lobe, barely separated from first tooth by shallow concavity (Fig. 1A, B); merus of third maxilliped subovate; exopod slender, flagellum absent (Fig. 3A); outer surfaces of palm of chela covered with small rounded granules, inner surface without transverse ridge; fingers longer than palm, dorsal margin of dactylus with 10 or 11 sharp, anteriorly directed sharp tubercles (Fig. 2A–D); ambulatory merus with sharp subdistal spine on dorsal margin, surface weakly rugose, propodus slender, relatively long (Figs 1A, 2E, F); pleon triangular; somite 3 widest, somite 6 with lateral margins gently convex; telson triangular, longer than broad, lateral margins gently convex (Fig. 2G); G1 relatively slender, proximal, distal part bent at angle of ca. 45° along longitudinal axis, subdistal part of outer margin gently angular with shelf-like feature (Figs 2H–K, 3B–D, F), distal part elongate, tapering in lateral view, spatuliform in marginal view, with small submedian cleft at tip when viewed mesially (Fig. 3E, G).

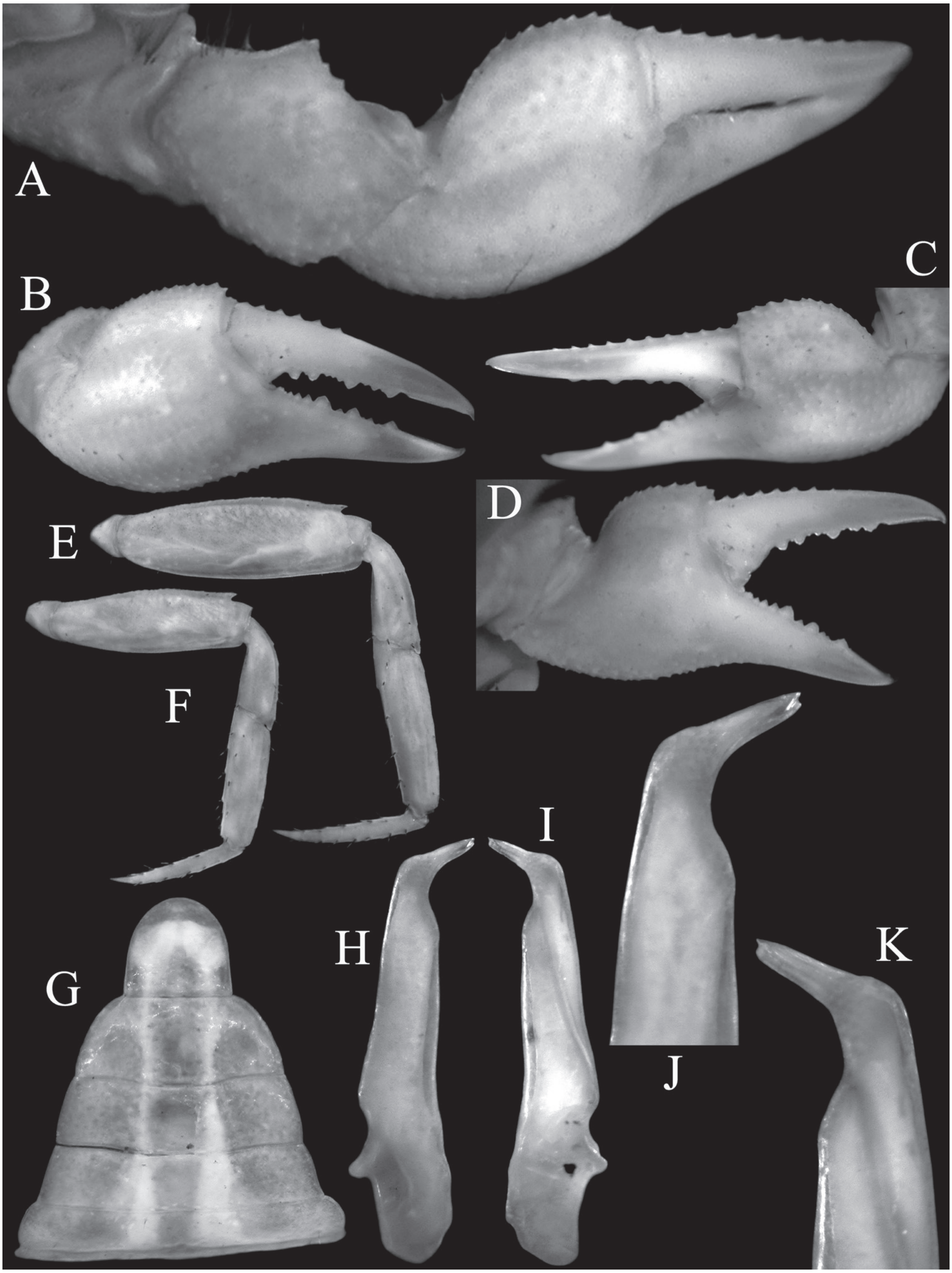

Figure 2. *Geosesarma sodalis* sp. nov., holotype male (10.1 × 9.8 mm) (ZRC 2020.0413), Sarawak **A** dorsal view of right cheliped **B** outer view of right chela **C** subdorsal view of left chela **D** inner view of right chela **E** right third ambulatory leg **F** right fourth ambulatory leg **G** pleonal somites 2–6 and telson **H** left G1 (ventral view) **I** left G1 (ventral view) **J** distal part of left G1 (ventral view) **K** distal part of left G1 (ventral view).

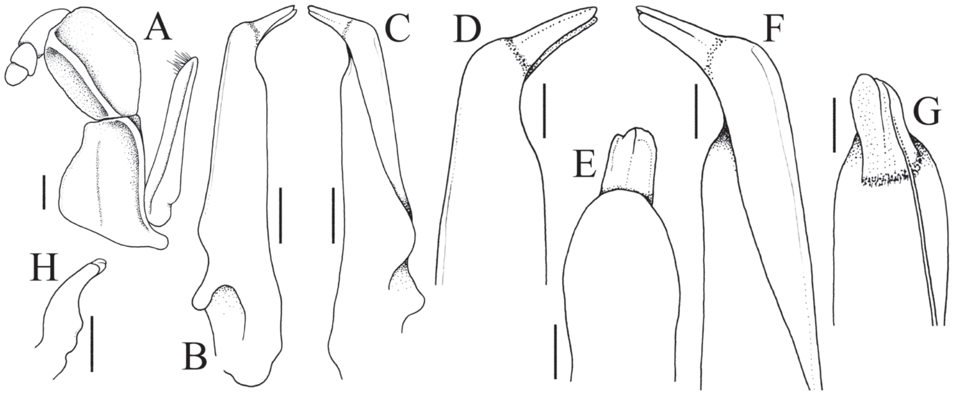

Figure 3. *Geosesarma sodalis* sp. nov., holotype male (10.1 × 9.8 mm) (ZRC 2020.0413), Sarawak **A** left third maxilliped (setae denuded) **B** left G1 (ventral view) **C** left G1 (ventral view) **D** distal part of left G1 (ventral view) **E** distal part of left G1 (distomesial view) **F** distal part of left G1 (ventral view) **G** distal part of left G1 (ventromesial view) **H** left G2. Scales bars: 0.5 mm (**A–C, H**); 0.25 mm (**D–G**).

Colour. Not known.

Females. Not known.

Etymology. The name is derived from the Latin noun for comradeship; alluding to the deep friendship the author has had over the last 30 years with the collector, Rob Stuebing, who has collected many interesting species for him.

Remarks. The island of Borneo has 13 known species of *Geosesarma*, all of which are endemic to the island. Five species occur in the state of Sarawak (Ng and Grinang 2018; Ng and Ng 2019). One group of *Geosesarma* species is characterised by their relatively quadrate carapace, presence of a row to sharp tubercles on the dorsal margin of the cheliped dactylus, absence of a flagellum on the third maxilliped exopod, and a relatively stout G1 with a tapering corneous distal part (in lateral view). In Borneo, the species in this group are *G. gracillimum* (De Man, 1902), *G. sabanus* Ng, 1992, *G. aurantium* Ng, 1995, *G. katibas* Ng, 1995, *G. danumense* Ng, 2002, *G. bau* Ng & Grinang, 2004, *G. ambawang* Ng, 2015, *G. pontianak* Ng, 2015, *G. larsi* Ng & Grinang, 2018, and *G. spectrum* Ng & Ng, 2019.

Five of the species in this group are present in Sarawak and Brunei: *G. gracillimum*, *G. katibas*, *G. bau*, *G. larsi*, and *G. sodalis* sp. nov. Compared to *G. gracillimum*, the carapace of *G. sodalis* sp. nov. is more quadrate with the lateral margins subparallel (Fig. 1A, b) (versus gently diverging in *G. gracillimum*; see Ng 2015: fig. 14A, B; Ng and Ng 2015: fig. 5F). The G1 of *G. sodalis* sp. nov. (Figs 2H, I, 3B, C) is distinct in that it is proportionately more slender than those of *G. gracillimum*, *G. katibas*, and *G. larsi* (cf. Ng 1995: fig. 12A–E; Ng and Grinang 2018: fig. 5B–F, Ng and Ng 2019: fig. 9B–E, G, H, I–M). In addition, the distal corneous part of the G1 is almost straight in *G. sodalis* sp. nov. (Fig. 3B–D, F, H–K) but gently upcurved in *G. gracillimum* (see Ng and Ng 2019: fig. 9I–M). Compared to *G. bau*, which also has a more slender G1, *G. sodalis* sp. nov. has the distal part bent at an angle of about 45° along the longitudinal axis and the subdistal part of the outer margin is more angular and shelf-like (Figs 2H–K, 3B–D, F) (versus G1 bent at about 30° along longitudinal axis and subdistal part of outer margin is gradually sloping in *G. bau*; see Ng and Grinang 2004: fig. 9D, F).

The relatively longer fingers (distinctly longer than the palm) and the outer surface of the chela with fewer small granules in *G. sodalis* sp. nov. (Fig. 2A–D), differ from the condition in *G. katibas* and *G. larsi*, with the shorter fingers and the outer surface densely covered with small rounded granules (see Ng and Grinang 2018: figs 2D, 3A; Ng and Ng 2019: fig. 1C). The longer fingers of the chela most closely resemble those of *G. gracillimum* and *G. bau* (see Ng 1995: fig. 13A; Ng and Grinang 2004: fig. 8A; Ng 2015: fig. 14E, F). The male pleon of *G. sodalis* sp. nov. (Fig. 2G) is similar to that of *G. katibas* (see Ng and Ng 2019: fig. 8D), but this character is not reliable to differentiate taxa as it varies some degree in relative widths of the somites and convexity of the lateral margins of somite 6 (Ng and Ng 2019).

The male chela and G1 differences between *G. sodalis* sp. nov. and *G. spectrum* (from Brunei) are the same as for the Sarawakian *G. katibas*. *Geosesarma sodalis* sp. nov. differs markedly from the two species in this group from Indonesian Kalimantan, *G. ambawang* and *G. pontianak*, in possessing a G1 that is proportionately stouter and the subdistal part of the outer margin has a prominent right angled hump-like arch (see Ng 2015: figs 9D–G, 13D–H, J–M). The three species in this group from the eastern Malaysia state of Sabah, *G. sabanus*, *G. aurantium*, and *G. danumense* differ markedly from *G. sodalis* sp. nov. in that the corneous G1 distal part is longer and distinctly spatuliform in lateral view (Ng 1992, 1995, 2002; Ng and Ng 2018).

Biology. Noteworthy is that *G. sodalis* sp. nov. was collected inside a cave where a cavernicolous species of gecarcinucid, *Arachnothelphusa sarang* Grinang & Ng, 2021, is present. Bukit Sarang is an isolated limestone outcrop with a complex of small caves, most of which probably have subterranean interconnections, and is part of the Tatau river basin in central Sarawak. The type specimen was obtained in moist areas several hundred meters from the cave entrance (RB Stuebing pers. comm.). Although more surveys in and around the Bukit Sarang were conducted in 2006 and more specimens of *A. sarang* were collected (Grinang and Ng 2021), no other specimens of *Geosesarma* were forthcoming.

Geosesarma sodalis sp. nov., however, does not have prominently elongated legs or reduced eyes typical of true troglobitic taxa, and must be treated as troglophile. It is probably more widespread outside the cave habitat. The site it was collected from is several hundred metres from the cave entrance and there was no light at all. The sympatric *Arachnothelphusa sarang* possesses some cave-dwelling characters-there is hardly any pigmentation on the body and legs and the pereopods are elongated, but the eyes are not reduced with the cornea still distinct, with Grinang and Ng (2021) treating it only as a troglophilic species.

No *Geosesarma* species had previously been recorded from caves, although one sesarmid genus *Karstarma* Davie & Ng, 2007, is known to live in or closely associated with limestone caves. *Karstarma* species are widely distributed in the Indo-West Pacific, with 18 recognised species (see Wowor and Ng 2018; Poupin et al. 2018; Ng 2020). Wowor and Ng (2018) recognised three species-groups in *Karstarma* and discussed the affinities of one of these groups with *Geosesarma*. They commented that the characters of some *Karstarma* species (e.g, *K. microphthalmus* (Naruse & Ng, 2007) and *K. malang* Wowor & Ng, 2018) are close to *Geosesarma*. Until the present discovery of *G. sodalis* sp. nov., no species of *Geosesarma* has previously been found in caves. *Geosesarma sodalis* sp. nov., however, has none of the morphological features associated with a cavernicolous lifestyle, e.g., reduced eyes and/or cornea and elongated pereopods. In any case, *G. sodalis* sp. nov. differs markedly from the group of *Karstarma* species highlighted by Wowor and Ng (2018) in its quadrate carapace, proportionately shorter ambulatory legs, and stouter G1, as well as its well-developed eyes with the large pigmented cornea.

Another species of sesarmid which was originally desrribed from near the entrance of a cave in Myanmar, *Pseudosesarma brehieri* Ng, 2018, is now known to normally live in mangrove habitats (Ng 2018; Schubart and Ng 2020).

Acknowledgements

The author is most grateful to Rob Stuebing for entrusting the material from Bukit Sarang to the author for study.

References

Davie PJF, Guinot D, Ng PKL (2015) Anatomy and functional morphology of Brachyura. In: Castro P, Davie PJF, Guinot D, Schram FR, Von Vaupel Klein JC (Eds) Treatise on Zoology – Anatomy, Taxonomy, Biology – The Crustacea (Vol. 9C–I): Decapoda: Brachyura (Part 1). Brill, Leiden, 11–163.

Davie PJF, Ng PKL (2007) A new genus for cave-dwelling crabs previously assigned to *Sesarmoides* (Crustacea: Decapoda: Brachyura: Sesarmidae). Raffles Bulletin of Zoology, Supplement 16: 227–231.

De Man JG (1892) Decapoden des Indischen Archipels. Zoologische Ergebnisse einer Reise in Niederlandisch Ost-Indien 2: 265–527. https://www.biodiversitylibrary.org/page/10886044

De Man JG (1902) Die von Herrn Professor Kükenthal in Indischen Archipel gesammelten Dekapoden und Stomatopoden. In: Kükenthal W (Ed.) Ergebnisse einer zoologischen Forschungsreise in den Molukken und Borneo. Abhandlungen der Senckenbergischen Naturforschenden Gesellschaft 25: 467–929. [pls 19–27.] https://www.biodiversitylibrary.org/page/10964510

Grinang J, Ng PKL (2021) A new species of the genus *Arachnothelphusa* Ng, 1991 (Crustacea: Decapoda: Gecarcinucidae) from a limestone cave in Sarawak (Malaysian, Borneo). Raffles Bulletin of Zoology 69: 1–7.

Naruse T, Ng PKL (2007) On a new species of cavernicolous crab of the genus *Sesarmoides* Serène & Soh, 1970 (Crustacea: Decapoda: Brachyura: Sesarmidae) from Sulawesi, Indonesia. Raffles Bulletin of Zoology 55(1): 127–130.

Naruse T, Ng PKL (2020) Revision of the sesarmid crab genera *Labuanium* Serène and Soh, 1970, *Scandarma* Schubart, Liu and Cuesta, 2003, and *Namlacium* Serène and Soh, 1970 (Crustacea: Decapoda: Brachyura: Sesarmidae), with descriptions of four new genera and two new species. Journal of Natural History 54(7–8): 445–532. https://doi.org/10.1080/00222933.2020.1763491

Ng PKL (1991) Bornean freshwater crabs of the genus *Arachnothelphusa* gen. nov. (Crustacea: Decapoda: Brachyura: Gecarcinucidae). Zoologische Mededelingen 65(1): 1–12.

Ng PKL (1992) *Geosesarma sabanus*, a new sesarmine crab (Decapoda, Brachyura, Grapsidae) from the forests of Sabah, East Malaysia, Borneo. Crustaceana 63(2): 210–213. https://doi.org/10.1163/156854092X00596

Ng PKL (1995) *Geosesarma aurantium*, a new sesarmine land crab (Crustacea: Decapoda: Brachyura: Grapsidae) from Sabah. Malayan Nature Journal 49: 65–70.

Ng PKL (2002) On a new species of terrestrial crab of the genus *Geosesarma* (Crustacea: Brachyura: Sesarmidae) from Sabah, Malaysia. Malayan Nature Journal 56(3): 303–310.

Ng PKL (2015) Semiterrestrial crabs of the genus *Geosesarma* De Man, 1892 (Crustacea, Brachyura, Sesarmidae) from western Borneo, Indonesia, with descriptions of three new species. Zootaxa 4048(1): 37–56. https://doi.org/10.11646/zootaxa.4048.1.2

Ng PKL (2017) On the identities of the highland vampire crabs, *Geosesarma foxi* (Kemp, 1918) and *G. serenei* Ng, 1986, with description of a new phytotelmic species from Penang, Peninsular Malaysia (Crustacea: Decapoda: Brachyura: Sesarmidae). Raffles Bulletin of Zoology 65: 226–242.

Ng PKL (2018) On two new species of potamid and sesarmid crabs (Decapoda, Brachyura) from caves in Myanmar. Crustaceana 91(2): 185–197. https://doi.org/10.1163/15685403-00003735

Ng PKL (2020) *Karstarma umbra*, a new species of cavernicolous crab (Brachyura: Sesarmidae) from Vanuatu, with a key to the genus. Crustacean Research 49: 73–88. https://doi.org/10.18353/crustacea.49.0_73

Ng PKL, Grinang J (2018) A new species of highland vampire crab (Crustacea: Brachyura: Sesarmidae: *Geosesarma*) from Serian, Sarawak. Zootaxa 4508(4): 569–575. https://doi.org/10.11646/zootaxa.4508.4.5

Ng PKL, Guinot D, Davie PJF (2008) Systema Brachyurorum: part I. An annotated checklist of extant brachyuran crabs of the world. Raffles Bulletin of Zoology, Supplement 17: 1–286.

Ng PKL, Schubart CD, Lukhaup C (2015) New species of "vampire crabs" (*Geosesarma* De Man, 1892) from central Java, Indonesia, and the identity of *Sesarma* (*Geosesarma*) *nodulifera* De Man, 1892 (Crustacea, Brachyura, Thoracotremata, Sesarmidae). Raffles Bulletin of Zoology 63: 3–13.

Ng PKL, Wowor D (2019) The vampire crabs of Java, with descriptions of five new species from Mount Halimun Salak National Park, West Java, Indonesia (Crustacea: Brachyura: Sesarmidae: *Geosesarma*). Raffles Bulletin of Zoology 67: 217–246.

Ng PYC, Ng PKL (2019) *Geosesarma spectrum*, a new species of semiterrestrial vampire crab (Crustacea: Decapoda: Brachyura: Sesarmidae) from Brunei Darussalam, Borneo. Zootaxa 4614(3): 529–540. https://doi.org/10.11646/zootaxa.4614.3.6

Poupin J, Crestey N, Le Guelte J-P (2018) Cave-dwelling crabs of the genus *Karstarma* from lava tubes of the volcano 'Piton de la Fournaise', in Réunion Island, with description of a new species and redescription of *Karstarma jacksoni* (Balss, 1934) from Christmas Island. (Decapoda, Brachyura, Sesarmidae). Zootaxa 4497(3): 381–397. https://doi.org/10.11646/zootaxa.4497.3.3

Schubart CD, Ng PKL (2020) Revision of the intertidal and semiterrestrial crab genera *Chiromantes* Gistel, 1848, and *Pseudosesarma* Serène & Soh, 1970 (Crustacea: Brachyura: Sesarmidae), using morphology and molecular phylogenetics, with the establishment of nine new genera and two new species. Raffles Bulletin of Zoology 68: 891–994.

Serène R, Soh CL (1970) New Indo-Pacific genera allied to *Sesarma* Say 187 (Brachyura, Decapoda, Crustacea). Treubia 27: 387–416.

Shy J-Y, Ng PKL (2019) *Geosesarma mirum*, a new species of semi-terrestrial sesarmid crab (Crustacea, Decapoda, Brachyura) from central Taiwan. ZooKeys 858: 1–10. https://doi.org/10.3897/zookeys.858.35198

Wowor D, Ng PKL (2018) A new sesarmid crab of the genus *Karstarma* (Crustacea: Decapoda: Brachyura) associated with limestone formations in East Java, Indonesia. Zootaxa 4482(2): 355–366. https://doi.org/10.11646/zootaxa.4482.2.7

ZooKeys 1031: 143–159 (2021)
doi: 10.3897/zookeys.1031.62181
https://zookeys.pensoft.net

RESEARCH ARTICLE

A peer-reviewed open-access journal
ZooKeys
Launched to accelerate biodiversity research

The first two blind troglobitic spiders of the genus *Ochyrocera* from caves in Floresta Nacional de Carajás, state of Pará, Brazil (Araneae, Ochyroceratidae)

Antonio D. Brescovit[1], Robson de A. Zampaulo[2], Igor Cizauskas[3]

1 *Laboratório de Coleções Zoológicas, Instituto Butantan, Av. Vital Brasil, 1500, Butantã, São Paulo, 05503-900, Brazil* **2** *Gerencia de Licenciamento Ambiental e Espeleologia, Vale SA, Avenida Doutor Marco Paulo Simon Jardim, 34006-200 Nova Lima, Minas Gerais, Brazil* **3** *Organização de Apoio à Pesquisa da Biodiversidade (OAPBio), Rua Frei Inácio da 238, 05362-040, São Paulo, Brazil*

Corresponding author: Antonio D. Brescovit (antonio.brescovit@butantan.gov.br)

Academic editor: A. Pérez-González | Received 17 December 2020 | Accepted 23 February 2021 | Published 15 April 2021

http://zoobank.org/85A6CB62-A350-4F16-954B-F3E1D657CC02

Citation: Brescovit AD, Zampaulo RA, Cizauskas I (2021) The first two blind troglobitic spiders of the genus *Ochyrocera* from caves in Floresta Nacional de Carajás, state of Pará, Brazil (Araneae, Ochyroceratidae). ZooKeys 1031: 143–159. https://doi.org/10.3897/zookeys.1031.62181

Abstract

The first two anophthalmic species of spiders of the genus *Ochyrocera* Simon, 1892, are described for caves located in the iron formation of Floresta Nacional (FLONA) de Carajás in southeastern Pará State, Brazil. The caves are located in the municipalities of Parauapebas and Canaã dos Carajás, in the eastern portion of the Amazon Forest domain. *Ochyrocera ritxoco* **sp. nov.** and *O. ritxoo* **sp. nov.** are described based on males and females. The species have similar body characteristics with the total absence of eyes and complete depigmentation, characteristics that indicate possible evolution in subterranean environments , and thus are classified as troglobites. Each species is associated with a single geomorphological unit (mountain range), with *Ochyrocera ritxoco* **sp. nov.** being restricted to caves of Serra Norte (North Mountain) and *O. ritxoo* **sp. nov.** to caves of Serra Sul (South Mountain). Both species were collected in aphotic zones of the caves. Small and tangled webs of *O. ritxoco* **sp. nov.** were observed under blocks of stone in the soil or in cracks of the walls.

Keywords

Amazonian region, blind ground weaver spider, Synspermiata, taxonomy, troglobite

Introduction

Ochyroceratidae currently contains 10 genera and 166 species (World Spider Catalog 2020), with the recent elevation of Psilodercidae reducing its diversity by half (Wunderlich 2008). Despite this, the distribution the family can be considered wide, occurring in tropical areas of the Neotropical, African and Indo-Pacific regions. Its species are common on the ground and in cave environments, with sizes not greater than 2 mm, and having six eyes and long, thin legs (Jocqué and Dippenaar-Schoeman 2006).

Although many ochyroceratids live in hypogean environments, few have morphological specializations related to life in caves, which would characterize them as troglomorphic. We highlight here, at least five species of the family whose members possess some type of troglomorphism, namely: *Speocera caeca* described by Deeleman-Reinhold (1995) from Indonesia, *Speocera eleonorae* Baptista, 2003 from Brazil, *Theotima pura* Gertsch, 1973 and *Theotima martha* Gertsch, 1977, which occur in caves on the Yucatan Peninsula, Mexico, and *Ochyrocera peruana* Ribera, 1978 from Peru. Only two species are blind spiders (*S. caeca* and *T. pura*), while the others are characterized by reduced or small size of the eyes, depigmented body and long thin legs (Gertsch 1977).

In this work, we describe two new troglobitic species of the ochyroceratid genus *Ochyrocera*. These species represent the first blind and depigmented members of the genus, which currently possesses 50 species worldwide (World Spider Catalog 2020).

The two species were collected from iron formation caves in FLONA de Carajás (Carajás National Forest), state of Pará, northern Brazil and expand the diversity of spiders known for this ferruginous region (Brescovit et al. 2018).

Materials and methods

Taxonomic descriptions

Specimens are deposited in the following collections (abbreviation and curator in parentheses): Instituto Butantan, São Paulo (IBSP, A.D. Brescovit) and Museu Paraense Emílio Goeldi, Belém (MPEG, A.B. Bonaldo).

Morphological terms follow Brescovit et al. (2018), except for macrosetae of endites which follow Baert (2014). Descriptions and measurements were performed using a Leica 165C stereomicroscope, while photographs were taken with a Leica DFC 500 digital camera mounted on a Leica MZ16A stereomicroscope. Focal range images were made using Leica Application Suite software, version 2.5.0. Total and femur lengths were measured in lateral view without detaching any part from the specimen. All measurements are in millimeters. Female genitalia were excised with a sharp needle and photographed mounted on Hoyer´s microscope slides. For scanning electron microscopy (SEM), body parts were dehydrated in a series of graded ethanol washes (80% to 100%), critical point dried, mounted on metal stubs using adhesive copper tape and nail polish for fixation and covered with gold. SEM images were taken with

FEI Quanta 250 and LEO 1450VP scanning electron microscopes, at Laboratório de Biologia Celular of Instituto Butantan, São Paulo and Museu Paraense Emílio Goeldi, Belém, respectively.

Study area

The caves where the spiders were sampled are inserted in iron formations located in the Carajás area in southeast state of Pará, in the eastern region of the Amazon Forest in Brazil (Fig. 10). The caves are within the FLONA de Carajás (Brazilian System of Conservation Units), which encompasses approximately 411 thousand hectares and includes parts of the municipalities of Parauapebas, Canaã dos Carajás and Água Azul do Norte. In the region of the park there is a mosaic of protected areas forming a continuous area of 1.31 million hectares of preserved forest (Rolim et al. 2006), which is surrounded by pastures that replaced original forest (Campos and Castilho 2012; Martins et al. 2012; Carmo and Jacobi 2013). The park area mainly comprises forest formations (ombrophilous or seasonal) and only 5% of campo rupestre (rocky/rupestrian fields), which develops on the laterite plates (crusts) of high areas of the region (Campos and Castilho 2012).

Taxonomy

Family Ochyroceratidae Fage, 1912
Genus *Ochyrocera* Simon, 1892

Ochyrocera ritxoco sp. nov.

http://zoobank.org/3A17CF00-CFE6-482A-89B7-2CF243171883
Figs 1–6, 10

Type material. ***Holotype*** male from Cave N1_0103 (GEM-1301 or Cipó cave; 6°0'13"S, 50°17'55"W), FLONA de Carajás, Parauapebas, Pará, Brazil, 28/XI-03/X/2007, R. Andrade et al. col. (IBSP 115497). ***Paratype*** female from Cave N1_0075 (GEM_1273 or Piranha cave; 6°1'14"S, 50°16'49"W), FLONA de Carajás, Parauapebas, Pará, Brazil, 28/XI–03/X/2007, R. Andrade et al. col. (IBSP 115499).

Other material examined. Brazil. Pará: Parauapebas, FLONA de Carajás, Cave N1_0015 (GEM-1211) (6°2'2"S, 50°16'16"W), 11/VI–02/VII/2014, 1♀ (IBSP 186123); 1♀ (IBSP 186124); 1♂ (IBSP 186125); 2♀ (IBSP 186126); Cave N1_0016 (GEM-1212) (6°1'10"S, 50°16'41"W), 04/IX–06/X/2014, 1♀ (IBSP 186130); 02–29/IV/2015, 2♀ (IBSP 186153); 3♀ (IBSP 186154); 1♀ (IBSP 186155); Cave N1_0055 (GEM-1253) (6°1'12"S, 50°16'43"W), 07–28/I/2015, 1♀ (MPEG 37086, ex IBSP 186147); Cave N1_0056 (GEM-1254) (6°1'11"S, 50°16'44"W), 07–28/I/2015, 1♂ (MPEG 37087, ex IBSP 186148); 1♂ 1♀ (IBSP 186149); Cave

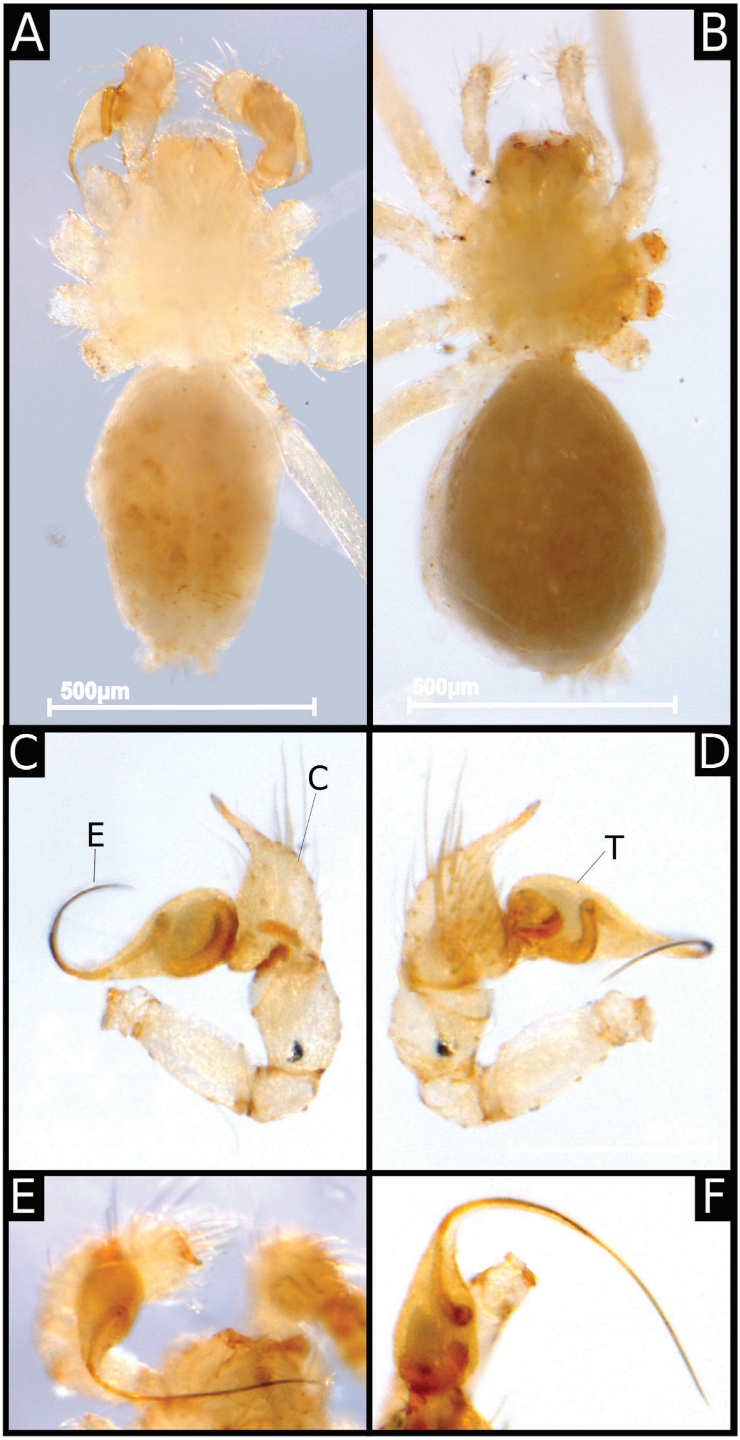

Figure 1. *Ochyrocera ritxoco* sp. nov., male IBSP 186160 (**A, C–F**), female IBSP 186146 (**B**) **A, B** habitus, dorsal view **C** left male palp, retrolateral view **D** same, prolateral view **E** right male palp, ventral view **F** same, dorsal view. Abbreviations: C = cymbium, CE = cymbial extension, E = embolus, T = tegulum.

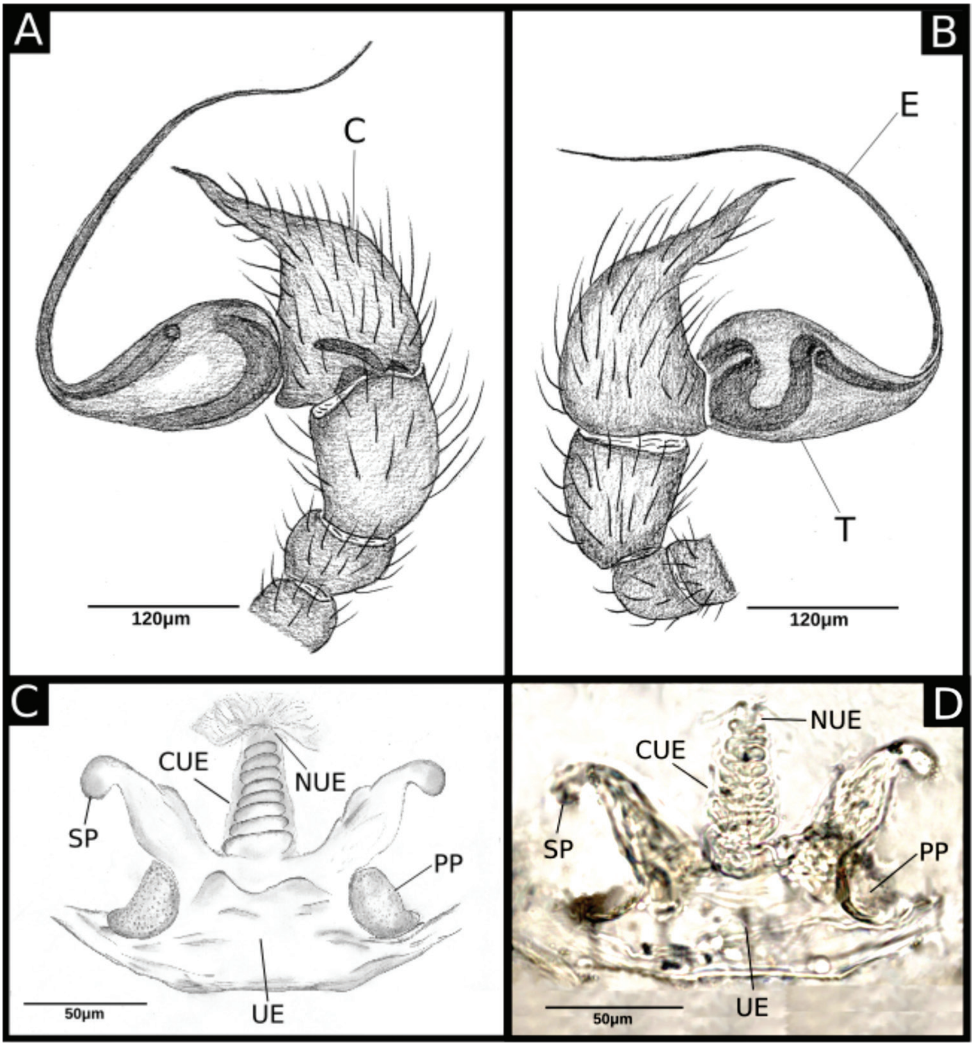

Figure 2. *Ochyrocera ritxoco* sp. nov. (**A, B**) **A** left male palp IBSP 186149, retrolateral view **B** same, prolateral view (**C, D**) **C** female genitalia IBSP 186149, enzyme cleared, dorsal view **D** same, dorsal view. Abbreviations: C = cymbium, CUE = columnar uterus externus, E = embolus, NUE = neck of uterus externus, PP = pore-plate, SP = spermathecae, T = tegulum, UE = uterus externus.

N1_0060 (GEM-1258) (6°1'12"S, 50°16'41"W), 11/VI–02/VII/2014, 1♀ (IBSP 186127); 1♀ (IBSP 186128); 07–28/I/2015, 1♀ (IBSP 186150); 1♀ (IBSP 186151); 1♂ 1♀ (MPEG 37088, ex IBSP 186152); Cave N1_0062 (GEM-1260) (6°1'10"S, 50°16'44"W), 04/IX–06/X/2014, 1♀ (IBSP 186131); 1♀ (IBSP 186132); 2♀ (IBSP 186133); 1♀ (IBSP 186134); 1♂ 2♀ (IBSP 186135); 02–29/IV/2015, 2♀ (IBSP 186157); 3♂ 1♀ (IBSP 186156); 1♀ (IBSP 186158); Cave N1_0073 (GEM-1271) (6°1'13"S, 50°17'17"W), 02–29/IV/2015, 1♀ (IBSP 186159); 1♂ (IBSP 186160); 1♀ (IBSP 186161); 1♀ (IBSP 186162); Cave N1_0084 (GEM-1282) (6°1'7"S, 50°17'1"W), 11/VI–02/VII/2014, 1♀ (IBSP 186129); Cave N1_0101 (GEM-1299)

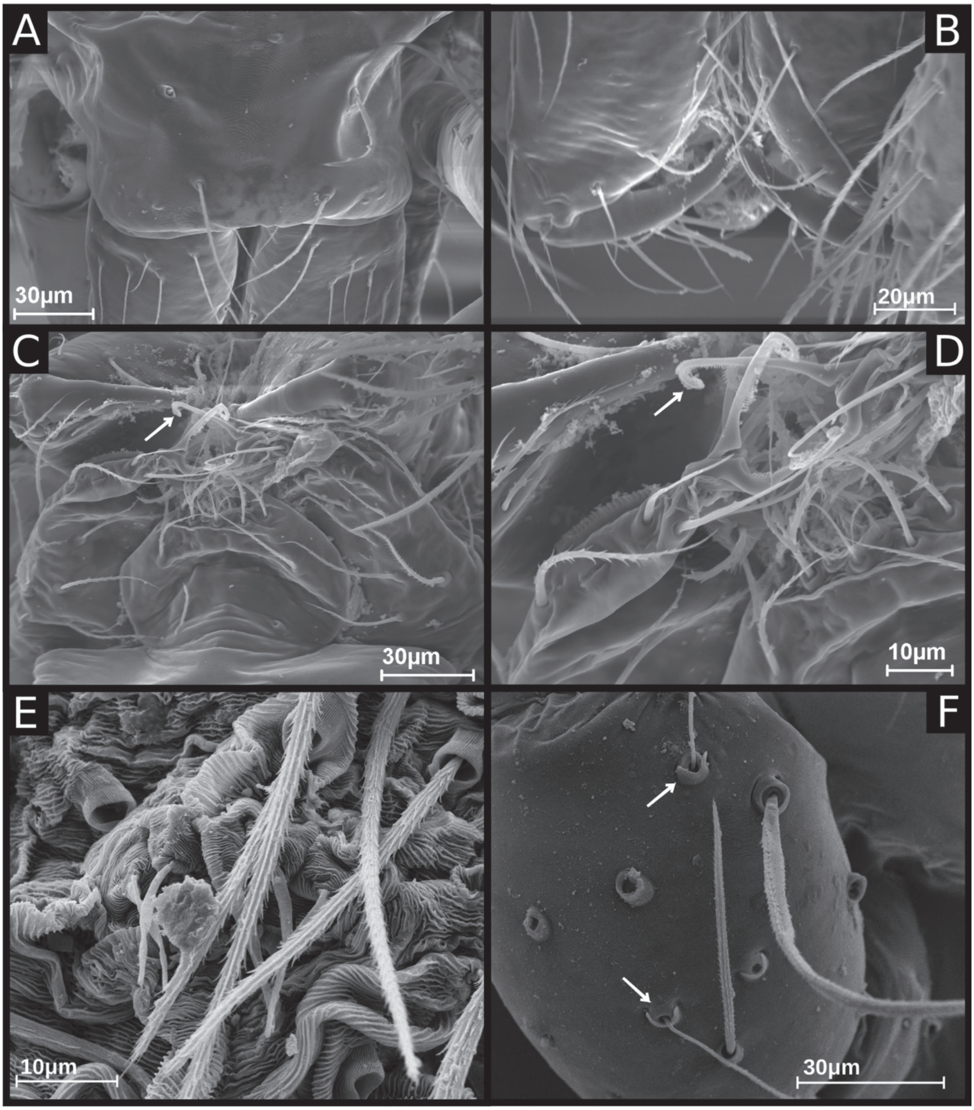

Figure 3. SEM images of *Ochyrocera ritxoco* sp. nov., male IBSP 260307 (**A–F**) **A** carapace, dorsal view **B** chelicerae, frontal view **C** endites and labium, ventral view **D** crosier-like macrosetae (arrow, detail) **E** epiandrous area, abdomen, ventral view **F** male palp, tibia (arrows, trichobothria), dorsal view.

(6°1'9"S, 50°16'46"W), 04/IX–06/X/2014, 1♂ (IBSP 186136); 1♀ (IBSP 186137); 1♀ (IBSP 186138); 1♂ (IBSP 186139); 2♀ (IBSP 186140); 1♂ (IBSP 186141); 1♂ (IBSP 186142); Cave N1_0240 (6°1'19"S, 50°16'26"W), 04/IX–06/X/2014, 1♂ (IBSP 186143); 1♀ (IBSP 186144); 1♂ (IBSP 186145); 1♀ (IBSP 186146); 02–29/IV/2015, 1♀ (IBSP 186163); 1♂ 1♀ (IBSP 186164); all collected by Equipe Carste; Cave N4WS_0067 (GEM-1846) (6°04'22"S, 50°11'30"W), 18/XI–01/XII/2010, F.P. Franco & C.A.R. Souza et al. col., 1♂ (IBSP 174069); 2♀ (IBSP 174070); Piranha,

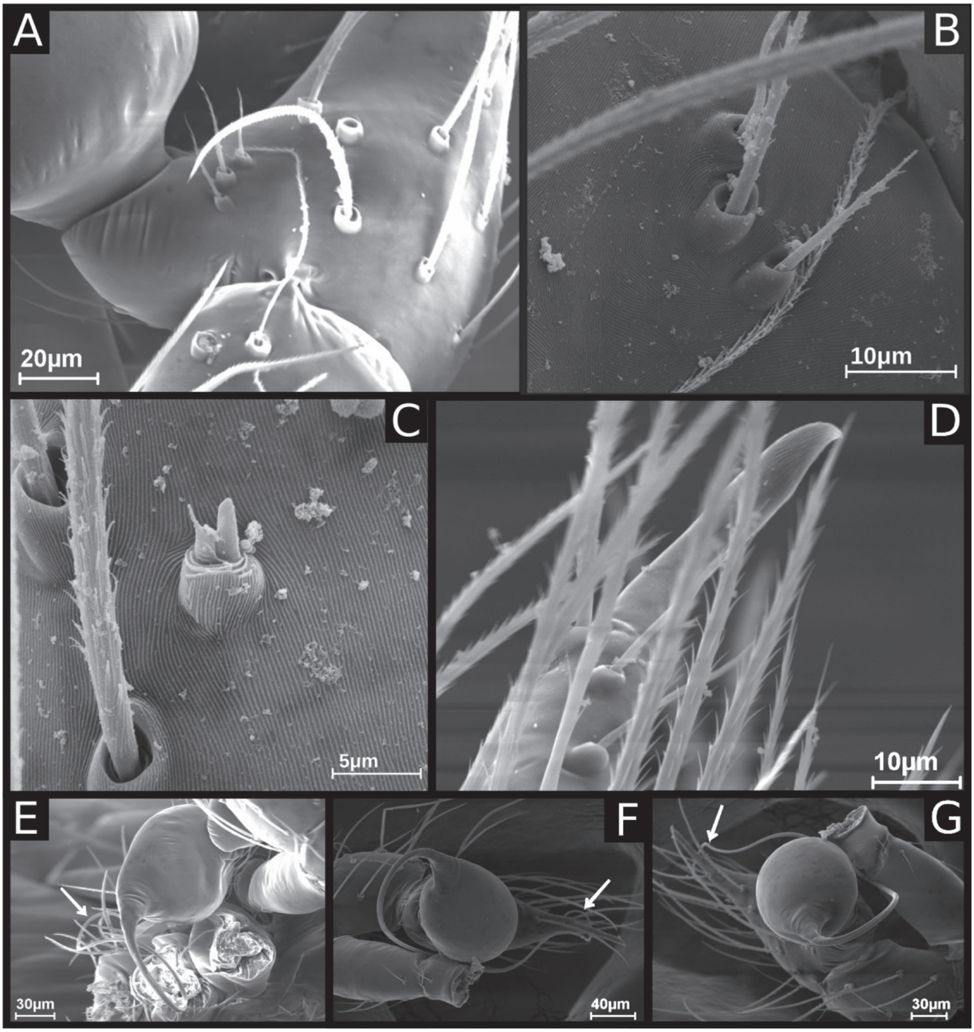

Figure 4. SEM images of *Ochyrocera ritxoco* sp. nov., male IBSP 260307 (**A–G**) **A** cymbium, retrolateral view **B** same, basal macrosetae, retrolateral view **C** same, tarsal organ, detail, retrolateral view **D** same, apex detail **E–G** male palp, arrows indicating the embolus **E** retrolateral view **F** same, prolateral view **G** same, frontal view.

Cave N1-75 (6°1’14"S, 50°16’49"W), 28/IX–03/X/2007, 1♂ 2♀ (IBSP 260307; 1♂ SEM; 1♀ SEM, ex IBSP 115499); all collected by R. Andrade et al.

Diagnosis. *Ochyrocera ritxoco* sp. nov. is distinguished from *O. ritxoo* sp. nov. by having an elongated embolus, which is two times longer than the bulb in the male palp (Figs 1F, 2A, B, 4E–G), while the embolus is one times longer than the bulb in *O. ritxoo* sp. nov. (Fig. 7C, D); a long and globose distal area in the spermathecae and an elongated columnar uterus externus with approximately eight internal chambers in the female genitalia (Fig. 2C, D); while *O. ritxoo* sp. nov. have a triangular distal area in

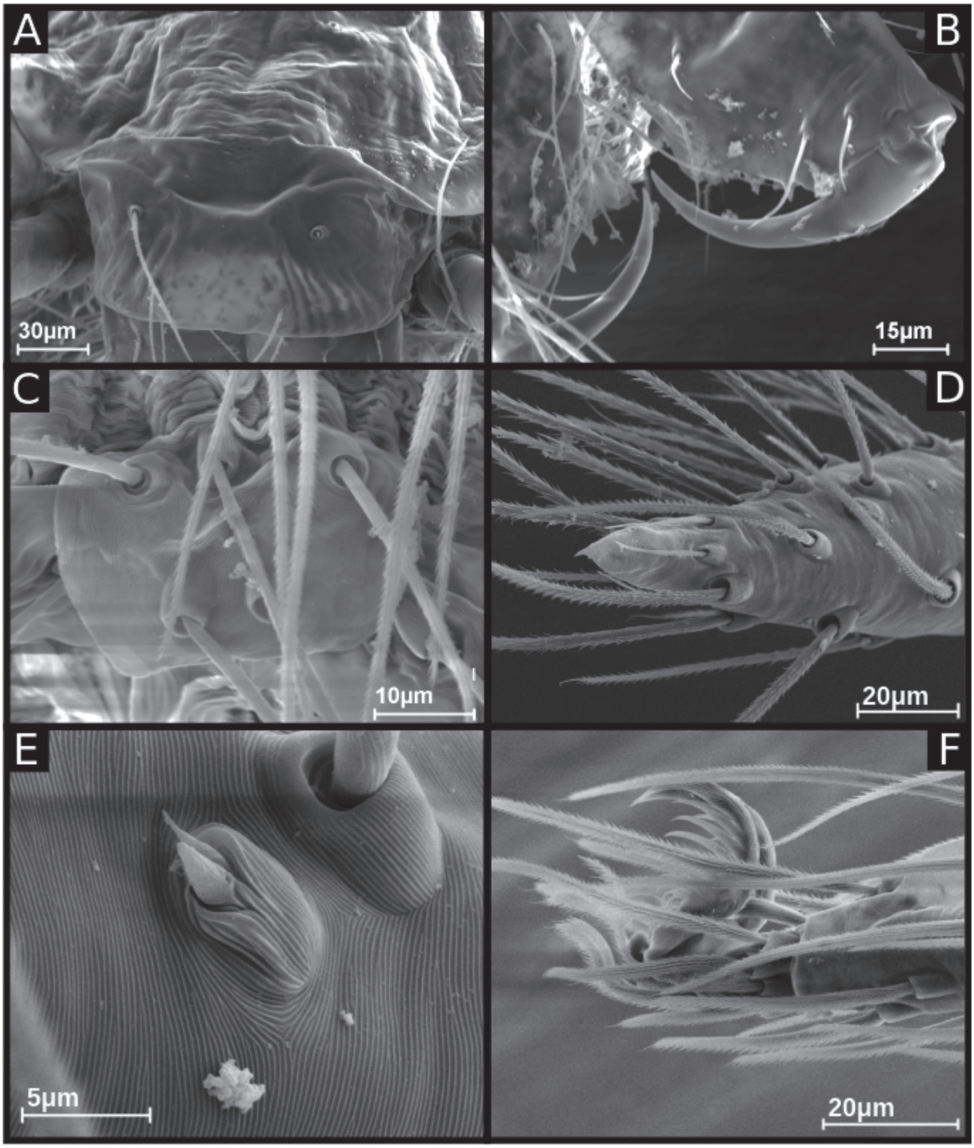

Figure 5. SEM images of *Ochyrocera ritxoco* sp. nov., female IBSP 260307 (**A–F**) **A** carapace, dorsal view **B** chelicerae, frontal view **C** colulus, ventral view **D** pedipalp, distal, prolateral view **E** same, tarsal organ **F** leg IV, claw, prolateral view.

the spermathecae and a shorter columnar uterus externus with 3–4 internal chambers in the female genitalia (Fig. 8C, D).

Description. Male (Holotype). Total length 1.1. Carapace length 0.45; ovoid, narrowing gradually anteriorly, yellowish and bright, pars cephalic flat, fovea absent (Figs 1A, 3A). Clypeus with two pairs of long bristles (Fig. 3A). Eyes absent. Chelicerae light yellow with orange fang, promargin with three teeth attached to a very long lamina (Fig. 3B), retromargin without teeth. Endites light yellow with large serrula with more than 30 denticles, distal macrosetae paired and crosier-like, many multifid macrosetae present (Fig. 3C, D). Labium cream-colored, rounded with 8–10 setae with an enlarged basally (Fig. 3C). Sternum light yellow. Legs cream-colored, formula 1423, total length I 4.5, II 3.8, III 3.1, IV 4.0. Male palp with palpal femur length 0.04, palpal tibia almost as long as wide with two long dorsal trichobothria (Fig. 3F), cymbium enlarged basally, narrowed distally, bearing elongated cuspule (Fig. 4D), three setae on projected bases retrolaterally (Fig. 4A, B), elongated tarsal organ subdistally (Fig. 4C), no basal setae on the rounded cymbial prolateral extension, bulb oval, embolus filiform, sinuous and at least twice as long as the cymbium (Figs 1F, 2A, B, 4E–G). Abdomen length 0.50, oval, uniformly gray. Six epiandrous spigots with a short base (Fig. 3E)

Female (Paratype IBSP 115499). Total length 1.15. Carapace length 0.55 as in male with light yellowish pattern (Figs 1B, 5A). Pedipalp without claw, with conical tip and subdistal trichobothrium (Fig. 5D–E). Clypeus, eyes, chelicerae (Fig. 5B), sternum, endites, and labium as in male. Legs as in male, formula 4123, total length I 4.1, II 3.6, III 2.4, IV 4.3. Claw of leg with five teeth (Fig. 5F). Abdomen length 0.65. Colulus rectangular with five long bristles (Fig. 5C). Internal genitalia with long spermathecae narrowed at tip, conspicuous pore-plate at base; medial columnar uterus externus long, with visible internal chambers. Uterus externus shorter than spermathecae. Oval pore-plates on spermathecae with approximately 20–30 glandular ducts (Fig. 2C, D).

Variation. Ten males: total length 1–1.25; carapace 0.4–0.5; femur I 1.05–1.4; ten females: total length 1–1.3; carapace 0.4–0.5; femur I 1–1.3.

Etymology. The specific name Ritxòkò means “ceramic dolls” in the female language of the Karajá people, an indigenous population of the region. The dolls are produced by Karajá women, who model, burn, paint, and sell them (Silva 2015).

Natural history. *Ochyrocera ritxoco* sp. nov. is a small troglobitic spider that is exclusive to caves in the Carajás karst region. Specimens were found only in aphotic zones of caves. They build small, tangled webs under blocks of stone on the ground or in slits (Fig. 6). The observed sex ratio for the species was 2.4F:1M (*N* = 66). *Ochyrocera ritxoco* sp. nov. was generally found in large cavities with horizontal projections varying from 9.5 to 216 meters (*N* = 13, mean = 107 m). All caves where the species was found have only one entrance and are located only in the middle and high slopes of Serra Norte. Most caves have aphotic zones or twilight zones (except for cavities N1_0103 and N1_0084) and high humidity, thus explaining the observed presence of small bodies of water in almost all cavities, especially during the wet season. The number of troglobitic species in these caves varied from one to ten (average 5.3 per cave), with species of the following taxa: spiders – Oonopidae (many species), Caponiidae (*Carajas paraua* Brescovit & Sánchez-Ruiz, 2016) and Ochyroceratidae (*Speocera* spp.); pseudoscorpions – Bochicidae, Chthoniidae and Ideoroncidae; springtails – Paronellidae (*Trogolaphysa* sp., *Cyphoderus* sp.), Entomobryidae (*Pseudosinella* sp.) and Sminthuridae (*Pararrhopalites* sp.); beetles – Carabidae (*Coarazuphium* spp.),

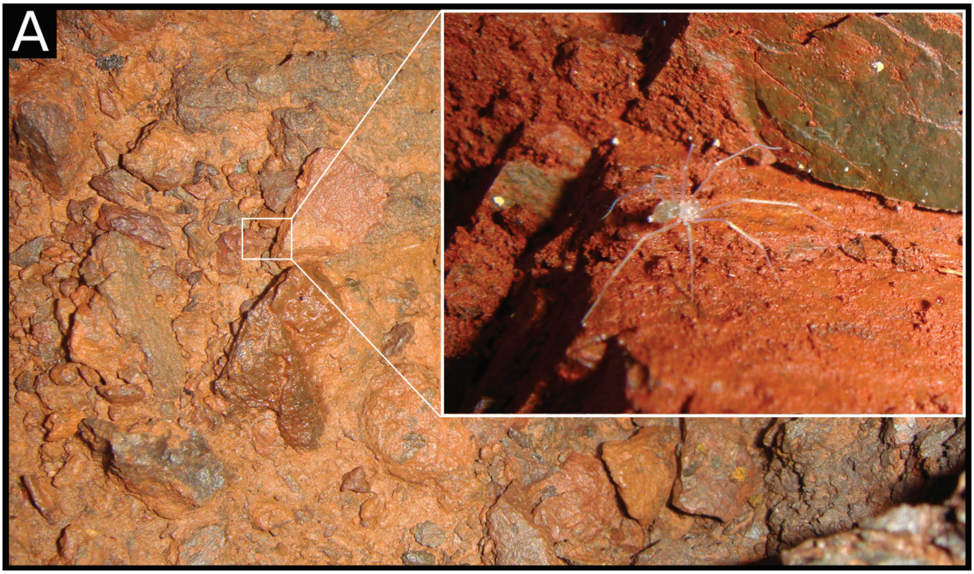

Figure 6. *Ochyrocera ritxoco* sp. nov., female in webs under rocks on the ground in the Cave N4WS_0067.

Dytiscidae (*Copelatus cessaima* Caetano, Bena & Vanin, 2013); isopods – Scleropactidae (*Circoniscus* spp.), Calabozoidae; amphipods – Bogidiellidae (*Bogidiella* sp.); planarian – Prorhynchidae (*Geocentrophora* sp.); and Harvestmen – Escadabiidae.

Distribution. Known exclusively from caves in a range of approximately 15 km of the Serra Norte (North Mountain), FLONA de Carajás, Parauapebas, state of Pará, northern Brazil (Fig. 10).

Ochyrocera ritxoo sp. nov.

http://zoobank.org/F161E5C9-B893-46D7-B724-737B01AF5705
Figs 7–10

Type material. ***Holotype*** male from Cave S11C_0201 (6°22'01"S, 50°23'07"W), FLONA de Carajás, Canaã dos Carajás, Pará, Brazil, 27/VII/2015, BioEspeleo Consultoria Ambiental col. (IBSP 193194). ***Paratype*** female from Cave S11C_0052 (6°23'56"S, 50°22'46"W), FLONA de Carajás, Canaã dos Carajás, Pará, Brazil, 09/III/2016, BioEspeleo Consultoria Ambiental col. (IBSP 193196),

Other material examined. Brazil. Pará: Canaã dos Carajás, FLONA de Carajás, Cave S11C_0194 (6°24'20"S, 50°23'34"W), 12/III/2016, 1♂ (IBSP 193078); Cave S11C_0046 (6°24'02"S, 50°22'43"W), 19/IV/2016, 1♀ imm. (IBSP 193083), all collected by BioEspeleo Consultoria Ambiental; Cave S11D_0064 (710) (6°23'31"S, 50°18'48"W), 13–30/I/2010, R. Andrade & I. Cizauskas et al. col., 1♂ 1♀ 3 imm. (IBSP 174071); 10–19/V/2011, D. Bebiano col., 1♀ (IBSP 196512); Cave S11D_0064 (710) (6°23'31"S, 50°18'48"W), 13–30/I/2010, 1♀ (IBSP 196513); 01–14/VII/2010, R. Andrade & I. Cizauskas et al. col., 2♀ (IBSP 196514); 2♂ (IBSP 196515; SEM);

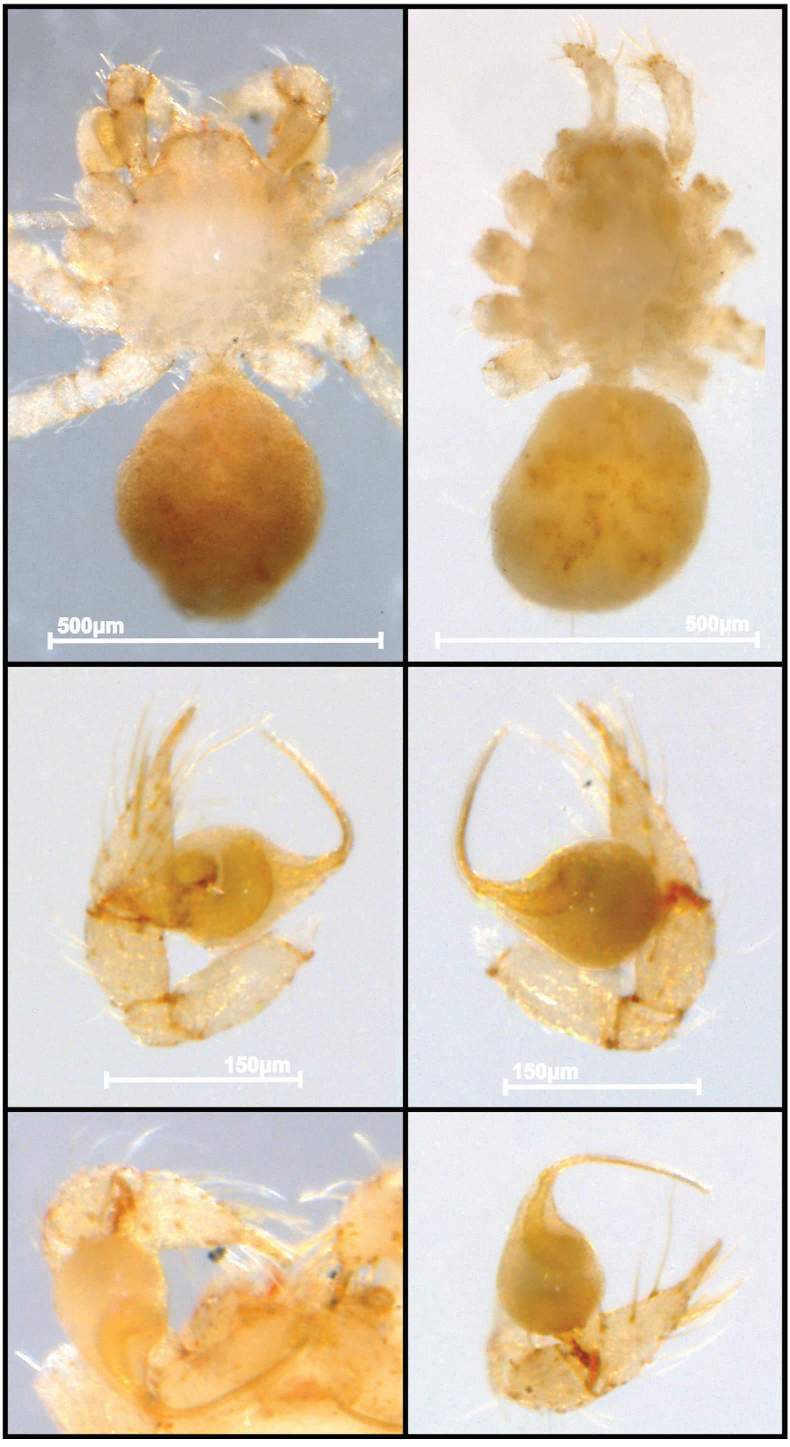

Figure 7. *Ochyrocera ritxoo* sp. nov., male IBSP 193194 (**A, C–F**), female IBSP 193196 (**B**) **A, B** habitus, dorsal view **C** left male palp, retrolateral view **D** same, prolateral view **E** right male palp, dorsal view **F** same, retro-ventral view. Abbreviations: C = cymbium, CE = cymbial extension, E = embolus, T = tegulum.

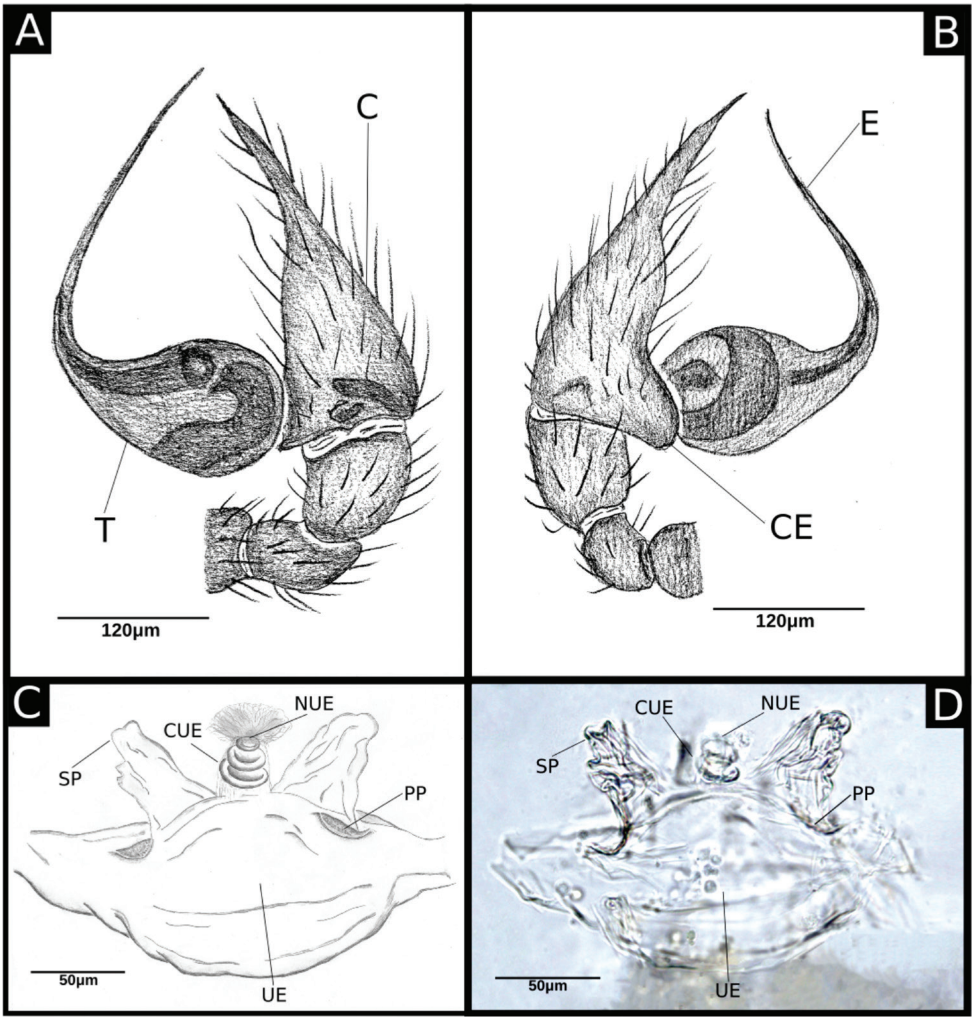

Figure 8. *Ochyrocera ritxoo* sp. nov. (**A, B**) **A** left male palp IBSP 193194, retrolateral view **B** same, prolateral view (**C, D**) **C** female genitalia IBSP 1741071, enzyme cleared, dorsal view **D** same, dorsal view. Abbreviations: C = cymbium, CE = cymbial extension, CUE = columnar uterus externus, E = embolus, NUE = neck of uterus externus, PP = pore-plate, SP = spermathecae, T = tegulum, UE = uterus externus.

Cave S11D_0096 (742) (6°23'37"S, 50°19'27"W), 13–30/I/2010, 1♂ (IBSP 196481); Cave S11D_0064 (710) (6°23'31"S, 50°18'48"W), 13–30/I/2010, 1♀ (IBSP 196482); Cave S11D_0064 (710) (6°23'31"S, 50°18'48"W), 1–14/VII/2010, 1♂ 1♀ (IBSP 196483) all collected by R. Andrade & I. Cizauskas et al.; Cave S11B_078 (6°21'33"S, 50°23'54"W), 28/IX/2018, Ativo Ambiental col. 1♂ (IBSP 260308).

Diagnosis. *Ochyrocera ritxoo* sp. nov. is distinguished from *O. ritxoco* sp. nov. by having the embolus as long as the bulb of the male palp (Figs 7C–F, 8A, B) while *O. ritxoco* sp. nov. have an elongated embolus, which is two times longer than the bulb in the male palp (Fig. 1F), and by a short and striped distal area of the spermathecae and a shorter columnar uterus externus with approximately 3–4 internal chambers in

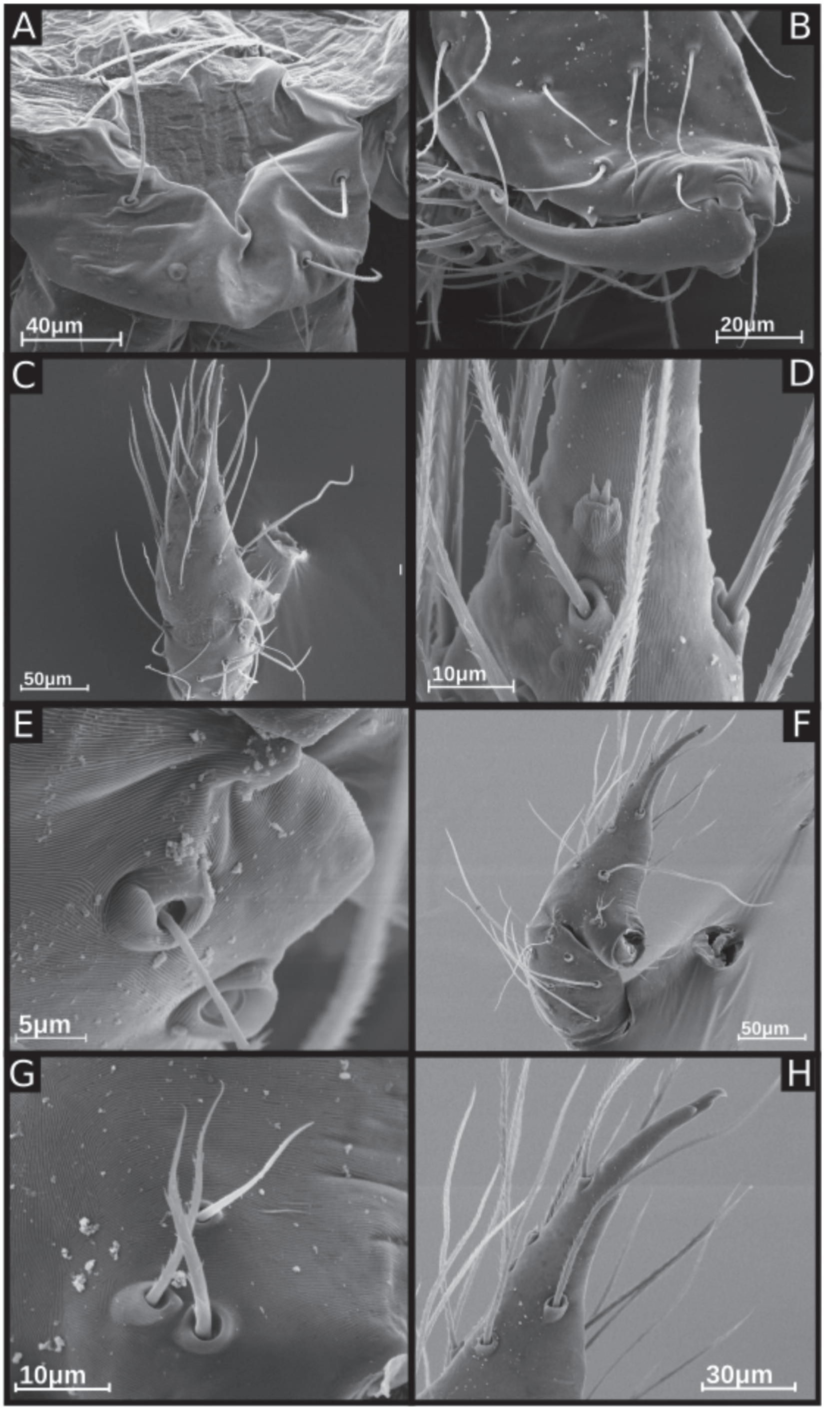

Figure 9. SEM images of *Ochyrocera ritxoo* sp. nov., male IBSP 196515 (**A–H**) **A** carapace, dorsal view **B** chelicerae, frontal view **C** cymbium, dorsal view **D** same, tarsal organ, detail **E** tibia of palp, trichobothria, apical dorsal view **F** cymbium, prolateral view **G** same, basal macrosetae, retrolateral view **H** same, cuspule, prolateral view.

the female genitalia (Fig. 8C, D) while the other species have a long and globose distal area in the spermathecae and an elongated columnar uterus externus with approximately eight internal chambers (Fig. 2C, D).

Description. Male (IBSP 193194) Total length 0.90. Carapace length 0.40, ovoid, narrowing gradually anteriorly, cream-colored and bright, pars cephalic flat, fovea absent (Fig. 7A). Clypeus with two pairs of long bristles (Fig. 9A). Eyes absent. Chelicerae light yellow, promargin with three teeth attached to a very long lamina (Fig. 9B); retromargin without teeth. Sternum cream-colored. Endites and labium as for *O. ritxoco* sp. nov.. Legs cream-colored, formula 1423, total length I 5.6, II 5.1, III 4.2, IV 5.4. Male palp with palpal femur length 0.03, palpal tibia enlarged, shorter than cymbium, with two long dorsal trichobothria (Fig. 8E), cymbium enlarged basally, slightly curved distally, bearing short apical cuspule; paired long setae on non-projected bases retrolaterally, elongated tarsal organ as in *O. ritxoco* sp. nov., basal setae on the rounded cymbial prolateral extension (Fig. 9F–H), bulb oval, embolus flattened, as long as cymbium (Fig. 7C–F, 8A, B). Abdomen length 0.6, oval, uniformly gray. Six epiandrous spigots with a short base.

Female. (Paratype IBSP 193196). Total length 1.0. Carapace length 0.35, as in male (Fig. 7B). Pedipalp without claw, with conical tip and subdistal trichobothrium. Clypeus, eyes, chelicerae, sternum, endites, and labium as in male. Legs as in male, formula 4123, total length I 5.3, II 4.9, III 4, IV 5.4. Abdomen length 0.65. Colulus triangular with six long bristles. Internal genitalia with enlarged spermathecae under the small pore-plate; medial columnar uterus externus short, internally with few visible chambers. Uterus externus ending in a narrow neck. Oval pore-plates on spermathecae with approximately 10–20 glandular ducts (Fig. 8C, D).

Etymology. The specific name Ritxòò also means “ceramic dolls” but in the male language of the Karajá people, an indigenous population of the region. The making of these dolls, however, is an exclusive activity of women (Silva 2015).

Natural history. *Ochyrocera ritxoo* sp. nov. is a small troglobitic spider that is exclusive to caves in the Carajás karst region. Specimens were collected only in aphotic zones of caves. The observed sex ratio for the species was 1.4F:1M (*N* = 17). *Ochyrocera ritxoo* sp. nov. was generally found in large cavities with horizontal projections varying from 26 to 245 meters (*N* = 7, mean = 102 m). These caves have one to three entrances and are located in all compartments of the Serra Sul landscape (top, high, medium and low slopes). All caves have aphotic zones and other troglobitic species were found in most caves, with the richness of troglobitic species per cave varying between one and six (average of four). The following taxa were found: spiders – Gnaphosidae (*Paracymbiomma carajas* Rodrigues, Cizauskas & Rheims, 2018), Caponiidae (*Carajas paraua* Brescovit & Sánchez-Ruiz, 2016) and Tetrablemmidae (*Matta* sp.); tailless whip scorpions – Charinidae (*Charinus ferreus* Giupponi & Miranda, 2016); pseudoscorpions, Chthoniidae; diplopods – Glomeridesmidae (*Glomeridesmus* sp.), Pyrgodesmidae, Pseudonannolenidae (*Pseudonannolene* spp.); springtails – Sminthuridae, Paronellidae; and beetles – Staphylinidae (Pselaphinae).

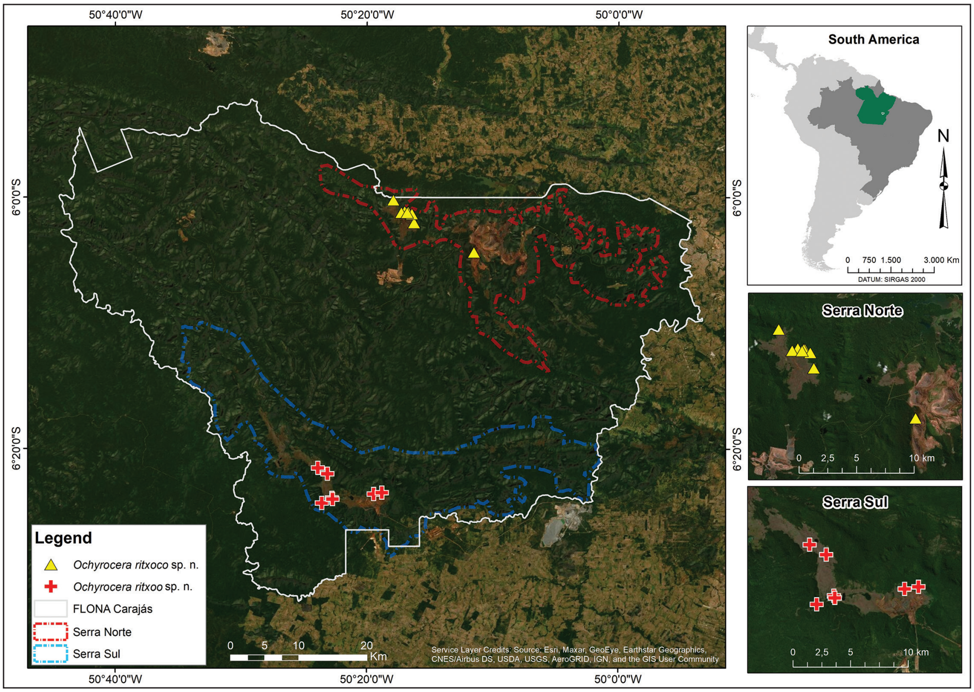

Figure 10. Distribution map of *Ochyrocera ritxoco* sp. nov., yellow triangles, and *Ochyrocera ritxoo* sp. nov., red plus signs, in FLONA de Carajás, Pará, Brazil.

Distribution. Known exclusively from caves in a range of approximately 10 km of the Serra Sul (South Mountain), FLONA de Carajás, Canaã dos Carajás, state of Pará, northern Brazil (Fig. 10).

Discussion

The fauna of subterranean spiders of the family Ochyroceratidae located in caves in Brazil is represented mainly by specimens of the genera *Ochyrocera* Simon, 1892, *Speocera* Berland, 1914, and *Theotima* Simon, 1893. The first two genera have troglomorphic spiders among their representatives and are a significant part of the yet unknown diversity of subterranean spiders in these environments (Baptista 2003). The genus *Ochyrocera* stands out for its abundance and diversity of species in ferruginous ecosystems, such as the Carajás system of the present study, with species colonizing the edaphic zone to the deep cave environment (Brescovit et al. 2018).

Both *Ochyrocera ritxoco* sp. nov. and *O. ritxoo* sp. nov. are troglobitic spiders that are restricted to iron formation caves in FLONA de Carajás. The description of these spiders expands the number of the endemic subterranean species (troglobites) and, together with *Carajas paraua* Brescovit & Sánchez-Ruiz, 2016 (Caponiidae) and *Paracymbiomma caecus* and *P. bocaina* (Gnaphosidae; Rodrigues et al. 2018), is evidence of a diversified subterranean araneofauna in the Carajás ferruginous system which must be considered in projects aimed at conservation and sustainable use of its natural resources.

Acknowledgements

We would like to thank to Beatriz Mauricio, microscope technician from Centro de Microscopia Eletrônica at Instituto Butantan, and Alexandre B. Bonaldo, from MPEG, for the SEM images. The authors are very grateful to the editor Abel Pérez González, and the reviewers Nadine Dupérré and Shuqiang Li for their careful reading of the manuscript. This work was supported by Vale S.A., Organização de Apoio à Pesquisa da Biodiversidade (OAPBio) and CNPq (ADB grant PQ 303903/2019-8).

References

Baert L (2014) Ochyroceratidae (Araneae) of Ecuador. Bulletin de la Société Royale Belge d'Entomologie 150: 70–82.

Baptista RLC (2003) *Speocera eleonorae* sp. nov., the first troglomorphic spider from Brazilian caves (Araneae: Ochyroceratidae). Revista Ibérica de Aracnología 7: 221–224.

Brescovit AD, Cizauskas I, Mota LP (2018) Seven new species of the spider genus *Ochyrocera* from caves in Floresta Nacional de Carajás, PA, Brazil (Araneae, Ochyroceratidae). ZooKeys 726: 87–130. https://doi.org/10.3897/zookeys.726.19778

Campos JF, Castilho A (2012) Uma Visão Geográfica da Região da Flona de Carajás. In: Martins FD, Castilho AF, Campos JF, Hatano FM, Rolim SG (Eds) Floresta Nacional de Carajás: Estudos sobre vertebrados terrestres. Nitro Imagens, São Paulo, 28–63.

Carmo FF, Jacobi CM (2013) A vegetação de canga no Quadrilátero Ferrífero, Minas Gerais: caracterização e contexto fitogeográfico. Rodriguésia 64: 527–541. https://doi.org/10.1590/S2175-78602013000300005

Deeleman-Reinhold CL (1995) The Ochyroceratidae of the Indo-Pacific region (Araneae). Raffles Bulletin of Zoology, Supplement 2: 1–103.

Jocqué R, Dippenaar-Schoeman AS (2006) Spider families of the world. Musée Royal de l'Afrique Central Tervuren, 336 pp.

Gertsch WJ (1973) A report on cave spiders from Mexico and Central America. Association for Mexican Cave Studies Bulletin 5: 141–163.

Gertsch WJ (1977) Report on cavernicole and epigean spiders from the Yucatan peninsula. Association for Mexican Cave Studies Bulletin 6: 103–131.

Martins FD, Esteves E, Reis ML, Costa FG (2012) Ações para Conservação. In: Martins FD, Castilho AF, Campos JF, Hatano FM, Rolim S (Eds) Floresta Nacional de Carajás: Estudos sobre vertebrados terrestres. Nitro Imagens, São Paulo, 198–229.

Ribera C (1978) Resultados faunisticos de diversas campañas realizadas en America Latina I: Una nueva especie cavernícola del norte de Perú: *Ochyrocera peruana* (Araneae: Ochyroceratidae). Speleon 24: 23–29.

Rolim SG, Couto HTZ, Jesus RM, França JT (2006) Modelos volumétricos para a Floresta Nacional do Tapirapé-Aquirí, Serra dos Carajás (PA). Acta Amazonica 36(1): 107–114. https://doi.org/10.1590/S0044-59672006000100013

Silva TC (2015) Ritxoko. Goiânia, Editora Cânone, 224 pp.

World Spider Catalog (2020) World Spider Catalog. Natural History Museum Bern. http://wsc.nmbe.ch [Version 21.5., accessed on 28 Nov 2020]

Wunderlich J (2008) The dominance of ancient spider families of the Araneae: Haplogynae in the Cretaceous, and the late diversification of the advanced ecribellate spiders of the Entelegynae after the Cretaceous-Tertiary boundary extinction events, with descriptions of new families. Beiträge zur Araneologie 5: 524–674.

ZooKeys 1031: 161–182 (2021)
doi: 10.3897/zookeys.1031.57836
https://zookeys.pensoft.net

RESEARCH ARTICLE

A peer-reviewed open-access journal
ZooKeys
Launched to accelerate biodiversity research

The resin bee subgenus *Ranthidiellum* in Thailand (Megachilidae, Anthidiini): nesting biology, cleptoparasitism by *Stelis*, and new species

Pakorn Nalinrachatakan[1], Prapun Traiyasut[2], Anupong Khongnak[2], Manop Muangkam[2], John S. Ascher[3], Natapot Warrit[1]

1 *Center of Excellence in Entomology and Department of Biology, Faculty of Science, Chulalongkorn University, Bangkok 10330, Thailand* **2** *Program in Biology, Faculty of Science, Ubon Ratchathani Rajabhat University, Ubon Ratchathani 34000, Thailand* **3** *Insect Diversity Lab, Department of Biological Sciences, National University of Singapore, 16 Science Drive 4 S3 Level 4, 117558, Singapore*

Corresponding author: Natapot Warrit (natapot.w@chula.ac.th)

Academic editor: M.S. Engel | Received 20 August 2020 | Accepted 22 February 2021 | Published 15 April 2021

http://zoobank.org/3D65C317-2F46-42ED-AE17-B9D48B30E8DA

Citation: Nalinrachatakan P, Traiyasut P, Khongnak A, Muangkam M, Ascher JS, Warrit N (2021) The resin bee subgenus *Ranthidiellum* in Thailand (Megachilidae, Anthidiini): nesting biology, cleptoparasitism by *Stelis*, and new species. ZooKeys 1031: 161–182. https://doi.org/10.3897/zookeys.1031.57836

Abstract

Resin bees of the subgenus *Ranthidiellum*, are rare and endemic to Southeast Asia. These bees are known to construct resinous entrance tubes to their nests. Here, the new species *Anthidiellum* (*R.*) *phuchongensis* **sp. nov.** is described along with a description of its nest collected from Phu Chong Na Yoy National Park, Ubon Ratchathani Province, Thailand. In addition, the bee cleptoparasite, *Stelis* (*Malanthidium*) *flavofuscinular* **sp. nov.,** and the male of *A.* (*R.*) *ignotum* Engel, 2009, are described for the first time. A key to *Ranthidiellum* species is also provided.

Keywords

Anthidiellum, *Malanthidium*, pollinator, systematics, taxonomy, wool carder bee

Introduction

Bees in genus *Anthidiellum* Cockerell, 1904 subgenus *Ranthidiellum* Pasteels, 1969 are rare, enigmatic, and restricted to Southeast Asia with only four reported species (Engel 2009; Ascher and Pickering 2020): *A.* (*R.*) *apicepilosum* (Dover, 1929), *A.* (*R.*) *meliponiforme* (Cockerell, 1919), *A.* (*R.*) *rufomaculatum* (Cameron, 1902), and the most recent *A.* (*R.*) *ignotum* Engel, 2009. *Ranthidiellum* bees are robust, of a moderate size with a reddish or fulvous infused integument, and possess an arcuate subantennal suture. Females of *Ranthidiellum* are equipped with an apically broad mandible (> 1.5× the base width), whereas an apical comb on S5 and median spine on T7 can be found in males (Pasteels 1969, 1972; Michener 2007). *Ranthidiellum* morphology was hypothesized to mimic its sympatric stingless bees (Cockerell 1919; Soh et al. 2016) and is clearly distinct from its most common sympatric congeners, such as *A.* (*Pycnanthidium*) *smithii* (Ritsema, 1874), which is a small bee with an overall black body and yellow maculation. Engel (2009) recently provided a provisional key to female *Ranthidiellum* species.

As *Ranthidiellum* species are rarely collected, they were not included in the recent phylogenetic studies of the Tribe Anthidiini (Combey et al. 2010; Gonzalez et al. 2012; Litman et al. 2016). Thus, insight into their evolution, together with their morphology, life history, and behavior are poorly understood. Pagden (1934) discovered the only known nests of *A.* (*R.*) *apicepilosum* in Bukit Kutu, Malaysia, which were burrowed in abandoned mud wasp nests using resins. Pasteels (1972) later provided supplementary details for this finding.

During a field collecting trip in October 2018 at Phu Chong Na Yoy National Park (PCNYNP), Ubon Ratchathani Province, Thailand, we discovered a small congregation of *Ranthidiellum* nests on a vertical earth bank. The nests were then excavated and brought back to the laboratory at the Ubon Ratchathani Rajabhat University, and reared until adult bees emerged. Here, we describe a new *Ranthidiellum* species discovered at PCNYNP, and also describe the cleptoparasitic bees that emerged from the host cells in the nest. Since the new *Ranthidiellum* described is morphologically similar to *A.* (*R.*) *ignotum* Engel, 2009, we examined additional *Ranthidiellum* material to facilitate comparison between the two, and a description of the male *A.* (*R.*) *ignotum* for the first time.

Material and methods

Ranthidiellum nests were discovered on a sandy earth bank on a walking trail leading to Kaeng Ka Lao Stream (Figs 1 and 8) [14°26'10.98"N, 105°16'37.05"E, alt. 322 m], PCNYNP, Ubon Ratchathani Province in October 2018 (we revisited the site again in December 2018 and 2019). Adjacent the Kaeng Ka Lao Stream is a secondary dipterocarp forest. All eight active nests (seven from 2018 and one from 2019) were carefully excavated from the earth bank using brushes and small hand shovels. A couple of abandoned nests were also found in the adjacent area. The collected nests were wrapped in

Figure 1. Study site at Kaeng Ka Lao Stream, PCNYNP, Ubon Ratchathani Province (Thailand), with the map produced using QGIS (3.16.0).

cotton wool, clumped paper, and saran ('cling') wrap before being put in a field box and transported back to the laboratory for examination.

Dissection of the seven nests collected from 2018 revealed a total of 18 individuals (six larvae, nine pupae, and three quiescent adults). Eight adult bees were collected: 2♀ from outside of the nesting area and 6 (3♀, 3♂) from the reared nest (see below), and were deposited at the Chulalongkorn University Natural History Museum (**CUNHM**) for morphological examination. Seven additional specimens of *Anthidiellum* (*Ranthidiellum*) *ignotum* Engel, 2009 (6♀, 1♂) deposited at **CUNHM** and the Department of Entomology and Plant Pathology, Chiang Mai University, Thailand (**CMU**), were also examined and compared with the collected individuals.

A single nest from 2019 was maintained in a plastic box under room temperature and relative humidity (22–25 °C, 70–90%) at Ubon Ratchathani Rajabhat University. Water spray was used to keep the humidity inside the box relatively constant. The first bee emerged after day 47. The time of eclosion of each remaining bee was recorded.

Ranthidiellum specimens were examined under light microscopy (Zeiss Stemi 508 stereomicroscope). Photographs were taken using a Canon 7D Mark II digital camera control via Canon EOS Utility software, attached to the stereomicroscope. All photographs were post-processed using Adobe Photoshop CC 2018 and Adobe Lightroom CC 2018 software. All terminology and abbreviations used follow Engel (2009), Kasparek (2015), Michener (2007), Michener and Griswold (1994), and Michener et al. (1994). Male specimens were dissected to reveal the genitalic structures using a protocol modified from Gonzalez et al. (2012). To clear most of the artifacts, we altered the process by immersing the genitalia in 3M KOH at room temperature (24 °C) for 20 h, or heating in hot water until ready to be dissected.

Photos or images of type specimens of *A.* (*R.*) *apicepilosum* Dover, 1929 (NHML 014026685), *A.* (*R.*) *meliponiforme* (Cockerell, 1919) (NHML 014026114), and *A.* (*R.*) *rufomaculatum* (Cameron, 1902) (NHML 014026141) at the Natural History Museum, London, UK (**NHMUK**), were examined through the "Apoidea (Bee) Type Digitization Project" digital platform from https://data.nhm.ac.uk/, and the images are provided by Mr. Chawatat Thanoosing and Ms. Natalie Dale-Skey (**NHMUK**).

Systematics

Genus *Anthidiellum* Cockerell, 1904

Subgenus *Ranthidiellum* Pasteels, 1969

Anthidiellum (*Ranthidiellum*) Pasteels, 1969: 48. Type species: *Protoanthidium rufomaculatum* Cameron, 1902, by original designation. [other aspects of type designation discussed in Michener and Griswold (1994)]

Anthidiellum (*Rhanthidiellum*) Pasteels, 1972: 102, unjustified emendation of *Ranthidiellum* Pasteels, 1969.

Diagnosis. Moderate size (around 7–10 mm); clypeus subtriangular as frontoclypeal suture curved upwards; subantennal suture arcuate; eyes convergent ventrally; preoccipital margin round, not carinate; pronotal lobe raised, extended, and lamellated; omaular carina complete to the ventral region of thorax; scutellum and axilla large, margin translucent; propodeum without dimple; abdomen appears oval, shiny with reddish, orangish, or ferruginous extended.

***Female*:** mandible apically broad, about 1.5× wider than base, with four small teeth; hind basitarsus enlarged; abdomen oval shaped, longer than wide, gradually smaller from third segment; T6 margin subtruncate, shield-like; S6 simple.

***Male*:** mandible tridentate, apex not wide as in female; T6 with apical transverse border; T7 short with median spine; S4 marginally with transparent membrane; S5 indented with black comb; gonoforceps bifid.

***Anthidiellum* (*Ranthidiellum*) *ignotum* Engel, 2009**

Figs 2, 4 (right), 5 (right)

Anthidiellum ignotum Engel, 2009: 30–34. (♀, holotype)
Anthidiellum ignotum Engel: Soh et al. 2016, 55. (♀)

Material examined 7 (6♀, 1♂). Thailand: Chiang Mai (new record), 2♀, 1♂, Chiang Dao, Pha Dang National Park, Srisuwan Waterfall, Suan Dok Mai (19°37'49.88"N, 98°57'12.40"E, alt. 527.96 m), 19 Dec. 2018, N. Warrit et al. (CUNHM: BSRU-AA-6708, 6709). 1♀, Mae Chaem District, Highway 1088, 9 Dec. 2016, N. Warrit

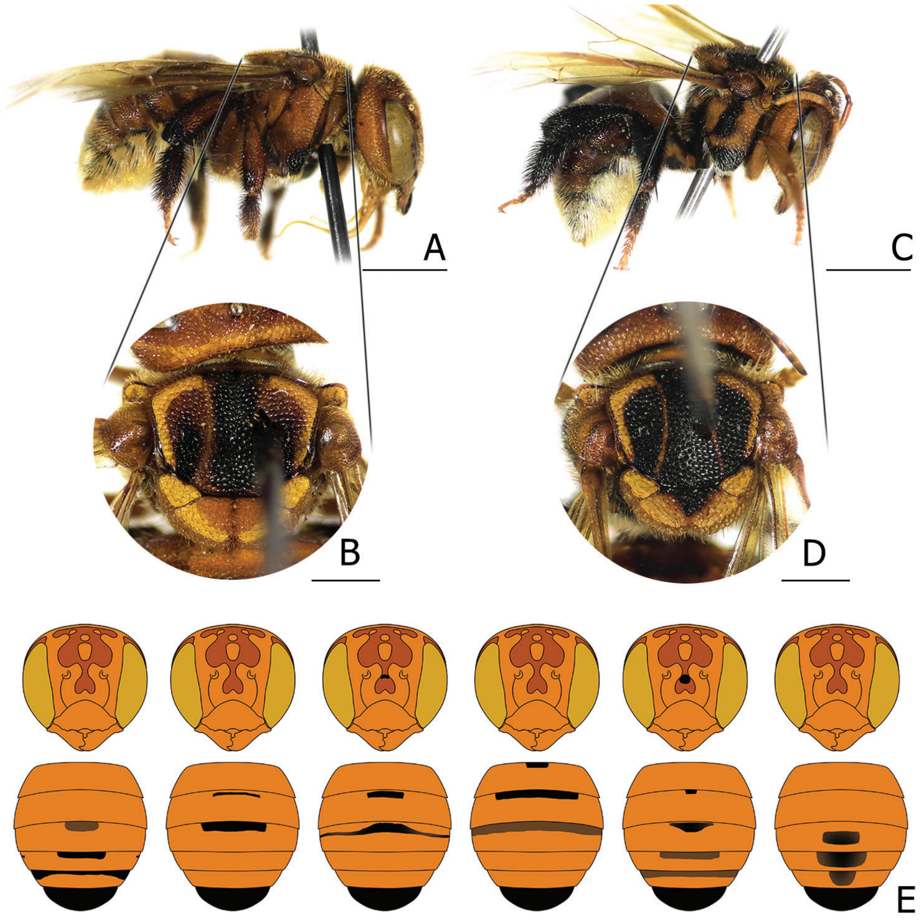

Figure 2. Female *Anthidiellum ignotum* Engel, 2009 **A, B** lateral habitus and mesosoma of the "less melanized" individual (BSRU-AA-1250) **C, D** lateral habitus and mesosoma of an individual with a black scutellum mark (BSRU-AA-6709) **E** female faces and metasoma, showing variations of black infused stigma. From left to right: BSRU-AA-2668, 1250, 1249, 6708, 6709, and CMU-0013. Scale bars: 2 mm (**A, B**) or 1 mm (**C, D**).

et al. (CUNHM: BSRU-AA-2668). 1♀, Samoeng, 13 Dec. 1992, Wichai [initially identified as "Apidae" by Wichit] (CMU-0013); 2♀, Phayao, Mueang, Maeka, Phayao University, 1 Jun. 2012, W. Suwannarak et al. [CUNHM: BSRU-AA-1249, 1250, same specimens in Soh et al. (2016)].

Distribution. Thailand [Chiang Mai (Chiang Dao, Mae Chaem, and Samoeng Districts) and Phayao (Maeka District) Provinces; Nakhon Ratchasima Province, Sakaerat Environment Research Area (type locality from Engel (2009))].

Diagnosis. This species can be distinguished from other *Ranthidiellum* by its remarkably bright ferruginous color, mostly without a black integument on their faces; tergites red-brown on marginal zone; T5 and T6 covered with pale-golden short tomentum; leg with reddish integument on coxa and femur of midleg and hindleg (see Engel 2009). Male with more extensive black maculation, especially on scutum and metasoma, whereas overall brighter than in female, predominantly on scutum; S4 gradulus incomplete (Fig. 5D); gonoforceps bifid, with extended medio-lateral carina with acute sharp edge.

Description. ♂: ***Structure*:** Length 7.8 mm, head width 3.2 mm, intertegulae distance 2.2 mm, wingspan 15.2 mm.

***Head*.** Overall prosomal coloration somewhat lighter than in female. Head lightly orange to yellow, gradually increasing in brightness ventrally, sparsely covered with bright yellow hairs. Maculation as in female but with dark contrast (Fig. 4H): inverted heart-shaped mark on paraocular area making median Y-shape bridge connecting two large ovoid marks above antennal socket, extending upwards, concatenated at ocellar triangle, and forming a transverse band on vertex. Eye margin with narrow black mark on dorsal margin to about half of outer orbital margin. Clypeus bright yellow. Mandible yellow, shiny, apex not as broad as in females. Outer ridge conspicuous making upper area shallowly depressed. Teeth black, tridentate with large acute tooth at apex. Labrum dark yellowish, without conspicuous large hairs on surface as in female. Scape orange to yellow. Pedicel brown. Antennal flagellum orange brown on 1st and basal half of 2nd segments, other flagellomere pale light brown with pits on front and shiny yellow surface without pits posteriorly.

***Mesosoma*.** Scutum largely black, with yellow inverted L-shaped band on antero-lateral margin extending to fine paramedial line and abutting posterior margin, slightly curved medially. Scutellum and axilla yellow, median with black inverted triangular shape. Tegula dark yellow, somewhat translucent. Pronotal lobe pale yellow, strongly carinate to lamellate. Metanotum yellowish, laterally black. Propodeum black with small orange spot anteriorly around propodeal spiracle. Anterior surface of mesepisternum black, lateral surface yellow-orange with extensive black marks dorsally and in area adhering to metepisternum. Metepisternum yellow-orange, black on anterior and dorsal margin. Overall mesosoma covered with bright yellow hairs, except for pale white hairs on lower part of mesepisternum.

***Wings*.** Forewing basally infuscated as in female, but with obvious hyaline patch covering parts of radial cell, 1st medial cell, and parts of 1st submarginal cell. Also, largely subhyaline on the marginal, submarginal, and 2nd medial cells.

***Legs*.** Foreleg yellow-orange, with black mark on upper part of coxa, and small basal mark on both anterior and posterior surfaces of trochanter and femur. Midleg and hindleg largely black with some obscure red-brown infused, except for dark yellow on middle coxa, posterior area on hind coxa dark brown, apical area of middle trochanter, especially on posterior surface, yellow-brown, upper and lower parts of middle femur with obscure yellow-brown band, and middle tibia with outer brown-yellowish band. Middle and hind tarsi dark brown to black but gradually lighter towards end. Claw dark yellowish to brown, black on both apical and subapical tooth. Arolia present, hair bright yellow on foreleg, the rest overall black but white on dorsal part of coxa, femur, and trochanter of midleg and hindleg. Tarsal hair generally dark brown, gradually becoming bright yellow at the end.

Metasoma. Yellow-orange with thin black band infused at basal terga. Apical margin subhyaline showing black area of the former. T1 black on frontal surface defined with carina, extended to upper lateral surface. T2–T5 with small lateral dots and black thin stripes on basal part. T6 apically curved inward, forming conspicuous apical border with black surfaces on back (Fig. 4F). T7 shield-like, black at margin, with median acute apex. Dorsal surfaces shiny and glabrous. Sternites overall yellow-orange except dark brown on S1. S4 (Fig. 5D) margin extended as transparent membrane, median of margin with two small black teeth. S5 widely emarginated in trapezoid shape, lined with 83 black round teeth on its black apical margin (Fig. 5F). S6 lined with black border slightly curved along basal margin, apical with broadly rounded projection. S7 thin, with laterally rounded angle. S8 inverted Y-shape (Fig. 5L). Genitalia (Fig. 5N) broad. Gonoforceps bifid with dorsal medio-lateral carina pointing as acute sharp edge. Penis valve simple. Hair bright yellow to white, black hair lining on lateral area of T1–T3 and covering some basal area of T4, extending more to the median on T3 but not abutted together.

Floral association. Unknown.

Remarks. Since a description of male *A.* (*R.*) *ignotum* is given here for the first time, variations in their color pattern are discussed later in the paper (see below).

***Anthidiellum* (*Ranthidiellum*) *phuchongensis* Nalinrachatakan & Warrit, sp. nov.**

http://zoobank.org/D7E83FBD-A9BA-4DCC-AEEA-5436A2EE699B
Figs 3, 4 (left), 5 (left)

Type locality. THAILAND: Ubon Ratchathani, PCNYNP, Kaeng Ka Lao [14° 26'10.98"N 105° 16'37.05"E, alt. 322 m]

Material examined 6 (5♀, 1♂). ***Holotype*:** 1♂, emerged from a reared nest on 6th Jan. 2020, A. Khongnak & M. Muangkam, (CUNHM: BSRU-AB-0161). ***Paratypes*:** 3♀, from the same nest as holotype, emerged on 27th Dec. 2019 (CUNHM: BSRU-AB-0158), 29th Dec. 2019 (CUNHM: BSRU-AB-0159), and 30th Dec. 2019 (CUNHM: BSRU-AB-0160).

Other materials. 2♀, collected on 5th Jan. 2019 (CUNHM: BSRU-AA-6706) and 9th Feb. 2019 (CUNHM: BSRU-AA-6936), aerial net, P. Traiyasut et al.

Diagnosis. This new species resembles *Anthidiellum ignotum* Engel, 2009 in overall appearance, but differs by its dark orangish to reddish integument; facial marks restricted on the frons; black apical bands on all terga except T6, making T6 clearly orangish (Fig. 3D), whereas all other females of *Ranthidiellum* species come with black T6; black hairs on T2, T3, and lateral of T1 and T4; black hind coxa on the upper part with a small black patch around its lower part. Midleg and hindleg covered with black hairs on tibia and basal part of tarsi, making these legs superficially brownish; male S4 gradulus complete.

Description. Male holotype: Body length 8.1 mm, head width 3.3 mm, intertegular distance 2.3 mm, wingspan 19.7 mm.

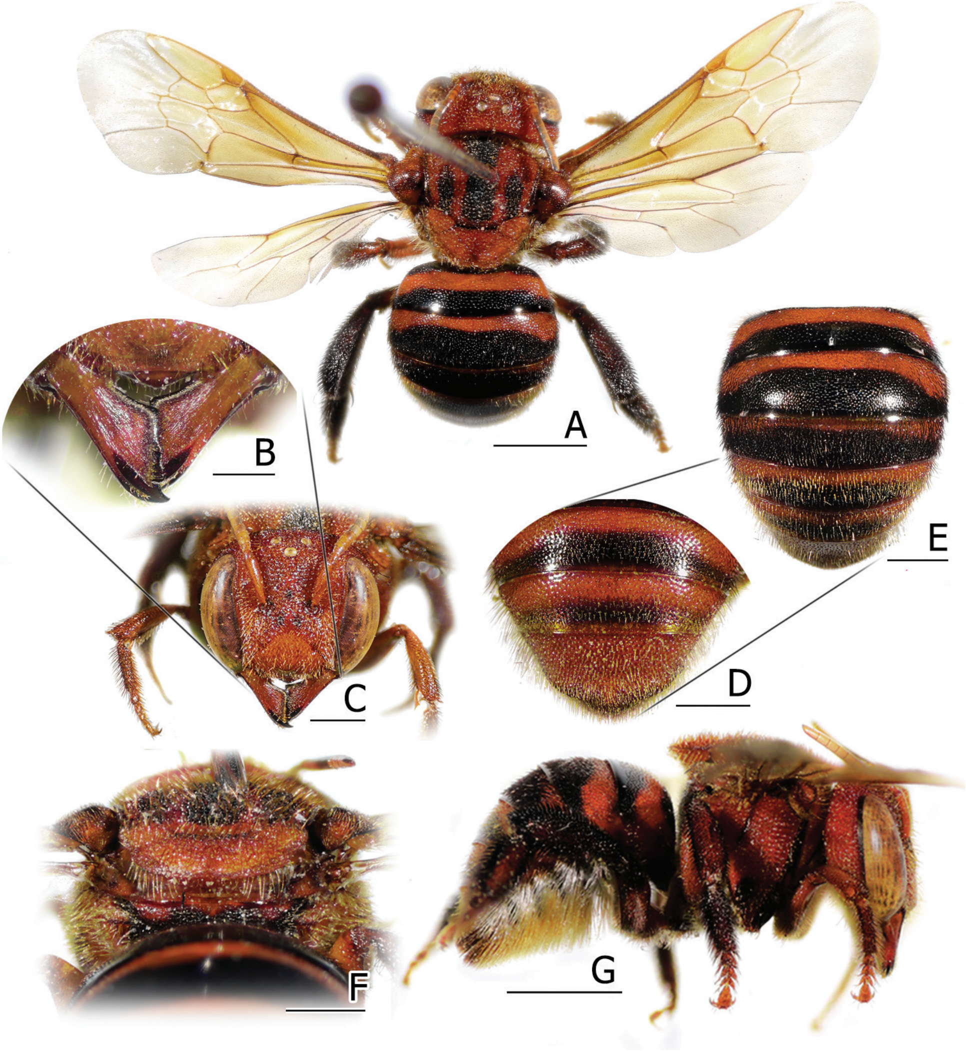

Figure 3. Female of *Anthidiellum phuchongensis* sp. nov. (BSRU-AA-6706) **A** dorsal habitus **B** mandible **C** face **D** metasomal apex **E** metasoma **F** propodeum **G** lateral habitus. Scale bars: 2 mm (**A, G**), 1 mm (**B, D–G**), or 0.5 mm (**C**).

Head. Orange to red-brown becoming brighter on clypeus and lower part of paraocular area; overall, sparsely covered with copperish-golden hair except black on preoccipital area and around ocelli triangle. Mandible orange, apically black. Maculation pattern showed as darker area, very obscured, similar to *A.* (*R.*) *ignotum*: mark on supraclypeal area [expressed as three marginal black dots, obscurely expressed in one dot while more extended for the rest (Fig. 4G)], mark along dorsal and posterior orbit, and noticeable large ovoid mark above antennal socket and stripe on ocellar triangle. Clypeus convex and depressed at apex. Clypeal punctures on lateral area coarse, becoming fine, dense, and irregular at median. Mandible apically black. Labrum yellow-orange, with conspicuous large hairs on apical surface. Scape orange to brownish. Pedicels brown. Antennal flagellum brown on 1st segment, orange on 2nd and 3rd segment; others pale, light brown with pits on front or shiny yellow-orange surface without pits on back.

Mesosoma. Covered with golden hairs. Pronotum orange, with black median stripe on anterior surface. Pronotal lobe orange, strongly carinate to lamellate. Scutum red-orange, with large black longitudinal median stripe, with two paramedial black stripes not reaching anterior and lateral margins. Scutellum yellow-orange, large, margin with median notch, median with orange area. Axilla yellow-orange. Tegula dark-brownish with anterior orange mark, somewhat translucent, with dark brown to black median mark on margin, dorsolaterally connected to inner circular mark. Metanotum orange. Propodeum extensively black except lateral orange area around propodeal spiracle. Mesepisternum anterior surface ventrally black, with orange area around lower part of inner margin. Lateral surface orange with dorsal black spots. Metepisternum without black mark except ventral stripe between midleg and hindleg.

Wings. Forewing subhyaline, basally infuscated. Second recurrent vein distally joining to 2nd submarginal crossvein.

Legs. Overall brown-orange, darker on inner surfaces of all tibia and tarsi of midlegs and hindlegs. Foreleg somewhat darker at basitarsus and nearby tarsi. Anterior surfaces of femur and tibia of foreleg yellow-orange, exposing shiny glabrous area. Black part infused on upper part of hind coxa and small lower mark. Hair copperish-gold with black intermix on foreleg, black on midlegs and hindlegs, becoming lighter on apical tarsi, copperish-white fringe on the ventral surfaces of coxa and trochanter. Claw yellow-orange, black on both apical and subapical teeth.

Metasoma. Orange with black apical band on T1–T5. T4–T5 black stripes dimmed. T6 rounded, overall orangish and lighter at apical border. T7 small, barely exposed, with acute median tooth. Hair bright gold except black on T2, T3 and lateral of T1 and T4. Sternites overall orangish, with white, dense, plumose pubescens laterally on S3–S5. S1 orangish with two lateral dark brown patches, median carina black. S2 with dark brown patches separated at median. S3 with a pair of minute dark brown patches. S4 gradulus complete, margin truncate, produced as thin transparent lobe, medially emarginated, middle of margin with three small black teeth. S5 margin black, with wide U-shaped emargination lined with a black comb of 92 blunt teeth. S6 margin produced as widely rounded lobe. S7 very narrow, with small rounded lateral lobe. S8 inverted Y-shape, basal margin strongly truncate. Apical lamina of gonoforceps enlarged, bilobed, outer lobe with prominent inner angular connected to dorsolateral carina (in *A.* (*R.*) *ignotum*, this angle is absent).

Female paratype (as in male except noted): Body length 8.2–9 (± 0.31) mm, head width 3.3–3.55 (± 0.05) mm, intertegular distance 2.5–2.8 (± 0.11) mm, wingspan 18.5–19.9 (± 0.58) mm.

Head. Overall, sparsely covered with copperish-gold hair. Maculation more distinct than in male, mark on supraclypeal area expressed as three marginal black dots in paratypes (Fig. 3C), fully black inverted heart-shape mark in BSRU-AA-6936. Mandible orange and slightly reddish at apex, extensive black margin on outer ridge. Apex conspicuously broader than base, teeth black, tridentate, with large acute tooth at apex.

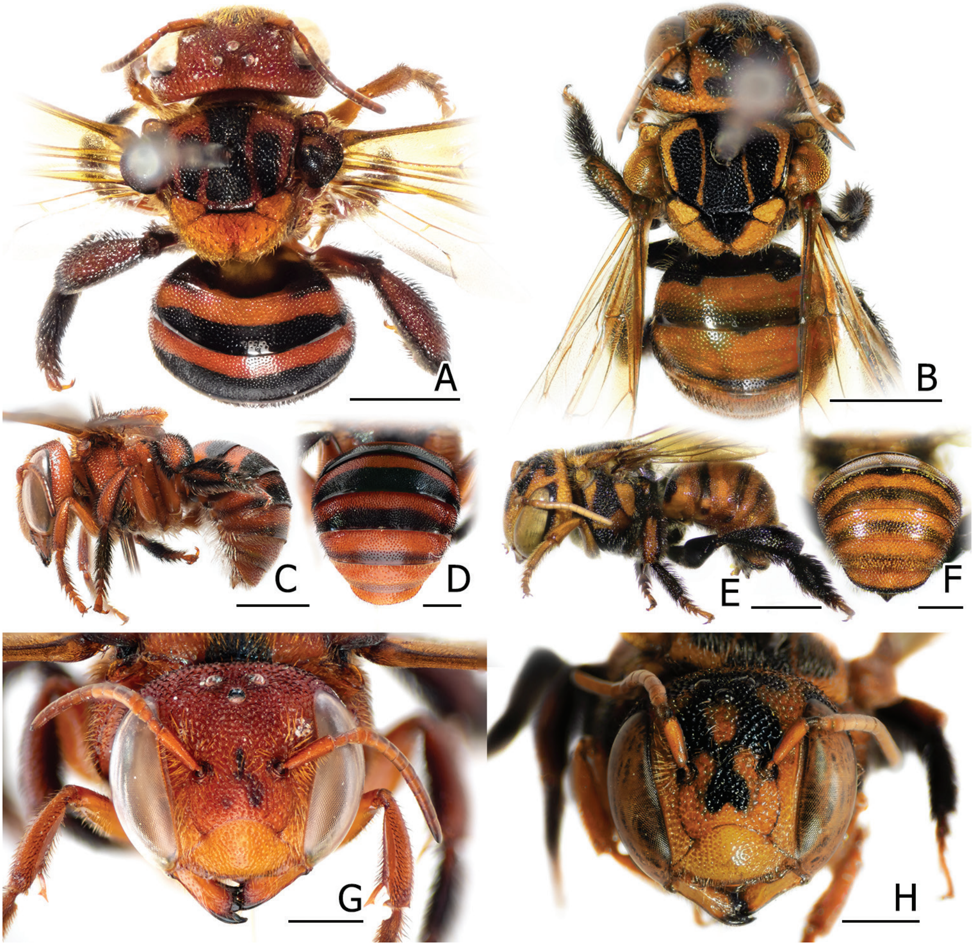

Figure 4. Males of *Anthidiellum phuchongensis* sp. nov. holotype (BSRU-AB-0161) (left) and *A. ignotum* Engel, 2009 (BSRU-AA-6707) (right) **A, B** dorsal habitus **C, E** lateral habitus **D, F** metasoma **G, H** face. Scale bars: 2 mm (**A, B, C, E**) or 1 mm (**D, F, G, H**).

Mesosoma. Covered with sparse copperish-gold hairs. Tegula brown-orange, with darker area at mesad. Mesepisternum black mark extended to dorsal half of anterior surfaces. Metepisternum orange with some black on anterior and posterodorsal margin.

Legs. Foreleg orangish, hair copperish-gold, becoming dark brown to black apically. Midleg and hindleg orange on coxa, femur, and trochanter. The rest of midleg, except apical of tarsi, darker to brown. Hindleg dark red-brown on apical of femur, tibia, and basitarsus. Hairs copperish-gold on coxa, trochanter and apical of tarsi, dark brown to black on the rest.

Metasoma. Orange with distinct black apical band on all terga, except T6. T6 obtuse. Sternite dark brown to black. Scopa yellow-gold, pale white laterally.

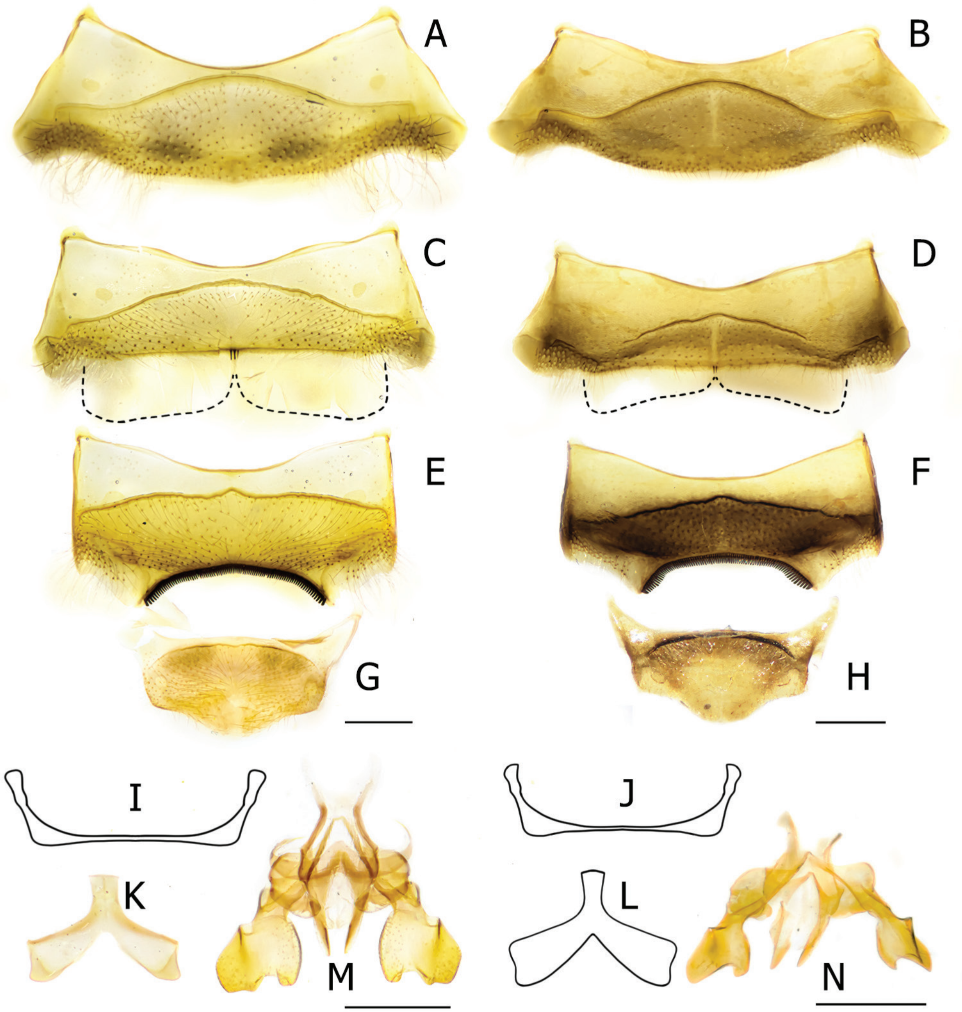

Figure 5. Genitalia and terminalia of male *Anthidiellum phuchongensis* sp. nov. holotype (BSRU-AB-0161) (left) and *A. ignotum* Engel, 2009 (BSRU-AA-6707) (right) **A, B** S3 **C, D** S4 **E, F** S5 **G, H** S6 **I, J** S7 **K, L** S8 **M, N** genitalia in dorsal habitus. Scale bars: 0.5 mm.

Etymology. The name is given to the PCNYNP, Ubon Ratchathani Province, where both the holotype and paratype were collected.

Floral association. Dipterocarpaceae. It is evident that *A. phuchongensis* utilized resins of *Dipterocarpus obtusifolius* Teijsm. ex Miq., a dominant plant in the area.

Bee kleptoparasites. *Stelis flavofuscinular* sp. nov. (see below).

Remarks. One *A.* (*R.*) *phuchongensis* female (BSRU-AA-6936) differs from the other paratypes in the black maculation, especially on the frons, which appeared as an inverted heart-shape, and the overall coloration was superficially darker than the other paratypes. These black extension markings are somewhat similar in female *A.* (*R.*) *ignotum* (see Fig. 2).

Genus *Stelis* Panzer, 1806

Subgenus *Malanthidium* Pasteels, 1969

Malanthidium Pasteels, 1969: 26. Type species: *Anthidium malaccense* Friese, 1914, by original designation.

Remarks. *Malanthidium* has an elongated body form, resembling most *Euaspis* species, and is of moderate size (8–11 mm). Only males are known. Straight subantennal suture; mandible tridentate; preoccipital margin rounded; omaulus carinated but not reaching ventral rim; distinct postero-lateral hook on axilla; scutellum large, rounded, and protruding posteriorly to overhang propodeum; wing dark brown to black; 2nd recurrent vein enters distal to 2nd submarginal crossvein; T6 margin with conspicuous border; S1 premarginal carina strong; S7 ventral surface smooth, margin with small median tooth.

Stelis (*Malanthidium*) *flavofuscinular* Nalinrachatakan & Warrit, sp. nov.

http://zoobank.org/AA054F28-B55D-4228-AF1A-652E032F763F
Figs 6, 7

Type locality. Thailand: Ubon Ratchathani, PCNYNP, Kaeng Ka Lao [14°26'10.98"N, 105°16'37.05"E, alt. 322 m]

Material examined 2 (2♂). ***Holotype*:** 1♂, emerged from a reared nest on the 25th Dec. 2019, A. Khongnak & M. Muangkam coll. (CUNHM: BSRU-AB-0157). ***Paratype*:** 1♂, same as in holotype, emerged on 23rd Dec. 2019 (CUNHM: BSRU-AB-0156).

Diagnosis. With only males known, *Stelis flavofuscinular* is distinct from its only known congener, *S. malaccensis* from Malaysia, as follows: head overall black, with yellow paraocular mark reaching close to the top of eyes, and narrow mark restricted close to apical area of clypeus; antennal scape black; Mesosoma overall black except yellow on postero-lateral hook of axilla; T1–T5 with large yellow strike band, with little median disruption that is pronounced more on rear metasomal segments; T6 with lateral yellow dots; S2–S4 with distinct median patch of long white hairs, while lacking black midapical comb. S4 and genitalia as in Fig. 7G.

Description. Male holotype: Body length 8.2 mm, head width 2.4 mm, intertegular distance 2.1 mm, wingspan 16.1 mm. **Paratype:** Body length 8.1 mm, head width 2.5 mm, intertegular distance 2.0 mm, wingspan 15.9 mm.

Head. Largely black, overall covered with sparse pale white hairs. Mandible black with red-brown infused, tridentate, with apically large acute tooth. Labrum black with rounded margin. Clypeus black with narrow yellow stigma (obscured in BSRU-AB-0156) on surface close to apex, punctures very dense, separated with less than half of its diameter, margin truncate, with small inconspicuous median tubercle. Subantennal suture strait. Frons punctures coarser than on clypeus, with two yellow stigmas

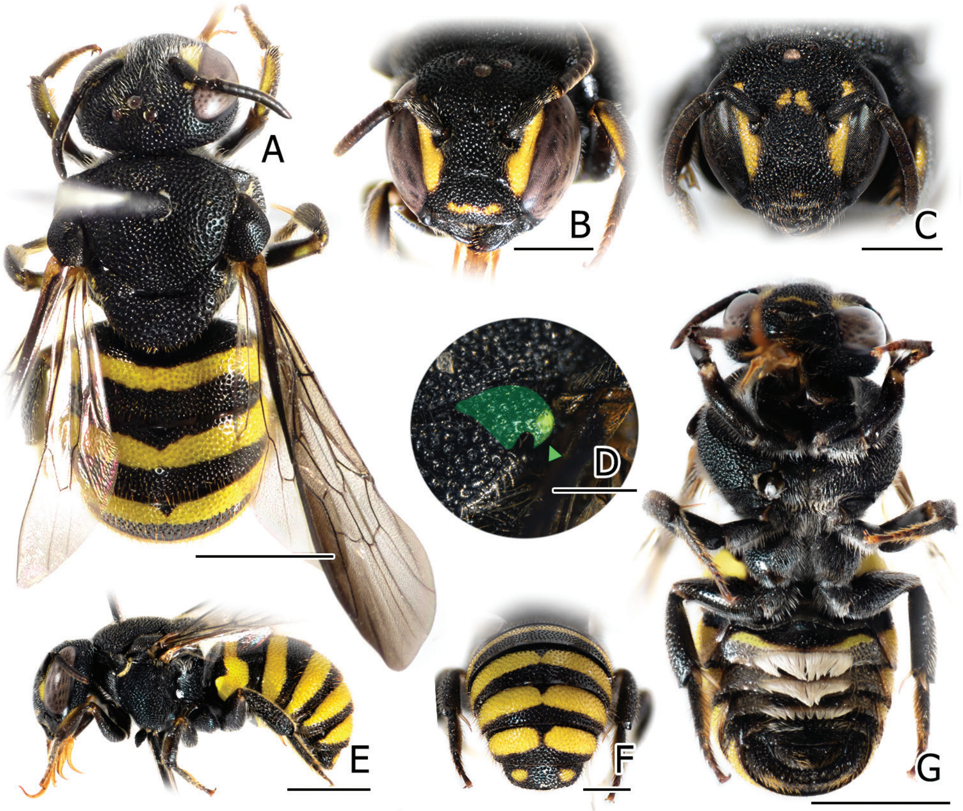

Figure 6. Male *Stelis flavofuscinular* sp. nov. [**A, B** holotype (BSRU-AB-0157) **C–G** paratype (BSRU-AB-0156)] showing the **A** dorsal habitus **B, C** face **D** axilla, with postero-lateral hook highlighted in green **E** lateral habitus **F** metasomal apex **G** ventral habitus. Scale bars: 2 mm (**A, E, G**), 1 mm (**B, C, F**), or 0.5 mm (**D**).

(Fig. 6B), typically very obscured but can be recognized in BSRU-AB-0157, present above area between antennal socket. Paraocular area with yellow mark extending along orbit close to top of ommatidia. Interocellar distance shorter than ocellooccipital distance. Vertex and preoccipital area with coarse and dense punctures, with distinct microsculptures. Surfaces nearby lateral ocelli shiny glabrous, with fewer punctures, whereas fine and dense around middle ocelli. Scape and pedicels brown-black, frontal surface covered with dense pale white hairs. Antennal flagellum dark brown, F1 color lighter in apical half, F2 almost broader than long.

Mesosoma. Overall black, covered with sparse pale white hairs. Pronotal lobe rounded. Omaulus carinated but does not reach venter of thorax. Mesepisternum swollen laterally, with fine dense punctures on anterior surface, very coarse and dense on lateral surface.

Scutum with coarse, dense punctures, separated by about half of its diameter, becoming fine and dense posteriorly. Scutellum rounded, extended posteriorly to overhang

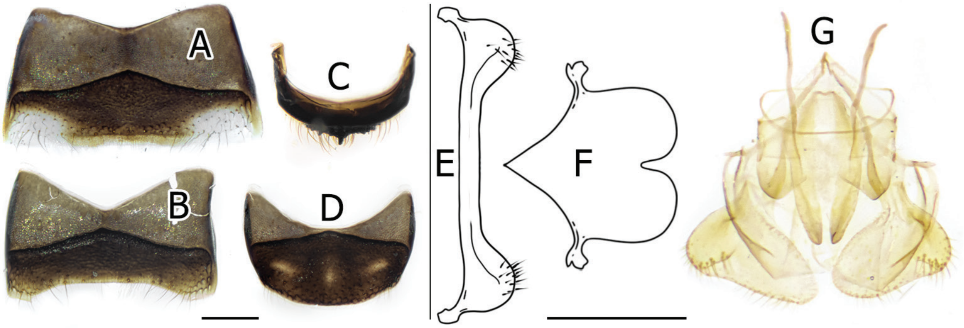

Figure 7. Genitalia and terminalia of male *Stelis flavofuscinular* sp. nov. (BSRU-AB-0157) **A** S4 **B** S5 **C** T7 **D** S6 **E** S7 **F** S8 **G** genitalia coupled with S8 in ventral habitus. Scale bars: 0.5 mm.

propodeum, punctation rather sparse in comparison with scutum. Scutoscutellar suture open, divided into two shiny bottom foveae. Axilla black (Fig. 6D), postero-lateral hook yellow, punctures fine and dense. Scutum, scutellum, and axilla come with distinct microsculptures. Tegula large, dark brown to black, with very fine, dense punctures. Propodeum black, median area shiny glabrous, with distinct fovea behind spiracle.

Wings. Dark brown to black especially on anterior half of forewing, and marginal cell. Stigma black. Second recurrent vein enters distal to 2nd submarginal crossvein, separating medial vein in 4:1 ratio.

Legs. Overall black-brown, with restricted yellow maculation present on anterior surface of tibia and apical femur of foreleg, dorsal surface of apical femur and basal tibia of midleg. Fore and mid tibia apically with two outer apical spines. Hind tibia apically with outer rounded projection. Tibial spur pale, bifid on foreleg. Hairs pale white, brown on tarsi. Hind basitarsus black, inner surfaces with brown dense hair fringe. Claw red-brown, apically black on hind tarsi. Arolia present, light brown.

Metasoma. Overall black with yellow maculation. Tergites covered with sparse, short, brownish hair, punctation coarse, separated by its diameter, uniformly distributed but somewhat confused on T6. T1–T5 with large yellow strike bands, with little median disruption that is pronounced more in rear metasomal segments. T6 large with lateral dots, apical margin rounded, carinated, forming ventral border. T7 small, marginal area depressed, median area of apical margin broadly crenulate with distinct median erected tooth that making lateral shallow emargination, ventral surface smooth with lateral angle making T7 weakly tridentate. Sternite black, with scattered brownish hairs. S1 median carina strong, premarginal carina strong, extended ventrally but not clearly overhanging margin. S2–S4 (Fig. 6G) laterally translucent, with distinct median white pubescent erected from premarginal band. S2 and S3 with yellow premarginal bands, but very narrow and medially restricted in the latter. S5 widely emarginated, with very sparse white pubescent. S6 margin rounded. S7 very narrow, ventral surface smooth, lateral margin with extended rounded lobe with dispersed erected hairs. S8 (Fig. 7F) very clear apically, extending to two rounded apical lobes separated with median U-shape notch, resembling inverted heart shape. Genitalia as in Fig. 7G.

Etymology. The word *flavo* means "yellow", while *fuscinular* means "hook". Thus, the specific epithet, *flavofuscinular*, principally refers to the yellow postero-lateral axilla hook of male bees that contrasts with its overall black mesosoma.

Bee host. *Anthidiellum phuchongensis* sp. nov. (see above). It is possible that *S. flavofuscinular* sp. nov. may also be a cleptoparasite of other *Megachile* species that are also frequently encountered in the PCNYNP area. Kasparek (2015) suggested that the hosts of *Stelis* species are mainly members of Megachilinae, and some *Stelis* species have a wide range of hosts.

Floral association. Unknown.

Remarks. Though the color pattern observed on the mesosoma and metasoma seems invariant, there are some variations in the yellow maculation especially on the face, noticeable in two specimens possibly from the same cohort, and so it is likely to have a greater level of variation in the population. *Stelis* (*M.*) *malaccensis* (Friese, 1914), redescribed by Pasteels (1969), differs mainly in coloration. It exhibits very dense punctures over all the thorax, a more subtriangular scutellum, yellow markings on the base of the mandible, scape, supraclypeal area, paraocular area, preoccipital area, vertex, mesopleuron, anterolateral margin of the scutum, and margin of the scutellum and axilla.

Key to female *Anthidiellum* (*Ranthidiellum*) species of the world

Modified from Engel (2009), see discussions below.

1 Face mostly without black area, if present, restricted to frons; metasoma largely reddish, orangish, or ferruginous **2**

– Face with extensive black areas; metasoma largely black, dark brown, or dark ferruginous **3**

2 T6 black; body ferruginous; T1–T5 without distinct black apical band, sometimes with black stigma infused (Fig. 2) .. ***A.* (*R.*) *ignotum* Engel, 2009**

– Body including T6 orangish (Fig. 3D); T1–T5 with prominent black apical band (Fig. 3) .... ***A.* (*R.*) *phuchongensis* sp. nov.**

3 Mesoscutum overall black; head black with clypeus, mandible, and antenna orangish to reddish; T6 covered with white to yellowish plumose tomentum; forewing conspicuously dark brown at basal half, apically hyaline **4**

– Mesoscutum with reddish to orangish anterolateral L-shape mark; head with more extensive lighter orangish to reddish area, especially on paraocular area along the inner and outer orbits, and oval mark below middle ocelli; T6 not covered with plumose tomentum; forewing without conspicuous dark-brown area .... ***A.* (*R.*) *meliponiforme* (Cockerell, 1919)**

4 Metasoma black, with red-brown to black infused basally on T1–T5; scutellum and axilla with narrow orangish to reddish marginal band .... ***A.* (*R.*) *rufomaculatum* (Cameron, 1902)**

– Metasoma dark brown to black, with orangish to reddish band present apically on T1–T5; band on the scutellum, and axilla margin broader .... ***A.* (*R.*) *apicepilosum* (Dover, 1929)**

Key to male *Anthidiellum* (*Ranthidiellum*) species of the world

The characters of male *A.* (*R.*) *rufomaculatum* (Cameron, 1902) and *A.* (*R.*) *apicepilosum* (Dover, 1929) are based on Pagden (1934) and Pasteels (1969). Male *A.* (*R.*) *meliponiforme* (Cockerell, 1919) remains unknown.

1 Metasoma largely reddish, orangish, or ferruginous **2**

– Metasoma largely black, dark brown, or dark ferruginous **3**

2 Body integument ferruginous (Fig. 4 right); face with extensive black area (Fig. 4H); Tergal apex translucent, covering black basal band of its successor; S4 gradulus incomplete (Fig. 5D) .... ***A.* (*R.*) *ignotum* Engel, 2009**

– Body integument orangish to reddish (Fig. 4 left); face with small black marks restricted on the frons (Fig. 4G); Tergal apex almost opaque, T1–T5 with black marginal band; S4 gradulus complete (Fig. 5C) .... ***A.* (*R.*) *phuchongensis* sp. nov.**

3 Metasoma uniformly dark red-brown, dark brown, or black, sometimes with broad reddish apical margins; T6 covered with plumose white tomentum; S5 apical comb with “± 80 teeth” ....***A.* (*R.*) *rufomaculatum* (Cameron, 1902)**

– Metasoma dark brown to black, with metallic reddish reflections infused apically predominantly on second and third segments; T6 not covered with white tomentum; S5 apical comb with “over 60 teeth”................................. .... ***A.* (*R.*) *apicepilosum* (Dover, 1929)**

Discussion

Taxonomic implications

It appears that sexual dimorphism in coloration is very strong in *A.* (*R.*) *ignotum* but very weak in *A.* (*R.*) *phuchongensis*. Both species are very similar in their morphology, but differ in their sternal and genitalic structures. The dorsolateral carina of the gonoforceps is present in both species, but it is still unclear whether this character is present in other *Ranthidiellum* species as the character is never reported. The genitalia descriptions and illustrations of *A.* (*R.*) *apicepilosum* (Dover, 1929) and *A.* (*R.*) *rufomaculatum* (Cameron, 1902) are vague (see Pagden 1934; Pasteels 1972), and males of *A.* (*R.*) *meliponiforme* (Cockerell, 1919) are unknown, though Ascher et al. (2016, see fig. 5A) reported an unknown male specimen of *Ranthidiellum* from eastern Cambodia that is presumed to be *A.* (*R.*) *meliponiforme*.

Color variations in *Ranthidiellum* are poorly understood as they are rarely found (Soh et al. 2016). In our study, although only six *A.* (*R.*) *ignotum* females were examined, several color variations were detected. We arbitrarily categorized these specimens into two forms based on the variations in the infused black integument as “normal” and “less melanized” forms (Fig. 2). One female collected from Phayao Province (BSRU-AA-1250) had “less melanized” traits, where the midleg, hindleg, and the anterior part of the scutum had reduced black areas. In addition, as the expression of the black pattern declined, the lateral black stripes on the anterior parts of the scutum appeared as red-brown. The "normal" form specimens had varying extensions of black areas, some obviously extended to the anterior surfaces of the mesonotum, propodeum, and anterior surfaces of T1. Also, more infused black marks were prominent on the face and T1–T5. One specimen from Chiang Mai (BSRU-AA-6709) showed a black triangular mark on the scutellum (Fig. 2D). It is noteworthy that this type of color variation can also be detected in *A.* (*R.*) *phuchongensis*.

We also examined the photographs of *Ranthidiellum* holotypes deposited at NHMUK: *A.* (*R.*) *apicepilosum* Dover, 1929, *A.* (*R.*) *meliponiforme* (Cockerell, 1919), and *A.* (*R.*) *rufomaculatum* (Cameron, 1902). All types had labels showing "TYPE (POSSIBLE)", and the labels were in accord with the original descriptions. Despite the type of *A.* (*R.*) *rufomaculatum* being labeled "Selected as types, Pasteels", the redescription by the author (Pasteels 1969) was not congruent with the material itself in some aspects. For example, Pasteels (1969, p 124, "Couleur" section) noted "En rogue ferrugineux … de larges bandes sur les tergites 1–5 (les deux dernières jaunâtres)" [reddish-ferruginous band on T1–T5, with the last two yellowish], while Cameron's (1902) original description and Mavromoustakis's (1936) notes are vague and did not mention any terga band. The character was shown in the material as obscured red-brown to black area infused basally for all denoted terga, thus, yellowish color stated by Pasteels should be a vague interpretation led by the distinct yellow tomentum, while color information can lead to misidentification since this will easily fit with the reddish-ferruginous broad apical band founded in *A.* (*R.*) *apicepilosum.* Materials of *A.* (*R.*) *apicepilosum* and *A.* (*R.*) *rufomaculatum* appear very similar in appearance, especially facial and mesosoma maculation (see Table 1), though these comparisons are based on very limited material. Considering current evidence presented with the synopsis of *Ranthidiellum* species (see Table 1), we revised and updated the identification keys based on Engel (2009) to both male and female species.

Michener (2007)'s diagnosis of *Stelis* denoted that males commonly have a midapical comb on S4, which is usually used as a diagnosis character. However, in the *S.* (*M.*) *flavofuscinular* sp. nov. described herein the midapical comb on S4 was absent. Besides S4, the studies on the genitalia and other hidden terga are very difficult to perform, with very few studies containing illustrations of these structures as mentioned in comprehensive revisions of *Stelis* by Kasparek (2015). It is very important to carefully prepare the genitalia and associated sclerites to deliver more comprehensive and accurate data.

Association of *Stelis* (*M.*) *flavofuscinular* sp. nov. with *Anthidiellum* (*R.*) *phuchongensis* sp. nov.

At the PCNYNP, *A.* (*R.*) *phuchongensis* putatively constructed their nests in preexisting cavities, mostly from abandoned mygalomorph spider nests that are abundant in the sandy earth bank, making protruding translucent resinous entrance tubes that curved downwards (Fig. 8C), similar to the nest described for *A.* (*R.*) *apicepilosum*, which utilize deserted potter wasp nests in Malaysia (Pagden 1934; Pasteels 1972).

Table 1. List of *Anthidiellum* (*Ranthidiellum*) and *Stelis* (*Malanthidium*) of the world. (***e***: emergence record; ***f***: flight record; ***t***: type locality).

Species	Original description	Supplementary literature	Documented localities	Phenology notes
A. apicepilosum (Dover, 1929)	Dover 1929	Pagden 1934; Pasteels 1969, 1972	Thailand (Nakhon Si Thammarat ***t***), Malaysia (Gunung Angsi, Negeri Sembilan; Batu Ferringhi, Penang; Bukit Kutu, Selangor)	February (24th***f***); March (8th***e***, 11***e***); April (15th***f***); August (24th***f***)
A. ignotum Engel, 2009	Engel 2009	Soh et al. 2016	Thailand (Chiang Mai, Nakhon Ratchasima ***t***, Phayao)	June (1st***f***); July (10th***f***); December (9th***f***, 13th***f***, 19th***f***: possibly mating flight)
A. meliponiforme (Cockerell, 1919)	Cockerell 1919	Pagden 1934; Pasteels 1969, 1972	Malaysia (Sandakan, Sabah, Borneo ***t***), Cambodia?* (Keo Seima)	not indicated
A. phuchongensis sp. nov.	this study	–	Thailand (Ubon Ratchathani)	January (5th***f***, ***e***, 6th***f***); February (9th***f***); October (10th, observed in habitat survey); December (27th***e***, 29th***e***, 30th***e***)
A. rufomaculatum (Cameron, 1902)	Cameron 1902	Mavromoustakis 1936; Pasteels 1969, 1972	Malaysia (Kuching, Sarawak, Borneo ***t***), Indonesia (Sumatra)	April (30th***f***)
S. malaccensis (Friese, 1914)	Friese 1914	Pasteels 1969; Michener and Griswold 1994; Michener 2007	Malaysia (Taiping Hill, Perak ***t***)	February (-)
S. flavofuscinular sp. nov.	this study	–	Thailand (Ubon Ratchathani)	December (emerge: 23rd***e***, 25th***e***)

*identified as *A. meliponiforme* in affinity (see Ascher et al. 2016).

This is the first report on the host-cleptoparasite relationship in *Ranthidiellum*. The *Anthidiellum* (*R.*) *phuchongensis* nest collected in December 2019 was maintained under a laboratory condition for 47 d until the first adult bee, a male *Stelis* (*M.*) *flavofuscinular* sp. nov., emerged, followed by another male 2 d later and then three *A.* (*R.*) *phuchongensis* females and a male over the remaining 12 d (Fig. 9C).

Stelis is known to adopt at least two strategies in attacking host cells (Litman 2019): the female *S.* (*Dolichostelis*) sp. is reported to attack closed host cells and to destroy the host offspring before laying eggs (Parker et al. 1987), whereas *S.* (*Stelis* s. str.) attacks open host cells to lay eggs and let the emerged larvae then kill the host eggs or larvae (Rust and Thorp 1973; Torchio 1989; Rozen and Hall 2011). Recent phylogenetic studies (Litman et al 2013, 2016) suggested *S.* (*Malanthidium*) to be more closely related to *S.* (*Stelis* s. str.) than to *S.* (*Dolichostelis*), and assumed that *S.* (*Malanthidium*) must be an open-cell attacker. Our work found evidence to suggest that *S.* (*M.*) *flavofuscinular* might be an open-cell attacker, since the host nest had no indication of resin modification by the parasite.

Taxonomic knowledge on *Stelis* in Southeast Asia is very scant (Michener 2007). Historically, there is only one species described: *S.* (*M.*) *malaccensis* (Friese, 1914), from Taiping hills, Perak, Malaysia (originally noted as "Taiping Hill, Malakka" by von Buttel-Reepen), previously a monobasic for *Malanthidium*. In this study, *S.* (*M.*) *flavofuscinular* is the second described *Malanthidium* species (see Table 1). Michener and Griswold (1994) and Michener (2007) also pointed out that there are at least two additional undescribed *Malanthidium* species, but the details were not provided.

Figure 8. Nesting habitat of *Anthidiellum phuchongensis* sp. nov. at PCNYNP, Ubon Ratchathani Province, Thailand **A, B** nest excavation process and area **C** resinous nest entrances **D, E** nest locations of *A. phuchongensis* on vertical earth bank (highlighted with yellow dots).

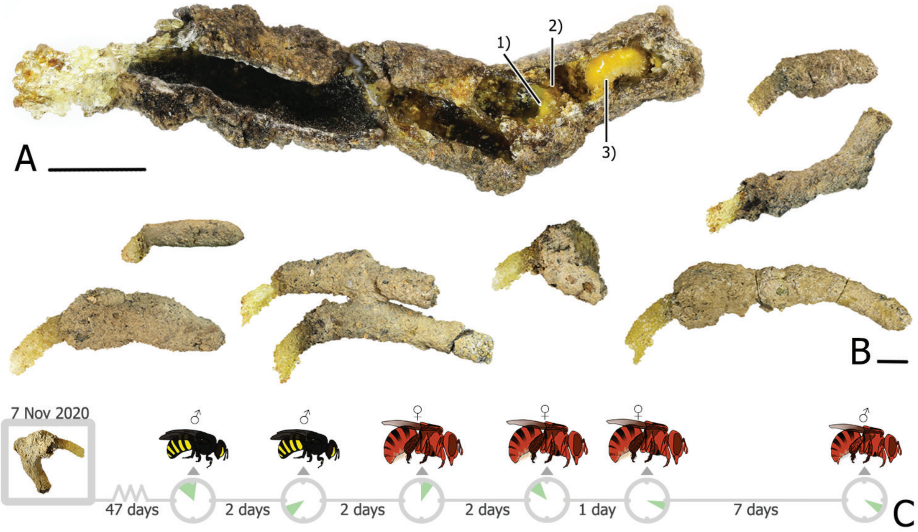

Figure 9. Nest structure of *Anthidiellum phuchongensis* sp. nov. **A** longitudinal dissected nest: 1) provisional mass, 2) resinous partition, and 3) predefecated larvae **B** showing diversity of nest morphology **C** timeline of bees emerging from the reared nest. Scale bars: 1 mm.

Acknowledgements

The authors express their deepest gratitude to Mr Chawatat Thanoosing (Imperial College London, UK; NHMUK) and Ms Natalie Dale-Skey (Curator of Hymenoptera, NHMUK) for providing relevant literature and the opportunity to access type specimens through the digital portal. Dr Victor Gonzalez (University of Kansas, USA) provided us with important literature. The Department of Entomology and Plant Pathology, Chiang Mai University, Thailand, graciously provided us with their specimens for examination. We also thank Mr Yongyut Kaewpaprab and members of the Bee and Spider Research Unit, Chulalongkorn University, Bangkok, Thailand, for field assistance. The manuscript was significantly improved with the assistance of Dr Michael S. Engel (University of Kansas, USA), Dr Max Kasparek (Natural Resources Management, Heidelberg, Germany), and an anonymous reviewer who provided useful comments.

This work was supported by the National Science and Technology Development Agency (NSTDA: JRA-CO-2563-11148-TH, MOU-CO-2563-11312-TH), and was conducted with official permission from the PCNYNP, Department of National Park, Wildlife and Plant Conservation (Ubon Ratchathani, Thailand). Funding was from the Center of Excellence in Biodiversity, Office of Higher Education Commission (Thailand) (PERDO-BDC: BDCPG2-159009/1) to NW, and the 90th Anniversary of Chulalongkorn University Scholarship (GCUGR1125631073M) to PN and NW, and the Asahi Glass Foundation Grant, Japan to NW.

References

Ascher JS, Pickering J (2020) Discover Life Bee Species Guide and World Checklist (Hymenoptera: Apoidea: Anthophila). http://www.discoverlife.org/mp/20q?guide=Apoidea_species [Accessed on 05.05.2020]

Ascher JS, Phallin H, Sokha K, Kang L, Sokchan L, Shao C, Greef SD, Chartier G, Sophany P (2016) A Report on the Bees (Hymenoptera: Apoidea: Anthophila) of Cambodia. Cambodian Journal of Natural History 2016: 23–39.

Cameron P (1902) On the Hymenoptera Collected by Mr. Robert Shelford at Sarawak, and on the Hymenoptera of the Sarawak Museum. Journal of the Straits Branch of the Royal Asiatic Society 37: 29–140.

Cockerell TDA (1919) XXXVII. Descriptions and records of bees.LXXXVII. Annals and Magazine of Natural History 4: 355–360. https://doi.org/10.1080/00222931908673902

Combey R, Kwapong P, Eardley C, Botchey M (2010) Phylogenetic Analysis of the Bee Tribe Anthidiini. Journal of Ghana Science Association 12(1): 26–38. https://doi.org/10.4314/jgsa.v12i1.56803

Dover C (1929) Wasps and Bees of the Raffles Museum, Singapore. Bulletin of Raffles Museum, Singapore 2: 43–70.

Engel MS (2009) A New Species of *Ranthidiellum* from Thailand, with a Key to Species (Hymenoptera: Megachilidae). Acta Entomologica Slovenia 17(1): 29–35.

Friese H (1914) Neue Bienenarten der orientalischen Region. Deutsche Entomologische Zeitschrift, 320–324. https://doi.org/10.1002/mmnd.48019140311

Gonzalez VH, Griswold T, Praz CJ, Danforth BN (2012) Phylogeny of the Bee Family Megachilidae (Hymenoptera: Apoidea) Based on Adult Morphology. Systematic Entomology 37: 261–286. https://doi.org/10.1111/j.1365-3113.2012.00620.x

Kasparek M (2015) The Cuckoo Bees of the Genus *Stelis* Panzer, 1806 in Europe, North Africa and the Middle East. Entomofauna. Supplement 18: 1–144.

Litman JR (2019) Under the Radar: Detection Avoidance in Brood Parasitic Bees. Philosophical Transactions of the Royal Society B: Biological Sciences 374: e20180196. https://doi.org/10.1098/rstb.2018.0196

Litman JR, Griswold T, Danforth BN (2016) Phylogenetic Systematics and a Revised Generic Classification of Anthidiine Bees (Hymenoptera: Megachilidae). Molecular Phylogenetics and Evolution 100: 183–198. https://doi.org/10.1016/j.ympev.2016.03.018

Litman JR, Praz CJ, Danforth BN, Griswold TL, Cardinal S (2013) Origins, Evolution, and Diversification of Cleptoparasitic Lineages in Long-Tongued Bees. Evolution 67(10): 2982–2998. https://doi.org/10.1111/evo.12161

Mavromoustakis GA (1936) XXV.–Notes on some Anthidiine bees (Apoidea) from Borneo. The Annals and Magazine of Natural History (10)18(104): 288–289. https://doi.org/10.1080/00222933608655193

Michener CD (2007) The Bees of the World (2nd edn). Johns Hopkins University Press, Baltimore, 953 pp.

Michener CD, Griswold TL (1994) The Classification of Old World Anthidiini (Hymenoptera, Megachilidae). The University of Kansas science bulletin 55: 299–327.

Michener CD, McGinley RJ, Danforth BN (1994) The Bee Genera of North and Central America (Hymenoptera: Apoidea). Smithsonian Institution Press, Washington, 209 pp.

Pagden HT (1934) Biological Notes on some Malayan Aculeate Hymenoptera III. Journal of the Federated Malay States Museums 17(3): 487–492.

Parker FD, Cane JH, Frankie GW, Vinson SB (1987) Host Records and Nest Entry by *Dolichostelis*, a Kleptoparasitic Anthidiine Bee (Hymenoptera: Megachilidae) Pan-Pacific entomologist 63(2): 172–177.

Pasteels JJ (1969) La Systématique Générique et Subgénérique des Anthidiinae (Hymenoptera, Apoidea, Megachilidae) de l'Ancien Monde. Mémoires de la Société Royale Belge d'Entomologie de Belgique 31: 1–148. [In French]

Pasteels JJ (1972) Revision des Anthidiinae (Hymenoptera Apoidea) de la Région Indo-Malaise. Bulletin et Annales de la Société Royale Belge d'Entomologie 108: 72–128. [In French]

Rozen Jr JG, Hall HG (2011) Nesting and Developmental Biology of the Cleptoparasitic Bee *Stelis ater* (Anthidiini) and Its Host, *Osmia chalybea* (Osmiini) (Hymenoptera: Megachilidae). American Museum Novitates 3707: 1–38. https://doi.org/10.1206/3707.2

Rust RW, Thorp RW (1973) The Biology of *Stelis chlorocyanea*, a Parasite of *Osmia nigrifrons* (Hymenoptera: Megachilidae). Journal of the Kansas Entomological Society 46(4): 548–562.

Soh EJ, Soh ZW, Chui SX, Ascher JS (2016) The Bee Tribe Anthidiini in Singapore (Anthophila: Megachilidae: Anthidiini) with Notes on the Regional Fauna. Nature in Singapore 9: 49–62.

Torchio PF (1989) Biology, Immature Development, and Adaptive Behavior of *Stelis montana*, a Cleptoparasite of Osmia (Hymenoptera: Megachilidae) Annals of the Entomological Society of America 82(5): 616–632. https://doi.org/10.1093/aesa/82.5.616

ZooKeys 1031: 183–204 (2021)
doi: 10.3897/zookeys.1031.56035
https://zookeys.pensoft.net

RESEARCH ARTICLE

A peer-reviewed open-access journal
ZooKeys
Launched to accelerate biodiversity research

Description of three new species of *Automeris* Hübner, 1819 from Colombia and Brazil (Lepidoptera, Saturniidae, Hemileucinae)

Thibaud Decaëns[1], Frédéric Bénéluz[2], Liliana Ballesteros-Mejia[3,4,5],
Diego Bonilla[6], Rodolphe Rougerie[3]

1 *CEFE, Univ Montpellier, CNRS, EPHE, IRD, Univ Paul Valéry Montpellier 3, Montpellier, France* **2** *Société entomologique Antilles-Guyane (SEAG), 18, Lotissement Amaryllis, F-97354 Rémire-Montjoly, French Guiana* **3** *Institut de Systématique, Evolution, Biodiversité (ISYEB), Muséum national d'Histoire naturelle, CNRS, Sorbonne Université, EPHE, Univ des Antilles, Paris, France* **4** *CESAB, Centre de Synthèse et d'Analyse sur la Biodiversité, Montpellier, France* **5** *Grupo de Investigación Diseño, Imagen y Comunicación. Facultad de Creación y Comunicación. Universidad El Bosque, Bogotá, Colombia* **6** *Tapuragua Reserva Natural de la sociedad civil, Yopal, Casanare, Colombia*

Corresponding author: Thibaud Decaëns (thibaud.DECAENS@cefe.cnrs.fr)

Academic editor: Christian Schmidt | Received 30 June 2020 | Accepted 1 March 2021 | Published 15 April 2021

http://zoobank.org/1014D0C2-C459-448C-A15E-69084DD2039E

Citation: Decaëns T, Bénéluz F, Ballesteros-Mejia L, Bonilla D, Rougerie R (2021) Description of three new species of *Automeris* Hübner, 1819 from Colombia and Brazil (Lepidoptera, Saturniidae, Hemileucinae). ZooKeys 1031: 183–204. https://doi.org/10.3897/zookeys.1031.56035

Abstract

The Saturniidae is one of the most emblematic families of moths, comprising nearly 3000 species distributed globally. In this study, DNA barcode analysis and comparative morphology were combined to describe three new species within the genus *Automeris*, which is the most diverse genus in the family. *Automeris llaneros* Decaëns, Rougerie & Bonilla, **sp. nov.**, *Automeris mineros* Decaëns, Rougerie & Bonilla, **sp. nov.**, and *Automeris belemensis* Decaëns, Rougerie & Bénéluz, **sp. nov.** are described from the Colombian Orinoco watershed, the Colombian Eastern Cordillera, and the area of endemism of Belém in the Brazilian Amazonia, respectively. They all belong to the *Automeris bilinea* (Walker, 1855) species subgroup, which comprises a number of species that are sometimes difficult to distinguish from each other using morphology alone. Here, the description of these three new species is based on significant differences from their closest relatives, either in terms of wing patterns, genitalia, DNA barcodes or a combination of these features.

Keywords

Amazonia, DNA barcoding, integrative taxonomy, Neotropics, new species, Orinoco, wild silkmoths

Introduction

The Saturniidae family, popularised as the wild silkmoths, is one of the most emblematic families of moths, because of the giant size, colourful patterns, or tailed hindwings of some of its species. In the latest published checklist (Kitching et al. 2018), as many as 3454 valid species were recognised in eight subfamilies and 180 genera. The diversity of the family is highest in the neotropics, where it is represented by six subfamilies and nearly 2400 species that can be found in a broad range of habitats, including the southmost areas of South America, from sea level to elevations exceeding 4000m. The diversity in habitus of these moths is also extreme: size ranges from small moths a few centimetres in wingspan (e.g., in the genus *Hylesia* Hübner, 1820) to very large ones approaching a wingspan of 20 cm (e.g., in *Arsenura* Duncan, 1841); wing patterns can be cryptic, mimicking leaves (e.g., in *Copaxa* Walker, 1855), can harbour large eyespots (e.g., in *Automeris* Hübner, 1919), or can be aposematic in colour (e.g., in *Citheronia* Hübner, 1919); wings can be rounded (e.g., *Dirphia* Hübner, 1919) or elongated (e.g., in *Syssphinx* Hübner, 1819 and *Ptiloscola* Michener, 1949), or some taxa have spectacular tailed hindwings (e.g., *Copiopteryx* Duncan, 1841).

Within subfamily Hemileucinae, the genus *Automeris* comprises species whose size ranges from small to very large; their main feature is the presence of a large eyespot on the dorsal surface of the hindwings. It is the most diverse genus within the family. In his monograph of the subfamily Hemileucinae, Lemaire (2002) listed 135 species in the genus, which he further organised into nine species groups based on the habitus and the structure of genitalia. Recently, the use of molecular approaches such as DNA barcoding, in addition to morphology, led to a significant increase in the pace of discovery and description of new species. Thus, in the past ten years only, as many as 155 new taxa were described, raising the total number of species in the genus to 313 (Kitching et al. 2018). In this paper, we use a combination of morphological features and molecular data (DNA barcodes) to propose the description of three new species from Colombia and Brazil within the group of *Automeris bilinea* (Walker, 1855), which was defined by Lemaire (2002) as a subgroup within the larger species group of *Automeris illustris* (Walker, 1855).

Materials and methods

Specimen collecting

Specimens were collected in the following three localities: from July to August 1999 in the savannah landscapes of the Eastern Plains of Colombia (Meta department, TD and DB leg.); in December 2002 in the Boyacá department, Colombia, in an area of humid Andean forest (1500 m in elevation) with moderate level of forest fragmentation (G. Lecourt and DB leg.); and from April to July 2008 in the state of Pará, Brazil, in an area of Amazonian forest with moderate to high levels of forest fragmentation

(TD leg.). Moths were attracted by a Mercury Vapour (MV) bulb powered by a small portable generator. A white sheet of 2 m height × 3 m width was used as a reflector. Collecting took place throughout each entire night, i.e., from 18:30 h to 06:30 h, in order to increase the probability of detecting species with different flight behaviours (Lamarre et al. 2015). Moths coming to the sheet were injected with ammonia, stored, and dried in labelled paper envelopes and brought to the lab to be mounted for morphological examination.

Morphological descriptions

All the specimens were mounted in a standard way to allow optimal examination of their body and wings. Male genitalia and eighth abdominal segment were prepared in 10% caustic potash solution to remove piliform scales, and were preserved in 75% ethanol. Body morphology, wing ornamentation and male genitalia structure were described using the terminology of Lemaire (1971, 2002).

Morphological features of the prepared specimens were compared with those of the species represented in Lemaire (2002) and Brechlin and Meister (2014). Additionally, type specimens of the three newly described species were compared with specimens from closely related species available in collections of TD and MNHN: 3 ♂ of *Automeris belizonensis* Brechlin & Meister, 2014; 2 ♂♂ and 1 ♀ of *Automeris bilinea* (Walker, 1855); 16 ♂♂ and 1 ♀ of *Automeris cinctistriga* (Felder & Felder, 1874); 5 ♂ of *Automeris fieldi* Lemaire, 1969; 5 ♂♂ of *Automeris godartii* (Boisduval, 1875); 3 ♂♂ of *Automeris lemensis* Lemaire, 1972; 28 ♂♂ and 1 ♀ of *Automeris midea* (Maassen & Weyding, 1885).

DNA barcoding and molecular analyses

DNA was extracted from dry legs removed from dry collection specimens of the suspected new species. We sampled two specimens of *Automeris llaneros* sp. nov., five specimens of *Automeris mineros* sp. nov. and 17 specimens of *Automeris belemensis* sp. nov., and we also included sequences of closely related species obtained from the Barcode of Life Data Systems (BOLD; Ratnasingham and Hebert 2007) and that had been generated as part of the DNA barcoding campaign for saturniid moths, coordinated by RR. Tissue samples were processed at the Canadian Centre for DNA Barcoding (CCDB). DNA was extracted using a routine silica-based 96-well extraction automation protocol (Ivanova et al. 2006). The part of COI used as a 'DNA barcode' (Hebert et al. 2003) was amplified with the primer set LepF1/LepR1 (Hebert et al. 2004), targeting a 658 bp fragment. The DNA extracts that did not amplify for the full-length DNA barcode were re-amplified with the internal primer pairs LepF1/MLepR1 and MLepF1/LepR1, targeting DNA fragments of 307 bp and 407 bp (Hajibabaei et al. 2006), respectively. All PCR amplifications were performed according to the standard PCR reaction protocol used in CCDB (Hajibabaei et al. 2005); PCR products were checked on a 2% E-gel 96 Agarose (Invitrogen, Burlington, ON, Canada). Unpurified PCR fragments were sequenced in both directions using the same primers as for the PCR reaction. The sequencing reactions followed CCDB protocols (http://ccdb.ca/resources/; Hajibabaei et al. 2005). All sequences were aligned and inspected for frame-shifts and stop codons for removal of editing errors and possible pseudogenes.

All records, including specimen and sequence data, and GenBank accession numbers, are given in Appendix 1, and are publicly accessible in the Barcode of Life Data system (BOLD) within dataset DS-AUTONSP (https://doi.org/10.5883/DS-AUTONSP). An unrooted neighbour joining (NJ) tree was computed on BOLD V4 using p-distances and the BOLD aligner option to compare the sequences obtained from the specimens of the three new species and those of closely related taxa. BOLD was used to calculate uncorrected p-distances between newly described species and their closest relatives. We also used the barcode identification numbers (BINs), i.e., clusters of barcode sequences automatically generated in BOLD which have a high concordance with species, as an additional source of information for species discrimination (Ratnasingham and Hebert 2013).

Distribution maps

We present maps of the current distribution for the three newly described species and their closest species within the *A. bilinea* subgroup (seven species, Fig. 3). Records of the other species within the *A. bilinea* subgroup were collected from BOLD and were georeferenced and carefully curated for locality and species identity excluding any possible error (a complete list of specimens and associated data is given in Appendix 1).

Collection abbreviations

CCGM	collection of Carlos G. Mielke (Ponta Grossa, Brazil);
CDB	collection of Diego Bonilla (Yopal, Colombia);
CFB	collection of Frédéric Bénéluz (Matoury, French Guiana);
CTD	collection of Thibaud Decaëns (Montpellier, France);
IAvH	Instituto de Investigación de Recursos Biológicos Alexander von Humboldt (Bogotá, Colombia);
MNHN	Muséum national d'Histoire naturelle of Paris (France);
MPEG	Museu Paraense Emilio Goeldi (Belém, Brazil).

Taxonomic account

***Automeris mineros* Decaëns, Rougerie & Bonilla, sp. nov.**
http://zoobank.org/CE1EAA15-8197-4B98-A2F4-062C40A83153
Figures 1A, B, E, F, 2A

Type material. ***Holotype.*** Colombia • ♂ (Fig. 1A, E); Boyacá department, near Quipama, Vereda Caviche; 5.575°N, 74.2595°W; elevation: 1500 m; 1–3 Dec.

2002; at MV light; DB and G. Lecourt leg.; BOLD SampleID: BC-Dec0551; Deposited in IAvH.

Paratypes (19 ♂♂ and 6 ♀♀). Colombia • 15 ♂♂ and 5 ♀♀, all same data as holotype; all specimens collected at MV light except one pair *ab ovo*, reared on *Pyracantha regersiana* in Rouen (France) by TD, and 3 ♂♂ and 2 ♀♀ ab ovo, reared on *Quercus* sp. in Bogotá (Colombia) by L.D. Ramirez and DB. Deposited as follow: 2 ♂♂ and 2 ♀ (Fig. 1B, F; allotype; BOLD SampleID: BC-Dec0547) in IAvH, 5 ♂♂ in MNHN (BOLD SampleID: BC-Dec0548, BC-Dec0549, BC-Dec0550), 6 ♂♂ and 1 ♀ in CTD, 1 ♂ in CFB, 4 ♂♂ and 2 ♀♀ in CCGM, 1 ♂ and 1 ♀ in CDB.

Diagnosis. *Automeris mineros* sp. nov. is similar to the reddish forms of *A. midea*, a species with a large and essentially Amazonian distribution (Fig. 3). However, the vivid coloration, which is occasional in the later, is consistent among all the specimens of *A. mineros* sp. nov. that have been examined. It is also possible to separate the two species by additional fine characters of the habitus. In *A. mineros* sp. nov., the antemedian area of the forewings appears lighter than the median area due to the presence of a dense dusting of yellow scales, while this zone is generally concolourous with or darker than the rest of the wing in *A. midea* (Fig. 4). The apex of the forewing tends to be less acute in *A. mineros* sp. nov. The width of the yellow periocellar ring of the hindwing is also wider in *A. mineros* than in most of the examined specimens of *A. midea*. Finally, the veins on the ventral side of the forewings are clearly highlighted in orange in *A. mineros* sp. nov., and are more sharply contrasting with the surrounding ground colour than in *A. midea*. Distinction based on male genitalia is less conclusive, although we can however note the truncated instead of triangular shape of the saccus, as well as the median plate of the gnathos which is less massive in *A. mineros* sp. nov. and clearly marked by a median projection. Interestingly, DNA barcodes clearly separate *A. mineros* sp. nov. from all closely related species in a distinct cluster of sequences (BIN BOLD:ABY4503; see fig. 4). The nearest neighbour is *A. belizonensis* (1.8% minimum p-distance), from which it can be distinguished by the more rounded shape of the forewings and the more vivid coloration of the hindwings.

Description. ♂ (Fig. 1A, E). ***Wingspan*:** 77–84 mm. ***Head*:** dark brown, labial palpi and antennae orange brown. ***Thorax*:** dorsally dark brown with red orange piliform scales on the ventral side; legs dark brown. ***Abdomen*:** dark orange brown with dark brown piliform scales on the dorsal side; eighth abdominal segment lacking any remarkable sclerotised structure. ***Forewings*:** length 40–42 mm, slightly elongated, rounded apex, straight outer margin; dorsal ground colour orange brown, suffused with yellow scales in the ante- and postmedian areas and, to a lesser extent, by pink scales in the median area; antemedial line faint, almost indistinct, only visible as yellow scales bordering its distal edge; postmedial line barely preapical (1–3 mm), slightly convex from apex to vein CuA2, then bent toward the anal margin, yellow in colour, lined distally by a line of black scales; discocellular mark rectangular, darker than the surrounding wing surface, with a dark brown spot in its centre, and three to four small spots of the same colour at its corners. Ventral side with a large dull orange area extending on the main basomedian area, with veins marked in distinctive orange scales; apical area dark brown, extending along outer margin and toward tornus. Postmedial line

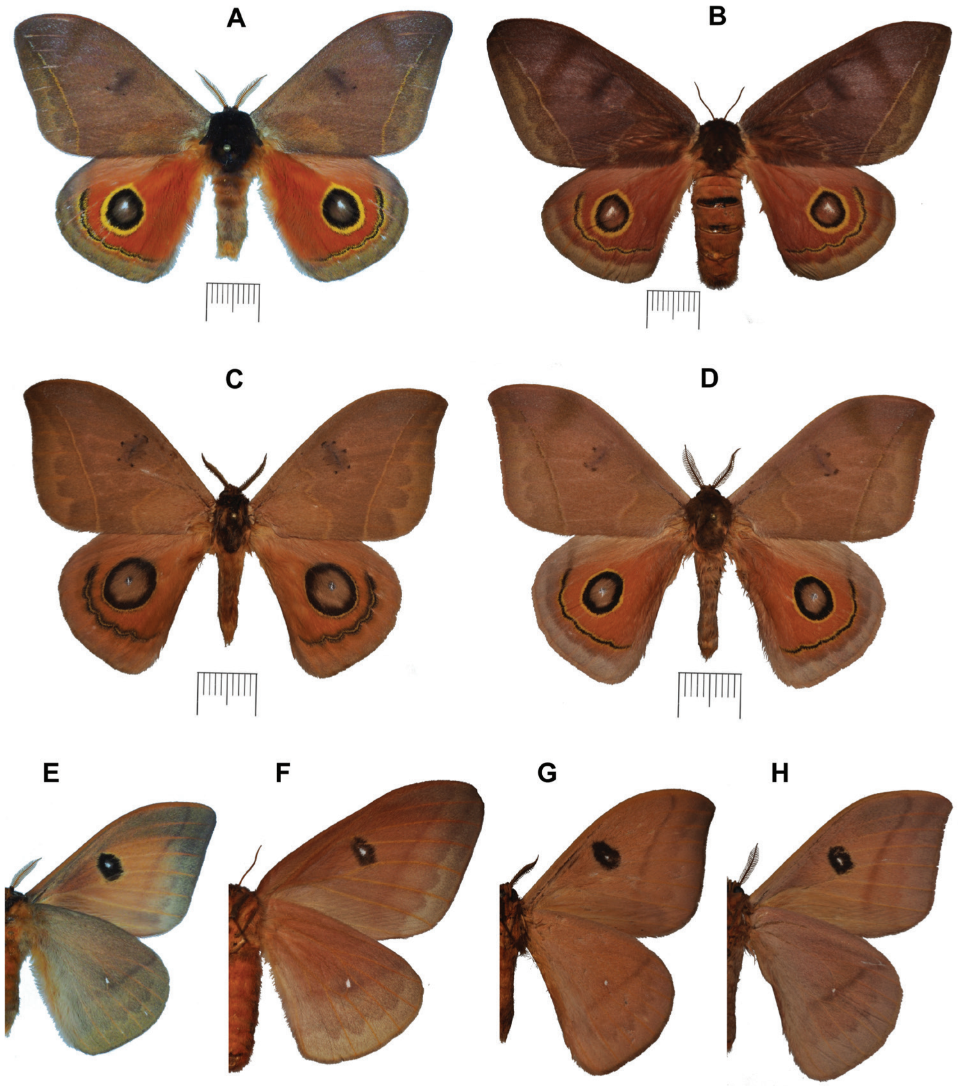

Figure 1. Specimens of the new species of *Automeris* spp. **A** dorsal view of *A. mineros* sp. nov., holotype ♂ **B** dorsal view of *A. mineros* sp. nov., paratype (allotype) ♀ **C** dorsal view of *A. belemensis* sp. nov., holotype ♂ **D** dorsal view of *A. llaneros* sp. nov., holotype ♂ **E** ventral view of *A. mineros* sp. nov., holotype ♂ **F** Ventral view of *A. mineros* sp. nov., paratype (allotype) ♀ **G** ventral view of *A. belemensis* sp. nov., holotype ♂ **H** ventral view of *A. llaneros* sp. nov., holotype ♂. Scale bars: 1 cm.

well marked, dark reddish brown; marginal band diffuse, suffused with yellow scales and disappearing toward apex. Discocellular mark large and black, with a white discal spot in its centre and surrounded by a thin diffuse ring of yellow scales. ***Hindwings*:** basomedian area vivid orange-red with a 7–12 mm × 6–8 mm eyespot in its centre formed by, from its centre: a small well marked white pupil surrounded by a dark brown iris, a first large black periocellar ring, a second large yellow ring of the same width, and finally a barely visible line of black scales enclosing the eyespot. Postmedial line black and lunular, distally bordered by a thin line of yellow scales, and proximally by another thin line of yellow and black scales; postmedian area formed by a thin vivid orange-red band and bordered by a large orange-brown marginal band covered with yellow scales. Ventral side light brown, suffused with yellow scales, particularly on the marginal band; venation distally marked with orange scales. Postmedial line dark brown, becoming faint toward the anal margin; discal cell with a small white spot.

Wingspan ♀ (Fig. 1B, F): 94 mm. ***Head, thorax, and abdomen*** of the same colour as in the male. ***Forewings*:** length 47 mm, elongated, rounded apex, almost straight border; dorsal ground colour dark purplish brown, suffused with light grey scales in the median area, except for a large oblique band lacking these scales approximately half way between the dark rectangular discal mark and the apex; postmedian area suffused with yellow scales. Both ante- and postmedial lines yellow, the latter straight and slightly preapical (3 mm). Ventral side light orange brown, the venation marked by orange scales, marginal band suffused with orange scales; postmedial line dark brown; large black discocellular mark, with a large white discal spot in its centre. ***Hindwings*:** Basomedian area brownish red; eyespot with the same structure as in the male, slightly duller in colour; black and lunular postmedial line, bordered by a line of yellow scales on both edges; postmedian area brownish red; marginal band covered with yellow scales. Ventral side light brown, suffused with yellow to pink scales; venation distally marked by orange scales; discal point small and white.

Genitalia ♂ (Fig. 2A): typical of the *A. bilinea* subgroup as described in Lemaire (2002). Uncus well developed, slightly extending beyond the distal end of the valves, with a broad bifid dorsal protuberance. Dorsal lobes of valves weakly developed and sharp. Median plate of gnathos strongly sclerotised with its posterior margin concave and with a small median projection. Saccus short and anteriorly truncated. Phallus straight, with a small lateral spine on its base; its posterior, tapering end slightly bent upward, with the weakly developed vesica expanding ventrally.

Genitalia ♀: not examined.

Immature stages. Eggs were obtained from a wild collected female. Larvae hatched 22 days after and readily fed on *Pyracantha regersiana* (Rosaceae) in France (rearing #17 by TD) and on *Quercus* sp. (Fagaceae) in Colombia (rearing by L. D. Ramirez and DB). Native foodplants remain unknown. Rearing was successful in plastic boxes, feeding larvae with fresh branches changed every 2–4 days. Larvae completed six instars within two months on *P. regersiana* and pupated in a brown cocoon.

Eggs are white with a black micropyle, laterally flattened, 2 mm diameter × 0.8 mm height, laid in dense cluster of several dozens. ***First larval instar*:** head black. Body 4 mm upon hatching, 6 mm maximal length; pale yellow with black scoli and spines. ***Second instar*:** Head black. Body 7–8 mm maximal length; brownish yellow dorsally, dull yellow ventrally; scoli and spines dark brown. ***Third instar*:** Head black. Body: 14 mm maximal length; brownish yellow dorsally, green yellow ventrally; scoli and spines dark brown. ***Fourth instar*:** Head black. Body 19–20 mm maximal length; dark brown dorsally with fine light green stripes, light green ventrally; scoli and spines dark brown to black. ***Fifth instar*:** Head green. Body: 35–40 mm maximal length; light green colour with pink dorsal ornamentation, a lateral ivory strip ventrally and dorsally bordered with a thin black line; scoli and spines light green. ***Sixth instar*:** Same colour and ornamentation as previous instar; 35–40 mm maximal length. ***Pupa and cocoon*:** Last instar larvae spin a thin and supple cocoon of beige silk. Pupa 24–37 mm long, dark brown. Reared adults emerged from the cocoon early in the morning one to two months after pupation.

Distribution. *Automeris mineros* sp. nov. is known form the type locality only, in the Oriental Cordillera of Colombia near Muzo (Fig. 3), a region from which a number of new taxa of Saturniidae were described recently (Decaëns and Rougerie 2008).

Etymology. This species is named in reference to emerald mining, which represents an emblematic economic activity in the region surrounding the type locality.

Automeris belemensis Decaëns, Rougerie & Bénéluz, sp. nov.

http://zoobank.org/A1CECFCF-0A6B-4128-B4FE-673D66FB6255
Figures 1C, G, 2B

Type material. ***Holotype*.** Brazil • ♂ (Fig. 1C, G); Pará state, Maçaranduba, Nova Ipixuna; Apr. 2008; 4.7990°S, 49.3630°W; elevation: 100 m; at MV light; TD leg.; BOLD SampleID: BC-TDMPEG0008; deposited in MPEG (catalogue number: MPEG.HLE 04018743).

Paratypes (16 ♂♂). Brazil • 13 ♂♂, same data as holotype with different sampling locations in the same area: 4.7990°S, 49.3630°W; 4.8110°S, 49.3670°W; 4.8050°S, 49.3690°W; 4.8040°S, 49.3230°W. Brazil • 1 ♂; Pará state, Pacajá; June 2008; 3.7060°S, 51.0390°W; at MV light; TD leg. Brazil • 2 ♂♂; Maranhão state, Reserva Biologica do Gurupi; 18 Apr. 2010; 4.0014°S, 46.8372°W; at MV light; TD leg. Deposited as follow: 3 ♂♂ in MPEG (BOLD SampleID: BC-TDMPEG0667, BC-TDMPEG0743, BC-TDMPEG0744; MPEG catalogue number: MPEG.HLE 04018744, MPEG.HLE 04018745, MPEG.HLE 04018746), 4 ♂♂ in the MNHN (BOLD SampleID: BC-TDMPEG0918, BC-TDMPEG0919, BC-INCT1136, BC-INCT1137), 3 ♂♂ in CFB (BOLD SampleID: BC-TDMPEG0956, BC-TDMPEG0957, BC-TDMPEG0982), 2 ♂♂ in CCGM (BOLD SampleID: BC-TDMPEG0983, BC-TDMPEG0920), 4 ♂♂ in CTD (BOLD SampleID: BC-TDMPEG0007, BC-TDMPEG0009, BC-TDMPEG0014, BC-TDMPEG0301).

Diagnosis. Phenotypically, *Automeris belemensis* sp. nov. is closely related to *A. cinctistriga* and *A. godartii* from which it is difficult to separate based on wing patterns, particularly if we consider the phenotypic variability that characterises these species (see Fig. 3 for distribution map of these species). However, the examination of a large number of specimens reveals subtle characters that make it possible to differentiate them. The distinction from *A. cinctistriga* is possible because of the general shape of the forewings in *A. belemensis* sp. nov. usually less elongated with a less prominent apex, and by the ornamentation of the eyespot of the hindwings, whose yellow ring is thinner, and highlighted externally by the presence of a line of black scales which is usually lacking in *A. cinctistriga*. The distinction from *A. godartii* is more difficult, but the general colouration of the wings is, however, different in the 22 specimens examined of the two species. In *A. belemensis* sp. nov., the ground colour of the forewings is a lighter orange-brown than the

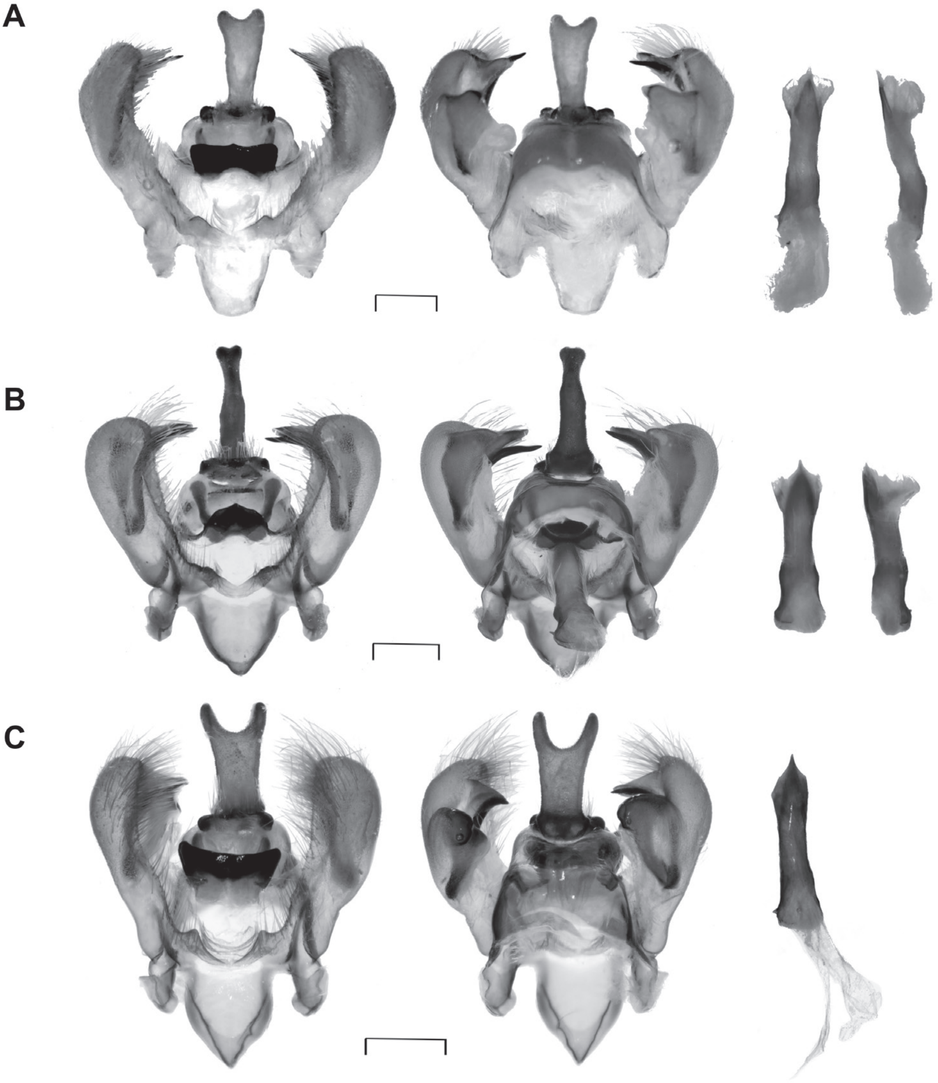

Figure 2. Genitalia ♂ of the new species of *Automeris* spp. **A** *A. mineros* sp. nov., paratype ♂ (BC-Dec0549) **B** *A. belemensis* sp. nov., paratype ♂ (BC-INCT1136) **C** *A. llaneros* sp. nov., paratype ♂ (BC-Dec0712). For each species, the dorsal and ventral views of the genitalia, and the dorsal and lateral views of the aedeagus are represented from the left to the right. Scale bars: 1 mm.

grey-brown ground colour that is characteristic of *A. godartii*. The dusting of silver scales generally present in *A. godartii*, in particular in the preapical triangle of the forewings, is weakly marked or completely absent in *A. belemensis* sp. nov. The ante- and postmedial lines are also lighter in *A. belemensis*, standing out in a more contrasted way compared to the surrounding wing colour. Finally, the line of black scales surrounding the eyespot of the hindwings, and sometimes even the yellow periocellar ring, which are continuous in *A. godartii*, are frequently interrupted towards the subcostal area in *A. belemensis* sp. nov.

It is likely that the male of *A. godartii* figured in Lemaire (2002: plate 40, fig. 4), originating from the state of Pará in Brazil, actually belongs to *A. belemensis* sp. nov.

With a long posteriorly produced uncus, male genitalia are similar to those of *A. godartii*, but also to those of *A. lemensis*, which is known only from the Gran Sabana region in southern Venezuela (Fig. 3). Interestingly, the DNA barcodes of the 11 sequenced specimens of *A. belemensis* sp. nov. form a distinct cluster in the NJ tree (BIN BOLD:AAA5242) with *A. lemensis* as the nearest neighbour with 2% minimum uncorrected p-distance (Fig. 4). However, both species can easily be distinguished by the ground coloration of their wings, which is much duller in the former, especially in the periocellar area of the hindwings, and an otherwise much rounder hindwing eyespot.

Description. ♂ (Fig. 1C, G). ***Wingspan*****:** 70–71 mm. ***Head*****:** dark brown, labial palpi and antennae orange brown. ***Thorax*****:** dorsally dark brown and ventrally orange brown; legs dark brown. ***Abdomen*****:** orange brown. ***Forewings*****:** Length 35–37 mm, slightly elongated, slightly prominent apex, straight outer border; dorsal ground colour orange brown; ante- and postmedial lines thin and yellow, the latter slightly convex, becoming barely visible upon reaching the costal margin 3–4 mm from the apex; discocellular mark rectangular, darker than the surrounding wing surface, with four to six dark brown spots at its angles. Ventral side yellow brown, slightly darker on the outer margin, with the postmedial line underlined by dark brown scales, and a large black discocellular spot, marked in its centre by a small white discal dot. ***Hindwings*****:** basomedian area dull orange with a large eyespot in its centre formed by, from its centre: a small black and white pupil, a large grey brown iris surrounded by a broad black periocellar ring, followed by a thin yellow ring, and finally by an external line of black scales. Postmedial line lunular, formed by a thin yellow line bordered proximally and distally by a wider black line; postmedian area dull orange; marginal band orange brown. Ventral side uniformly yellow brown, with a straight, weakly marked postmedial line, a faint zigzagging premarginal line, and with a small white discal spot.

Female unknown.

Genitalia ♂ (Fig. 2B): similar general structure as in other species of the *bilinea* subgroup. Uncus well developed, long and bent downwards, apically barely bifid. Dorsal lobes of valves well developed and broadly triangular. Median plate of gnathos strongly sclerotised with its posterior margin convex, a developed median projection, and long lateral appendages. Saccus well developed, triangular and acute anteriorly. Phallus straight, with a small lateral spine on its base; its posterior end slightly bent upward, with a weakly developed vesica.

Distribution. *Automeris belemensis* sp. nov. is known from the lower Amazonian watershed in the Brazilian states of Pará and Maranhão, Brazil (Fig. 3). It has not been found despite of extensive collecting efforts in neighbouring region of French Guiana, and is also unknown from other areas of Brazilian Amazonia. This suggests it could be restricted to the Belém area of endemism as defined in Cardoso da Silva et al. (2005), which was recently highlighted as a hotspot for the diversity of so far undescribed moth species (Lamarre et al. 2016).

Etymology. *Automeris belemensis* sp. nov. is named as a reference to the area of endemism of Belém where this species has been found and to which it is likely endemic.

***Automeris llaneros* Decaëns, Rougerie & Bonilla, sp. nov.**

http://zoobank.org/790F11B2-06F1-4CCF-9AA1-423401D11432

Figures 1D, H, 2C

Type material. ***Holotype.*** Colombia • ♂ (Fig. 1D, H); Casanare, Orocue; 4.7943°N, 71.3353°W; elevation: 150 m; Aug. 1999; at MV light; TD and DB leg.; BOLD SampleID: BC-Dec0711; deposited in the IAvH.

Paratype. Colombia • 1 ♂; Meta, Carimagua research station; 4.5716°N, 71.3320°W; elevation: 170 m; July 1999; at MV light; TD and DB leg.; BOLD SampleID: BC-Dec0712; deposited in CTD.

Diagnosis. *Automeris llaneros* sp. nov. is phenotypically very similar to *A. cinctistriga*, from which it is quite difficult to distinguish based on wing patterns alone. However, the two known specimens of *A. llaneros* sp. nov. have less elongated forewings with less acute apices than most of the examined specimens of *A. cinctistriga*. The background colour of the forewing is also duller in *A. llaneros* sp. nov., less orange, and the ante- and postmedian lines are finer, beige instead of yellow, and contrasting much less markedly with the general colour of the wings. Finally, the distance between the ante- and postmedian lines at the point where they join the anal edge of the forewings seems greater in *A. llaneros* sp. nov. (1 cm in the two known specimens) than in *A. cinctistriga* (4–7 mm). The DNA barcodes of *A. llaneros* sp. nov. are assigned to a different BIN than those of *A. cinctistriga* (see discussion), and the two species are very clearly separated in the DNA barcode tree, bringing additional support to their treatment as two distinct species.

DNA barcodes place *A. llaneros* sp. nov. near *A. belizonensis*, *A. mineros* sp. nov., and *A. fieldi* on the NJ tree (Fig. 4). This proximity seems to be confirmed by the examination of the male genitalia, whose bifid protuberance of the uncus is strongly developed, exceeding the tip of the valves, as in *A. mineros* sp. nov. (described here), *A. belizonensis*, and *A. fieldi* (Lemaire 1971; Brechlin and Meister 2014). In comparison, *A. cinctistriga* generally presents a less developed and less deeply indented uncus (Lemaire 1971). The new species is also easily distinguished from these close relatives based on its wing shape and patterns. For instance, *A. belizonensis* has more elongated forewings with more pointed apex, and an overall more vivid and orange colouring. *Automeris mineros* sp. nov. also has a very different coloration, notably due to the contrasting orange-red periocellar area of the hindwings. Finally, *A. fieldi*, a species occurring from the Pacific slopes of the Andes to Costa Rica (Fig. 3) and probably north to Honduras (Bénéluz, pers. comm.), stands out again by the slightly more elongated shape of the forewings, but also by the presence of a continuous ring of black scales external to the eyespot of the hindwings, which is lacking in *A. llaneros* sp. nov.

Description. ♂ (Fig. 1D, H). ***Wingspan*****:** 72–74 mm. ***Head*****:** Dark brown, labial palpi and antennae brown. ***Thorax*****:** dorsally dark brown and ventrally light brown; legs light brown. ***Abdomen*****:** dorsally orange brown, ventrally light brown. ***Forewings*****:** Length 32–35 mm, slightly elongated, slightly prominent apex, straight to slightly convex outer border; dorsal ground colour dull orange brown; antemedial line thin and beige, doubled with a brown line proximally; postmedial line slightly convex, barely visible as it reaches the costal margin 2–3 mm from the apex, thin and beige, distally

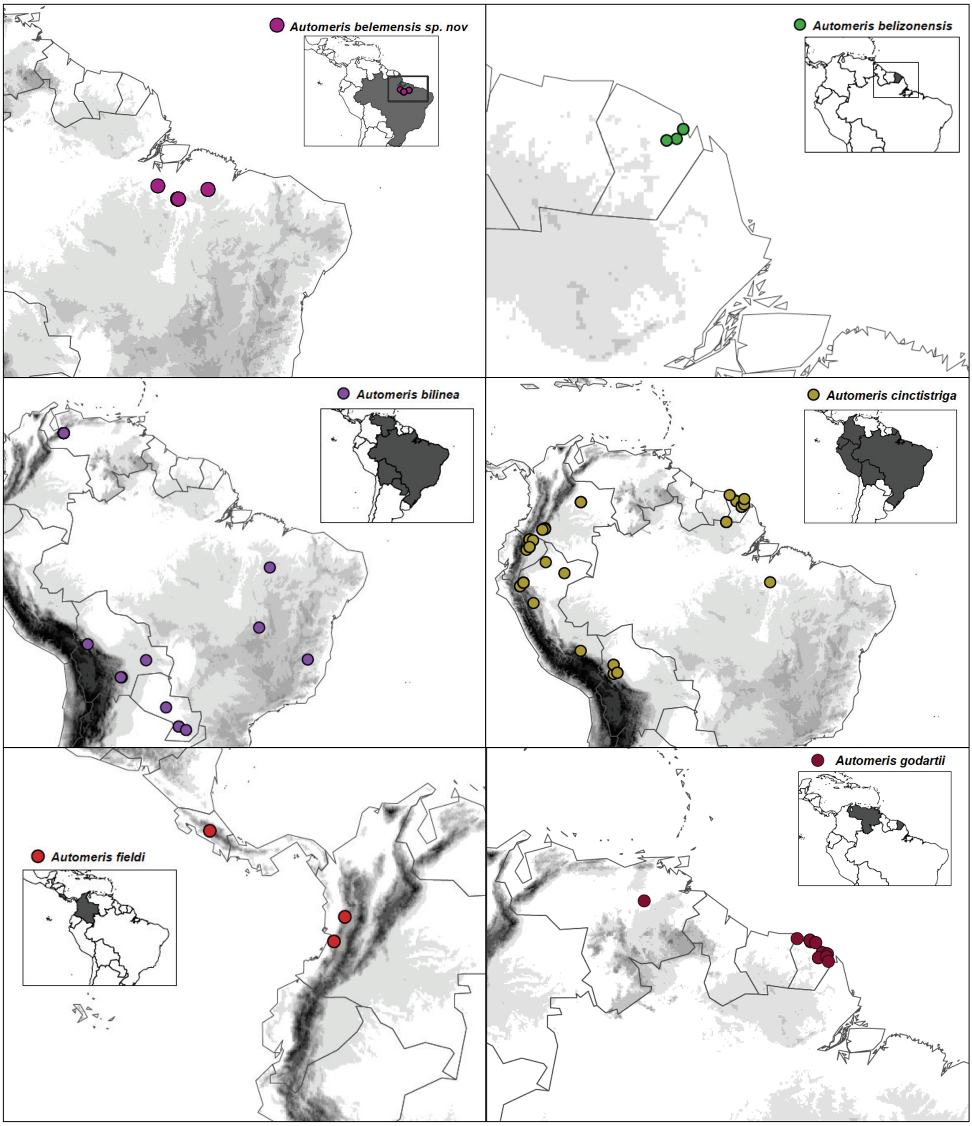

Figure 3. Distribution maps of *Automeris* species within the subgroup of *A. bilinea*, based on georeferenced records collected from BOLD, and known geographic distribution of the three new species of *Automeris* spp.

bordered by dark brown scales; basal and median areas concolorous; discocellular mark of the median area rectangular, darker than the surrounding wing surface, with three clearly visible dark brown spots at corners and one faint central spot. Ventral side yellow brown, with darker postmedial and premarginal lines, and a large black discocellular mark, marked in its centre by a white discal spot; venation marked with orange scales. ***Hindwings***: Basomedian area dull orange suffused by dark brown scales, with a large eyespot in its centre formed by, from its centre: an almost completely white small pupil, suffused with few black scales, a large grey brown iris, surrounded by a large black ring

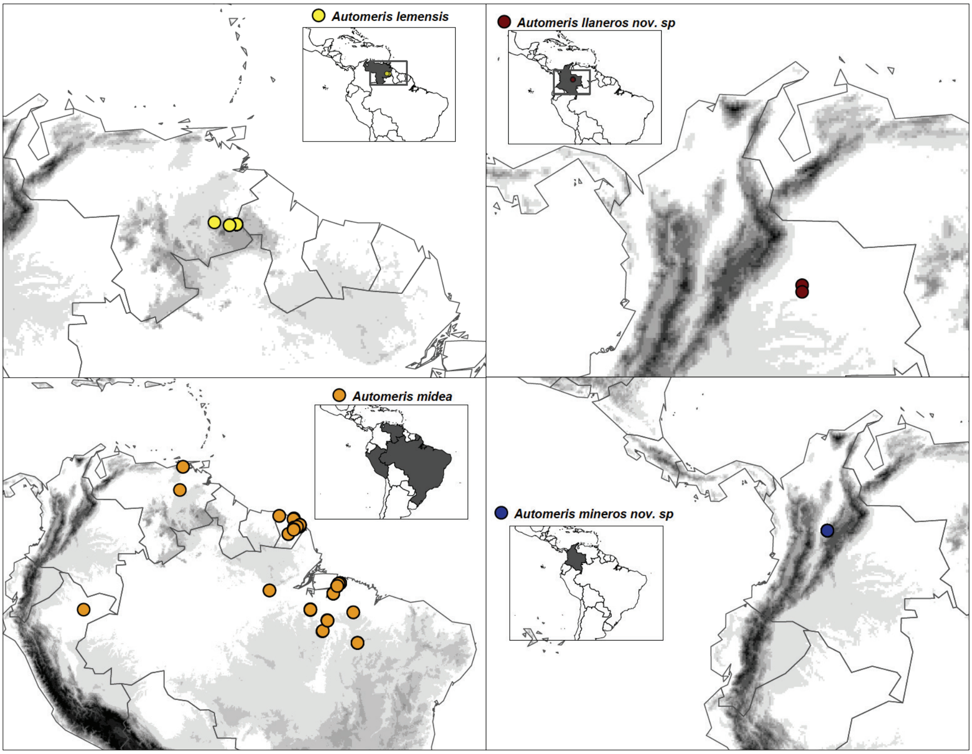

Figure 3. Continued.

and then a thinner yellow ring (in paratype specimen we observed a few black scales external to this outer yellow ring of the eyespot); postmedial line black, lunular, bordered proximally and distally by thin lines of yellow scales; postmedian area dull orange; marginal band large and grey. Ventral side uniformly orange brown, with a weak oblique postmedial line interrupted before it reaches the costal margin, a vestigial premarginal line forming darker U-shaped marks between veins, and a small white discal point.

Female unknown.

Genitalia ♂ (Fig. 2C): very similar to those of *A. mineros* sp. nov. Uncus elongated, large and strongly bifid apically, largely extending beyond the valves. Valves relatively short, rounded, with a broad, rounded dorsal lobe; arms short and strongly curved. Median plate of the gnathos highly sclerotised, as wide as the saccus and subrectangular. Saccus well developed, triangular and acute anteriorly.

Distribution. *Automeris llaneros* sp. nov. is only known from the region of Carimagua and Orocué, in the Colombian part of the Orinoco watershed, the so called "Llanos Orientales" of Colombian Eastern Plains (Fig. 3). The region has been poorly investigated for saturniid diversity but is known to host a few endemics whose exact distributions need to be clarified (see for example Decaëns et al. 2005).

Etymology. This species is named in reference to the Llanos region, which refer to the large area of savannahs that cover most of the Colombian and Venezuelan Orinoco watershed.

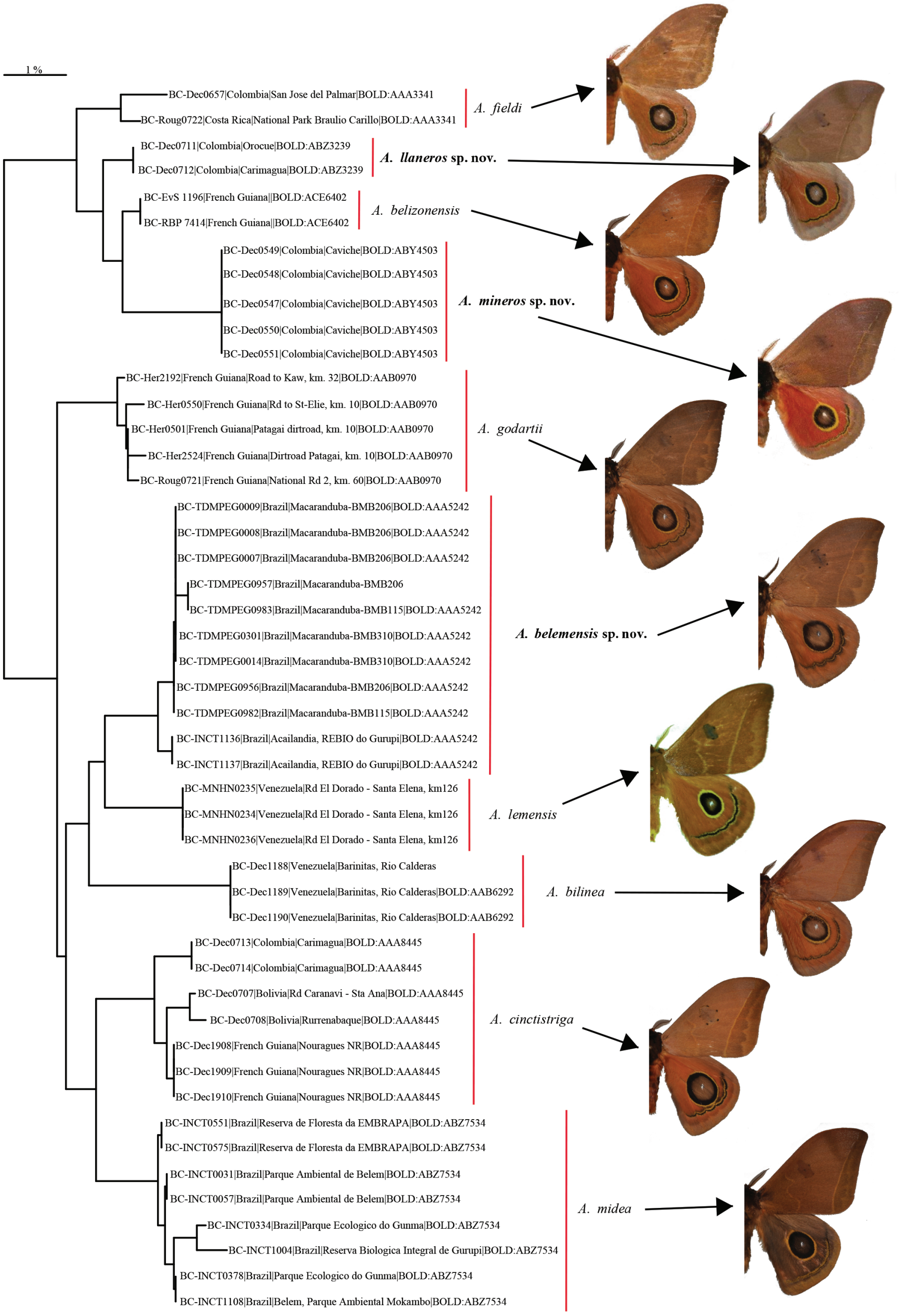

Figure 4. Neighbour joining tree (K2P distances) built from DNA barcodes (COI) of specimens from the three new species of *Automeris* and their closest relatives. The labels of the terminal branches successively give the following information: sample ID code in the Barcode of Life Data system, country, and exact collecting site when available, Barcode Identification Number (BIN) automatically assigned to each sequence in BOLD. All specimens of *A. lemensis* and one of *A. bilinea* have no BIN number due to the short length of their COI sequences.

Discussion

The description of three new species of *Automeris* within the highly cryptic *A. bilinea* species-subgroup is a new illustration of the value of DNA barcoding, when combined with morphological diagnostic characters and distribution data, in disclosing hidden diversity (Hebert et al. 2004). Our study illustrates two different methodological approaches, which can allow the identification and support the description of new species in such taxonomically difficult groups.

In the case of *A. mineros* sp. nov., the species had appeared clearly distinct from other known species by the study of its external habitus, showing in particular a unique coloration of the hindwing periocellar area. This singularity is however shared with some specimens representing extreme variants of another species belonging to this subgroup (*A. midea*). This led us to further explore the question, first by a comparison of male genitalia, used conventionally but whose discriminating characters between closely related species in this group sometimes remains uncertain or even equivocal (Lemaire 1971). Finally, we used DNA barcodes as an independent dataset to confirm the separation of *A. mineros* sp. nov. from its relatives.

For *A. llaneros* sp. nov. and *A. belemensis* sp. nov., the approach was different. The use of DNA barcodes first revealed the existence of cryptic species, i.e., species presenting different barcodes but that were not discriminable from their habitus, or differing from each other only by subtle characters. The subsequent analysis of the genetic distances revealed affinities with species which were not necessarily the most similar in their wing pattern, but such affinities were corroborated in both cases by the structure of the male genitalia. Thus, it is the combination of the genitalia, the habitus, and the DNA barcodes which concomitantly characterise these species within the group.

In the case of *A. llaneros* sp. nov., the problem of the real identity of *A. cinctistriga*, a species with which it is impossible to rule out confusion, also deserves to be considered carefully. *Automeris cinctistriga* was described from a male collected in Colombia, and Lemaire (1971) already stated that the exact identity of this species could be problematic, as the abdomen of the lectotype had been destroyed. It is also most likely that the type-locality of the lectotype, Bogotá (2600m asl), is wrong, as no similar species seems to fly at such high elevation Andean forests of the Colombian Eastern cordillera (pers. obs.). Within the material collected in the eastern plains of Colombia, we found several specimens corresponding to the description of *A. cinctistriga* based on their wing patterns, and DNA barcoding of these specimens revealed two distinct clusters of barcodes corresponding to two distinct BINs in BOLD. These two BINs were clearly separated in the barcode tree (Fig. 4), making *A. cinctistriga* in its former definition paraphyletic, and clearly suggesting that they correspond to two different species (Mutanen et al. 2016). In the absence of genitalia and available DNA sequences from the old lectotype of *A. cinctistriga*, it was formally impossible to define which of the two species corresponded to each of these BINs. We therefore adopted the more conservative position. We considered that *A. cinctistriga* corresponded to the BIN BOLD:AAA8445, which in BOLD, is defined by a large distribution around the Amazonian watershed (including Bolivia, Brazil, Colombia, Ecuador, French Guiana, Peru), perfectly fitting the distribution of *A. cinctistriga* as described in the literature (Lemaire 1971, 2002). The other BIN (BOLD:ABZ3239) was represented by the two Colombian specimens used herein as type material for the description of *A. llaneros* sp. nov. This position is also consistent with wing ornamentation, since the lectotype represented by Lemaire (1971) broadly presents the characteristics that we have attributed to *A. cinctistriga*.

Overall, the discovery of new species, including some cryptic ones, in a highly diverse genus such as *Automeris* does not represent a surprising finding. The cryptic diversity of *Automeris* has already been highlighted by recent taxonomic studies, in which traditionally recognised species with large geographical distributions have been divided into several new species based primarily on differences in DNA barcodes (Brechlin and Meister 2014). This underlines the extent of the taxonomic deficit that characterises the family Saturniidae, which nevertheless is among the best studied within the "Heterocera".

The fact that species traditionally recognised as having a wide distribution prove to be in fact complexes of cryptic species with more restricted distributions also raises new and interesting questions concerning the specificity of the different biogeographical areas which constitute the neotropics. The three regions from which the species described in our study originate are a perfect example. The saturniid fauna is considered to be made up of a mixture of endemics and widely distributed species, with variable proportions depending on the regions. For instance, the Eastern Cordillera of Colombia is considered to be a hotspot of diversity, harbouring a significant proportion of endemics (Lemaire 2002; Decaëns et al. 2007; Decaëns and Rougerie 2008), whereas faunas of the Orinoco and Amazon lowlands are generally considered to be dominated by species with wide distributions (Lemaire 2002). In all cases, however, it is likely that due to this cryptic diversity, a significant proportion of species diversity has been underestimated by the predominant use of morphology in previous estimations. This is well illustrated by our case study, where we describe three new species with probably restricted distributions based largely on the information provided by DNA barcoding. As described in other groups of organisms (Guarnizo et al. 2015), we can therefore expect that the generalisation of the use of DNA barcoding will continue to fragment the expansive distributions of widespread species, thus modifying our current perception of diversity distributed among biogeographical areas.

Acknowledgements

Field work in Brazil was supported through grants from the Agence Nationale de la Recherche (ANR, France) and the Brazilian National Council of Research (CNPq, Brazil) to the project AMAZ_BD ("Amazonian landscape biodiversity"; ANR 06 BIODIV 009-01; IFB_ANR). This research also benefited from the support by the synthesis centre CESAB of the French Foundation for Research on Biodiversity (FRB; www.fondationbiodiversite.fr) to the ACTIAS group. We are particularly grateful to Patrick

Lavelle (IRD-CIAT, Cali, Colombia), Marlucia Bonifacio Martins (MPEG, Belém, Brazil), and staff from the Carimagua Research Station (CIAT-CORPOICA, Colombia) for their support during field collecting in Brazilian Amazonia and Colombian Eastern Plains, and Gilbert Lecourt for kindly providing the specimens collected in the region of Muzo. We finally thank Paul Hebert for facilitating DNA barcode sequencing through the international Barcode of Life project.

References

Brechlin R, Meister F (2014) Neu taxa der Gattung *Automeris* Hübner, [1819] (Lepidoptera: Saturniidae). Entomo-Satsphingia 4(1): 5–89.

Cardoso da Silva JM, Rylands AB, da Fonseca GAB (2005) The fate of the Amazonian Areas of Endemism. Conservation Biology 19(3): 689–694. https://doi.org/10.1111/j.1523-1739.2005.00705.x

Decaëns T, Bonilla D, Naumann S (2005) *Dirphia carimaguensis*, a new Hemileucinae from the Eastern Plains of Colombia (Lepidoptera: Saturniidae). Galathea (Nuremberg, Germany), suppl. 15: 13–21.

Decaëns T, Rougerie R (2008) Description of two new species of Hemileucinae (Lepidoptera: Saturniidae) from the region of Muzo in Colombia – evidence from morphology and DNA barcodes. Zootaxa 1944: 34–52. https://doi.org/10.11646/zootaxa.1944.1.2

Decaëns T, Rougerie R, Bonilla D, Ramiréz LD (2007) Contribution to the knowledge of the Saturniidae fauna of Muzo (Boyacá, Colombia), with the redescription of *Copaxa apollinairei* Lemaire, 1978 (Lepidoptera, Saturniidae). Nachrichten des Entomologischen Vereins Apollo (Frankfurt, Germany) 28(1/2): 69–75.

Felder C, Felder R (1874) "Helf 4" Heterocera. Bombyces & Sphinges. In: Felder C, Felder R, Rogenhofer AF (Eds) Reise der österreichischen Fregatte Novara um die Erde in den Jahren 1857, 1858, 1859. Zoologischer Theil, Zweiter Band, Zweite Abtheilung: Lepidoptera. K.-k. Hof- und Staatsdruckerei, Vienna, plates 75–107.

Guarnizo CE, Paz A, Muñoz-Ortiz A, Flechas SV, Méndez-Narváez J, Crawford AJ (2015) DNA barcoding survey of anurans across the Eastern Cordillera of Colombia and the impact of the Andes on cryptic diversity. PLoS ONE 10(5): e0127312. https://doi.org/10.1371/journal.pone.0127312

Hajibabaei M, deWaard JR, Ivanova NV, Ratnasingham S, Dooh RT, Kirk SL, Mackie PM, Hebert PDN (2005) Critical factors for assembling a high volume of DNA barcodes. Philosophical Transactions of the Royal Society B Biological Sciences 360: 1959–1967. https://doi.org/10.1098/rstb.2005.1727

Hajibabaei M, Janzen DH, Burns JM, Hallwachs W, Hebert PDN (2006) DNA barcodes distinguish species of tropical Lepidoptera. Proceedings of the National Academy of Sciences of the USA 103: 968–971. https://doi.org/10.1073/pnas.0510466103

Hebert PDN, Penton EH, Burns JM, Janzen DH, Hallwachs W (2004) Ten species in one: DNA barcoding reveals cryptic species in the Neotropical skipper butterfly *Astraptes fulger-*

ator. Proceedings of the National Academy of Sciences of the USA 101: 14812–14817. https://doi.org/10.1073/pnas.0406166101

Hebert PDN, Ratnasingham S, deWaard JR (2003) Barcoding animal life: cytochrome c oxidase subunit 1 divergences among closely related species. Proceedings of the Royal Society B Biological Sciences 270: S96–S99. https://doi.org/10.1098/rsbl.2003.0025

Ivanova NV, deWaard JR, Hebert PDN (2006) An inexpensive, automation-friendly protocol for recovering high-quality DNA. Molecular Ecology Notes 6: 998–1002. https://doi.org/10.1111/j.1471-8286.2006.01428.x

Kitching I, Rougerie R, Zwick A, Hamilton C, St Laurent R, Naumann S, Ballesteros-Mejia L, Kawahara A (2018) A global checklist of the Bombycoidea (Insecta: Lepidoptera). Biodiversity Data Journal 6: e22236. https://doi.org/10.3897/BDJ.6.e22236

Lamarre GPA, Decaëns T, Rougerie R, Barbut J, Herbin D, Laguerre M, Thiaucourt P, Martins Bonifacio M (2016) An integrative taxonomy approach unveils unknown and threatened moth species in Amazonian rainforest fragments. Insect Conservation and Diversity 9: 475–479. https://doi.org/10.1111/icad.12187

Lamarre GPA, Mendoza I, Rougerie R, Decaëns T, Hérault B, Béneluz F (2015) Stay out (almost) all night: contrasting responses in flight activity among tropical moth assemblages. Neotropical Entomology 44: 109–115. https://doi.org/10.1007/s13744-014-0264-3

Lemaire C (1969) Description d'Attacidae nouveaux de Colombie et de Panama (Lep.). Annales de la Société entomologique de France (Paris) 5: 73–94.

Lemaire C (1971) Révision du genre *Automeris* Hübner et des genres voisins. Biogéographie, éthologie, morphologie, taxonomie (Lep. Attacidae). Mémoires du Muséum national d'Histoire naturelle (Paris) (A) Zoologie 68: 1–232.

Lemaire C (1972) Description d'Attacidae (= Saturniidae) nouveaux du Venezuela et du Pérou (Lep.). Bulletin de la Société entomologique de France (Paris) 77: 29–41.

Lemaire C (2002) The Saturniidae of America (= Attacidae). Vol 4 – Hemileucinae. Goecke & Evers, Keltern, 1388 pp. [140 pls.]

Maassen JP, Weyding A (1885) Beiträge zur Schmetterlingskunde. Elberfeld 5: 1–6. [pls [41–50], figs 82–126.]

Mutanen M, Kivelä SM, Vos RA, Doorenweerd C, Ratnasingham S, Hausmann A, Huemer P, Dincă V, van Nieukerken EJ, Lopez-Vaamonde C, Vila R, Aarvik L, Decaëns T, Efetov KA, Hebert PDN, Johnsen A, Karsholt O, Pentinsaari M, Rougerie R, Segerer A, Tarmann G, Zahiri R, Godfray C (2016) Species para- and polyphyly in COI gene trees. Systematic Biology 65(6): 1024–1040. https://doi.org/10.1093/sysbio/syw044

Ratnasingham S, Hebert PDN (2007) BOLD: The Barcode of Life Data System (http://www.barcodinglife.org). Molecular Ecology Notes 7: 355–364. https://doi.org/10.1111/j.1471-8286.2007.01678.x

Ratnasingham S, Hebert PDN (2013) A DNA-based registry for all animal species: the Barcode Index Number (BIN) System. PLoS ONE 8(8): e66213. https://doi.org/10.1371/journal.pone.0066213

Walker F (1855) List of the specimens of lepidopterous insects in the collection of the British Museum. Part VI: Lepidoptera, Heterocera. Order of the trustees, London, 1259–1507.

Appendix I

List of the specimens included in the dataset DS-AUTONSP of the Baorcode of Life Data system, collecting data and accession codes in BOLD and GenBank.

Species	Sex	Status	Collectors	Collection Date	Country	State/ Province	Exact Site	Latitude / Longitude	Elevation (m)	Collection Date	Collectors	COI-5P Seq. Length	Sample id	Process ID	BIN	GenBank accession
Automeris belemensis sp. nov.	♂	Holotype	T. Decaens	01-Apr-2008	Brazil	Para	Macaranduba	-4.7990, -49.3630	102	01-Apr-2008	T. Decaens	658[0n]	BC-TD-MPEG0007	TDMPE007-09	BOLD:AAA5242	JN827467
	♂	Paratype	T. Decaens	18-Apr-2010	Brazil	Maranhao	Acailandia, REBIO do Gurupi	-4.0014, -46.8372	275	18-Apr-2010	T. Decaens	658[0n]	BC-INCT1136	STDB692-14	BOLD:AAA5242	KX051423
	♂	Paratype	T. Decaens	18-Apr-2010	Brazil	Maranhao	Acailandia, REBIO do Gurupi	-4.0014, -46.8372	275	18-Apr-2010	T. Decaens	658[0n]	BC-INCT1137	STDB693-14	BOLD:AAA5242	KX051458
	♂	Paratype	T. Decaens	01-Apr-2008	Brazil	Para	Macaranduba	-4.7990, -49.3630	102	01-Apr-2008	T. Decaens	658[0n]	BC-TD-MPEG0008	TDMPE008-09	BOLD:AAA5242	JN827466
	♂	Paratype	T. Decaens	01-Apr-2008	Brazil	Para	Macaranduba	-4.7990, -49.3630	102	01-Apr-2008	T. Decaens	658[0n]	BC-TD-MPEG0009	TDMPE009-09	BOLD:AAA5242	JN827465
	♂	Paratype	T. Decaens	01-Apr-2008	Brazil	Para	Macaranduba	-4.8110, -49.3670	111	01-Apr-2008	T. Decaens	658[0n]	BC-TD-MPEG0014	TDMPE014-09	BOLD:AAA5242	JN827464
	♂	Paratype	T. Decaens	01-Apr-2008	Brazil	Para	Macaranduba	-4.8110, -49.3670	111	01-Apr-2008	T. Decaens	658[0n]	BC-TD-MPEG0301	TDMPE284-10	BOLD:AAA5242	HQ581446
	♂	Paratype	T. Decaens	01-Jun-2008	Brazil	Para	Pacaja	-3.7060, -51.0390	111	01-Jun-2008	T. Decaens	0[n]	BC-TD-MPEG0667	AMAZ546-12	–	–
	♂	Paratype	T. Decaens	01-Apr-2008	Brazil	Para	Macaranduba	-4.8050, -49.3690	127	01-Apr-2008	T. Decaens	0[n]	BC-TD-MPEG0743	AMAZ622-12	–	–
	♂	Paratype	T. Decaens	01-Apr-2008	Brazil	Para	Macaranduba	-4.8050, -49.3690	127	01-Apr-2008	T. Decaens	0[n]	BC-TD-MPEG0744	AMAZ623-12	–	–
	♂	Paratype	T. Decaens	01-Apr-2008	Brazil	Para	Macaranduba	-4.8110, -49.3670	111	01-Apr-2008	T. Decaens	0[n]	BC-TD-MPEG0918	AMAZ797-12	–	–
	♂	Paratype	T. Decaens	01-Apr-2008	Brazil	Para	Macaranduba	-4.8110, -49.3670	111	01-Apr-2008	T. Decaens	0[n]	BC-TD-MPEG0919	AMAZ798-12	–	–
	♂	Paratype	T. Decaens	01-Apr-2008	Brazil	Para	Macaranduba	-4.8110, -49.3670	111	01-Apr-2008	T. Decaens	0[n]	BC-TD-MPEG0920	AMAZ799-12	–	–
	♂	Paratype	T. Decaens	01-Apr-2008	Brazil	Para	Macaranduba	-4.7990, -49.3630	102	01-Apr-2008	T. Decaens	594[0n]	BC-TD-MPEG0956	AMAZ835-12	BOLD:AAA5242	MT257065
	♂	Paratype	T. Decaens	01-Apr-2008	Brazil	Para	Macaranduba	-4.7990, -49.3630	102	01-Apr-2008	T. Decaens	491[0n]	BC-TD-MPEG0957	AMAZ836-12	–	MT257050
	♂	Paratype	T. Decaens	01-Apr-2008	Brazil	Para	Macaranduba	-4.8040, -49.3230	116	01-Apr-2008	T. Decaens	625[2n]	BC-TD-MPEG0982	AMAZ861-12	BOLD:AAA5242	MT257047
	♂	Paratype	T. Decaens	01-Apr-2008	Brazil	Para	Macaranduba	-4.8040, -49.3230	116	01-Apr-2008	T. Decaens	538[0n]	BC-TD-MPEG0983	AMAZ862-12	BOLD:AAA5242	MT257063

Species	Sex	Status	Collectors	Collection Date	Country	State/ Province	Exact Site	Latitude / Longitude	Elevation (m)	Collection Date	Collectors	COI-5P Seq. Length	Sample id	Process ID	BIN	GenBank accession
Automeris belizonensis	♂	Holotype	local collector	01-Jan-2012	French Guiana	Cayenne	Kaw mountain	4.5595, -52.2067	290	01-Jan-2012	local collector	658[0n]	BC-RBP 7414	SARBE1594-13	BOLD:ACE6402	MT257076
	♀	Paratype	local collector	28-Jun-2003	French Guiana	Cayenne	Belizon	4.2697, -52.6415	80	28-Jun-2003	local collector	658[0n]	BC-EvS 1196	SAVSA1196-11	BOLD:ACE6402	JN273152
Automeris bilinea	♂		B. Wenczel		Venezuela	Barinas	Barinitas, Rio Calderas	8.7900, -70.4570	420		B. Wenczel	268[0n]	BC-Dec1188	STDB238-07	–	MT257049
	♂		B. Wenczel		Venezuela	Barinas	Barinitas, Rio Calderas	8.7900, -70.4570	420		B. Wenczel	658[0n]	BC-Dec1189	STDB239-07	BOLD:AAB6292	MT257046
	♀		B. Wenczel		Venezuela	Barinas	Barinitas, Rio Calderas	8.7900, -70.4570	420		B. Wenczel	658[0n]	BC-Dec1190	STDB240-07	BOLD:AAB6292	MT257072
Automeris cinctistriga	♂		T. Decaens, G. Lecourt	01-Dec-1991	Bolivia	La Paz	Rd Caranavi – Sta Ana	-15.5190, -67.5160	875	01-Dec-1991	T. Decaens, G. Lecourt	612[0n]	BC-Dec0707	STDA697-07	BOLD:AAA8445	MT257057
	♂		T. Decaens, G. Lecourt	01-Dec-1991	Bolivia	Beni	Rurrenabaque	-14.4640, -67.5570	380	01-Dec-1991	T. Decaens, G. Lecourt	574[0n]	BC-Dec0708	STDA698-07	BOLD:AAA8445	MT257069
	♂		T. Decaens	01-Apr-1995	Colombia	Meta	Carimagua	4.5660, -71.3330	170	01-Apr-1995	T. Decaens	635[0n]	BC-Dec0713	STDA703-07	BOLD:AAA8445	MT257054
	♀		T. Decaens	01-Apr-1995	Colombia	Meta	Carimagua	4.5660, -71.3330	170	01-Apr-1995	T. Decaens	595[0n]	BC-Dec0714	STDA704-07	BOLD:AAA8445	MT257048
	♂		T. Decaens	01-Jun-2011	French Guiana		Nouragues, Inselberg RS	4.0882, -52.6798	124	01-Jun-2011	T. Decaens	658[0n]	BC-Dec1908	STDB704-14	BOLD:AAA8445	MT257066
	♂		T. Decaens	01-Jun-2011	French Guiana		Nouragues, Inselberg RS	4.0882, -52.6798	124	01-Jun-2011	T. Decaens	658[0n]	BC-Dec1909	STDB705-14	BOLD:AAA8445	MT257062
	♂		T. Decaens	01-Jun-2011	French Guiana		Nouragues, Inselberg RS	4.0882, -52.6798	124	01-Jun-2011	T. Decaens	658[0n]	BC-Dec1910	STDB706-14	BOLD:AAA8445	MT257061
Automeris fieldi	♂	Paratype	H. & L. Dehez	01-Nov-1965	Colombia	Valle del Cauca	Anchicaya	3.5350, -76.8692	400	01-Nov-1965	H. & L. Dehez	407[0n]	BC-MNHN0241	STDB581-09	BOLD:AAA3341	MT257064
	♂		T. Decaens, D. Bonilla	01-Jul-2002	Colombia	Choco	San Jose del Palmar	4.9170, -76.2500	1200	01-Jul-2002	T. Decaens, D. Bonilla	658[0n]	BC-Dec0657	STDA647-07	BOLD:AAA3341	MT257058
	♂		J. Barbut et al.	11-May-2005	Costa Rica	Cartago	National Park Braulio Carillo	9.7620, -83.8820	600	11-May-2005	J. Barbut et al.	658[0n]	BC-Roug0722	SATWA741-07	BOLD:AAA3341	MT257053
Automeris godartii	♂		D. Herbin & M. Laguerre	02-Mar-2006	French Guiana		Dirtroad to Patagai, km. 10	5.3930, -53.1910	48	02-Mar-2006	D. Herbin & M. Laguerre	658[0n]	BC-Her0501	SDHA501-07	BOLD:AAB0970	MT257074
	♂		D. Herbin & M. Laguerre	01-Mar-2006	French Guiana		Road to St-Elie, km. 10	5.2980, -53.1500	28	01-Mar-2006	D. Herbin & M. Laguerre	658[0n]	BC-Her0550	SDHA550-07	BOLD:AAB0970	MT257055

Species	Sex	Status	Collectors	Collection Date	Country	State/ Province	Exact Site	Latitude / Longitude	Elevation (m)	Collection Date	Collectors	COI-5P Seq. Length	Sample id	Process ID	BIN	GenBank accession
Automeris godartii	♂		D. Herbin & M. Laguerre	05-Mar-2006	French Guiana		Road to Kaw, km. 32	4.5443, -52.1529	200	05-Mar-2006	D. Herbin & M. Laguerre	658[0n]	BC-Her2192	SDHC192-08	BOLD:AAB0970	MT257052
	♂		D. Herbin & M. Laguerre	02-Mar-2006	French Guiana		Dirtroad to Patagai, km. 10	5.3934, -53.1915	45	02-Mar-2006	D. Herbin & M. Laguerre	658[0n]	BC-Her2524	SDHC524-09	BOLD:AAB0970	GU703600
	♂		D. Carlot	10-Apr-1997	French Guiana		National Rd 2, km. 60	4.5170, -52.4030	64	10-Apr-1997	D. Carlot	639[0n]	BC-Roug0721	SATWA740-07	BOLD:AAB0970	MT257073
Automeris lemensis	♂	Paratype	C. Lemaire	17-Jun-1971	Venezuela	Bolivar	Rd El Dorado – Santa Elena, km126	5.7322, -61.4021	1350	17-Jun-1971	C. Lemaire	307[0n]	BC-MNHN0234	STDB574-09	–	MT257051
	♂	Paratype	C. Lemaire	17-Jun-1971	Venezuela	Bolivar	Rd El Dorado – Santa Elena, km126	5.7322, -61.4021	1350	17-Jun-1971	C. Lemaire	307[0n]	BC-MNHN0235	STDB575-09	–	MT257071
	♂	Paratype	C. Lemaire	17-Jun-1971	Venezuela	Bolivar	Rd El Dorado – Santa Elena, km126	5.7322, -61.4021	1350	17-Jun-1971	C. Lemaire	307[1n]	BC-MNHN0236	STDB576-09	–	MT257070
Automeris llaneros sp. nov.	♂	Holotype	T. Decaens, D. Bonilla	01-Aug-1999	Colombia	Casanare	Orocue	4.7943, -71.3353	150	01-Aug-1999	T. Decaens, D. Bonilla	658[0n]	BC-Dec0711	STDA701-07	BOLD:ABZ3239	MT257067
	♂	Paratype	T. Decaens, D. Bonilla	01-Jul-1999	Colombia	Meta	Carimagua	4.5716, -71.3320	170	01-Jul-1999	T. Decaens, D. Bonilla	613[0n]	BC-Dec0712	STDA702-07	BOLD:ABZ3239	MT257068
Automeris midea	♂		T. Decaens	07-Apr-2010	Brazil	Para	Parque Ambiental de Belem	-1.4330, -48.4110	25	07-Apr-2010	T. Decaens	658[0n]	BC-INCT0031	INCTA031-10	BOLD:ABZ7534	HQ961129
	♂		T. Decaens	07-Apr-2010	Brazil	Para	Parque Ambiental de Belem	-1.4330, -48.4110	25	07-Apr-2010	T. Decaens	658[0n]	BC-INCT0057	INCTA057-10	BOLD:ABZ7534	HQ961154
	♂		T. Decaens	11-Apr-2010	Brazil	Para	Parque Ecologico do Gunma	-1.2130, -48.2900	22	11-Apr-2010	T. Decaens	658[0n]	BC-INCT0334	INCTA334-10	BOLD:ABZ7534	HQ568029
	♂		T. Decaens	11-Apr-2010	Brazil	Para	Parque Ecologico do Gunma	-1.2130, -48.2900	22	11-Apr-2010	T. Decaens	658[0n]	BC-INCT0378	INCTA378-10	BOLD:ABZ7534	HQ568071
	♂		T. Decaens	13-Apr-2010	Brazil	Para	Reserva de Floresta da EMBRAPA	-2.1800, -48.8020	19	13-Apr-2010	T. Decaens	658[0n]	BC-INCT0551	INCTA551-10	BOLD:ABZ7534	HQ568235
	♂		T. Decaens	13-Apr-2010	Brazil	Para	Reserva de Floresta da EMBRAPA	-2.1800, -48.8020	19	13-Apr-2010	T. Decaens	658[0n]	BC-INCT0575	INCTA575-10	BOLD:ABZ7534	HQ568259

Species	Sex	Status	Collectors	Collection Date	Country	State/ Province	Exact Site	Latitude / Longitude	Elevation (m)	Collection Date	Collectors	COI-5P Seq. Length	Sample id	Process ID	BIN	GenBank accession
Automeris midea	♂		T. Decaens	18-Apr-2010	Brazil	Maranhao	Reserva Biologica Integral de Gurupi	-4.0010, -46.8370	275	18-Apr-2010	T. Decaens	658[0n]	BC-INCT1004	INCTB005-10	BOLD:ABZ7534	HQ568662
	♂		T. Decaens	08-Apr-2010	Brazil	Para	Belem, Parque Ambiental Mokambo	-1.4335, -48.4111	25	08-Apr-2010	T. Decaens	658[0n]	BC-INCT1108	STDB664-14	BOLD:ABZ7534	KX051429
Automeris mineros sp. nov.	♂	Holotype	G. Lecourt, D. Bonilla	01-Dec-2002	Colombia	Boyaca	Vereda Caviche	5.5756, -74.2595	1500	01-Dec-2002	G. Lecourt, D. Bonilla	658[0n]	BC-Dec0551	STDA541-07	BOLD:ABY4503	MT257075
	♀	Paratype	G. Lecourt, D. Bonilla	01-Dec-2002	Colombia	Boyaca	Vereda Caviche	5.5756, -74.2595	1500	01-Dec-2002	G. Lecourt, D. Bonilla	658[0n]	BC-Dec0547	STDA537-07	BOLD:ABY4503	MT257056
	♂	Paratype	G. Lecourt, D. Bonilla	01-Dec-2002	Colombia	Boyaca	Vereda Caviche	5.5756, -74.2595	1500	01-Dec-2002	G. Lecourt, D. Bonilla	658[0n]	BC-Dec0548	STDA538-07	BOLD:ABY4503	MT257060
	♂	Paratype	G. Lecourt, D. Bonilla	01-Dec-2002	Colombia	Boyaca	Vereda Caviche	5.5756, -74.2595	1500	01-Dec-2002	G. Lecourt, D. Bonilla	658[0n]	BC-Dec0549	STDA539-07	BOLD:ABY4503	MT257059
	♂	Paratype	G. Lecourt, D. Bonilla	01-Dec-2002	Colombia	Boyaca	Vereda Caviche	5.5756, -74.2595	1500	01-Dec-2002	G. Lecourt, D. Bonilla	373[0n]	BC-Dec0550	STDA540-07	BOLD:ABY4503	–